JSPS ASIA AND AFRICA SCIENCE PLATFORM PROGRAM

GEOMOPHOLOGICAL COMPARATIVE RESEARCH ON NATURAL DISASTER MITIGATION IN THE COASTAL REGIONS OF TROPICAL ASIA

PROCEEDINGS
OF
PHUKET, HO CHI MINH, AND PATTAYA CONFERENCES

March 2008
Nagoya University, Japan

JSPS ASIA AND AFRICA SCIENCE PLATFORM PROGRAM

GEOMOPHOLOGICAL COMPARATIVE RESEARCH ON NATURAL DISASTER MITIGATION IN THE COASTAL REGIONS OF TROPICAL ASIA

PROCEEDINGS
OF
PHUKET, HO CHI MINH, AND PATTAYA CONFERENCES

March 2008
Nagoya University, Japan

Photographs on first/back cover pages by M. Umitsu

The chapters in this publication were first presented at the International Conferences about "Geomorphological comparative research on natural disaster mitigation in the coastal regions of tropical Asia", which were held at Phuket, Thailand, August 2006, Ho Chi Minh, Vietnam, August 2007, and Pattaya, Thailand, November 2007, as shown in the Appendix of this volume in detail. No part of this publication may be reproduced without any permission of the concerned authors.

Includes 200 + iv pages
Also available as a PDF file at: www.geog.lit.nagoya-u.ac.jp/aaplat/

EDITOR	Masatomo Umitsu, Professor of Department of Geography, Graduate School of Environmental Studies, Nagoya University
	Makoto Takahashi, Associate Professor of Department of Geography, Graduate School of Environmental Studies, Nagoya University
STAFF	Taro Sasaki, Researcher of International Cooperation Center for Agricultural Education, Nagoya University
	Midori Kobayashi, Secretary of Department of Geography, Graduate School of Environmental Studies
SUPPORT	Japan Society for the Promotion of Sciences (JSPS): www.jsps.go.jp
	Nagoya University: www.nagoya-u.ac.jp
DATE OF ISSUE	20th March 2008
PUBLISHER	Nagoya, Japan: Department of Geography, Graduate School of Environmental Studies, Nagoya University: www.geog.lit.nagoya-u.ac.jp
PRINT	Nagoya University Cooperative: http://www.nucoop.jp/

PREFACE

We are pleased to publish the proceedings of the International Conferences about the "Geomorphological comparative research on natural disaster mitigation in the coastal regions of tropical Asia", supported by the Asia and Africa Science Platform Program, Japan Society for the Promotion of Science (JSPS).

We had three conferences in Phuket, Thailand, Ho Chi Min City, Vietnam, and Pattaya, Thailand. The first conference in Phuket was held on August 31 and September 1, 2006, and the topic of the conference was focused on the giant Indian Ocean tsunami disaster. The huge tsunami caused severe damage to the regions surrounding the Indian Ocean, especially the Andaman Sea Coast of Southwest Thailand, Banda Aceh and Nanggroe Aceh Darussalam in Indonesia. In order to share the information about the tsunami overwhelmingly, we met together at Phuket and had fruitful discussion both in the workshop and in the field from the cross-regional and inter-disciplinary perspectives.

The topic of Ho Chi Minh Conference held on August 26 and 27, 2007 was focused on mangroves. Mangrove ecosystem is one of the most important environmental elements in tropical coastal zone. It plays a role not only as the place of nursery for shrimps and fishes but also as the shelterbelt against storm surges, tsunamis or other coastal erosion. It also contributes as a very important life zone for the local people of the coastal region. Moreover, mangrove forest plays a role in CO_2 sequestration to reduce global warming. In the recent years, mangrove areas have been reduced by shrimp culture and developing infrastructure such as industrial zone, residence, port, etc. Mangrove area is also considered to be vulnerable to the effect of sea-level rise. For these reasons, we have planned to organize the International Conference on Mangroves in Ho Chi Minh City, Vietnam.

Pattaya Conference was held on November 3 and 4, 2007 and its main topic was coastal erosion. Coastal erosion is one of the crucial on-going problems in most coasts of Asia. Human activities in drainage basins and coastal plains have been giving the decrease of sediment supply to the coasts due to mainly dam construction, sand mining and irrigation, and relative sea-level rise (subsidence) due to excess ground water extraction, together with the destruction of coastal ecosystems, e.g., deforestation of mangroves.

Each of these conferences was consist of two parts: 1) a workshop on the topics including physical and human aspects of the issue including methodologies such as GIS/RS, and 2) a field excursion to the coastal regions. We think that they provided very good opportunities to exchange our experience and knowledge about those topics each other and brought very fruitful results. This publication is a compilation of some papers presented at the conferences. We expect that the publication will be beneficial for the consideration about the coastal issue in the tropical Asia. As we esteemed the originality of the authors, we only changed and edited the format of the articles.

Finally, we would like to express our sincere thanks to the all participants of the conferences, especially Dr. Charlchai Thanvud at Prince of Songkhla University, Thailand, Dr. Nguyen Van Lap at Vietnamese Academy of Science and Technology (VAST), Dr. Ta Thi Kim Oanh at VAST, Dr. Vien Ngoc Nam, Nong Lam at University, Vietnam, and Dr. Thanawat Jarpongsakul, Chulalongkorn University, Thailand as local organizers of the conferences.

Prof. Masatomo UMITSU (Project Leader, Department of Geography, Nagoya University)
Dr. Makoto TAKAHASHI (Department of Geography, Nagoya University)

CONTENTS

PART III – PATTAYA CONFERENCE [129]

PART I

PHUKET CONFERENCE
ON
TSUNAMI DISASTER

31 August - 1 September 2006

DSM Accuracy Generated by Combining Single-images from IKONOS and QuickBird: A Case Study of Nam Khem Plain, Thailand

Satoshi Ishiguro[1], Toshiro Sugimura[2], Shigeki Sano[3], Yasuhiro Suzuki[4]

[1] *Graduate School of Environmental Studies Nagoya University, Furo-cho, Chikusa-ku, Nagoya-city, 464-8601, Japan*
[2] *Remote Sensing Technology Center of Japan, Tsukuba-Mitsui BLDG 18, 1-6-1 Takezono, Tsukuba-city, 305-0032, Japan*
[3] *Tamano Consultants Co., Ltd., 1-3-15 Aoi-cho, Higashi-ku, Nagoya-city, 464-0004, Japan*
[4] *Nagoya University, Furo-cho, Chikusa-ku, Nagoya-city, 464-8601, Japan*

Abstract

Microtopography is essential for reconstructing water flows resulting from tsunami events and for estimating the resultant damages. In order to construct the microtopography efficiently, it is essential to (1) develop a high-resolution digital surface model (DSM) of the flooded region on the basis of stereo-pair images and (2) quantify the accuracy of the generated model. However, using the stereo-pairs of aerial photographs may not be feasible because tsunamis generally affect coastal regions to a broader spatial extent. Moreover, in many cases, the archives of stereo-pair satellite images of tsunami-affected areas are not satisfactory because such images are captured only when they are requested.

In this study, we attempt to construct a DSM by using two single images captured by the satellites IKONOS and QuickBird for the Nam Khem plain located along the south-western coastline of Thailand, which was affected by the December 26, 2004, Sumatra-Andaman tsunami. These satellites have different satellite azimuths and elevation angles.

The DSM is generated using the stereo pattern matching algorithm. We experiment with template sizes of 11, 15, 19, and 23 pixels, and from the observation of stereoscopic satellite imagery, it is found that the template size of 19 pixels is the most accurate DSM.

For the DSM of the Nam Khem plain, the root mean square error (RMSE) of the elevation is calculated to be 1.32 m.

STUDY AREA AND METHOD

Nam Khem plain, Thailand was chosen as our study area. The reason we chose this area is following: this area is Tsunami disaster area and two single-images existed already which are taken from heterogeneous satellites (IKONOS and QuickBird) for its investigation, and there are aerial photographs we can obtain. With these aerial photographs we carry out photogrammetry for inspecting accuracy of DSM.

The method we adopted for generating DSM is stereo-matching by applying the theory of image matching. Satellite images which we used are IKONOS (resolution of 1 m) and Quick-

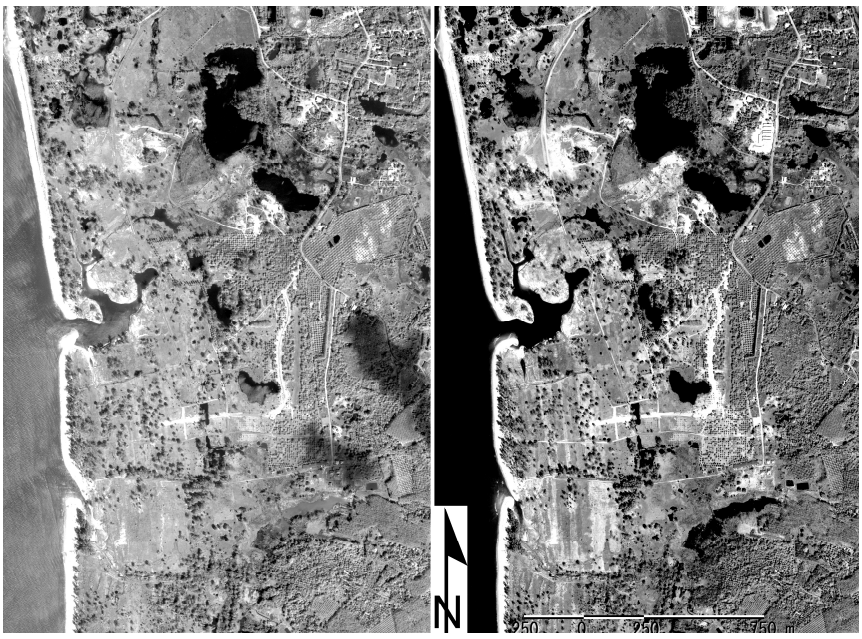

Fig.1 Stereo pair of studied area combined by IKONOS and QuickBird images

Bird (resolution of 0.6 m): thus we had to make same resolution both of the satellite images because by using stereo-matching theory resolution of satellite images should be same. In this study, resolution of the image from QuickBird is changed to 1 m. Moreover theoretically there is no parallax between two images where height is 0 m. Clearly distinguishable 34 objects along shoreline are used for overlapping two images as height 0 m. We used ArcGIS 9 for overlapping two images and to re-sample the image from QuickBird.

RESULT AND ACCURACY INSPECTION

The DSM we generated could explain some artificial mounds, roadside trees, buildings and some beach ridges. For inspecting accuracy of the DSM, we carried out photogrammetry by using a pair of aerial photograph. We measured 159 ground points for inspecting accuracy by using digital photogrammetry and compared with value of DSM. As the result of inspecting accuracy, it emerged that this DSM could be generated with a standard deviation of 1.32 m.

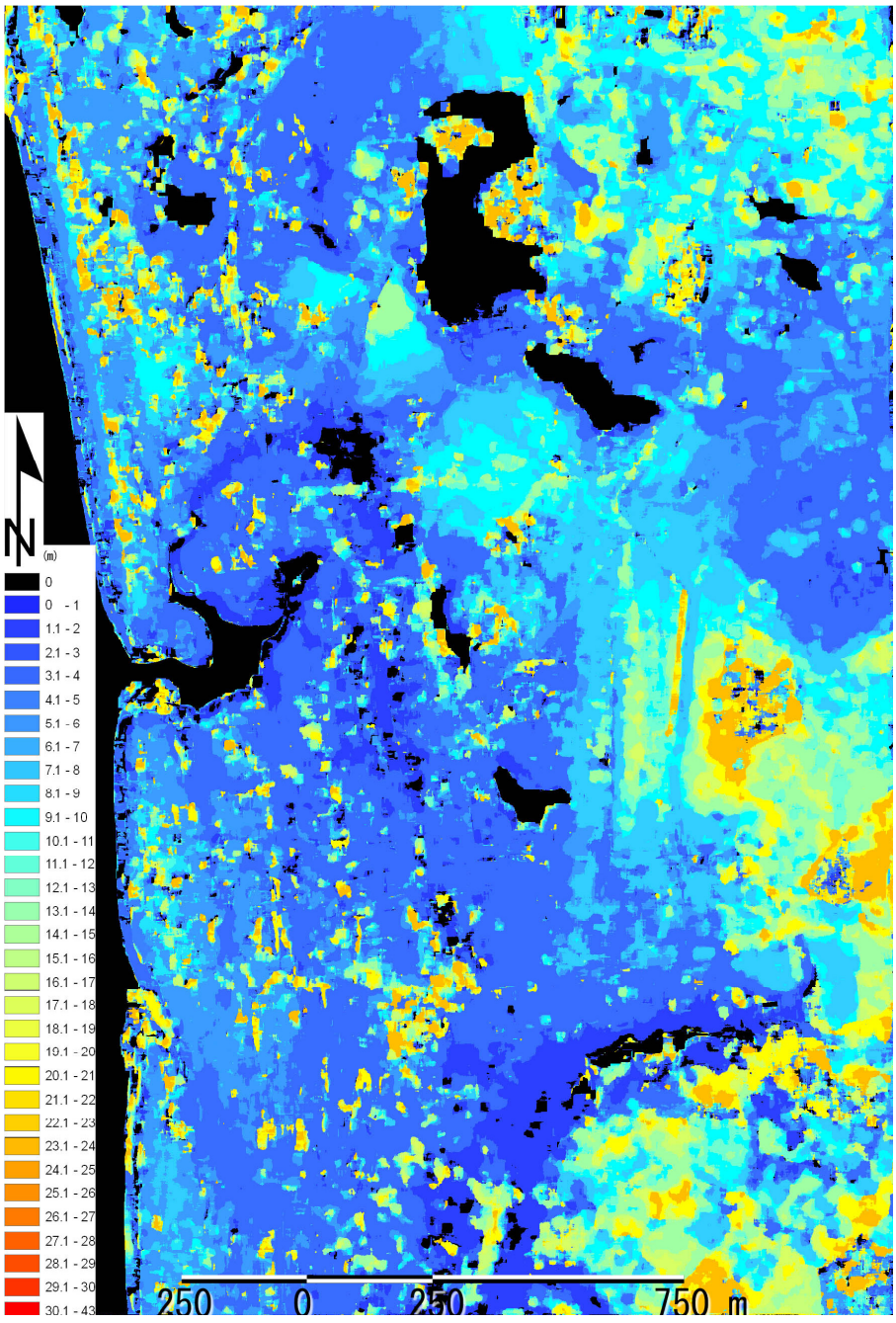

Fig.2 DSM generated by IKONOS and QuickBird images

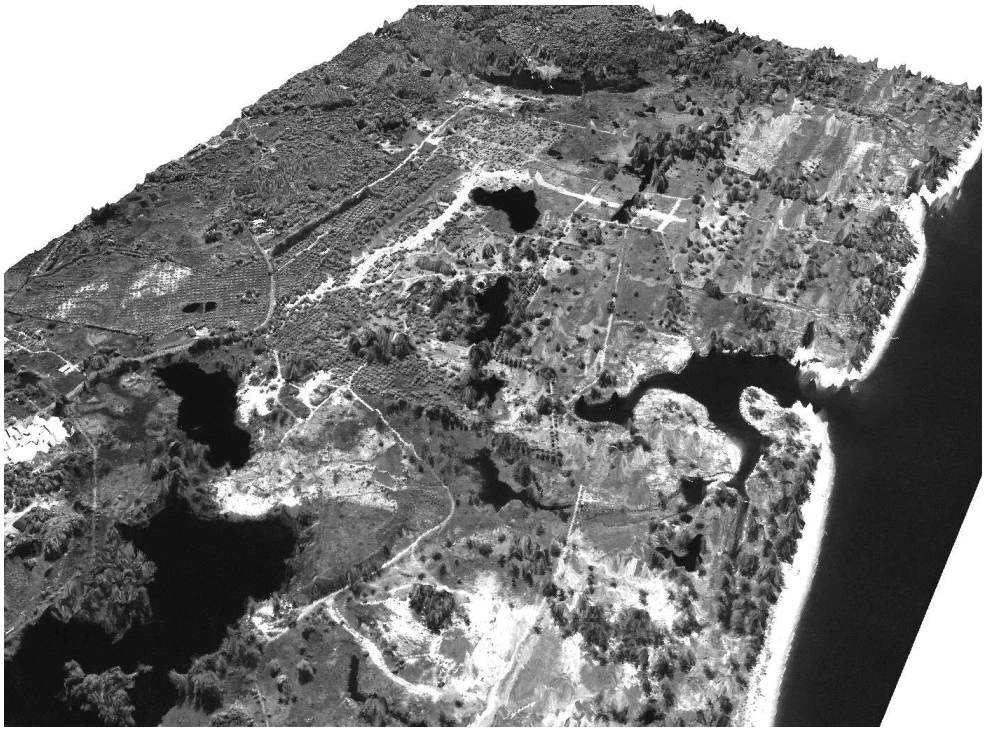

Fig.3 A birds-eye view of overlapping DSM and IKONOS image aspect from northwest toward southeast

PRESUMPTION OF ACCURACY OF DSM MADE FROM TWO SATELLITE SINGLE-IMAGES

We also attempt to make the expression that presumed accuracy, when it used single-images taken from heterogeneous satellites to generate DSMs. As a result, we succeeded in showing the equation by the expression of simple proportion, and only satellite azimuth and satellite elevation are necessary for estimating accuracy as the parameter.

CONCLUSION

We succeeded to generate DSM by using two single-images taken from IKONOS and QuickBird. To inspect the accuracy of DSM, we carried out digital photogrammetry and it emerged that this DSM could be generated with a standard deviation of 1.32m. We also attempted to make the equation to presume accuracy of DSM which generated by using heterogeneous satellites images. The equation can be shown by simple proportion and we need only satellite azimuth and satellite elevation for this equation as the parameter.

References

Thierry Toutin: Comparison of stereo-extracted DTM from different high-resolution sensors: SPOT-5, EROS-A, IKONOS-II, and QuickBird, *IEEE Transactions on Geoscience and Remote Sensing*, 42, 10, 2004

C. S. Fraser, H. B. Hanley and T. Yamakawa: Three-Dimensional geopositioning accuracy of IKONOS imagery, *Photogrammetric Record*, 17(99), pp.465-479, 2002

M. Noguchi, C. S. Fraser, T. Nakamura, T. Shimono and S. Oki: Accuracy assessment of QuickBird stereo imagery, *The Photogrammetric Record*, 19(106), pp.128-137, 2004

H. B. Hanley and C. S. Fraser : Geopositioning accuracy of IKONOS imagery : Indications from two dimensional transformations, *Photogrammetric Record*, 17(98), pp.317-329, 2001

Quick Assessement & Mapping of Earthquake Damage Using Remote Ssensing Imagery: Case Yogyakarta, Indonesia

Suharyadi, Taufik Heri Purwanto

Lecturer in Remote Sensing Department, the Faculty of Geography, Gadjah Mada Univeresity, Yogyakarta - Indonesia

Abstract

On May, 27 2006, an earthquake occurred in Yogyakarta, Indonesia. Earthquake disaster is a quick type natural disaster with occur suddenly and little warning or without warning. The earthquake disaster in Yogyakarta, on May, 27 2006, cause severe property damage and large number of deaths people. Yogyakarta local goverment has not an experienced enough devastating earthquake disaster, even the local goverment close and has an experienced devastating volcanic dissater. One of the active volcano in Indonesia name is Merapi Volcano, located in the norther part of Yogyakarta. The Yogyakarta Province is located in Java Island has short-listed by Government of Republic Indonesia as one of the most volcanic eruption. Because the local goverment has not an experienced to face the disaster, there is no preparation to face the earthquake disaster. When the dissater occurred, local goverment lack of spatial information related to the building damage and its residents. Spatial information related to the disaster location are needed for emergency response and recovery/ rehabilitation after the disaster. One of the spatial data are needed for the activities of emergecy response and recovery are a map of building damage. The objective of the research is to (a). quick response activities; quick response activities is to provide spatial information related to the disaster location, victim's needs and aid distribution for the volunteers. (b). quick assessment and mapping of the damage inflicted by this earthquake and to develop database to make recommendations in recovery phases.

Triple C method is used to find out the first activities, and the second activities use combination of remote sensing technique and field survey. The second methode in the research is a combination of remote sensing interpretation, and short interview including quick assessment for the building damage, and plotting building position into imagery. Primary data are IKONOS imagery May 28, 2006, a day after the disaster.

The results of the research are maps of building damage and detail database of each building. The map of building damage consist 3 classes, include low, medium, and high damage. The level of damage base on government's damage classification (FORM-1), and building suitability assessment by Civil Engineering Gadjah Mada University. The building damage map figure out the damage in Yogyakarta after earthquake. The database consist detail tabular information of building characteristics and its residents.

Key words: earthquake, quick assessment, building damage

INTRODUCTION

During the last five years Indonesia have to face a lot of natural disasters, one of the natural disaster seem occurred continuously are earthquake disasters. The disaster is a hazard because most of the disaster occurred in the human live areas.

Developing countries are more vulnerable to hazards because of their increasing rate of development and urban growth. The lack of proper disaster management leads to increase in risk in more densely populated cities. Most of the growth in terms of civil structures and infrastructure will concentrate in the developing countries for the next few decades. These countries are already loaded with various urban problems like population growth, urban sprawl, building density and lack of financial strength. The risk is continuously increasing in these countries at an alarming rate. The sole purpose of all mitigation processes in the world is to save human lives and property from the impact of natural disasters (Sokhi, 2000 in Khatsu, 2005).

When we live in Indonesia, it is impossible to live in a disaster free environment but it is possible to reduce the impact of disasters by proper risk management strategies. The pre-planned mitigation activities not only save the human lives but also reduce the potential effect of disasters. The proper disaster management strategy at initial planning level improve the overall functioning of the areas and help us to face the ill effects of disaster.

Earthquakes can create disasters of high magnitudes when they hit human live areas of large population and infrastructure. Damage of building and its infrastructure occurred in dense settlement during the

disaster. A lot of victim has to be helped in short time, and some time its locations in remote area. To face the disaster, we should do quick response activities, especially to save the victims and provide aid logistics.

On May, 27 2006, an earthquake occurred in Yogyakarta and its surrounding. Earthquake disaster is a quick type natural disaster with occur suddenly and little warning or without warning. The earthquake disaster in Yogyakarta, cause severe property damage and large number of deaths people. Yogyakarta local goverment has not an experienced enough devastating earthquake disaster, even the local goverment close and has an experienced devastating volcanic eruption. One of the active volcano in Indonesia name is Merapi Volcano, located in the norther part of Yogyakarta. The Yogyakarta Province is located in Java Island has short-listed by Government of Republic Indonesia as one of the most volcanic disaster. Because the local goverment has not an experienced to face the disaster, there is no preparation to face the earthquake disaster. When the dissater occurred, local goverment lack of spatial information related to the building damage and its residents. Spatial information related to the disaster location are needed for emergency response and recovery/ rehabilitation after the disaster. One of the spatial data are needed for the activities of emergecy response and recovery are a map of building damage.

OBJECTIVES

The objective of the research is to:

(a). Develop quick response activities to face an earthquake disaster in Yogyakarta and its surrounding. Quick response activities are to provide spatial information related to the disaster: location, victim's needs and aid distribution for the volunteers.

(b). Develop quick assessment and mapping of the damage inflicted by this earthquake and to developed database to make recommendations in recovery phases.

METHOD

Material used:

- Ikonos imagery, May 28 2006
- Topographic map

Equipment used:

- GPS
- Digital camera
- Image map
- Questioner

Triple C method is used to find out the first activities. There are three components to support the activities. These components are community, communication, and cartography. Community are victim earthquake or persons were injured who need help from the volunteer; communication are communication facilities who create direct communication between victim and volunteers, and cartography is a map that presenting the location of victim, victims need, and aid distribution. In general, the triple C method is shown in

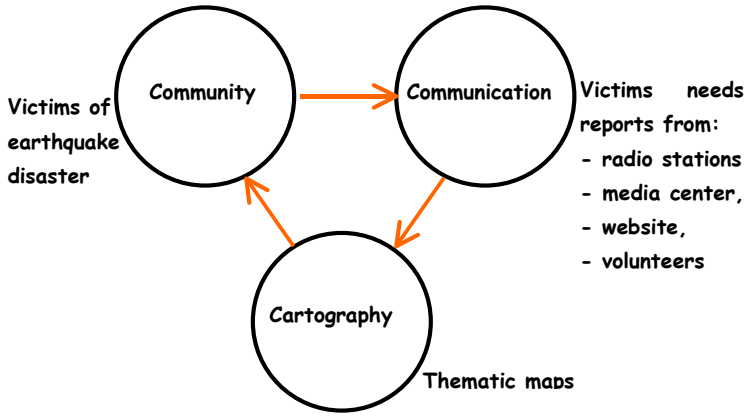

Figure 1. Triple C Method (Suharyadi, 2006)

figure 1 below.

The method to reach the second activities is a combination of remote sensing technique and field survey. Primary remote sensing data are IKONOS imageries May, 28 2006, a day after the disaster. The technique to interpretation the building damage was plotting building position into imagery in the field and short interview including quick assessment for the building condition. Plotting building position used GPS in the center of building researcher.

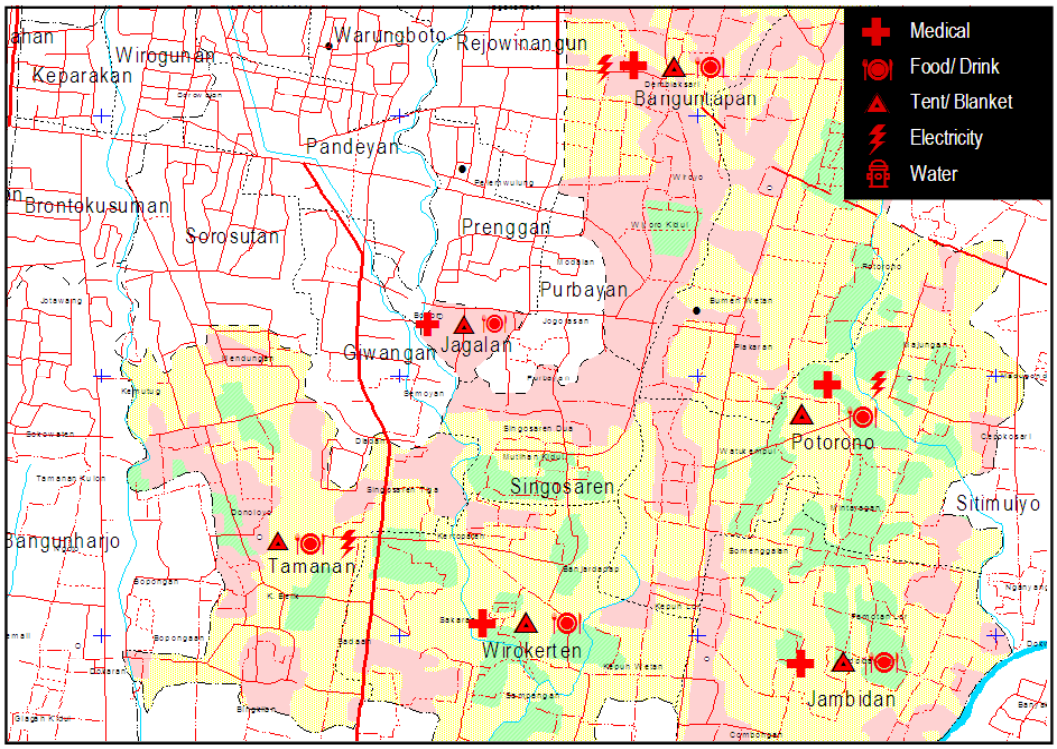

Figure 2. Victim's need map in Banguntapan Sub District

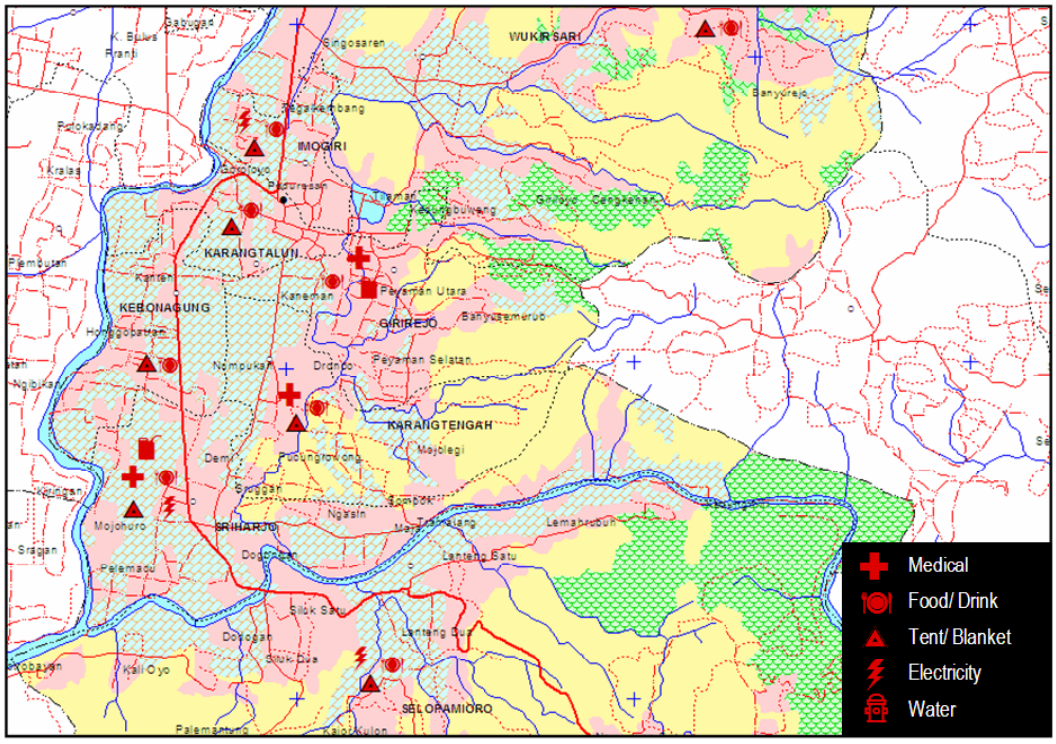

Figure 3. Victim's need map in Imogiri Sub District

RESULT

The results of these activities in brief are:

1. Spatial Information related to disaster
   Developed quick response activities to face an earthquake disaster in Yogyakarta and its surrounding.

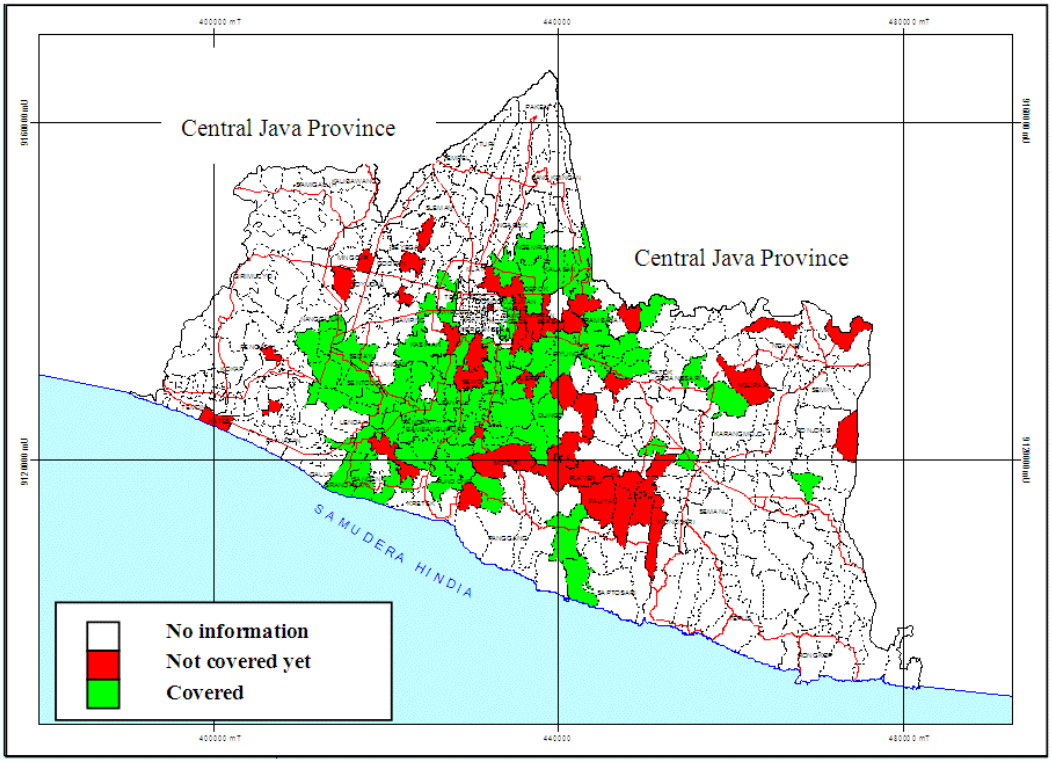

Figure 4. Aid distribution map of Yogyakarta Special Province

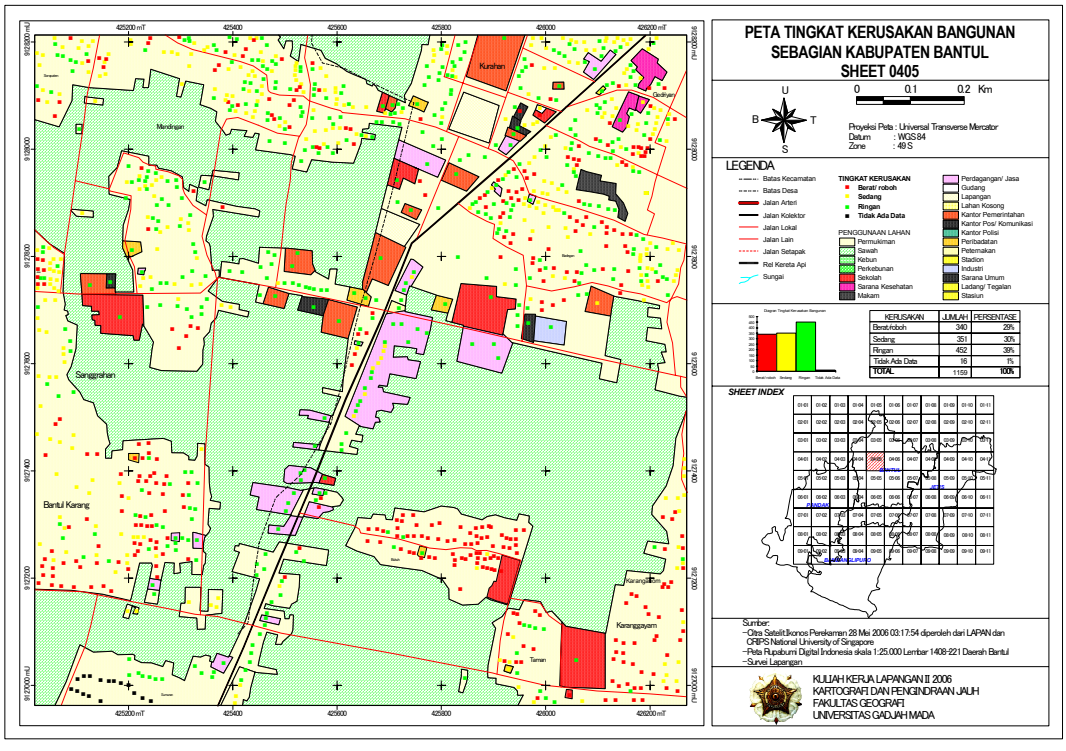

Figure 5. Example of building damage map

Quick response activities are to provide spatial information related to the disaster, the victim, and aid distribution from the volunteers.

The spatial information have been updated 3 times a day in the period of quick response activities, include: early morning, mid day, and in the afternoon. The spatial information consists of: location of damage, location of victims, victim's need, and persons were injured, and aid distribution from the volunteers.

The forms of spatial information are: hard copy form (hard copy map), softcopy format, and Web-GIS format. Example of the maps were enclosed in figure 2, figure 3.

Based on the victim's need map in Banguntapan Sub District (enclosed in figure 2), it can be seen that, on 2 June 2006, in the morning, the victims in Banguntapan Village need electrical power, drugs, food, and tent. The need of victims in Jagalan Village was electrical power; tent and food, while in Tamanan village were tent, food and electrical power. The same characteristic also figure out at figure 3 (enclosed map) in Imogori villages the victim's need were electrical power, tent and food, while in Karangtalun village only require tent and food. The condition of victim's need usually differ in the morning, afternoon and evening because some areas have been helped already by the volunteers.

The spatial information about victim's need of the earthquake disaster areas was provided to the volunteers who come to location of disaster, and they used the spatial information as guidance in pointing aid and help. By using spatial information, updated continuously, the distribution of aid to the victim was expected better distributed and it reduced overlap of aid.

To know the distribution coverage which have been executed by volunteer can be seen in figure 4 (aid distribution map). From the map, which creates on 2 June 2006, there were some areas which have received the aid and some districts have not received yet.

2. Spatial database of building damage

The map consists of building damage and its attribute. The building damage is classified in three classes, low damage, medium, damage, and, high damage. The level of damage base on government's damage classification, Table -1 (enclosed in appendix-1), and building suitability assessment by Civil Engineering Department Gadjah Mada University. The map of building damage figure out the damage in Yogyakarta after earthquake. The database consist detail tabular information of building characteristics and its residents. The example of the map and its attribute is enclosed in figure 5.

Developer quick assessment and mapping of the damage inflicted by this earthquake and to develop database to make recommendations in recovery phases. Base on the map, the local government was possible to estimate budget for rehabilitation and reconstructions of damage housing. The method have good result and to reduce error estimation of housing damage.

CONCLUSION

Spatial information related to the disaster: location, victim's needs and aid distribution for the volunteers can be developed using triple C Method. The form of spatial information is: hard copy form (hard copy map), softcopy format, and Web-GIS format. The information can be used as a tool to guide the volunteers.

Level of housing damage in the disaster areas which be inflicted by the earthquake can be develop using high spatial resolution of remote sensing imageries and minimal field survey. The form of information is in spatial form (map form). The damage maps consist of level of housing damage, and detail information related to its residents. The spatial information related to the damage can be used as a recommendation in recovery phases.

References

Khatsu, Petevilie. 2005. *Urban Multi-Hazard Risk Analysis Using GIS and Remote Sensing: A Case Study of a Part of Kohima Town, India*. ITC, The Netherlands

Suharyadi. 2006. *Quick assessment of building damage after earthquake disaster*. The Faculty of Geography, Gadjah Mada University, Yogyakarta

Acknowledgements

I take this opportunity to thank to Professor Makoto Takahasi, Ph.D., from The Faculty of Geography, Nagoya University Japan for supporting us to come in this conference and providing facilities during the conference. I would like to express my heartfelt gratitude to my friend in "Geography Base Camp for Disaster Aid" for necessary support and motivation for these activities. Finally the most important support, inspiration, and encouragement that never be forgotten, I dedicate this work to my colleagues and friends in Yogyakarta.

Table 1. The level of damage base on government's damage classification

1. Building Identity : Sheet _____ ID _____
2. Owner/ Tenant :
3. Location Identity :
   Dusun/ Kampung : _____
   RT/RW : _____
   Village : _____
   District : _____
4. Building Function :
   - ☐ House
   - ☐ Commercial
   - ☐ Gov./Private Office
   - ☐ Health Facility
   - ☐ Education
   - ☐ Tourism
   - ☐ Industrial
   - ☐ Public Facility
   - ☐ _____
5. Number of Floor :
   ☐ 1 ☐ 2 ☐ 3 ☐ ___
6. Building Structure Material :
   - ☐ Iron
   - ☐ Reinforced concrete
   - ☐ Brick
   - ☐ Wood
   - ☐ Bamboo
7. Building Roof Material :
   - ☐ Cement
   - ☐ Cement Tile
   - ☐ Clay Tile
   - ☐ Asbestos tiled roof
   - ☐ Iron sheeting
8. Level of Damage :
   - ☐ High/ Collapse
   - ☐ Medium
   - ☐ Low

Notes :

The Impact of Java Tsunami 17th July 2006 to the South Coast of Java Island – Indonesia

Djati Mardiatno[1, 3], Sutikno[2], Sunarto[3], Franck Lavigne[4], Johann Stoetter[1]

[1]Institut of Geography, University of Innsbruck, Innsbruck-Austria
[2]Faculty of Geography Gadjah Mada University, Yogyakarta-Indonesia
[3]Research Centre for Disaster, Gadjah Mada University, Yogyakarta-Indonesia
[4]University of Paris I, Pantheon-Sorbonne, Paris-France

(contact: mardiatno@yahoo.com)

Abstract

The last significant tsunami in Indonesia was happened in south Java on July 17, 2006. Although the magnitude was less than Banda Aceh tsunami in 2004, that event still caused seriously impact in the destructed area. The most serious damage was found particularly in Pangandaran beach and surrounding area. In Central Java Province, almost all of coastal area was also attacked by that tsunami.

The aims of this research are to observe the tsunami wave characteristics on the land and the tsunami impact to the attacked areas. Several areas were selected and assessed using rapid survey technique to know the tsunami action on the land and the damage objects in each area. Furthermore, the result was also directed to illustrate the damage level and certain problem in the environmental context.

Based on the field survey result, it was found that run-up height reach more than 5 meters in several areas. Flowdepth varied between 1 meter and 2 meters and the inundation could reach more than 500 m into the land. Regarding to the building, almost all of the semi-permanent building was completely destroyed by tsunami. Most of them were located near to the shoreline, even less than 200 meters. Generally, permanent buildings were still in existence, although they experienced variously damage. The tsunami action also destroyed other objects, such as fisherman's boats and paddy field areas. Most of the boats in the beach were shifted up far to the land and almost all of them were totally broken. At certain areas, tsunami also inundated paddy field areas and could leave the salt content problem in the soil body there. More than 600 people dead caused by that tsunami with the highest number (413) can be found in Ciamis regency. With regard to the tsunami earthquakes phenomena, it is essential to create appropriate tsunami mitigation measures in south Java for reducing total loss when tsunami takes place again in the future.

Keywords: *flowdepth, run-up, tsunami wave, damage, Java Island*

INTRODUCTION

The South coastal area of Java Island is a part of the Indonesia archipelago that faces directly the subduction zone between the India-Autralian Plate and Eurasian Plate. The subduction zone is situated in the Indian Ocean. Collision between these plates result in the endogenic activity in that zone being very dynamic. As a consequence, this area is very vulnerable to earthquakes. If earthquakes take place under seawater and there is a vertical dislocation in the seafloor, it will result in tsunamis.

In Indonesia, tsunami magnitude usually is varied between 1.5 and 4.5 (Imamura scale), maximum wave height is in a range 4 to 24 meters and wave penetration in to the land is in a range 50 to 200 meters from the shoreline. Based on the "Katalog Gempa" (Earthquake Catalogue) year 1629-2002, tsunami occurred in Indonesia 109 times, i.e. one was caused by landsliding, 9 times were triggered by volcanic eruption and 98 times were caused by tectonic earthquake (http://www.bmg.go.id). Latief et al (2000) noted that during the period 1600-1999, 105 tsunami have occured in Indonesia and 90% of them were caused by earthquakes.

The last tsunami in Indonesia was happened in south Java on July 17, 2006 (Figure 1). It was triggered by an earthquake Mw=7.7 located in 34 km of depth (source: USGS). That event was the second significant tsunami in South Java. The first was in 1994, which struck Banyuwangi region (East Java), triggered by an earthquake Ms=7.2 (Maramai and Tinti, 1997) or Mw=7.8 (USGS). Although the magnitude of tsunamigenic earthquake in 2006 was less than Banda Aceh tsunami in 2004, that event still caused seriously im-

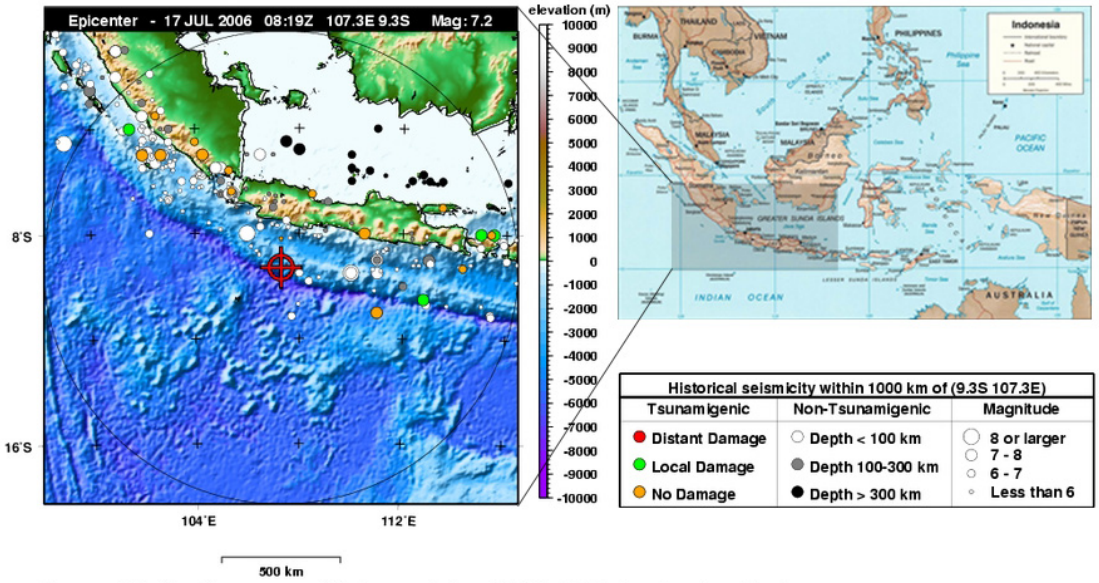

Source: http://ioc3.unesco.org/itic/images/upload/17July2006_Java.jpg (modified)

Figure 1. Epicentre location that triggering tsunami 17 July 2006

pact in the destructed area. The most serious damage was found particularly in Pangandaran beach and surrounding area. In Central Java Province, almost all of south coastal area was also attacked by that tsunami.

The aims of this research are to observe the tsunami wave characteristics on the land and the tsunami impact to the attacked areas. Several areas were selected and assessed using rapid survey technique to know the wave action on the land and the damage objects in each area. Furthermore, the result was also directed to illustrate the damage level and certain problem in the environmental context.

METHOD

This research used survey method, i.e. the analysis is based on the field survey data. Field survey was begun one day after tsunami happened, i.e. on July 18 until one week after for the first step. The second step was carried out on July 31 until 4 of August. First survey was carried out by Laboratoire de Geographie Physique/LGP (Paris-France)-UGM/PSBA (Yogyakarta-Indonesia) team and the UGM/PSBA-Geographie Innsbruck team conducted the second survey. Topographic maps (Rupabumi Indonesia/RBI maps) scale 1:25.000 and some images from aerial photos and high resolution satellite images were used in conducting this survey. Some equipments were also used in this survey, i.e. handheld GPS, Geodetic GPS Trimble, range finder (Laser ACE ® 300), geological compass and digital camera.

The first step survey was emphasized to observe the wave characteristic and damage objects, for instance run-up height, flowdepth distribution on the land, inundation and the types of damage objects. Then, the second step survey was directed to complete data from the first survey and emphasized more on damage assessment. Short visit to local authorities was also carried out to collect more data about damage and estimated fatalities.

The survey covered part of the coastal area destroyed by tsunami wave. Administratively, the survey covered several regencies (Kabupaten/Kota) as follow, i.e. Ciamis, Cilacap, Kebumen, Purworejo, and Bantul. Otherwise, several areas also represent the different kind of area, for instance tourism area, settlement area and agricultural area.

RESULTS AND DISCUSSIONS

Based on the field survey result, there were some variations in wave height on the land. Run-up height on the coast could reach more than 5 meters and water height on the land varied between 1 meter and 2 meters. Otherwise, wave inundation could reach more than 500 m into the land. Other team from Coastal Dynamic Research Agency (BPDP-BPPT) reported that the highest wave was 4.6 metres, founded in Widarapayung, Cilacap (Kedaulatan Rakyat, 2006). Table 1 shows the variation of run-up height, flowdepth and the inun-

Table 1. Field measurement of some tsunami wave characteristics in some selected areas

Location	x (UTM)	y (UTM)	Tide level from m.s.l.	Flow-depth	Run-up height (above m.s.l.)	Reference point	Dist. (m)	Flow dir	Additional comments from eyewitnesses
Cimerak	222038	9136696	-0.6	2.5					
(Bulakbenda)	222652	9137464	-0.6	4.0					
Pangandaran	223910	9143605	-0.6		10.4	Pylon	89		Breaking on the road.
(Batukaras)	224019	9142803	-0.5	1.9	5.5	Tree	121		
Pangandaran	228007	9148960	-0.05	1.4					Sound like bomb and/or like
(Batu hiu)	228062	9149163	-0.25	1.4					toppled trees; sea withdrawal.
	228162	9148945	-0.3	1.5					
Pangandaran	233658	9150479	-0.3	0.8					
(Karangtirta)	234080	9050358	-0.4	1.2					
	234413	9150371	-0.3	2.7					
Pangandaran	240051	9149490	0.4	3.9					3 waves; sea retreat, sound like
(Pananjung)	240184	9149380	0.4	5.8					bomb; earthquake slightly felt.
	240603	9149515	0.4	0.5		Wall			
	241325	9147732	-0.15		4.5	Tree			
	241404	9148280	0.1		4.1	Wall	50		
	241494	9147893	-0.1		4.6	Tree			
	240089	9149393	-0.1		6.4	Tree			
	240205	9149365	0	3.8	7.4	Wall			
Pangandaran	245864	9150880	-0.2		9.2	House			Sound like bomb; earthquake
(Keboncarik)	245864	9150886	-0.2		8.5	Tree			slightly felt; 3 main waves; Breaking of the 2nd wave.
Pangandaran	246721	9150820	-0.3	3.7		Wall			3 waves; 1st wave at 16:15; 2nd
(Karangsari)	246651	9150805	0.4	5.1	8.4	Tree	10	N178	wave 8m high before breaking;
	247021	9150777	0.2	0	7.9				breaking of the 2nd wave;
	246910	9150859	0.2	3.1	6.8	Wall			backwash parallel to the shoreline N238 to N30.
Cilacap	289181	9149800	-0.4		2.9	PLTU			Earthquake slightly felt; sea
(city)	289181	9149629	-0.4		3.7	PLTU			retreat.
Cilacap	299654	9149309	-0.35	5.0					
(Sodong)									
Cilacap	308108	9148743	-0.3	1.2					3 waves: arrival time around
(Widarapayung)	308440	9148939	-0.25	3.5					16:30; wave broken on the beach;
	308597	9148693	-0.3	4.0					slight backwash between the waves
Cilacap	320609	9146716	-0.3	1.5					Sea withdrawal; unusual sound of
(Jetis)									sea waves.
Kebumen	322425	9145916	-0.3	3.5					Sound like bomb (twice); 3 waves;
(Ayah)	322867	9145913	0.4		6.7	Tree			wave broken on the dyke
	327741	9141227	-0.2	1.4					
Kebumen	330922	9149140	0.45	3.4	5.0				
(Karangbolong)	330990	9142142	-0.3	4.6					
	330926	9142156	-0.3	2.0					
Kebumen	331558	9142166	-0.05	0	3.9	Dune			Wave broken on the beach.
(Puring)	331205	9142261	-0.1	3.5					
	331268	9142403	-0.1	2.0					
Kebumen	343556	9140262	-0.5		6.7				
(Ketawang)	342472	9140381	-0.1	4.0					
	343455	9140306	-0.1	2.2					
Purworejo	378139	9132210	-0.6	0	6.7	Dune	32	N270	Sound like bomb; earthquake not
(Keburuhan)	380163	9131677	0.2	1.7					felt.
	380188	9131860	0.2	2.7	3.0				
Bantul	413739	9116926	0.5	1.5					
(Pandansimo)									
Bantul	418958	9115022	-0.5		3.7		75	N350	Sound like bomb.
(Samas)									
Bantul	425728	9112977	-0.4		5.5	Riverbank			Sound like bomb; 3 waves almost
(Parangtritis)	426151	9112904	-0.75		4.6	Sanddune	170	N11	simultaneous, after 16.00; no sea
	426780	9112807	0.4	2.4					withdrawal; since the tsunami
	425508	9113054	-0.4		4.2			N340	event, sedimentation problems due to sand

Note: data collected by two teams (Laboratoire de Geographie Physique/LGP and UGM/PSBA-Geographie Innsbruck)

dation distance from the shoreline. On the other hand, the area condition before and after tsunami can be seen in Figure 2. It is clear as showed in Figure 2 that tsunami debris will be useful in determining wave inundation distance. Most of the debris was deposited at the boundary of inundating water.

Concerning to the damage, Table 2 shows the number of damage objects (buildings, boats and land) caused by 2006 Java tsunami. Almost all of the semi-permanent building was completely destroyed by tsunami. Refer to Papathoma Tsunami Vulnerabiliy Assessment (PTVA) model by Papathoma *et al*. (2003), it is appropriate that high and medium vulnerable buildings, i.e. partly permanent or permanent buildings with moderate strength, will have serious, even completely damage if tsunami occur. Most of them were

Figure 2. The images showing selected area condition before and after tsunami

Table 3. South Java tsunami 2006 casualties

No	Locations	Dead	Injuries	Missing	Refugees
West Java					
1	Ciamis	413	379	15	4190
2	Tasikmalaya	63	103	-	1650
3	Garut	2	2	-	-
Central Java					
1	Cilacap	157	8	10	306
2	Kebumen	10	24	8	581
3	Purworejo	2	1	-	-
Yogyakarta					
1	Bantul	-	3	-	-
2	Gunungkidul	3	-	-	-

Source: Bakornas PBP (data per 1 August 2006)

located near to the shoreline, even less than 200 meters. Generally, permanent buildings were still in existence, although they experienced variously damage. For boats, most of them parked in the beach were shifted up far to the land and almost all of them were totally broken. At certain areas, tsunami also inundated paddy field areas and could leave salt content problem in the soil body. Marine sand layer was depos-

Figure 3. Type of damage objects caused by tsunami 2006

Table 2. Damage objects caused by tsunami 2006

No	Locations	Buildings (permanent & semi permanent)	Boats	Land (paddy field/ garden/forest)
West Java				
1	Ciamis	1997	1239	137 ha
2	Tasikmalaya	231	30	*n/a*
3	Garut	10	-	*n/a*
Central Java				
1	Cilacap	224	1605	463.7 ha
2	Kebumen	121	606	*n/a*
3	Purworejo	-	90	*n/a*
Yogyakarta				
1	Bantul	*n/a*	*n/a*	*n/a*

Source: Bakornas PBP (data per 1 August 2006); n/a: data not available

ited in the soil surface and destroyed some productive vegetations, especially paddy. Figure 3 shows the type of damage objects.

Regarding to the number of casualties, more than 600 people dead caused by that tsunami (Table 3). The highest number of deadly people can be found in regency of Ciamis (413), followed by Cilacap (157) and then Tasikmalaya (63). Ciamis had the highest victims because this regency received direct effect of tsunami (especially in Pangandaran and Batu Hiu) while in Cilacap was caused by a number of people collected snails in the coast at that time (*personal communication with some local people*). Fortunately, the presence of Nusakambangan Island in the front of Cilacap city avoid that area from the worse effect to tsunami.

Tsunami in 2006 also affected some morphological features in the coastal area. Figure 4 shows some morphological changes caused by that tsunami. That changes was performed in the short time and they might be used in identifying rapid geomorphological processes during the event. Refer to Oya (2001), predictions about tsunami disaster can also utilise physical properties of landform. It is reasonable that rapid morphological changes after tsunami will be very useful in predicting the impact of 'future' tsunamis.

PROSPECTIVE MITIGATION MEASURES

Very little discussion was given to the threat of tsunami along coastlines where historical records are minimal (Bryant, 2005). However, the records availability will be useful in the area which are situated adjacent

Figure 4. Some morphological changes caused by tsunami 2006

to tsunami sources. This case could also be found in South Java where only two significant tsunamis (1994 and 2006) provided very good records. Both events presented the similar phenomena of specific tsunamis, which had been well-known as 'tsunami earthquakes'.

As in 1994, Java tsunami 2006 was fairly strong although the magnitude of the tsunamigenic earthquake was not big enough to justify such a large destruction and so many victims. Some people felt no strong earthquake, therefore it will be necessary to consider more about tsunami warning system in south Java. Fortunately, that event was in the day time, quite different with 1994 tsunami where the event was in the evening. Moreover, especially in Pangandaran resort area, the holiday period was over so that only a few people visited that place.

Tsunami 2006 took place when the installation of tsunami early warning systems (TEWS) by the national government had not reached south Java area. On the other hand, only a few people recognised about TEWS. Based on rapid interview with local people, TEWS should be established by considering to the common knowledge of local people. Traditional sign will be necessary, i.e. using alarm sounded by the drum made from bamboo or wood which is struck to sound it. Regarding to tsunami earthquake, it is necessary to highlight the importance of "composite-indicator" beside 'strong earthquake' as the first warning. Two significant tsunamis in South Java (1994 and 2006) provided evidence that some eyewitnesses didn't feel strong groundshaking before tsunamis. Other team (Widjo Kongko *et al*.) also presented similar result that Java tsunami 2006 was not initiated by a strong earthquake.

Hazard is an inescapable part of life and it is best viewed as a naturally occurring or human induced process or event with the potential to create loss, i.e. a general source of danger (Smith, 1996). South Java area has complex landform and will be developed by the national government to increase its economic growth. The government has had a long planning to develop this area by road development as the first step. Furthermore, the towns and districts in this area will gain their economic condition and give the multiplier effect to the local people, and also can invite people from the other places. On the other hand, tsunami is the real threat within this area, hence the development planning should consider the hazard potential from the ocean, e.g. tsunami, to minimize risk in the future.

CONCLUSION

More than 600 people became tsunami victims. Thousands buildings, boats and hundreds square meters land had been damaged. Many fatalities caused by tsunami 17 of July 2006 had increased people awareness to the hazard potential from the ocean. At present, they understand that their regions are very vulnerable to tsunami.

Tsunami is a real threat along the south coast of Java Island. Therefore, it is essential to create a systematic tsunami mitigation program for reducing total loss in that area when tsunami occurs again in the future, e.g. by using traditional sign for TEWS. It is also necessary to consider the "composite-indicator" beside 'strong earthquake' as the first warning. Both tsunamis, i.e. in 1994 and 2006 proved that some eye-witnesses slightly felt earthquakes prior to tsunamis.

Acknowledgement

This research can be realized by the support from Research Centre of Disaster (PSBA) Gadjah Mada University Yogyakarta-Indonesia, University of Innsbruck-Austria and Tsunarisque Project- France. A special thank is provided to the Head of PSBA in supporting all materials and equipments which can be used in this research.

Notes from the authors:

Because of the late publication, some part of this article, i.e. field measurement results, has been published in Natural Hazard and Earth System Science (NHESS) as follow: Lavigne, F., Gomez, C., Gifo, M., Wassmer, P., Hoebreck, C., Mardiatno, D., Prioyono, J. and Paris R., Field Observations of the 17 July 2006 Tsunami in Java. *Natural Hazard and Earth System Science*, 2007, **7**(1), 177 - 183.

References

Bakornas PBP, 2006. *Laporan Perkembangan dan Penanganan Bencana Gempabumi dan Tsunami di Jawa Barat, Jawa Tengah dan DI Jogjakarta*, 1 Agustus 2006 at 15.00 WIB, Jakarta.

Bryant, Edward, 2005. *Natural Hazard*, Second Edition, Cambridge University Press, Cambridge.

Kedaulatan Rakyat, 2006. *Tsunami Tertinggi di Cilacap*, 29 Juli 2006, page 1 and 24.

Latief, H., Puspito, N.T. and Imamura, F., 2000. Tsunami Catalog and Zones in Indonesia, *Journal of Natural Disaster Science*, **22**(1), 25 - 43.

Maramai, A. and Tinti, S., 1997. The 3 June 1994 Java Tsunami: A Post-Event Survey of the Coastal Effects, Natural Hazards, **15**(1), 31-49.

Oya, Masahiko, 2001. *Applied Geomorphology for Mitigation of Natural Hazards*, Kluwer Academic Publisher, London.

Papathoma, M., Dominey-Howes, D., Zhong, Y. and Smith, D., 2003. Assessing Tsunami Vulnerability, an Example from Heraklio, Crete. *Natural Hazards and Earth System Sciences*, **3**(5), 377 - 389.

Smith, Keith, 1996. *Environmental Hazards Assessing Risk and Reducing Disaster*, Second Edition, Routledge, London.

VSI, 2006. *Pengenalan Tsunami* (*http://merapi.vsi.esdm.go.id/?static/tsunami/pengenalan.htm*), retrieved on 22nd July 2006, at 13.30.

Widjo Kongko, Suranto, Chaeroni, Aprijanto, Zikra and Sujantoko, 2006. Rapid Survey on Tsunami Jawa 17 July 2006, available online at: *http://ioc3.unesco.org/itic/files/tsunami-java170706_e.pdf*

Effects of Landforms on the Tsunami Flow in the plain of Banda Aceh, Caused by the Giant Earthquake off Sumatra, Indonesia

Masatomo Umitsu [1*], Charlchai Tanavud [2], Boonrak Patanakanog [3]

1: Department of Geography, Nagoya University, Nagoya 464-8601, Japan
2: Faculty of Natural Resources, Prince of Songkhla University, Hat Yai, Songkhla 90112, Thailand
3: Soil Survey and Land Use Planning Office, Land Development Department, Phaholyothin Road, Chatuchak, Bangkok 10900, Thailand

** Corresponding author: Masatomo UMITSU*
Tel: +81-52-789-2270, Fax: +81-52-789-3254, E-mail: umitsu.m@gmail.com

1. INTRODUCTION

The catastrophic tsunami accompanying the giant earthquake off Sumatra on December 26, 2004, inundated and caused severe disaster in the coastal lowlands of northern Sumatra, Indonesia. In this paper, we will describe and discuss how coastal plain landforms affected tsunami flow on the coastal plains of Banda Aceh in Sumatra. (Fig.1).

2. REGIONAL SETTING

The Band Aceh coastal plain is located along the lower reaches of the Aceh River. It is situated in a graben formed by movement of the Sumatra Fault (Fig. 2). The coastal plain is characterized by deltaic and tidal lowland in the central and western parts, and by distinct rows of beach ridges in the eastern part. Elevation of the plain is 1-3 meters high above sea level in the central and western parts, except the higher parts of natural levees along the present and abandoned channels. The eastern coastal area is also low-lying, but there is a small sand dune along the coast and rows of beach ridges, 1-2 m above the swales, exist in the inner area. Shrimp and fish ponds are formed in tidal lowlands of the central and western parts of the plain. Deltaic lowland and beach ridges are occupied by houses, and the Banda Aceh urban area is located on the deltaic plain in the central part of the coastal plain (Fig.3). Calculated high and low tide levels of the

Fig. 1. Map showing the location of the Banda Aceh

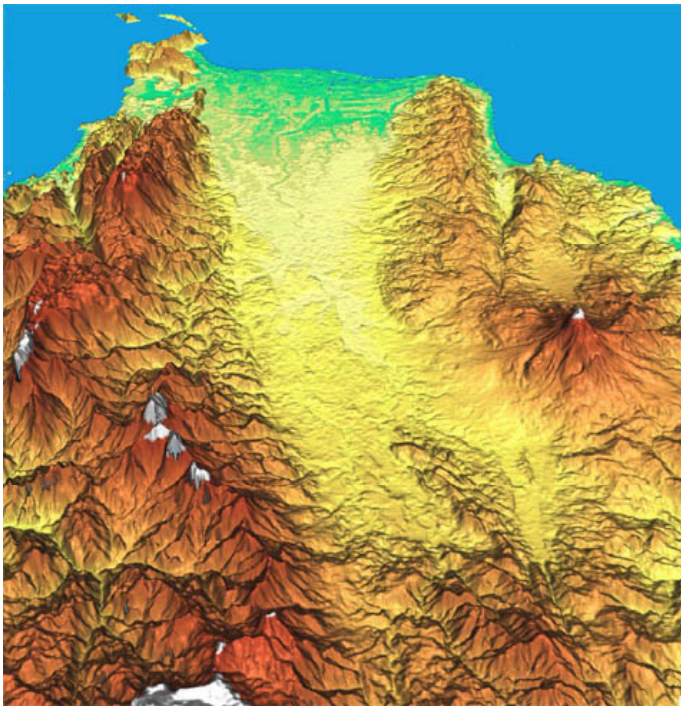

Fig. 2. 3D view of the Banda Aceh coastal plain

Fig.3 Destroyed buildings about 200 m inland from the coast

Fig.4 Destroyed buildings in the central part of the plain about 1.5 km inland from the coast

Fig.5 Destroyed buildings in the western part of the plain about 2 km inland from the coast

Fig.6 Destroyed building in the eastern part of the plain about 1.5 km inland from the coast

Oleelheue near Banda Aceh on Dec. 26, 2004 are 172 cm and 42 cm, respectively, and the tidal range of the region is less than 1.5 m (based on the data by Tsuji et al, 2005).

Generally speaking, destruction of buildings in the Banda Aceh plain is related to the distance from the coast. Distinct regional difference of the destruction of buildings was also seen among the eastern and the central and western parts of the Banda Aceh coastal plain (Figs. 4-6).

3. METHODS

Landforms were classified through interpretation of satellite images of the plains, and field surveys in the regions. The 1:50,000 scale topo-sheets of Band Aceh, the SPOT 2 image of the Banda Aceh plain taken just after the tsunami on December 26, and the IKONOS satellite images taken on December 29 were used for the interpretation. SRTM-dem data were also used for the interpretation and classification of landforms.

During the field surveys, heights and directions were measured of flow indicators related to tsunami flow on the plains. The orientation of fallen columns of destroyed buildings and the scratches on the floors of buildings are also good markers of run-up flow directions in the Banda Aceh coastal plain (Fig. 7, 8).

4. TSUNAMI FLOW AND LANDFORM CHANGE IN THE BANDA ACEH PLAIN

Flow indicators on the Banda Aceh coastal plain generally show inundation from the northwest. However, some areas show different directions of the flow (Fig. 11). On the northeastern coast, flows spread out in a

Fig. 7. Scratches on a floor near the coast of the Banda Aceh coastal plain

Fig. 8. Fallen columns indicating run-up tsunami direction

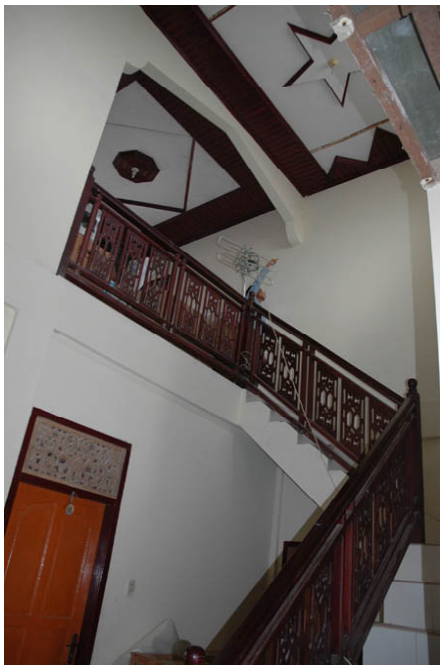

Fig. 9. Inundation heights were measured from the water mark of the tsunami

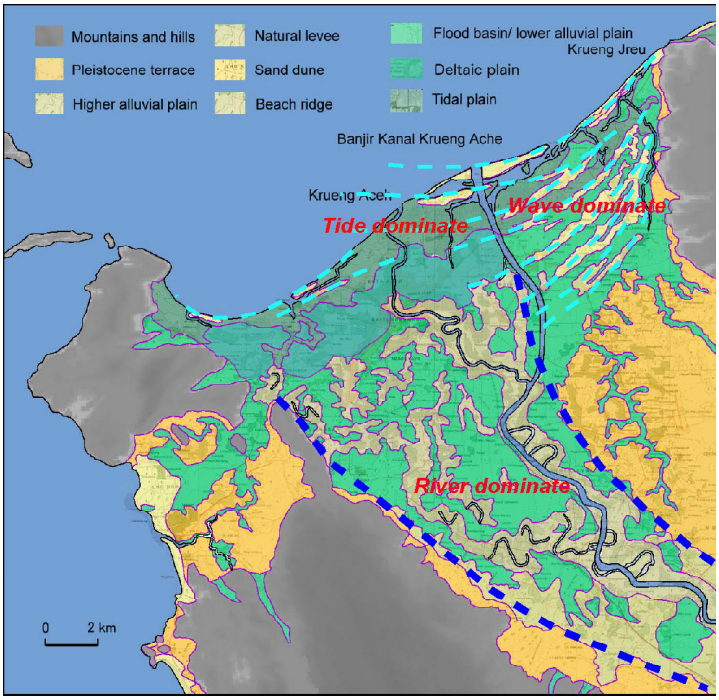

Fig.10. Landforms and geomorphic agency of the Banda Aceh

radial pattern from a gap in the sand dune along the coast. In the southwestern part of the plain, northeastward tsunami flow from the west coast penetrated the plain and the flow met in a gap of hills with the southward run-up tsunami flow
of the Banda Aceh coastal plain. We also mapped indicators in the western part of the coastal plain that show southward flows deflected due to the existence of hills.

Tsunami flow extended inland in the central and western parts of the plain for about 4 km, and for about 3 km in the eastern part. Remarkable invasion of the run-up tsunami flow along the Aceh, the Aceh drainage and the Jreu rivers was recorded on the SPOT 2 image (Fig. 12). The distances of the invasion of the flow from the coast into the rivers were 8 km, 8.5 km, and 6 km, respectively.

Inundation heights at similar distances from the coast were variable, with greater heights in the central and western part of the plain. The tsunami reached a height about 9 m on the ground near the port of the Banda Aceh and about 6-8 m in the western part of the plain about 2 km inland. In the eastern part of the plain about 2 km from the coast, however, tsunami heights were mostly lower than 3 m (Fig. 11, 13).

Severe coastal erosion occurred in the parts of the tidal plain used for shrimp or fish ponds. The small narrow banks separating the ponds were easily eroded by the tsunami returning these areas to former tidal flat conditions (Fig. 14). The conversion of these areas to tidal flats was due to erosion by the tsunami rather than tectonic subsidence. Interviews with local people confirmed that tidal areas are now exposed at low tide to the same extent as they were before the tsunami, and tide levels marked on several bridge are

almost similar to levels before the tsunami. It was difficult to reconstruct the flows of the tsunami backwash flow in the Banda Ache plain because there are few indicators of backwash flow on the ground.

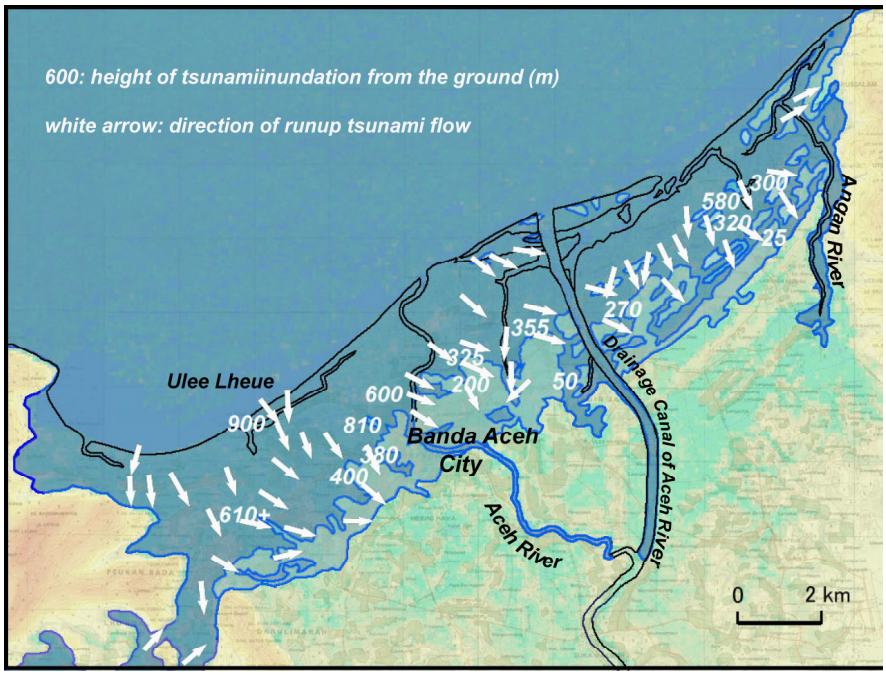

Fig. 11. Direction and height of tsunami flow in the Banda Aceh coastal plain

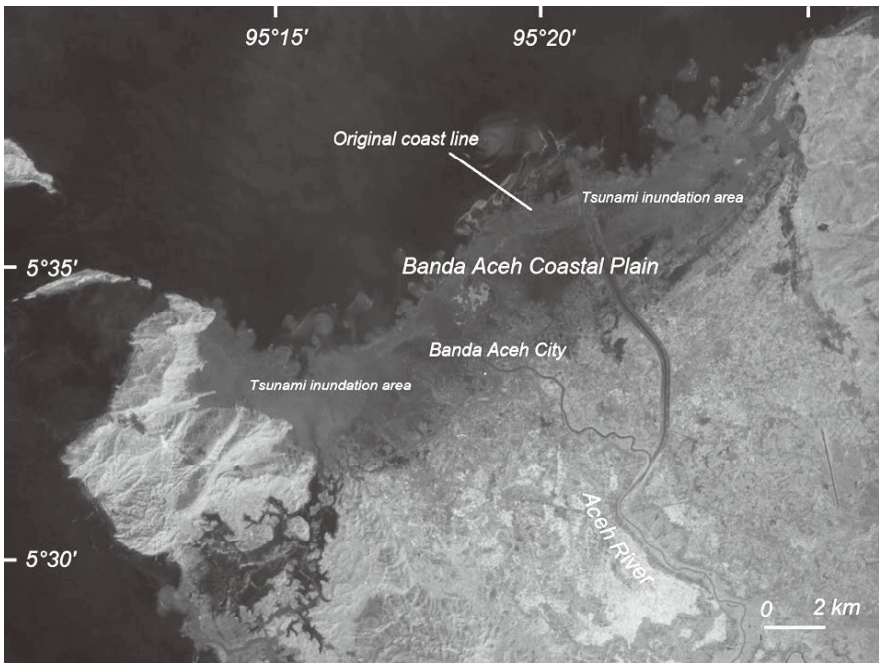

Fig. 12. SPOT-2 image of the Banda Aceh coastal plain about 3.5 hours after the tsunami inundation. The image was taken at 11:23:40 (local time) on December 26, 2004. (Includes material from CNES2005, Distribution Spot Image S.A., France, all rights reserved).

7. EFFECT OF LANDFORMS ON TSUNAMI FLOW IN THE PLAINS

Regional differences in tsunami flow patterns and tsunami height can be seen on the Banda Aceh coastal plain. The differences are related to the characteristics of the landforms of the plains. In the case of the Banda Aceh Plain, erosion of channels was not violent and the linear erosion is not observed on the plain. In some areas of the plain, however, coastal landforms were greatly modified. Shrimp and fish ponds on the tidal plain were extremely damaged and some of them disappeared after the tsunami. This indicates that the

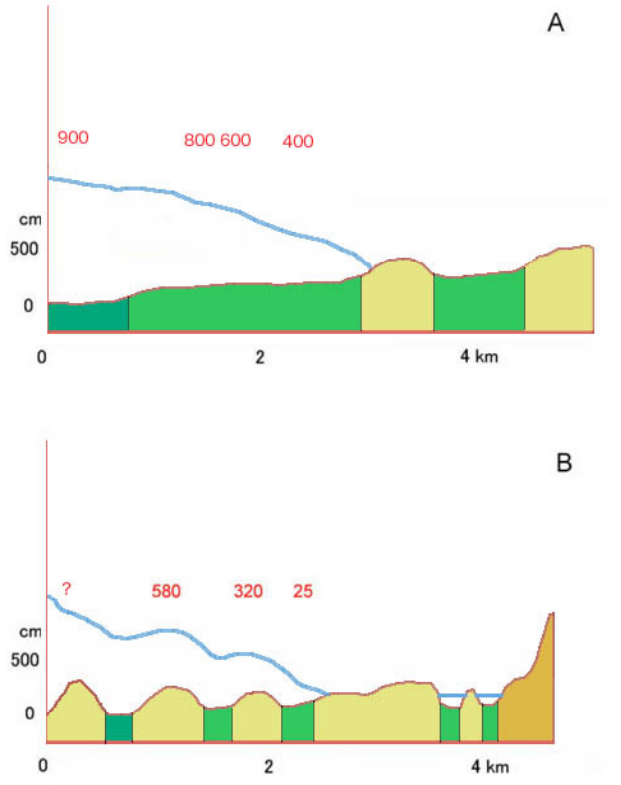

Fig. 13. Schematic cross section of the tsunami flow in western (A) and eastern (B) parts

Fig. 14. Tidal flat of the central part of the coastal lowland

Fig. 15. Coastal sand dune in the eastern part of the plain

backwash flow was not concentrated linearly in the Banda Aceh plain, and sheet erosion of backwash flow dominated in the plain. This condition is shown on the SPOT image taken four hours after the tsunami intrusion (Fig. 12).

The primary reason for the dominance of sheet erosion is that the ground level is related to the geo-environment of the Banda Aceh coastal plain. There is a broad tidal plain in the central and western coastal area of the Banda Aceh plain, and the ground surface is low and flat. This environment did not pro-duce the concentration of backwash and linear-flow erosion was not remarkable.

The tsunami heights in the central and western parts of the Banda Aceh coastal plain at similar dis-tances from the coast were higher than in the eastern parts. It is suggested that the existence of low-lying tidal and deltaic plains in the western and central parts of the plain facilitated intrusion of tsu-nami flow inland. The tsunami inundation height also did not decrease in the regions of the plain. In the eastern coastal region, relatively higher landforms such as dunes and beach ridges prevented the tsunami flow from penetrating inland.

8. CONCLUSIONS

Tsunami flow and inundation in the Banda Aceh plain, Indonesia are related to its landforms. The landforms of the Banda Aceh coastal plain are characterized as deltaic lowlands with tidal plain in the west and central parts and the strand plain and beach ridges in the eastern part of the plain. Coastal erosion of the plains was caused by direct attack of tsunami wave in both the Banda Aceh plain, and the broad tidal flat of the Banda Aceh coastal plain was severely damaged by the tsunami flow. Sheet erosion dominated in the Band Aceh tidal plain. Micro-landforms such as beach ridges and natural levees prevented the flow of the tsunami from penetrating further inland in the area near the margin of tsunami inundation.

Acknowledgements

This paper is based on the article of Umitsu et al. (2007). The authors wish to express gratitude to Prof.

Fumiaki Kimata at Nagoya University, Japan and Mr. Didik Sugiyanto at Syiah Kuala University, Indonesia, for their support of our field survey in Banda Aceh. The research was supported by the Grant-in-Aid for Scientific Research (B1500302) sponsored by Japan Society for the Promotion of Science, the Science and Technology promotion Budget by FY 2004 for the Urgent Indian Ocean Tsunami Research by Ministry of Education, Culture, Sports, Science and Technology, and the Discretion Budget of FY 2005 by the Chancellor of Nagoya University for the Indian Ocean Tsunami Survey. This paper is a contribution to IGCP-Project 495 “Quaternary Land-Ocean Interactions: Driving Mechanisms and Coastal Responses”.

References:

Tsuji, Y, Namegaya, Y. and Ito, J., 2005. Astronomical Tide Levels along the Coasts of the Indian Ocean. (URL-http://www.eri.u-tokyo.ac.jp/namegaya/sumatera/tide/) (Earthquake Research Institute, the University of Tokyo)

Umitsu, M., Tanavud, Charlchai and Patanakanog, B. (2007) Effects of landforms on tsunami flow in the plains of Banda Aceh, Indonesia, and Nam Khem, Thailand. Marine geology, 239, 163-172

Tsunami Wave Force and its Estimation Method
－ Forces on a Rectangular Body －

Norimi Mizutani, Tomoaki Nakamura

Department of Civil Engineering, Nagoya University, Nagoya 464-8603, Japan

Abstract

Wave force due to run-up tsunami is investigated in this paper. Laboratory experiments have been conducted to measure wave pressure and forces on a rectangular body. Numerical simulation has also performed to compute deformation of tsunami on apron and resultant wave pressure and wave forces on the body. Present numerical simulation method has been shown to have excellent performance in simulating wave deformation and wave forces. Moreover, a simple estimation method of the wave force has been proposed in this study.

INTRODUCTION

On December 26, 2004, the Indian Ocean Tsunami attacked coastal areas of Indonesia, Thailand, India, Sri Lanka and other countries along the Indian Ocean. A series of tsunamis killed a large number of people and destroyed many coastal structures. These structures were damaged not only by tsunamis themselves but also by floating debris such as timbers, vehicles and vessels, resulted in serious structural damages.

In ports, many vessels are usually moored. Once such a huge tsunami strikes the port area, drifted vessels due to run-up tsunami waves may cause severe destructions of port facilities. In recent years, a huge demand for container ships due to the economic growth of Asian countries leads to the increase in containers piled up on an apron. Thus, indirect damage from tsunami-induced drifted containers is now a great concern for port and harbor disaster prevention. Using hydraulic model experiments, Mizutani et al. (2005) investigated a run-up tsunami on an apron for clarifying tsunami force acting on a fixed container and collision force due to a drifting container. They consequently found that the tsunami force was evaluated with the drag term of the Morison equation. However, few detailed measurements of wave field in the vicinity of the container, in particular wave pressure acting on the container, were performed.

As far as tsunami-induced wave pressure is concerned, there are some empirical formulae (Tanimoto et al.,1984; Asakura et al., 2000; Ikeno et al., 2001, 2003). Using a model experiment, Ikeya et al. (2005) investigated temporal-spatial variation of tsunami-induced wave pressure on a land-based structure. Summarized these studies, maximum run-up height in front of a vertical structure due to a tsunami wave was three times higher than maximum water level in the absence of structures and maximum wave pressure on the structure was predicted with the maximum runup height in front of the structure. Furthermore, Asakura et al. (2000) and Ikeno et al. (2001, 2003) indicated that impulsive pressure around the bottom of the structure exceeded the above pressure. However, a few contributions have been devoted to the detailed mechanism of tsunami-induced wave pressure on a structure, particularly the impulsive pressure.

In this study, we investigated run-up tsunami deformation in the vicinity of containers, which is approximated as a rectangular body in this study, fixed on an apron for clarifying tsunami force and wave pressure acting on the containers with a three-dimensional numerical simulation as well as hydraulic model experiments. Also, a simple estimation method of wave force is proposed and its validity is investigated.

NUMERICAL SIMULATION

In this study, we adopted a numerical model composed of the following governing equations, i.e., a continuity equation (Eq. (1)) with a wave source, modified Navier-Stokes equations (Eq. (2)) with both inertia and drag forces due to porous media developed by Golshani et al. (2003), surface tension force based on the CSF (Continuum Surface Force) model of Brackbill et al. (1992) and eddy viscosity based on the Smagorinsky model (Smagorinsky, 1963), and an advection equation (Eq. (3)) of the VOF function F, which represents the volume fraction of water in a numerical mesh (Hur et al., 2007):

$$\frac{\partial\left(mv_j\right)}{\partial x_j}=q* \tag{1}$$

$$\left(1+C_A\frac{1-m}{m}\right)\frac{\partial v_i}{\partial t}+\frac{\partial\left(v_iv_j\right)}{\partial x_j}=-\frac{1}{\hat{\rho}}\frac{\partial p}{\partial x_i}-g_i+\frac{f_i^s}{\hat{\rho}}+\frac{\partial}{\partial x_j}\left(-\tau_{ij}+2\hat{\nu}D_{ij}\right)-R_i+Q_i-\beta_{ij}v_j \tag{2}$$

$$\frac{\partial\left(mF\right)}{\partial t}+\frac{\partial\left(mv_jF\right)}{\partial x_j}=Fq* \tag{3}$$

where v_i is the seepage velocity vector, p is the pressure, $x_i=\left[x,y,z\right]^{\mathrm{T}}$ is the position vector, t is the time, $g_i=[0,0,g]^{\mathrm{T}}$ is the gravitational acceleration vector, g is the gravitational acceleration, $\hat{\rho}=F\rho_w+\left(1-F\right)\rho_a$ is the fluid density, ρ_w and ρ_a are the densities of water and air, respectively, $\hat{\nu}=F\nu_w+\left(1-F\right)\nu_a$ is the kinematic molecular viscosity of fluid, ν_w and ν_a are the kinematic molecular viscosities of water and air, respectively, m is the porosity, $q*$ is the wave source (see Kawasaki, 1999), C_A is the added mass coefficient, $D_{ij}=\left(\partial v_i/\partial x_j+\partial v_j/\partial x_i\right)\big/2$ is the strain rate tensor, f_i^s is the surface tension vector modeled with the CSF model, τ_{ij} is the turbulent stress based on the Smagorinsky model, R_i is the drag force vector derived by Golshani et al. (2003), Q_i is the wave source vector, $\beta_{ij}=\beta\delta_{i3}\delta_{j3}$ is the dissipation factor matrix, β is the dissipation factor which equals zero except for added dissipation zones (Hinatsu, 1992), δ_{ij} is the Kronecker delta. In the present model, we applied f_i^s, τ_{ij}, R_i and Q_i formulated as follows:

$$f_i^s=\sigma\kappa\frac{\partial F}{\partial x_i}\frac{\hat{\rho}}{\overline{\rho}}, \tag{4}$$

$$\tau_{ij}=-2\left(C_S\Delta\right)^2\left|D\right|D_{ij}, \tag{5}$$

$$R_i=\frac{12C_{D2}\hat{\nu}\left(1-m\right)}{md_{50}^2}v_i+\frac{1}{2}\frac{C_{D1}\left(1-m\right)}{md_{50}}v_i\sqrt{v_jv_j}, \tag{6}$$

$$Q_i=v_i\frac{q*}{m}-\frac{2}{3}\frac{\partial}{\partial x_i}\left(\hat{\nu}\frac{q*}{m}\right), \tag{7}$$

where σ is the surface tension coefficient of water, κ is the local surface curvature, $\overline{\rho}=\left(\rho_w+\rho_a\right)\big/2$ is the fluid density at the water-air interface, C_S is the Smagorinsky coefficient, $\Delta=\sqrt[3]{\Delta x\Delta y\Delta z}$ is the filter width, Δx, Δy and Δz are the mesh widths in the x, y and z directions, respectively, $\left|D\right|$ is the absolute value of the strain rate tensor D_{ij}, C_{D2} and C_{D1} are the linear (laminar) and nonlinear (turbulent) drag coefficients, respectively, and d_{50} is the median diameter of porous media. This simulation employed the SMAC method for coupling the continuity equation (Eq. (1)) and the modified Navier-Stokes equations (Eq. (2)). The 3rd-order Adams-Bashforth, 3rd-order TVD (Total Variation Diminishing) proposed by Chakravarthy and Osher (1985) and 2nd-order central difference schemes were applied to the time derivative, convective and other terms of Eq. (2), respectively. For tracking a free surface location, Eq. (3) was calculated with the MARS of Kunugi (2000), one of the PLICs (Piecewise Linear Interface Calculation) such as PLIC (Youngs, 1982) and TELLURIDE (Rider and Kothe, 1998). In this paper, we adopted the cold start, which means all velocities at the initial time were zero.

MODEL EXPERIMENT

For investigating runup tsunami deformation around containers on an apron, hydraulic model experiments were conducted with a scale of 1/75 using a 28.0m long, 8.0m wide and 0.8m high wave basin with a piston-type wave generator at the Department of Civil Engineering, Nagoya University. As shown in Figure 1,

a 1.0m long, 4.0m wide and 0.25m high apron was placed at 12.0m onshore from the wave generator. In this study, two types of containers were adopted: the first was a 20ft container (32x80x35 mm) and the other was a 40ft container (32x163x35 mm).

The measurements of (i) water surface elevation in front of the apron, (ii) water level on the apron, (iii) runup height in front of containers and (iv) tsunami force acting on containers were conducted in each experimental run. First, water surface elevation was measured at 5, 50 and 100mm offshore from the front of the apron with capacitance-type wave gages. At the same time, the measurement of water level on the apron was performed at 100, 200, 300, 400 and 500mm onshore from the front of the apron using the wave gages. As for runup height in front of containers, we fixed containers at 105, 205, 305, 405 and 505mm from the front of the apron, and then we measured runup height at 5 mm offshore of the containers with the wave gage. Finally, we measured wave-directional tsunami force acting on containers located at 105, 305 and 505mm from the front of the apron using a cantilever-type wave force meter, as shown in Photo 1. Wave conditions are listed in Table 1.

Similar experiments were also conducted using two-dimensional wave tank which can generate long-

Table 1 Incident wave conditions (3D experiments)

Case	Wave Period T [s]	Wave Height H [cm]	Still Water Depth h [cm]
Case 1	4.0	2.8	22.0
Case 2	3.0	3.8	22.0
Case 3	3.0	3.0	22.0
Case 4	3.0	2.8	22.0
Case 5	2.0	6.8	22.0
Case 6	2.0	6.0	22.0
Case 7	2.0	5.0	22.0
Case 8	2.0	4.0	22.0

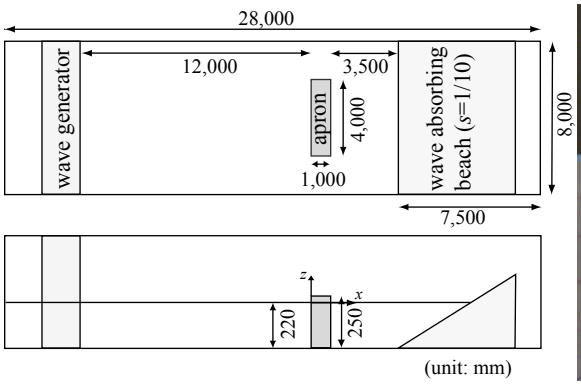

Figure 1 Experimental setup (3D)

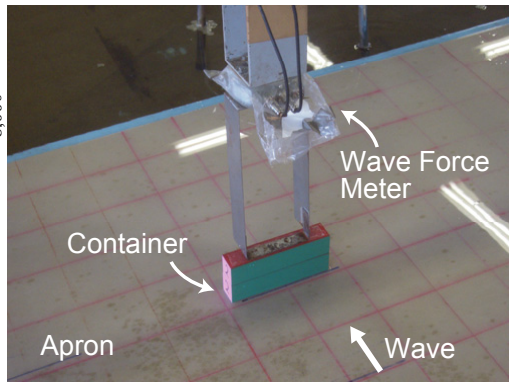

Photo 1 Measurement of tsunami force

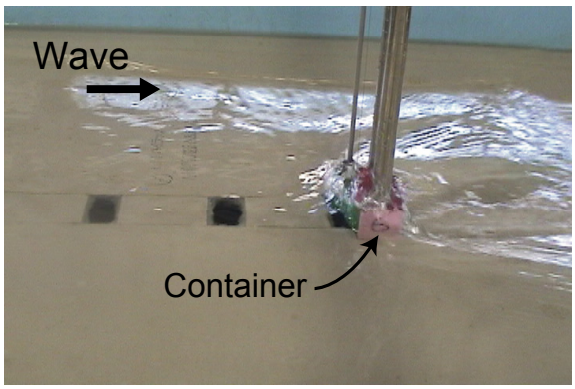

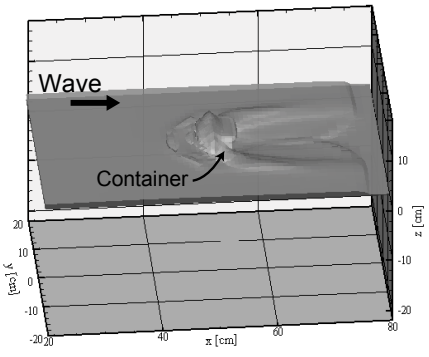

Figure3 Runup tsunami deformation due to a 20 ft container
(Experimental result and computed result, $x = 505\,\text{mm}$ for Case 7)

period waves as well as solitary waves, in order to discuss the effect of wave period.

RESULTS AND DISCUSSIONS

Figure 3 shows an example of runup tsunami deformation due to a 20 ft container, in which the left and right figures correspond to experimental and numerical results, respectively. Computed tsunami deformation agrees well with the experimental result. Figure 4 represents a comparison between experimental and numerical water surface elevation in front of apron and on the apron. The numerical results are in excellent agreement with the experimental ones, and we hence concluded that the numerical method was valid both qualitatively and quantitatively. Figure 5 shows a comparison of wave-directional tsunami force acting on containers. As indicated in Figure 5, the numerical data slightly underestimate the experimental ones, particularly in the case of a long runup distance, although the numerical results show a good agreement with the experimental ones. It is revealed that the present numerical simulation was very useful in directly calculating tsunami force acting on containers using no empirical equation such as the Morison equation.

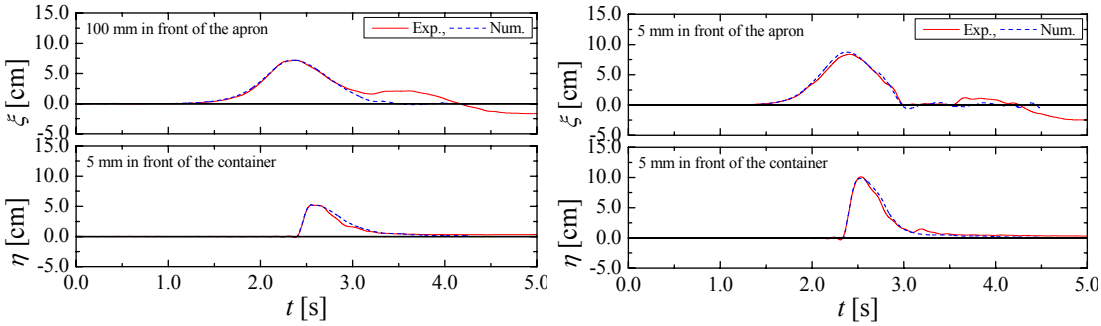

(a) single 20 ft container (Case 2) (b) double 40 ft containers (Case 6)

Figure 4 Water surface fluctuation ξ in front of the apron and runup height η_f at 5 mm offshore from the front of containers placed at $x = 205\,\mathrm{mm}$

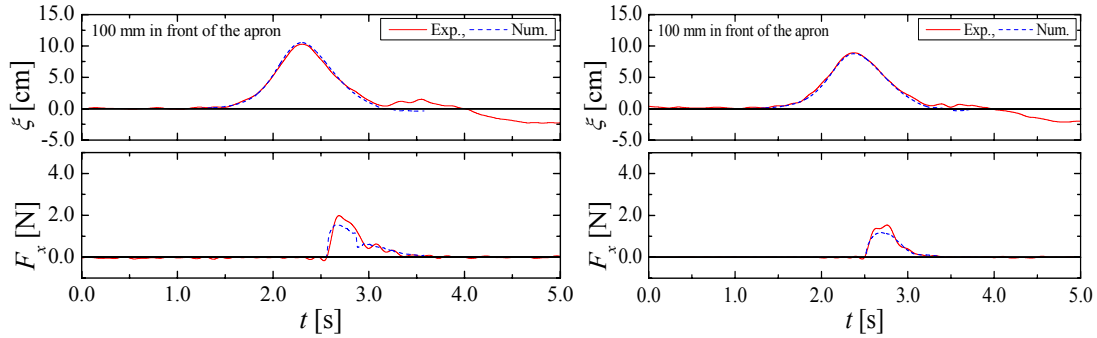

(a) 20 ft at $x = 505\,\mathrm{mm}$ (single, Case 6) (b) 20 ft at $x = 305\,\mathrm{mm}$ (double Case 6)

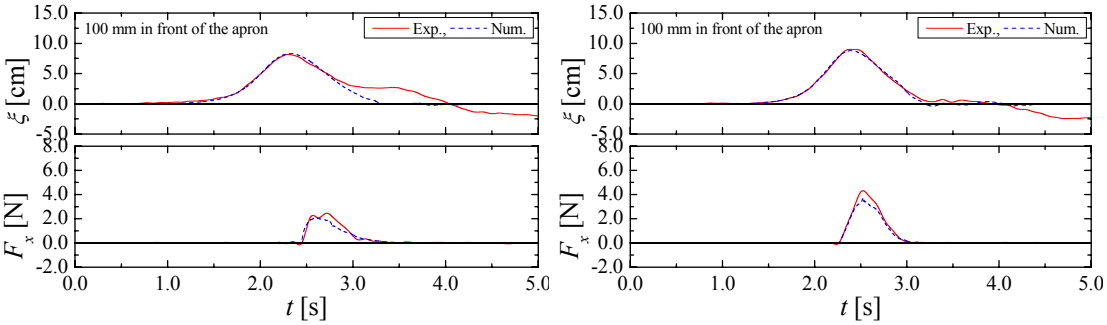

(c) 40 ft at $x = 305\,\mathrm{mm}$ (single Case 2) (d) 40 ft at $x = 105\,\mathrm{mm}$ (double Case 7)

Figure 5 Wave-directional tsunami force acting on containers F_x

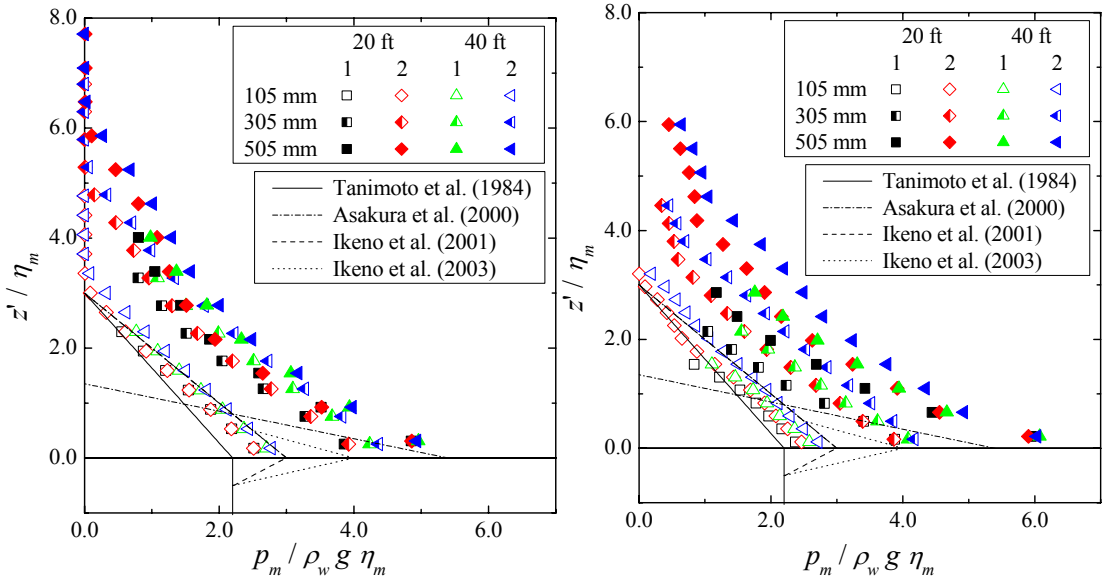

(a) Case 3 (b) Case 7

Figure 6 Maximum wave pressure p_m normalized by maximum water level η_m

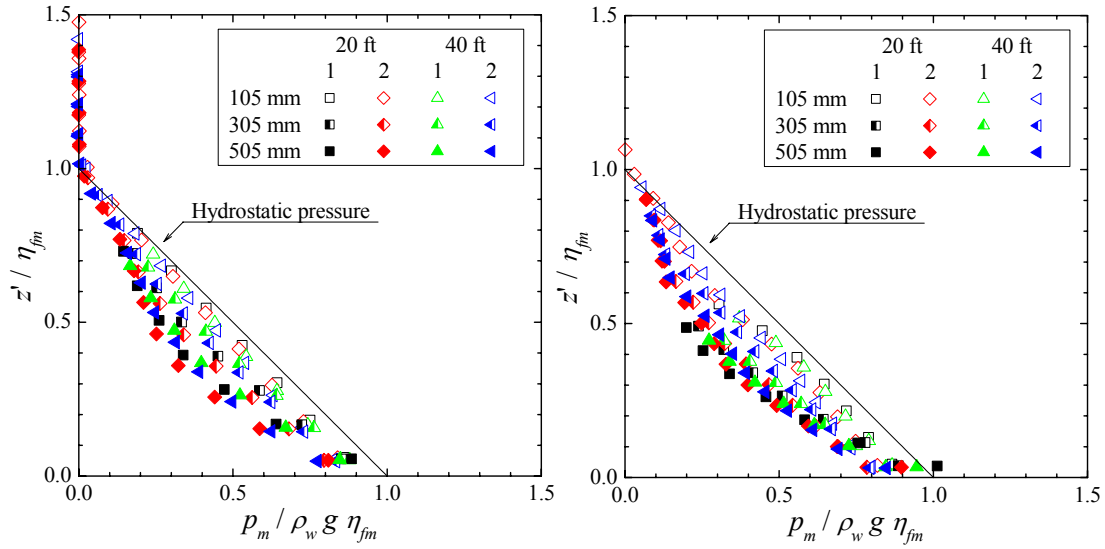

(a) Case 3 (b) Case 7

Figure 7 Maximum wave pressure p_m normalized by maximum runup height η_{fm}

As mentioned in the first chapter, Tanimoto et al. (1984), Asakura et al. (2000) and Ikeno et al. (2001, 2003) proposed empirical formulae for predicting tsunami-induced wave pressure acting on a structure. Figure 6 shows maximum wave pressure acting on the centerline of containers, in which the solid, dashed-dotted, broken and dotted lines represent respectively their formulae. As shown in Figure 6, the numerical data have similar inclinations as the empirical equations, i.e., a hydrostatic condition. As mentioned above, the previous studies found that η_{fm} was three times higher than η_m, but the present numerical results indicate that z'/η_m at $p_m/\rho_w g\eta_m = 0.0$ is larger than 3.0 in certain conditions. This phenomenon was also confirmed with experimental results (Mizutani et al., 2006).

Figure 7 shows p_m normalized by η_{fm} instead of η_f, in which the solid line is a hydrostatic pressure distribution which is zero at $z'/\eta_{fm} = 1.0$. As indicated in Figure 7, an upper limit of p_m is evaluated with the maximum runup height, assuming a hydrostatic condition. However, the slope of $p_m/\rho_w g\eta_{fm}$ is de-

pendent on z'/η_{fm} , and it is possible that $p_m/\rho_w g\eta_{fm}$ around the bottom of the containers ($z'/\eta_{fm} \approx 0.0$)exceeds the hydrostatic pressure distribution for Case 7. In order to clarify this mechanism in detail, we here treat tsunami-induced wave pressure p_w acting on layered two 40 ft containers piled up at $x = 505\,\mathrm{mm}$ for Case 8.

Distributions of maximum wave pressure $p_m/\rho_w g\eta_{fm}$ of the abovementioned case at different phase are shown in Figure 8, in which t is the time from the instance when the wave hit the lowest point of the containers. As indicated in Figure 8, impulsive pressure of the runup tsunami wave caused maximum wave pressure around the bottom of the containers at $t = 0.00\,\mathrm{s}$. After that, since the nonlinearity of p_w weakened due to a decrease in velocities in front of the containers, the wave pressure p_w approached a hydrostatic pressure distribution, as shown in the bottom of Figure 8. In summary, the mechanism of maximum wave pressure acting on containers p_w strongly depended on the positions on the containers, that is to say, around the bottom of the containers resulted from the impulsive pressure due to the impact of the runup tsunami wave, p_w near the maximum runup height was caused by the nonlinear pressure distribution due to large velocities in front of the containers, and p_w between them arose from the hydrostatic pressure distribution.

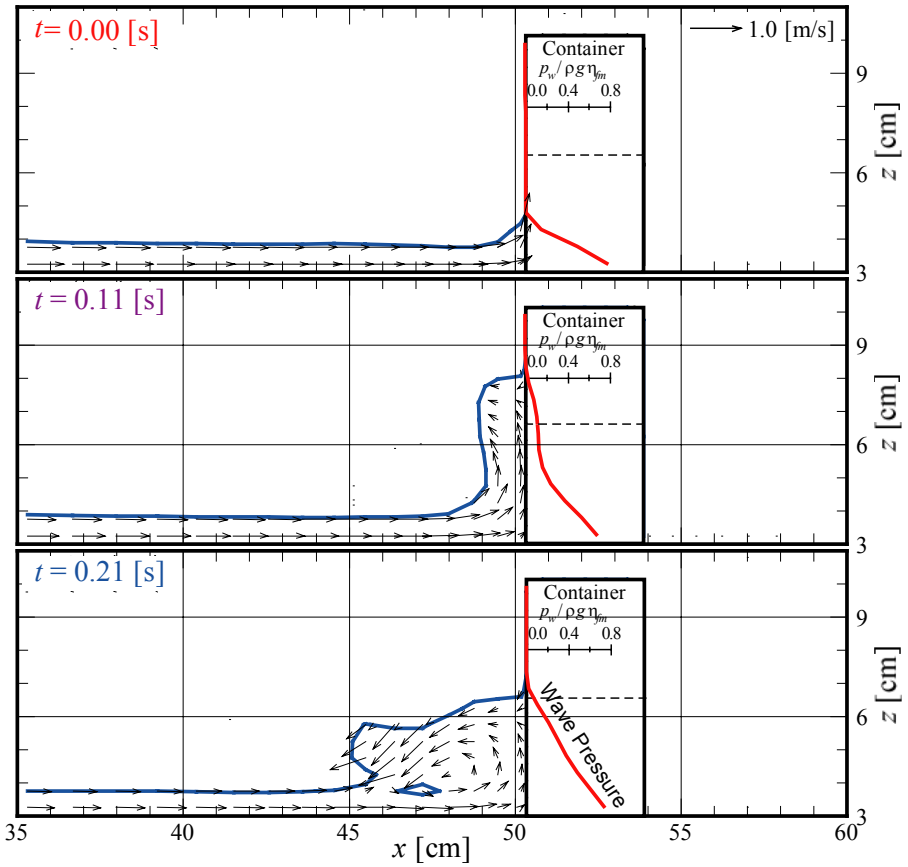

Figure 8 Wave field around the containers and wave pressure acting on the containers p_w

CONCLUSIONS

In this study, we treated runup tsunami deformation around containers plied up on an apron for investigating tsunami force and wave pressure acting on the containers with a three-dimensional numerical simulation based on the MARS as well as hydraulic model experiments. As a result, we confirmed the validity of the numerical simulation through a comparison of runup height in front of the containers, and we revealed that the numerical method was very useful in predicting tsunami force acting on the containers using no

empirical equations. Furthermore, it was found that an upper limit of maximum wave pressure acting on the containers was evaluated with maximum runup height in front of the containers, assuming a hydrostatic condition; however, it was possible that impulsive pressure around the bottom of the containers exceeded the hydrostatic pressure distribution due to the impact of the runup tsunami wave.

Acknowledgements

The authors express their sincere thanks to former graduate students, Mr.Yusuke Takagi, Mr.Kazutomo Shiraishi and Atsuhiro Usami for their great contribution in conducting the experiments.

References

Asakura, R., Iwase, K., Ikeya, T., Takao, M., Kaneto, T., Fujii, N. and Omori, M. (2000). An experimental study on wave force acting on on-shore structures due to overflowing tsunamis. Proc. Coastal Eng., JSCE, 47: 911-915 (in Japanese).

Brackbill, J. U., Kothe, D. B. and Zemach, C. (1992). A continuum method for modeling surface tension. J. Comp. Phys., Elsevier, 100: 335-354.

Chakravarthy, S. R. and Osher, S. (1985). A new class of high accuracy TVD schemes for hyperbolic conservation law. AIAA Paper, 85-0363.

Fenton, J. (1972). A ninth-order solution for the solitary wave. J. Comp. Phys., Elsevier, 53: 257-271.

Golshani, A., Mizutani, N., Hur, D.-S. and Shimizu, H. (2003). Three-dimensional analysis on nonlinear interaction between water waves and vertical permeable breakwater. Coastal Eng. J., 45(1): 1-28.

Hinatsu, M. (1992). Numerical simulation of unsteady viscous nonlinear waves using moving grid system fitted on a free surface. J. Kansai Soc. Naval Architects, 217: 1-11.

Hur, D.-S., Nakamura, T. and Mizutani, N. (2007). Sand suction mechanism in artificial beach composed of rubble mound breakwater and reclaimed sand area. Ocean Eng., Elsevier, 34(8-9), pp.1104-1119.

Ikeno, M., Mori, N. and Tanaka, H. (2001). Experimental study on tsunami force and impulsive force by a drifter under breaking bore-like tsunamis. Proc. Coastal Eng., JSCE, 48: 846-850 (in Japanese).

Ikeno, M. and Tanaka, H. (2003). Experimental study on impulse force of drift body and tsunami running up to land. Proc. Coastal Eng., JSCE, 50: 721-725 (in Japanese).

Ikeya, T., Asakura, R., Fujii, N., Ohmori, M., Iriya, T. and Yanagisawa, K. (2005). Spatio-temporal variation of tsunami wave pressure acting on a land structure. Ann. J. Civil Eng. Ocean, JSCE, 21: 121-126 (in Japanese).

Kawasaki, K. (1999). Numerical simulation of breaking and post-breaking wave deformation process around a submerged breakwater. Coastal Eng. J., 41(3-4): 201-223.

Kunugi, T. (2000). MARS for multiphase calculation. CFD J., 9(1): IX-563.

Mizutani, N., Shiraishi, K., Usami, A., Miyajima, S. and Tomita, T. (2006). Experimental study on tsunami excitation on container rested on apron and collision force of drift container. Ann. J. Coastal Eng., JSCE, 53: 791-795 (in Japanese).

Mizutani, N., Takagi, Y., Shiraishi, K., Miyajima, S. and Tomita, T. (2005). Study on wave force on a container on apron due to tsunamis and collision force of drifted container. Ann. J. Coastal Eng., JSCE, 52: 741-745 (in Japanese).

Rider, W. J. and Kothe, D. B. (1998). Reconstruction volume tracking. J. Comp. Phys., Elsevier, 141: 112-152.

Smagorinsky, J. (1963). General circulation experiments with the primitive equations. Mon. Weath. Rev., 91(3): 99-164.

Tanimoto, K., Tsuruya, H. and Nakano, S. (1984). Tsunami force and damage factor of revetments due to 1983 Nihonkai-Chube earthquake tsunami. Proc. Coastal Eng., JSCE, 31: 257-261 (in Japanese).

Youngs, D. L. (1982). Time dependent multimaterial flow with large fluid distortion. Numerical Methods for Fluid Dynamics, ed. Morton, K. M. and Baines, M. J., Academic Press, 27-39.

Geomorphological Mapping and Regional Features of the Lower Mekong Plain (Cambodia)

Sumiko Kubo

Department of Geography, Waseda University, Tokyo, 169-8050, Japan
E-mail: sumik@waseda.jp

Abstract

Geomorphological analyses of the Lower Mekong Plain in Cambodia were carried through mapping of micro-landforms of the plain by interpreting aerial photographs and satellite images, with field surveys. The plain is to be classified into upland, gentle fan, natural levee, higher alluvial surface, back marsh and former river channels. Floods, or certain water level changes occur every year, and seasonal water level changes are seen individually that depends on micro-landforms. Unique water management systems are developed to adapt the water level changes. Geomorphological mapping therefore shows the integration of landforms, land use and water use in the plain.

Keywords: The Lower Mekong Plain, micro-landforms, flood, water

INTRODUCTION

The Mekong River has its catchment area about 795,000 km^2. The upper part of its drainage basin is relatively narrow and lower part is broad. Cambodian Plain occurs in the southern part of the broader part (Figure 1). The plain consists of the Mekong floodplain and the Tonle Sap Great Lake with its surrounding plains. The Lower Mekong River Basin is also characterized by monsoon climate, which has heavy summer rainfall and dry winter. Therefore vast discharge is seen for the Mekong during the wet season (May to October) with large inundation area, while the discharge decreases considerably during dry season (November to April).

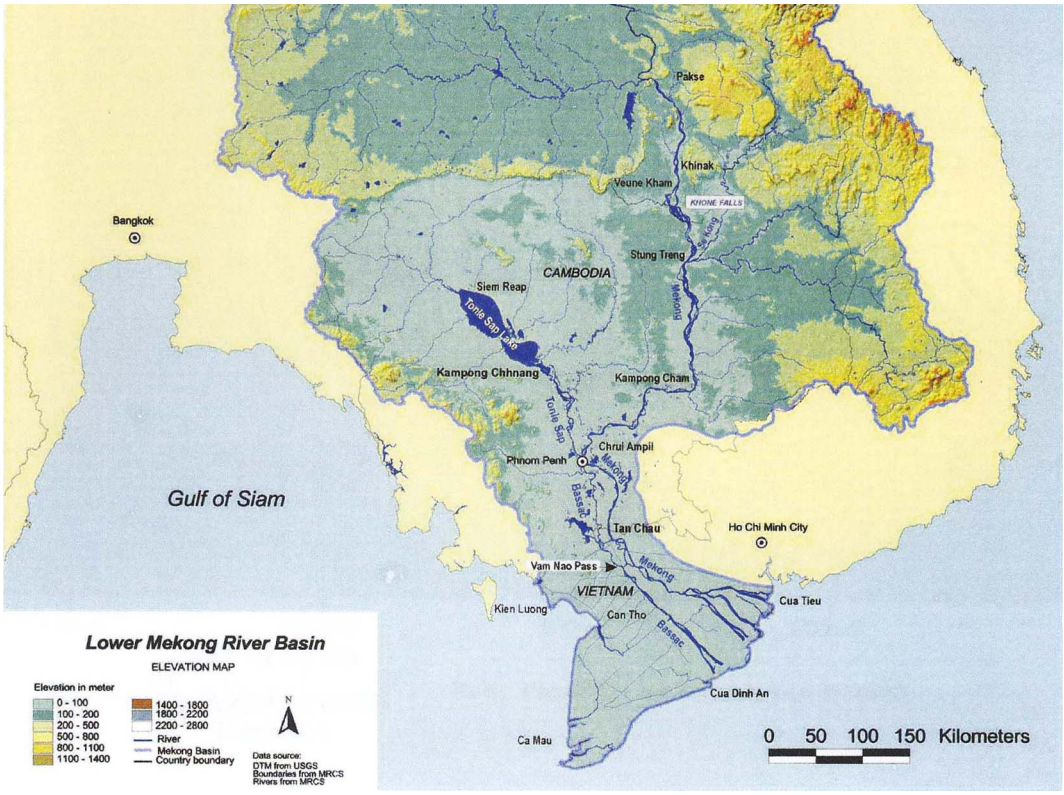

Fig. 1. The Lower Mekong River Basin (MRC, 2000)

Based on the geomorphological mapping of the plain, I intended to integrate the relationships between micro-landforms, land-use and water-use in the plain (KUBO, 2004, 2006). This paper will show some distinctive landform features in the plain related with unique land-use system.

Geomorphological analyses were carried out by interpreting aerial photographs (approx. scale 1:25,000; taken in 1992 by FINNMAP) and various satellite images (CORONA, LANDSAT, SPOT, JERS-1 etc) with field surveys. Field surveys include the scopes on landforms, land-use, water-use and archeological features. Topographic maps (scale 1:50,000 and 1:100,000), hydrological data and preceding reports were also used.

LANDFORM FEATURES OF THE CAMBODIAN PLAIN

Major Rivers in the plain

The Mekong flows through the Cambodian Plain from the North to South. It has little floodplain from the Laotian border to Kracheh Town, then it forms relatively narrow floodplain to Kampong Cham City, some 70 km upstream of Phnom Penh City. The width of the floodplain between Kracheh and Campong Cham is about 10 km. The channel form of the Mekong is braided, and deposits are sandy. From Kampong Cham City to the downstream, the floodplain starts to extend to form the middle part of the Cambodian Plain.

The Tonle Sap River flows from Lake Tonle Sap to join with the Mekong at Phnom Penh. At the same point the Bassac River splits from the Mekong. These four river channels form a 'K' shape, giving the area around Phnom Penh named 'Chaktomuk', or 'Four Faces' (but French name 'Quatre Bras' means Four Arms).

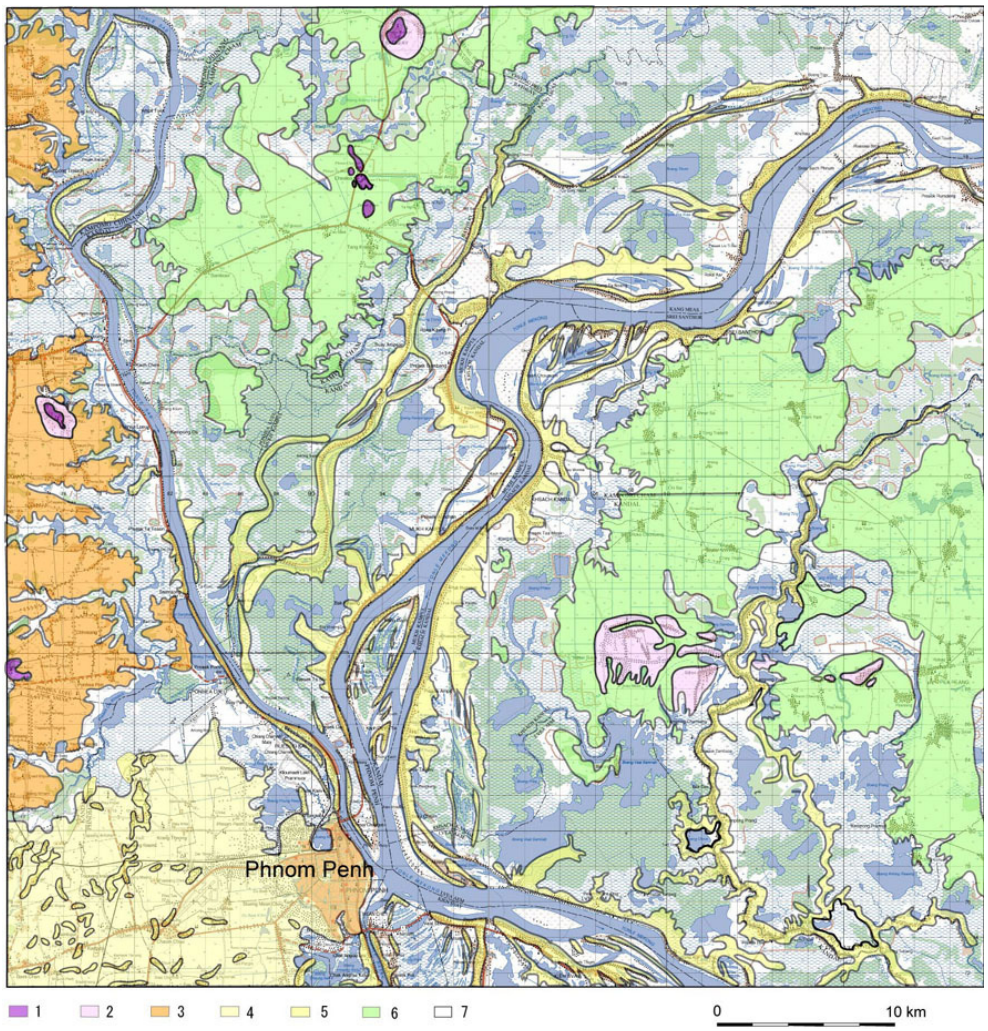

Fig. 2. Geomorphological map of the Lower Mekong Plain (Kubo, 2006)
1: mountain and hill, 2: pediment, 3: upland, 4: gentle fan,
5: natural levee, 6: higher alluvial surface, 7: back marsh

The Chaktmuk area has very unique fluvial characters (e.g. Mekong River Commission, 2003; 2005). The Tonle Sap River connects Lake Tonle Sap in the upstream with the Mekong in the downstream. During the rainy season, the flow direction of the river reverses, and the lake acts as a floodwater-retarding reservoir, expands into area by three times. At the end of the rainy season, the flow direction of the Tonle Sap River reverts to drain into the Mekong again. During the rainy season the Mekong itself causes floods in the plain around Phnom Penh.

Geomorphological mapping

Following geomorphologic units were distinguished in the plain (Figure 2): mountain and hill, pediment, upland, gentle fan, natural levee, higher alluvial surface, back marsh and former river channel.

Based on the landform features, the plain near Chaktomuk Junction was divided into following parts: 1) Upland terraces and alluvial fan in the western part, 2) The Mekong floodplain, 3) The Tonle Sap River floodplain, and 4) The Bassac River floodplain. Features are summarized as follows: 1) higher alluvial surfaces surround the floodplain, 2) the Mekong floodplain is characterized by braided channel pattern in the upper reaches, and by natural levees/back marshes in the lower reaches, 3) the Tonle Sap river floodplain is very flat, and 4) the Bassac river is characterized by artificial features called Colmatage canals (Kubo, 2004; 2006).

REGIONAL FEATURES ON WATER LEVEL CHANGE AND FLOODS

The Cambodian Plain has distinct seasonal change in water levels. During the rainy season water level of the Mekong River increases and the inundation along the floodplain progresses gradually. In September and October, water level reaches its highest and broad area is inundated. In November and December water level decreases again. The range between low and high water level is nearly 10 m near Phnom Penh. Because the floodplain is strongly affected by this water level change, land-use, water-use and agricultural practices vary by regions.

Regional features related to water level changes and the situations during the extreme flood in 2000 are shown below.

The Mekong floodplain

Along the Mekong River, inundation occurs extensively during every rainy season. Narrow natural levees are slightly higher than others; they provide lands for roads and dwellings. Agricultural use is restricted in the inundated areas so that small amount of recession (dry season) rice cultivation is seen along the natural levees. This floodplain functioned as floodwater channel during the rainy seasons. The former main river channels such as Preak Kang Chak and Preak Mukh Kampul became influential flood water courses. Several bridges of National Route 6A near Preak Mukh Kampul were heavily damaged by the 2000 flood and preceded floods. Similarly, National Route 1 on the left bank of the Mekong near Neak Loeang was also damaged. Flood water in this area flowed through the floodplain of left bank. Any facility in the floodplain that prevents water flow during high water periods should be deeply concerned.

On the higher alluvial surface, rainy season rain-fed paddy fields are seen like the upland surface. Square farm ponds and so-called Pol Pot canals (canals constructed during the Khmer Rouge age) are also seen in this area. While normal floods do not reach the surface except peripheral areas, large floods occasionally inundate this area. During the large floods in the year 2000, higher alluvial surface on both sides of the Mekong were inundated extensively (Kubo, 2003).

The Tonle Sap River floodplain

This is the floodplain where the water comes from the Mekong via the channel of Tonle Sap River. Water also comes from the right side of Preak Mukh Kampul. According to these specific behaviors of flood water, water velocity and sediment deposition are smaller than that of the Mekong. As a result, broad marshy area exists. Recession rice cultivation (paddy cultivated during receding water) is also seen in parts of this area.

Rectangular/ circular or arc-shaped small embankments (tomnup) are fringing the higher alluvial surfaces (Figure 3). They store floodwater and rainwater during the rainy season, and the water is used for neighboring recession (dry-season) paddy fields.

The Bassac floodplain

Dense colmatage canals characterize the area (Figure 4). Colmatage is a system of artificial canals con-

nected perpendicular to the main river. Some canals have water gates at the inlet but canals without gates are also common. During the rainy season when the water level increase, water from the main river flow into the canals and drain into back marsh area. Simultaneously sediments deposit along the channel and form slightly elevated lands. In this manner land reclamation progressed. Reclaimed land is used for upland crops as maize etc. This is the system said to be established during French colonial period. On the other hand, back marsh areas remain between the Bassac and Mekong.

Very little area was inundated along the Bassac River in the year 2000 flood. Flood water movement was predominantly through colmatage channels into back-marsh areas. Therefore floodwater does not overflow at the main channel. Overflow occurs along the colmatage canals so that the flood can be well controlled. The flood in 2000 did not cause severe damage in this area Colmatage system therefore seems to be suitable and sustainable for controlling water in the area.

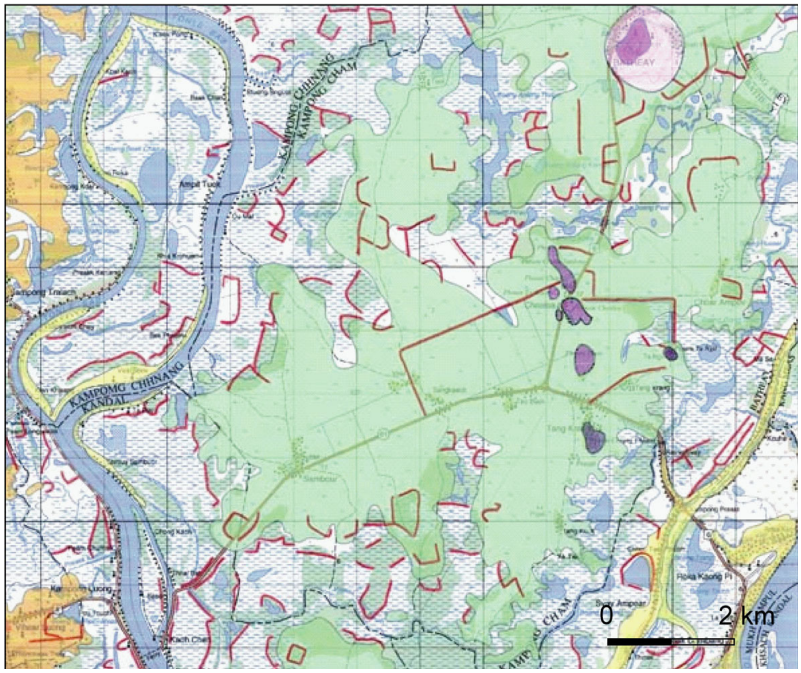

Fig. 3a. Geomorphological map showing the area between the Tonle Sap River and the Mekong
Each mesh represents 2*2 km grid. Bold lines show dikes.
The Tonle Sap River is seen on the left side and the Mekong on the right.
Note that tomnup dikes fringe higher alluvial surface.

Fig.3b. A tomnup dike
Water is stored on the right side and used for paddy field on the left.

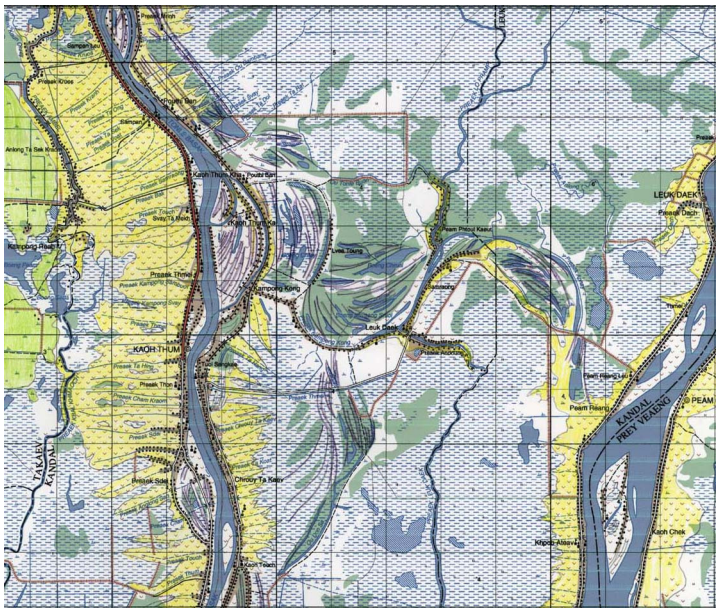

Fig. 4a. Geomorphological map showing the area between the Bassac and the Mekong
The Bassac is seen on the left and the Mekong on the right.
Note that colmatage canals and accompanied features develop along the Bassac.

Fig. 4b. Colmatage canal leads water from the Mekong (back) to back marsh (front)

Colmatage canals are also seen along the Mekong but their density is far lower than that of the Bassac. The Mekong itself is too large to control and hard to maintain canals directly connected with the main channel. In the year 2000 flood, several colmatage gates along the Mekong were destroyed. The Tonle Sap River has no colmatage canals probably by its small sediment supply.

RICE ECOSYSTEM AND WATER

Traditional rice ecosystem in Cambodia is classified into following four categories (Save Cambodia's Wildlife, 2006): 1) Rain-fed lowland rice, 2) Rain-fed upland rice, 3) Deepwater/floating rice and 4) Re-

cession (dry season) rice. Within these categories, upland rice of 2) often practiced in shifting cultivation so that is very rare in the Cambodian plain. The rest three are seen in the plain; harvesting and transplanting rice is often seen along the Mekong and Tonle Sap floodplains. As rice harvest is generally once a year in Cambodia, it does not mean second or third cropping. They have different conditions for water availability.

Rice ecosystem is therefore understood with micro-landforms and water behaviors in the plain. Rain-fed lowland rice is available during the rainy season on upland, alluvial fan and higher alluvial surfaces. Farm ponds and so-called Pol Pot canals are countermeasures for water scarcity in these areas.

In the back marshes of the Mekong and Tonle Sap River floodplain, deep inundation during the rainy season prevents cropping. There are some areas for deep water floating rice cultivation but the yield is low. Recession rice cultivation is dominant in the peripheral parts of these deep water areas. Transitional area between higher alluvial surface and floodplain is characterized by distribution of tomnup dikes. Many tomnup dikes function as storing water during high water level and water is used for recession rice.

Natural levees along the Mekong are relatively flood-safe. National roads and settlements are located on natural levees. Colmatage canals and canal-side reclaimed land generated artificial landforms. Silted land extends to the back marsh area nearly 5 km from the Bassac River. Upland crops are practiced in this field.

CONCLUDING REMARKS

The Lower Mekong Plain (Cambodian Plain) has distinct regional geomorphological features. It is facing water surplus and shortage as the area is affected by monsoon climate. Seasonal water level change, different rice ecosystem, unique water management systems are seen in this area. People clearly consider the landform condition to control water and cultivate rice. The author attempts geomorphological analyses to integrate the relationships between land, water and their management in regional features.

Acknowledgments

This paper was extracted and modified from Kubo (2006); Proceedings of the International Conference on "Mekong Research for the People of the Mekong" held at Chiang Rai in October 2006, a month after the International Conference on the Mitigation of Natural Disasters in the Tsunami Affected Coastal Regions of Tropical Asia held at Phuket.

I explain my thanks to the following institutes and staffs for their support: Nagoya University (JSPS Grant-in-Aid research), Mekong River Commission, Cambodia National Mekong Committee, Ministry of Public Works and Transportation, Japan International Cooperation Agency, Japanese Embassy, National Institute for Rural Engineering.

The Ministry of Education, Science and Culture of Japan supported this study (Research Revolution 2002 Project: Yamanashi University; Grant-in-Aid for Scientific Research: Waseda University).

References

Hori, H., 2000, *The Mekong: Environment and Development*. United Nations University Press.

Kubo, S., 2003, Geomorphological features and flood characters around Phnom Penh, Lower Mekong River Plain. *Proceedings of the 1st International Conference on Hydrology and Water Resources in Asia Pacific Region*, Vol. 2, 692-696, Kyoto.

Kubo, S., 2004, Geomorphological features, flood characters, land-use and water-use in the Lower Mekong Plain in Cambodia. *Proc. of International Conference on Advances in Integrated Mekong River Management*, 201-205, Vientiane.

Kubo, S., 2006, Land, water and land use in the Lower Mekong Plain (Cambodia): Geomorphological integration. *Proc. of International Conference on "Mekong Research for the People of the Mekong"* (CD-ROM), 309-316, Chiang Rai, Thailand.

Mekong River Commission, 2003, *State of the Basin Report 2003*, Phnom Penh, 300p.

Mekong River Commission, 2005, *Overview of the Hydrology of the Mekong Basin*, Vientiane, 73p.

Save Cambodia's Wildlife, 2006, *The Atlas of Cambodia: National Poverty and Environment Maps*. Phnom Penh, 141p.

Future Issues on Supply of Disaster Information to Residents with Foreign Nationality in Hamamatsu City, Shizuoka Prefecture (JAPAN)

Hiromi Kataoka

Kinki University, Higashi-Osaka. Japan

I. INTRODUCTION

The Immigration Control and Refugee Recognition Act (hereafter referred to as the Immigration Act) was amended in Japan in 1990. With the amendment of this act, the scope of the employment-permitted residence visa was increased, and 2nd and 3rd generation Nikkei (person of Japanese descent) and their families were granted 'Spouse or Child of Japanese National Visa' and 'Long Term Resident Visa' which do not restrict activities. In addition, it is possible for a non Japanese-descended spouse of a Nikkei up to the 3rd generation to have the same residency qualification as a Japanese-descended person. Due to this, the number of Nikkei and families of South American origin centering on Brazil increased in Japan. The number of Brazilians registered in Japan in December 2004 (end of the month) was 286,557; this is 14.5% of all foreign residents. Looking at the residing areas of Brazilians, there are many in the Tokai area which is centered on Aichi prefecture and Shizuoka prefecture. The primary factor for this is the manufacturing industry-related enterprises and automobile industry-related enterprises and sub contractors and sub-sub contractors in this region at which many Brazilians are employed. However, recently the number of Brazilian workers in the food processing industry and the like has also increased.

The influx of Brazilians after the Immigration Act amendment has two major features in addition to the regional deviation of residence. The first is "family stay", and the second is "long-term stay". In Hamamatsu city[1)] in Shizuoka prefecture which has the highest number of Brazilians registered of all the municipalities in Japan, the case is seen, the figure for 'single' Brazilians decreased from 22.5% (1996) to 5.3% (2000) and the figure for 'married couples with children' increased greatly from 18.1% (1996) to 66.3% (2000). The transition from singles to families with children is notable (Hamamatsu City International Division 1996 and 2000). This is against the background of the economic downturn resulting in lower income and therefore leading to longer working hours and the continued stagnation of the Brazilian economy.

The change from 'migrant worker' to 'long term resident" and "citizen" has resulted in various social systems and services for foreigners in the affected areas.

Fig. 1. The location of Hamamatsu city, Shizuoka

II. THE INFLUX OF BRAZILIANS IN SHIZUOKA PREFECTURE HAMAMATSU CITY

The industrial city of Hamamatsu city in Shizuoka prefecture has a population of 593,899 (end of March 2003) and city limits and peripheral municipalities are home to many equipment manufacturers and their supplier companies etc. Although the economic downturn has seen the deterioration of business in recent years, the employment level of Hamamatsu city is still high compared to the national level. These present conditions have been an important factor in the increase of guest workers.

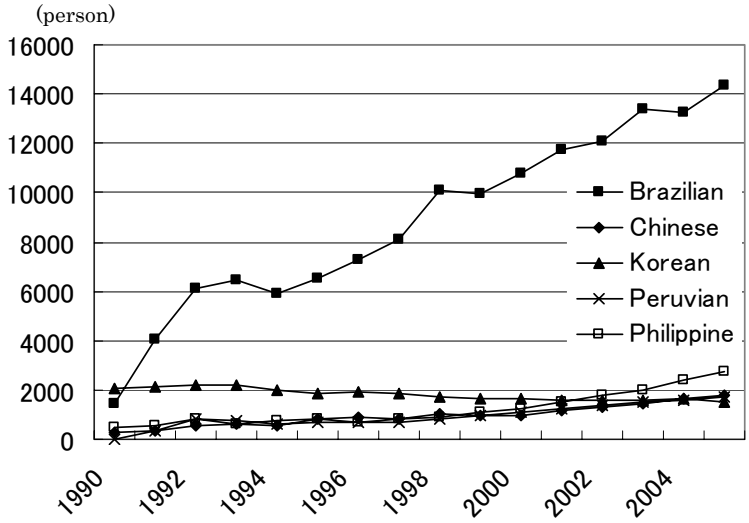

Fig. 2. Transition of the foreigner population in Hamamatsu city

After the Immigration Act amendment of 1990, in Hamamatsu city, Nikkei and their family of South American origin increased, and the number of foreigners registered in Hamamatsu city at the end of March 2002 was 20,395; 3.43% of the entire Hamamatsu population. Within this figure, the number of Brazilians was 12,111 and the number of Peruvians was 1,382, approximately seven-tenths of all foreigners. Thus, Hamamatsu city has become an area which specializes in South Americans.

Also in Hamamatsu city, in Brazilians' family structure, the shift to family stay and family stay especially accompanied by a child from solo emigration is remarkable like other cities in Japan. In addition, recently, the permanent residence visa applicants are also increasing rapidly and the movement towards family stay and settlement is progressing.

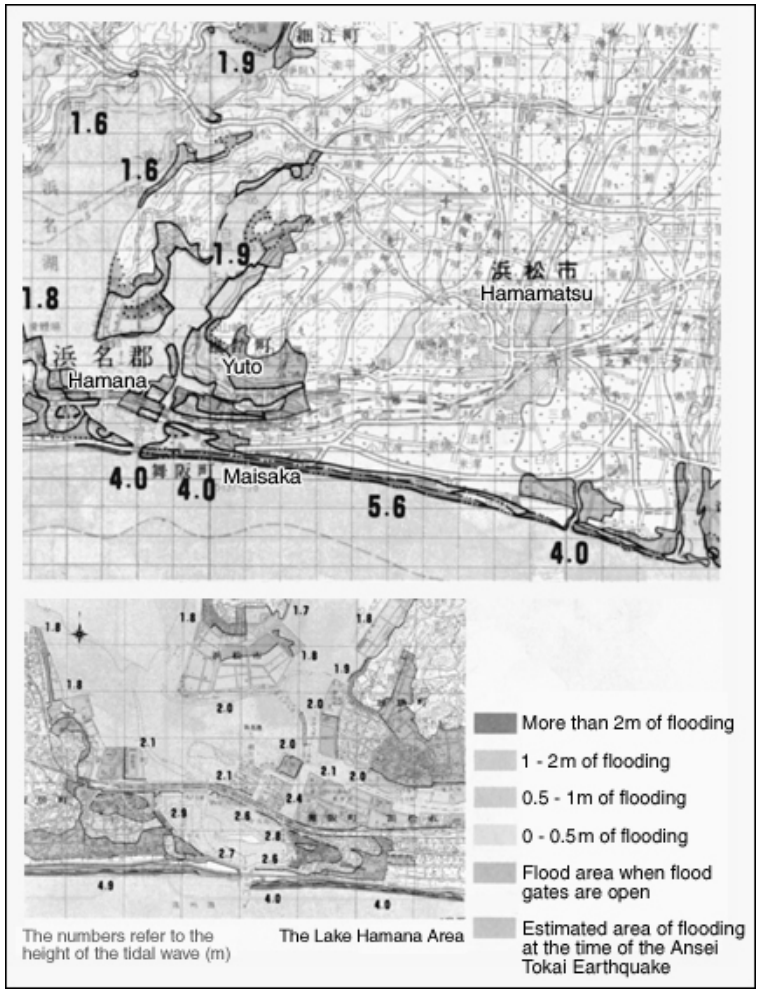

Fig. 3. Supply of disaster information to foreigners (1)
The hazard map in case of the Tokai earthquake

III. Supply of disaster information to a foreigner in Hamamatsu city, Shizuoka

This progress of Brazilians' inflow and longer residence in Hamamatsu city has significantly affected the recipient local community. In Hamamatsu city, various social systems and services for foreigners by the government, Japanese citizens' organizations, and NPOs are expanding, accompanying the increase of Brazilians. Hamamatsu city conducts widely ranging measures for Brazilians, including daily living consultation in Portuguese, which started in 1991, establishment of a foreign children/students consultation

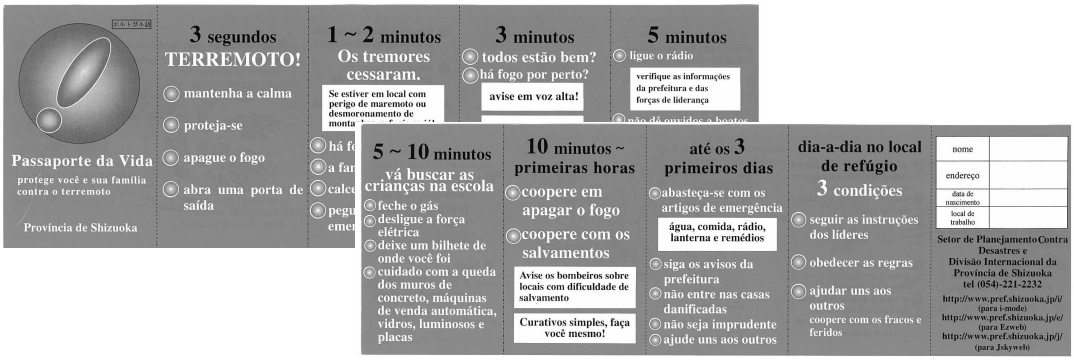

Fig.4. Supply of disaster information to foreigners (2). *"The passport of a life"* (the Portuguese version, the Spanish version, English-language edition)

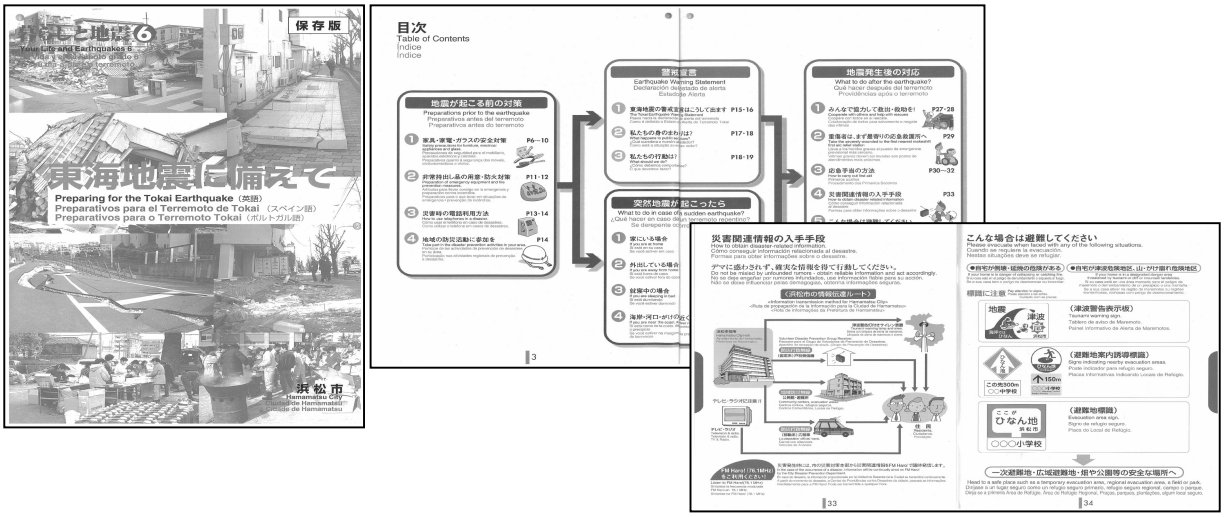

Fig. 5. Supply of disaster information to foreigners (3). Pamphlet *"hich prepares for disaste"* (Portuguese, English, Japanese writing together)

room, allocation of personnel who can speak Portuguese at administration service counters, offering Japanese language classes, providing social welfare to elderly foreigners, and publication of city bulletins in Portuguese. Recently, classes to support foreign children who do not attend school and foreigner employment issue management conferences are being conducted. In addition to these measures by the government, services such as Japanese language classes and free health checkups by local resident volunteers and NPOs are implemented.

Note that Hamamatsu city belongs to a region that can be greatly damaged in the event of the Tokai Earthquake (Figure 3). As such, the government and related organizations aggressively work to provide foreigners with information on disaster prevention and earthquake disasters.

Figure 4 shows the "Passaporte da Vida" (four language editions: Japanese, Portuguese, Spanish, and English), published by Shizuoka prefecture. This "Passaporte da Vida" explains in detail the actions one should take from the first minute to ten minutes after occurrence of an earthquake.

Figure 5 shows the pamphlet prepared by Hamamatsu city, "Preparing for a Tokai Earthquake" (written in English, Portuguese, Spanish, and Japanese). To prepare for disasters such as the Tokyo Earthquake and tsunamis, everyday disaster prevention measures, how to act after occurrence of an earthquake, etc., are written in detail.

Figure 6 is the website prepared by Hamamatsu city, "CANAL HAMAMATSU." This website explains in detail information on daily living, the mechanism of earthquakes and tsunamis, disaster prevention measures, how to respond in the event of an earthquake, etc., in preparation for a Tokai Earthquake. This information can be read in Portuguese, English, and Japanese.

Figure 7 shows the video, "Earthquake Enlightenment," which is a disaster prevention video jointly prepared and distributed by Shizuoka prefecture and a TV station called IPC in Brazil. Both Portuguese edition and English edition were prepared to explain the details, including daily disaster prevention measures and how to respond in the event of an earthquake disaster, also using actual images from the Great Hanshin Awaji Earthquake.

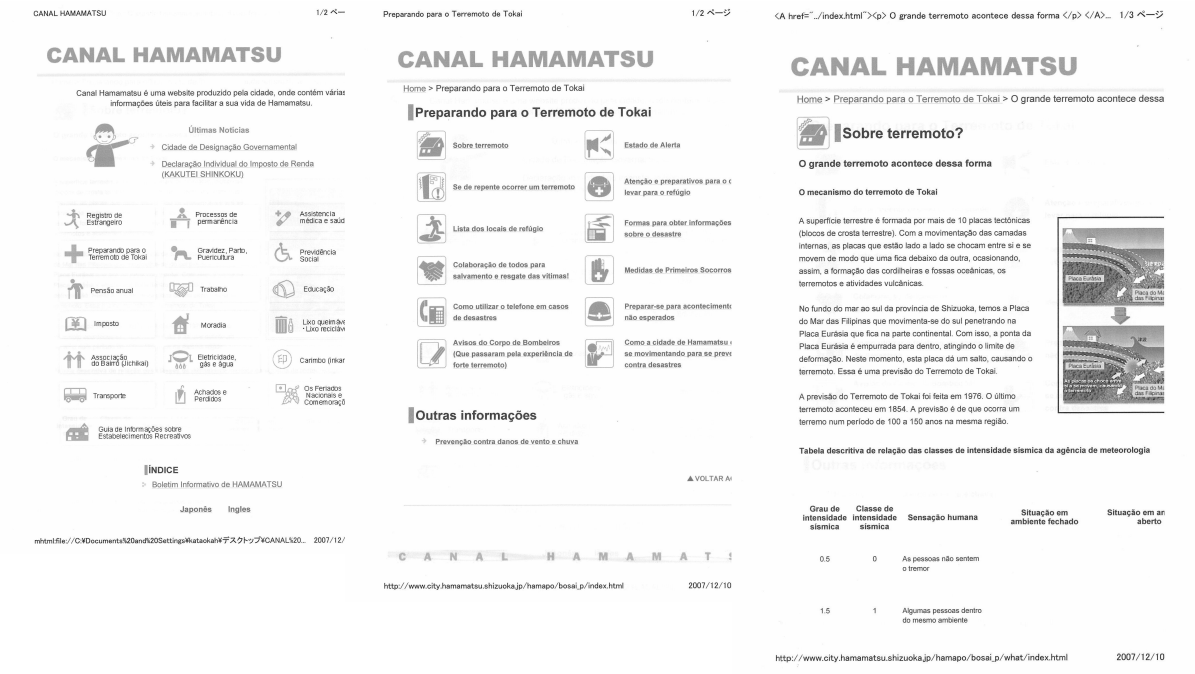

Fig. 6. Supply of disaster information to foreigners (4). Internet *"CANAL- HAMAMATSU"* (Portuguese, English)

Fig. 7. Supply of disaster information to foreigners (5). “Video Earthquake Enlightenment” (Portuguese version, English version)

IV. FUTURE ISSUES ON SUPPLY OF DISASTER INFORMATION TO RESIDENTS WITH FOREIGN NATIONALITY IN HAMAMATSU CITY, SHIZUOKA PREFECTURE

In this way, supply of disaster prevention and disaster information to residents with foreign nationality in Hamamatsu city is increasing, for example through the use of city bulletins, pamphlets, videos, and the Internet. However, it is quite doubtful that the services conducted by the government and related organizations, such as supply of disaster prevention / disaster information and other daily living information, as well as measures for residents with foreign nationality, are well known to the party concerned – residents with foreign nationality.

According to the latest survey on the actual state of living, which Hamamatsu city conducted with 1,253 South American people who live in the city, more than half of the residents with foreign nationality said, “I don’t know” or “I know but I have never used it” regarding most of the government’s services or measures for foreigners. The result shows that the city bulletins, pamphlets, videos, and website that have been prepared are not effectively used (2007 Hamamatsu City International Division). Furthermore, events such as locally conducted disaster prevention training are participated in by only a small number of foreigners. This is considered to be because local events are mainly advertised through passing bulletins (a form of communication in which a document that carries information is circulated from household to

household), and many of the residents with foreign nationality work at night and stay at home on a different time schedule from the Japanese, and have a different language and lifestyle; so, they end up not receiving the information. As such, a future issue to be resolved is how appropriately and effectively the government, related organizations, and citizens' organizations convey information to the party concerned – residents with foreign nationality.

South American residents mostly obtain information related to the recipient region through TV programs and newspapers in their native language, work colleagues, and ethnic business stores. In the future, it is desired to build effective information conveyance routes in a form that involves companies that employ residents with foreign nationality and ethnic businesses. At the time of an actual disaster, many people suffer from damages, regardless of nationality. In order to build a foundation for people to help each other and overcome such difficult situations, beyond the border of language and lifestyle, it is necessary to work on a daily basis to maintain interaction and friendly relations among residents with foreign nationalities and Japanese residents.

Services and measures for foreigners, including supply of disaster information, expand and improve according to the increase of residents with foreign nationalities, but it can be said that information is provided in the true sense only when effective functioning of such information is also considered. Aiming to thoroughly convey disaster prevention / disaster information, and to maintain mutual friendly relations, thus minimizing damages in the event of a disaster, the government, related organizations, private companies, residents with foreign nationalities, and Japanese residents need to make mutual efforts in the future.

References

The Hamamatsu City International Division. 1996, 2000, 2007. *Report of the Investigation of actual attitude of foreigners – focusing on people of South American – Japanese descent*. Hamamatsu City.

Notes

1) New Hamamatsu city contains 11 municipalities of Tenryugawa-Hamanako regions from July 1st, 2005. However, this chapter uses the former Hamamatsu city.

PART II

HO CHI MINH CONFERENCE
ON
MANGROVES

25 - 26 August 2007

An Assessment of the Changes of the Ecological Significance of Wetlands and Mangroves in the Red River Coastal Zone, Vietnam

Nguyen Tien Cong[1], Nguyen Thanh Phuong[2]

[1] *Researcher, Center for Remote sensing & Geomatics- Institute of Geological Sciences-Vietnamese Academy of Science and Technology*
tiencong@hn.vnn.vn
[2] *PhD Candidate School of Geosciences, the University of Sydney, NSW. 2006 Australia*
ntphuong197x@yahoo.com

Abstract

The coastal zone of the Red River Delta is classified and qualified for coastal wetland and mangrove by using remote sensing data of 1986 – 2003. Analysis data demonstrates that a large part of the original wetlands of the coastal area have been converted to other land use purpose. However, is has been created new other wetlands by coastal evolution and development consequences during this time. To this coastal area, a significant conflict between purposes of economic development and wetlands protection is a continuous major concern of management and researches.

To provide information and planning tools for the protection of wetland resources in the study area, Geographic Information Systems (GIS) and remote sensing data have been applied to assess the changes of the ecological significance of wetlands. The research includes three parts. Firstly, the SPOT images have been classified to delineate wetlands. The second part is an assessment of the ecological significance of wetlands given each period which of them are the most important in maintaining the environmental integrity of the area. Models introduced by Sutter (Sutter L.A., 2000, 2001), which are modified and applied, are the watershed and landscape-based wetlands functional assessment models. The models are based on using GIS software and remote sensing data to assess the level of water quality, wildlife habitat, and hydrologic functions of individual wetlands. The methodology does not apply for visiting and collecting information in individual wetlands and is the only practical approach for dealing with a large geographic area containing many wetlands within the limited amount of time and budget (Sutter L.A., 2000). The results are maps of the ecological significance of wetlands in which each wetland polygon as rating of level of functions a wetland provides to its watershed. Finally, temporal and spatial changes of wetland and their ecological significance on different periods are assessed by analyzing result maps in model on GIS environment.

INTRODUCTION

Wetlands are important ecosystem transitional position between land and water and contribute to water quality, flood attenuation, and wildlife habitat for coastal watershed (Sutter, 2001). Wetlands are usually delineated by combining characteristics of hydrology, saturated soils and vegetation (Lyon, 1993; Kent 2000; Kusler, 2003).

Coastal zone of the Red River delta is one of two the largest wetland area in Vietnam. To date, there are approximate 200 bird species in which has about 60 migration bird species, and 50 water bird species recognized in area study (Pedersen, 1996). Many rare birds as globally threatened such as Nordmann's Greenshank *Tringa guttifer*, Asian Dowitcher *Limnodromus semipalmatus*, Spoon-billed Sandpiper *Calidris pygmeus*, Grey-headed Lapwing *Vanellus cinereus*, Saunders's Gull, Chinese Egret *Egretta eulophotes*, Black-headed Ibis *Threskiornis melanocephalus*, Black-faced Spoonbill, Spot-billed Pelican *Pelecanus philippensis*, Painted Stork *Mycteria leucocephala* and Japanese Paradise-flycatcher *Terpsiphone atrocaudata* have been listed in the Vietnamese Redbook as endangered species (Pedersen. 1996). The unique habitats in this area are characterized by mudflat, alluvial ground on river mouths, salt marsh, and the thousands of hectare mangrove. Furthermore, the Red River delta has the most densely populated area in the world (Pedersen, 1996; Hien, 2005).

Vietnam economy has dramatically developed by the "Doi Moi" policy – economic liberalization began in 1986 and GDP grows in 8.5% each year. Wetlands in the coast of the Red River delta are also suffered by replacing land-use purposes. Either transforming wetland to paddy field by building new dykes seaward, or converting large mangrove area to shrimp ponds or performing weakness management manner lead to loss significant wetland along the coast. Two natural reserves, Xuan Thuy and Tien Hai locating Ba Lat mouth between Thai Binh and Nam Dinh provinces have been established in 1994. This is to give spe-

cific solution to contribute conservation, restoration, and sustainability for the coastal wetland on the Red River delta from Vietnam government.

In the historic delta evolution of the coastal Red River delta, riverine and marine hydrodynamic processes have been playing major role in accreting new tidal wetland (Nguyen Van Cu, 2006), accretion rate about 25 m/year in last several decades. Basically, mangrove forest has been raised in tidal flats by ecological progress (Hong. P, 1993).

The first natural reserve Xuan Thuy was designated as a Ramsar Site by the Bureau of the Convention on Wetlands of International Importance (the Ramsar Convention) on 20 September 1988, with an area of 12,000 ha (Hong. P 2004). The establishment of the Xuan Thuy Nature Reserve was decreed by Official Letter 4893/KGVX of the government of Vietnam, with an area of 7,100 ha on 5 September 1994. Changing area of the Xuan Thuy Nature Reserve indicates the lost of large wetland area in this site.

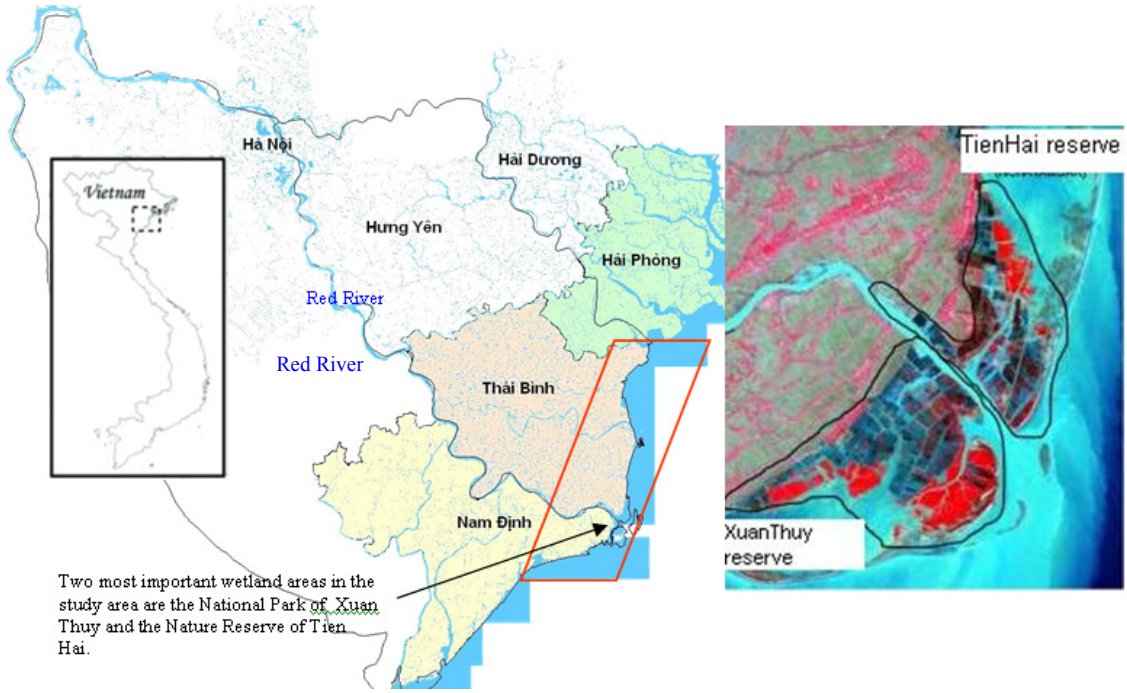

Figure 1: Area study including: The Xuan Thuy national park and the nature reserve of Tien Hai, Vietnam.

The establishment of a nature reserve at Tien Hai was decreed on 5 September 1994 the Vietnam Government. Tien Hai Nature Reserve is situated at the Balat mouth of the Red River. The site is bordered by Xuan Thuy Nature Reserve to the south, a small river to the north and the main sea dyke to the west. There are two islands within the nature reserve: Vanh Island covering 2,000 ha and Thu Island covering 50 ha (Hong. P 2004).

Evaluating sustainability of coastal natural resources management through functional wetland analysis has been paid attention by many researches (Adamus et al 1991;Hruby et al. 2000; Sutter. 2001; Turner. 2000). In general, wetland functions are refers to a process that occurs in a wetland (Adamus *et al.* 1991). The process of wetland system is grouped by its functions like water quality, flood control, habitat supply. According to Kusler (2003) all wetland do not present the same function and a wetland can performs a certain function which plays high degree comparing with another by low degree. Zaladis and Gelakis (1999) monitored and assessed change of wetland functions to evaluate efficient wetland management solutions. Assessment change of ecological wetland is carried out in wetland functions assessment models. Thiesing (1998), Hrubby(199), Kusler (2003) reviewed systematically methodologies of wetland function assessment. These researches reviewed about 90 different methods following two scales: landscape (watershed) and site-specific characteristics. Sutter (1999, 2001) built two models to assess ecological significance, which refers to the contribution that a wetland makes to its watershed as determined by the functions that the wetland performs. The most contribution to tidal wetland functions assessment is SWAMP model reported by Sutter (2001) because it can be widely applied to coastal individual wetland based on rating ecological significance of three primary wetland functions (water quality, hydrology, and habitat).

The objectives of this study is to apply GIS and remote sensing data to assess the changes of the ecological significance of wetlands based on wetland functions to provide information and planning tools for the protection and conservation of wetland resources in the study area

MATERIALS AND METHODS

Our study project includes three main stages:

- To create wetland maps from satellite imagery to monitor wetland changes though three dates: 1986 and 1991: before and after Xuan Thuy, the first wetland reserve of Vietnam recognized by the Ramsar Convention, and 2003.
- To apply wetland functions assessment model to evaluate the ecological significance of wetlands. Parameters and structure of SWAMP model is modified to correspond with geographic features of the study area. Modified SWAMP model is applied to meet with our requirements:
  - This model is the only practical approach for dealing with a large geographic area containing many wetlands within the limited amount of time and budget and does not apply for visiting and collecting information in individual wetlands.
  - This model is applied to tidal wetland study.
  - Model assessing wetland functions are constructed as a set of hypotheses about relationships between environmental conditions and the performance or sustainability of a function.
  - The models are based on using GIS data and software to assess the performance of water quality, wildlife habitat, and hydrologic functions of individual wetland.
  -
  - The result of model is a map representing the overall assessment rating that uses a hierarchical structure in which individual parameters are rated and successively combined three wetland functions mentioned above
- To assess spatial and temporal changes of wetlands and wetland functions and relate to policy conservation and resource management in the coastal Vietnam.

Figure 2: Classification sub-watersheds on SPOT image acquired in 2003

Remote sensing data

In this study SPOT imagery with ground resolution 25m and 10m acquired 3rd June 1986, on 25th May, 1991, and 23rd December, 2003 are used. SPOT imagery have been interpreted manually to identify wetland polygons of three main wetland categories such as mangrove, tidal flat, and shrubs marsh. Other land-use types like aquaculture, paddy field, village is also classified.

GIS data

Digital topographic maps was digitized with ARCGIS program from topographic maps scale 1:25.000 published in 2000, and scale 1:50.000 published in 2005. Three dimensions topographic maps depict the

geographic feature of the Red River basin and prepare to estimate its wetland boundary. In addition, land-use maps scale 1:50.000 in 2000 and 2005, hydrology system maps, and soil maps are also used to input the wetland functional assessment model. Whole data is converted to VN 2000 projection in ARCGIS software in order to standardize GIS data from different sources.

RESULTS AND DISCUSSION

Topographic maps scale 1:50.000 and 1:25.000 are digitized to create DEM of the whole delta to extract the geographical features of the Red River delta. Sub-watershed boundaries are extracted from DEM by ISRISI software. Coastal sub-watersheds are selected as boundary to identify for coastal wetland. Sub-watersheds are numbered from 11, 12, 13, 14 to 15 locating on the left side of the Red River sub-basin; and 21 covering the two wetland reserves on the right side of the Red River sub-basin (Fig 2). This wetland classification in sub-watersheds is basic to analyze and assess spatial wetland change.

Table 1: Sub-watershed's area (ha) and its percentage of wetland area in 1986, 1991, and 2003.

WSDID	11	12	13	14	15	21
subwatershed (ha)	38,703.29	1,872.65	37,123.75	6,719.25	35,716.02	26,560.31
wetland 1986	366.76	0.00	333.75	194.41	84.59	2,287.74
% per watershed	0.95	0.00	0.90	2.89	0.24	8.61
1986	L	L	L	M	L	H
wetland 1991	139.47	18.48	73.15	120.17	30.73	672.92
% per watershed	0.36	0.99	0.20	1.79	0.09	2.53
1991	L	L	L	L	L	M
wetland 2003	1,191.28	297.26	694.28	167.85	374.15	2,061.62
% per watershed	3.08	15.87	1.87	2.50	1.05	7.76
2003	M	H	L	M	L	H

A criteria based on percentage of wetland area per sub-watershed area is created to evaluate the wetland's significance in terms of its role in the landscape. The fewer wetlands there are and the more intensively used is the land in the watershed, the more significant is the wetland's function (Sutter, 1999). This criteria assigned high (H), medium (H), and low (L) is from 0 to <2%, from 2-<% to 5%, larger than 5%, respectively. Wetland area in sub-watershed 21 has either the largest area or higher significance criteria than others sub-watershed in region study. Decrease wetland's significance in 1991 and quickly increase in 2003 relative closely to mangrove restoration projects funded by non-governmental organizations and to the suitable coastal zone integration management project from 2000 (Hong. P, 2004). Table 2 and figure 3 illustrate that increasing mangrove area is an important factor to result in raising wetland's significance in sub-watersheds in region study. Besides, aquaculture area increase is one of major reasons for considerably decrease wetland area.

In Ba Lat mouth, there was obvious a large mangrove area has been recovered in the Xuan Thuy nature reserve but it is not to compare with 1000ha wetland lost and aquaculture area jumped approximately fivefold (table 3).

Wetland boundaries and types from classification results were used as one of four layer data input the assessment wetland model. Others are land cover, hydrology, and sub-watershed boundaries.

The assessment model can assess and examines how individual wetlands within a watershed contribute to three wetland functions: water quality, hydrology, and habitat in sub-watersheds for 3 dates 1986, 1991, and 2003. According to Preston, E. and B. Bedford (1990) three wetland functions were defined as:

Table 2: Comparing wetland and aquaculture area in 1986, 1991, and 2003

CODE	w86	w91	w2003
Tidal flat	9,054.48	6,855.16	3,525.57
Shrub	1,181.98	828.89	943.64
Mangrove	3,267.25	1,102.85	4,786.44
wetland Total(ha)	13,503.72	8,786.90	9,255.65
Aquaculture	766.87	1,343.61	5,840.77

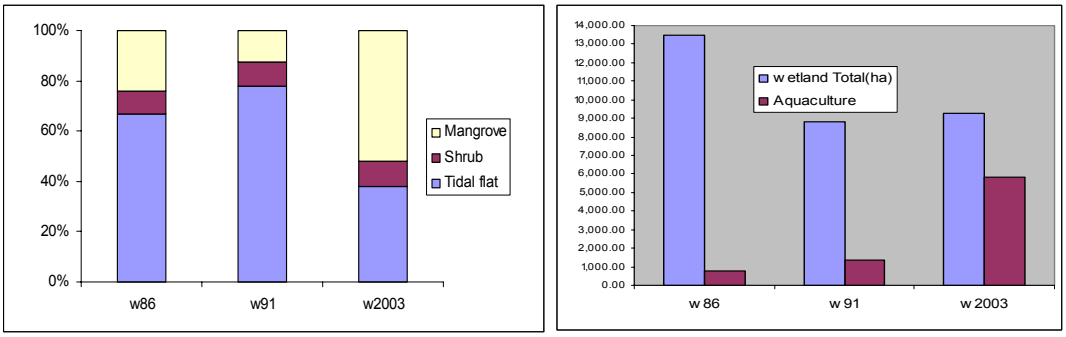

Figure 3: Relationship between aquaculture and wetland area in different periods

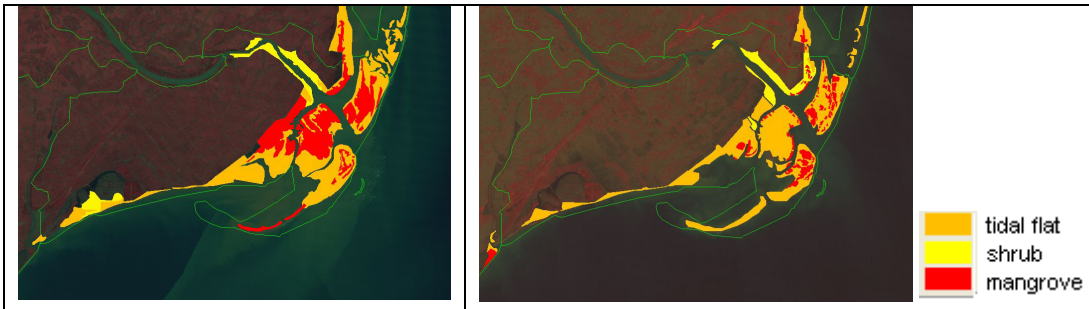

1986

1991

2003

Figure 4: The result of classification wetland from SPOT images in period 1986 – 1991 shows evolution progress: mangrove deforestation causing bare flats to prepare shrimp ponds. It is clearer to see classification result in 1991 and in 2003, tidal flats were converted to shrimp ponds; mangrove were afforested; new tidal flats were formed by accretion process. Especially, whole wetland in southern part of Ba Lat mouth was lost.

Table 3: Comparing wetland and aquaculture area in 1986, 1991, and 2003 in sub-watershed 21, Balat mouth.

CODE	2003_21	1991_21	1986_21
Tidal flat	1351.886	3305.93	3214.668
Shrub	382.427	571.383	706.872
Mangrove	2061.62	672.918	2287.738
wetland Total(ha)	3795.933	4550.231	6209.278
Aquaculture	2923.122	735.604	667.738

Hydrologic function: the capacity of wetlands to reduce and desynchronize peak flood discharge, influence base flow, and modify groundwater interactions with surface water.

Water quality function: the capacity of wetlands to remove or transform excess nutrients, organic compounds, trace metals, sediment, and refractory chemicals from water as it moves downstream.
Habitat function: the capacity of wetlands to supply the requirements (qualitatively and quantitatively) of the biota normally using a wetland system.

The model is used landscape characteristics (obtained from geographic information system analyses) rather than uses site-specific characteristics (obtained from vegetation, and land use descriptions) to derive the parameters used for examining these wetland functions because of limitation of time and budget to sur-

vey data onsite. Analyzing GIS data to derive the parameters are carried out in Arc/View® Spatial Analyst® and ARCGIS, produced by the Environmental Systems Research Institute (ESRI).

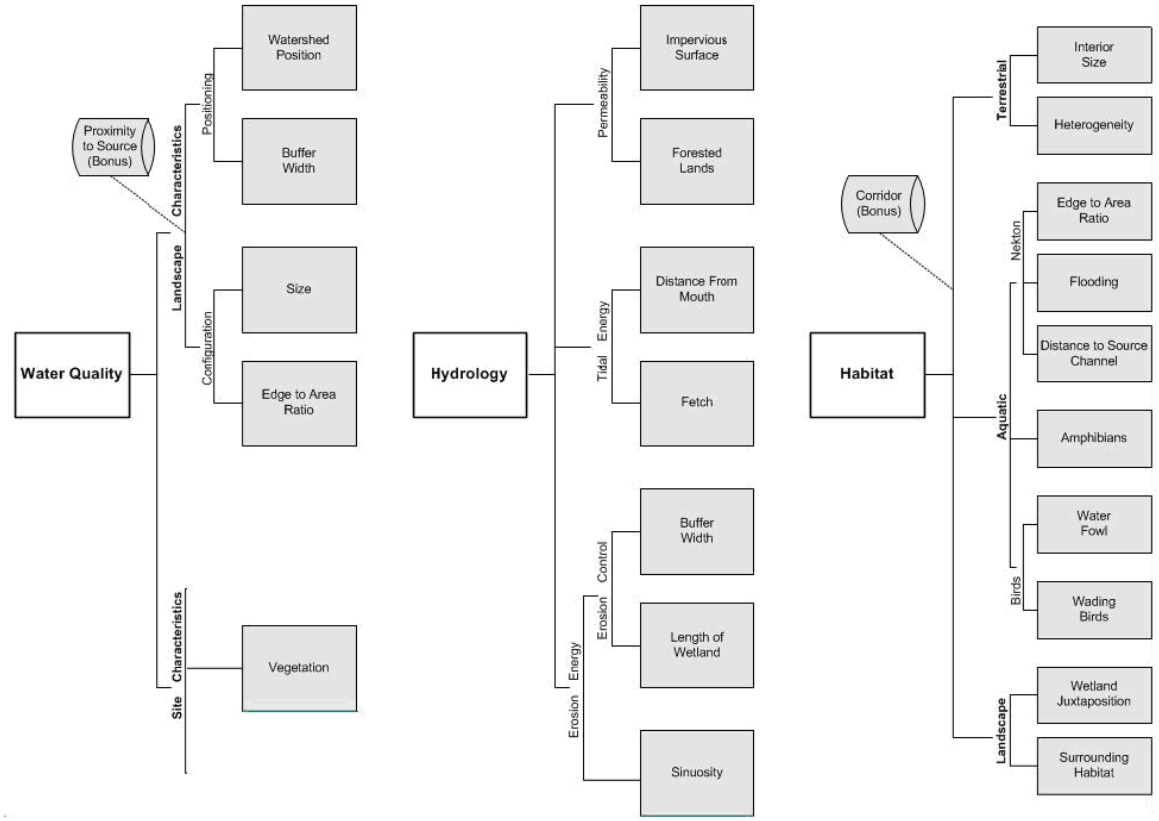

Figure 4: Structure of spatial wetland assessment for management and planning tidal module (modified from SWAMP of Sutter, 2001)

Similar SWAMP model, the hierarchal structure in the model is determined at three levels. The highest level is the wetland overall significance as well as Overall Wetland Rating (OWR). The second hierarchal level consists of the three primary functions (hydrology, water quality, and habitat) which is estimate the wetland significance functions. Basically, parameters are used to perform the wetland functions and each parameter is assigned high (H), medium (M), and low (L). The ratings of three functions is integrated an Overall Wetland Rating as rating of the wetland functional significance. This integration and evaluation are very complex. Each parameter is evaluated based on assumes relate with fundamental ecological principles about how a wetland performs a specific function. More detail about assumes see Sutter (1999, and 2001).

The result of the model is set of component maps of water quality, hydrology, habitat, and OWR maps. For example, analysis results from three wetland functions in Ba Lat mouth presents that excessive exploitation of wetland locating on the mouth causes decline wetland functions level from H to M. On the contrary, wetlands in the Lu island and Ngan island have restoration and then keep wetland functions level at H due to be limited exploration, and recover and afforest mangrove after 1991 (fig 5).

All most of wetland polygons have OWR index reaches M and H in 1986, 1991, and 2003 although wetland area decreased significantly (table 4). More 80% wetland area has OWR at M in the study time. Percentage of wetland reaching H (19%) strongly decreased to 0.94% in 1991; fortunately, the percentage recovers its old value as growth of mangrove area about 1000ha in 2003. Furthermore, identification wetland from SPOT image with spatial resolution 10x10m acquired in 2003 can delineate smaller wetland polygons than classification results in 1986 and 1991. Wetland polygons having quite small area cause landscape parameters such as edge to area ratio (water quality and habitat function), size (water quality function), sinuosity (hydrologic function), and interior size (habitat function) having low level.

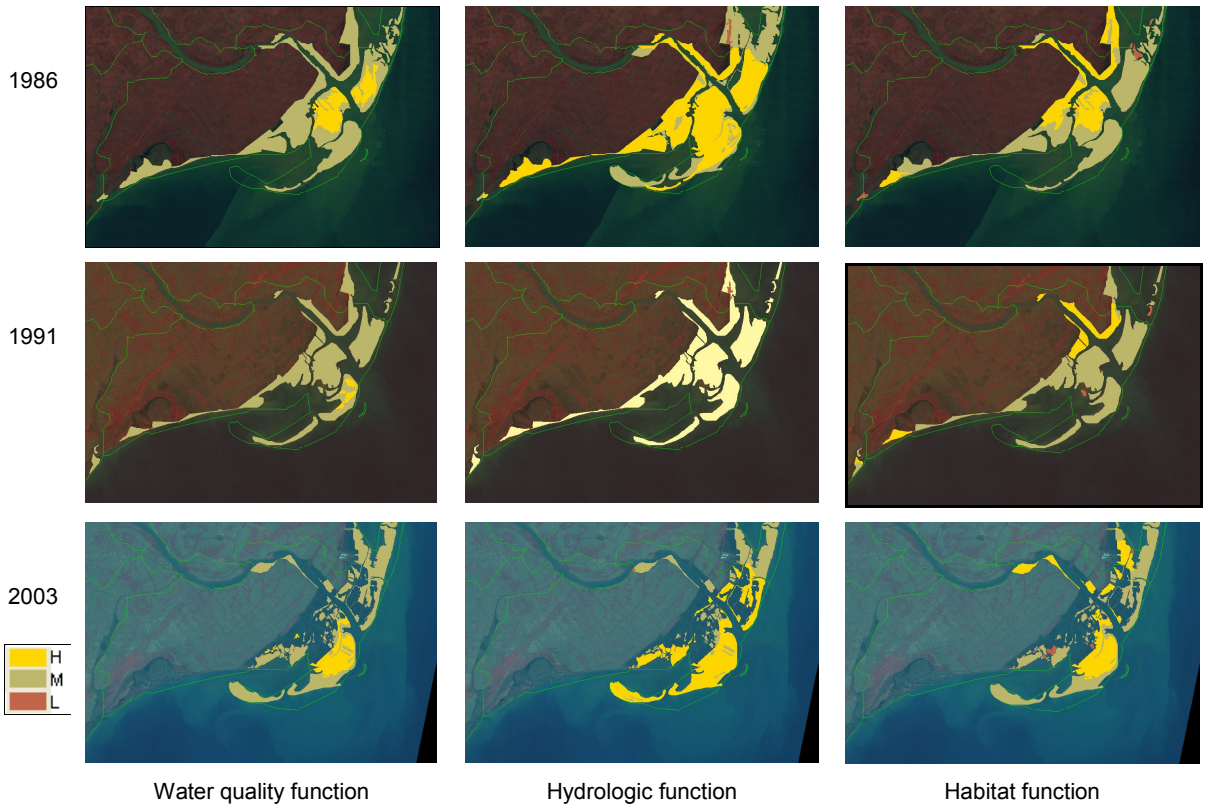

Figure 5. Assessment three wetland functions in Ba lat mouth in 1986, 1991, and 2003.

Table 4: OWR index for wetland in Ba Lat mount in 1986, 1991, and 2003

OVR/Year	L	M	H	WetlandTotal(ha)
OVR2003	7.39	7494.34	1753.92	9255.65
OVR91	0.00	8704.70	82.20	8786.90
OVR86	0.00	10961.33	2542.37	13503.70

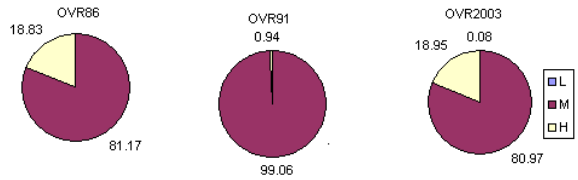

Figure 6. OWR index for wetland in Ba Lat mount in 1986, 1991, and 2003.

In Ba Lat mouth, significantly falling wetland area (from 6200ha in 1986 to 4500ha in 1991) brings to decrease OWR index from level H to level M in 1991; consequently, increase mangrove area leads increase OWR index in 2003. Studying change of land-use purposes in the two nature reserves by Hien. P *et al.* (2005) shows that "changes in mangroves are variable; there is a decrease between 1988 and 1994 followed by an increase between 1994 and 2001". Change of land-use purposes damages landscape and transforms wetland habitat features e.g. wetlands fragment that reducing their size, and coming between shrimp ponds. They lead to reduce levels of landscape parameter (habitat function) and of edge to area ration (habitat and water quality functions). Losing mangrove and change of land-use purposes in tidal flat reduce also levels of erosion and tidal energy (hydrologic function). This means that capacity of coastal wetland preventing shoreline erosive forces is worse (Sutter. 2001).

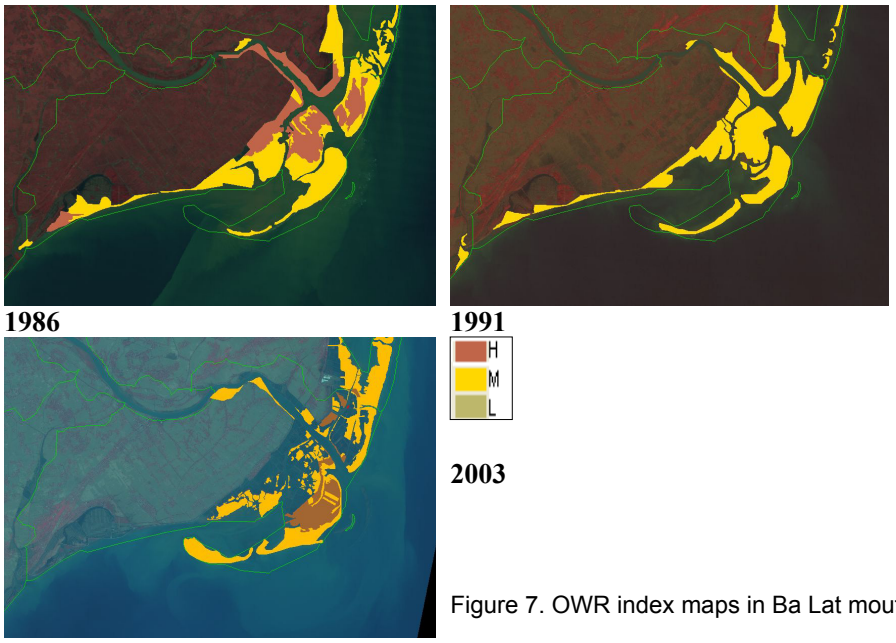

Figure 7. OWR index maps in Ba Lat mouth

To overlay OWR index maps between 1986 and 1991; and 1991 and 2003, spatial and temporal change of wetland functions is analyzed. In Ba Lat mouth (fig 8a, 8b), wetland polygons in Con Ngan Island and on two sides of this mouth decrease OWR index in period 1986 – 1991, completely lost from after 1991. OWR index of wetland polygons in Con Lu Island are fairly stable in period 1986 - 1991, because this area is the core of Xuan Thuy, the Ramsar site. Conservation and afforestation policies have contributed to enhance the ecological signification index during period from after 1991 to 2003.

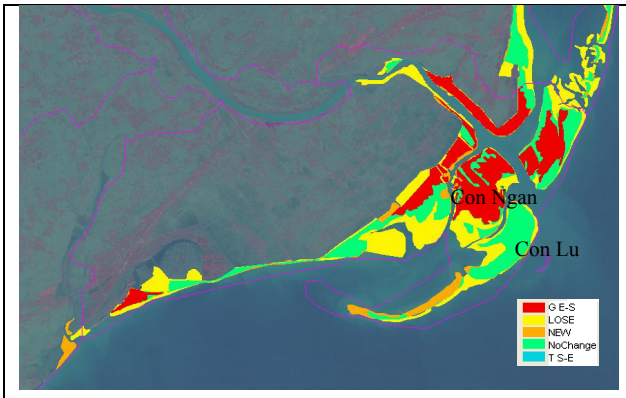

Figure 8a. Changing OWR index from 1986 to 1991 in Balat mouth

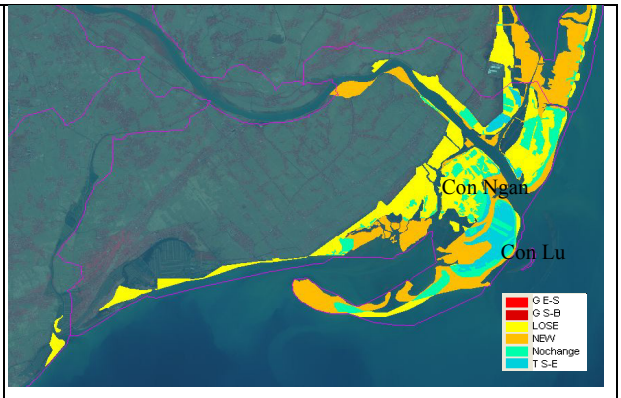

Figure 8b. Changing OWR index from 1991 to 2003 in Balat mouth

Result of analysis in change of ecological's significance of wetland for whole area study (table 5) points:

Table 5: Changing ecological's significance of wetland for whole area study

CHANGE 86-91	s(HA)	%
Decrease H to M	2,119.53	14.53
LOSE	5,785.68	39.68
NEW	1,104.30	7.57
No change	5,490.72	37.65
Increase M to H	82.20	0.56

Change 91-03	s(HA)	%
Decrease H to M	0.42	0.00
Decrease M to L	0.98	0.01
LOSE	5,227.76	36.09
NEW	5,716.79	39.47
No change	2,719.70	18.78
Increase M to H	817.77	5.65

To compare change of OWR index between two periods 1986 – 1991 and 1991 – 2003 presents that in the last period there are limitation in decline OWR index from H to M, and the area of wetland polygons having increase OWR index from M to H level grows tenfold than the previous period. Cross-table analysis in change of wetland types and change of OWR index shows that OWR index rose from M to H during period 1991 - 2003 in places including:

- over 450ha where mangrove was afforested on tidal flat, shrubs
- 40ha damaging mangrove was recovered
- about 190ha existence mangrove because afforested mangrove next to them leads to increase their landscape parameters (habitat function) and position parameters (water quality).
- about 50ha tidal flat was covered by vegetation due to ecological progress.

Change of OWR index from H to M in period 1986 – 1991 exists in 2100ha wetland area in which there were 1260ha mangrove deforested completely and 120ha mangrove deforesting.
There was 10.000ha wetland, which had been lost from 1986 to 2003. Only do wetland lose trend improves after 1991 in Xuan Thuy, Tien Hai, Thai Thuy, where applying suitable afforestation and conservation policy.

River and marine processes had continuously formed new tidal flats. There is formation of over 1000 ha in 5 years from 1986 to 1991. During 12 years (1991 – 2003) wetland area, that restored and formed, had raised tenfold (more 5000ha). These new wetland compensates to some extent the loss of wetland. It seems that, the policy to minimizing wetland loss is applied locally and whole coastal zone of the Red River delta had continuously lost wetland in constant rate from 1986 to 2003. Rising aquaculture ponds area from 700 ha (1986) to 5800 ha (2003) shows that conflict between economic development and nature conservation is happening strongly.
We have used the Pressure-State-Response framework (P-S-R) in order to analyze the relationship between wetland management and conservation policies and the result of study on changing wetlands and ecological significance of wetlands. Based on Turner (2000), we define components of this framework as following:
Pressure (P): (1) requirement of economic development leads to change land-use purposes such as dyke seaward and transform wetland to aquaculture ponds. (2) Natural coastal evolution such as accretion, shoreline position movement in the coast helps to bring about landscape status change.

State (S): spatial and temporal wetland's distribution and functions

Response (R): wetland conservation and management policies in particular and coastal zone and watershed management in general issued by the central and local government.
The relationship between these conservation and management polices and the change of wetland and its functions in the coastal zone of the Red River delta can describes as two stages:
Stage I (from 1986 to 1991): there were unsuitable wetland management and conservation policies causing large amount of wetland area lost and its function decreased under pressure of economic development (P). From 1986 Vietnam government has begun a progress of economic liberalization and integration that leads to change awareness of policy maker on sustainable development. From 1988 the Vietnamese government had been preparing planes to respond the risk of wetland lost.

Stage II (from after 1991 to 2003): since 1994, the government established the Wetland reserves as Xuan Thuy and Tien Hai. International projects focus on investigating wetland biodiversity (Pedersen, 1996), restoring and afforesting mangrove (Hong. P. 2004), and applying on integrated coastal zone management issues which improve wetland management and conservation policies of the central and local government. During this time, response (R) had influenced component of pressure (P) e.g. afforesting mangrove on new formed tidal flats, and restricting to replace mangrove by shrimp ponds as solutions to counterpoise converting existence tidal flats to shrimp ponds. These solutions have also contributed to improve wetland functions. Although, the lost rate of wetland in this period (435 ha/year) is more decrease than previous period (1157 ha/year), but amount of wetland lost is significantly large. Thus, policy makers have to improve response policies. For example, it needs to have coastal watershed's specific land-use planning and to monitor planning implementation for the Red River delta.

CONCLUSIONS

The results of analyzing spatial and temporal wetland change and its function in coastal zone of the Red River shows that wetland evolution from 1986 to 2003 describes two stages: decreasing area and functions of wetland from 1986 to 1991; recovering wetland functions from 1991 to 2003. These changes demon-

strate the relationship between economic development and protection nature resources in the study area and impact of the wetland management policies on coastal wetland ecosystems.

Applying GIS-based wetland functions assessment model and remote sensing is suitable approach to support wetland management in particular, and coastal zone management in general. The approach provides an excellent tool for regional planners to determine and rank current wetland in coastal watershed under human activities and environmental stress, estimate future impacts of land use management decisions and set achievable sustainable development goals.

In the next step, this study can be developed (1) in doing more accurate satellite image classification to identify intertidal wetland, (2) in verifying criteria to evaluate parameters in the model. That expects to make decision support system to manage more effectively the wetland in the coastal watershed of the Red River delta.

Reference

1. Adamus, P.R., L.T. Stockwell, E.J. Clairain, Jr., M.E. Morrow, L.P. Rozas, and R.D. Smith. 1991. Wetland Evaluation Technique (WET) Volume I: Literature Review and Evaluation Rationale. Wetlands Research Program Technical Report WRP-DE-2. US Army Corps of Engineers Waterways Experiment Station, Vicksburg, MS.
2. Bedford, B.L. and E.M. Preston. 1988. Developing the Scientific Basis for Assessing Cumulative Effects of Wetland Loss and Degradation of Landscape Functions: Status, Perspectives and Prospects. Environmental Management 12(5): 751-771.
3. Cu Nguyen Van 2004 - Bãi bồi ven biển cửa sông Bắc Bộ, Việt Nam. Nhà xuất bản khoa học. Hà Nội 2004 (Vietnamese version)
4. Hien Pham Thi Thanh , Martin Béland, Ferdinand Bonn, Kalifa Goïta et al. 2005. Assessment of land-cover changes related to shrimp farming in two districts of northern Vietnam using multitemporal Landsat data, EARSeL: 2nd Workshop on Remote Sensing of the Coastal Zone, Porto, Portugal, 9-11 June 2005
5. Hồng Phan Nguyên 2004 – Hệ sinh thái rừng ngập mặn ven biển đồng bằng sông Hồng, đa dạng sinh học, sinh thái học, kinh tế-xã hội-quản lý và giáo dục-NXB Nông nghiệp, 2004 (Vietnamese version).
6. Hong, Phan Nguyen and Hoang Thi San, 1993. Mangroves of Vietnam. IUCN, Bangkok, Thailand, 173p
7. Hruby, T, S. Stanley, T. Granger, T. Duebendorfer, R. Friesz, B. Lang, B. Leonard, K. March, and A. Wald. 2000 Methods for Assessing Wetland Functions Volume II: Depressional Wetlands in the Columbia Basin of Eastern Washington. WA State Department Ecology Publication #00-06-47.
8. Kent Donald M. (Edited) 2000- Applied Wetlands Science and Technology, Second Edition, CRC Press.
9. Kusler, J. 2004. Wetland assessment for regulatory purposes final report: Assessing functions and values. Institute for Wetland Science and Public PolicyScience and Public Policy, Association of State Wetland Managers, Inc., Berne, NY. [Online] URL: http://www.aswm.org.
10. Lyon, John G. 1993 Practical Handbook for Wetland Identification and Delineation. Ann Arbor, MI: Lewis Publishers, Inc.
11. Pedersen, A. and Nguyen Huy Thang 1996 The *Conservation of Key Coastal Wetland Sites in the Red River Delta*. BirdLife International Vietnam Programme, Hanoi, Vietnam
12. Sutter, L.A. et.al, 1999 - NC-CREWS: North Carolina Coastal Region Evaluation of Wetland Significance A REPORT OF THE STRATEGIC PLAN FOR IMPROVING COASTAL MANAGEMENT IN NORTH CAROLINA
13. Sutter, L.A. 2001- Spatial Wetland Assessment for Management and Planning (SWAMP): Technical Discussion. NOAA Coastal Services Center. Publication No. 20129-CD. Charleston, South Carolina, USA.
14. Thiesing MA. 1998 - An evaluation of wetland assessment techniques and their applications to decision making - Wetland inventory, assessment and monitoring: Practical techniques and identification of major issues, CM Finlayson, NC Davidson & NJ Stevenson (editors) Proceedings of Workshop 4, 2nd International Conference on Wetlands and Development, Dakar, Senegal, 8.14 November 1998
15. Turner R. Kerry, Jeroen C.J.M van den Bergh, Tore Soderqvist, Aat Barendregt, Jan van der Straaten, Edward maltby, Ekko C. van Ierland. 2000. Ecological-economic analysis of wetland: scientific integration for management and policy. Ecological Economics. Vol 35 (p 7-23)
16. Zalidis, G.C., and A. Gerakis. 1999. Evaluating the sustainability of watershed resources management through wetland functional analysis. Environmental Management 24:193-207.

Diatom and Foraminifera as Indicators of Environmental Change in Mangrove Swamps of Ca Mau Peninsula, Vietnam

Ta Thi Kim Oanh[1], Nguyen Van Lap[1], Bui Thi Luan[2], Masatomo Umitsu[3]

[1] HCMC Institute of Resources Geography, Vietnamese Academy of Science and Technology, 1 Mac Dinh Chi Str., Dist. 1, HoChiMinh City, Vietnam. E-mail: sedlap@hcm.vnn.vn
[2] College of Natural Sciences, Vietnam National University
[3] Nagoya University, Japan

Key words: Diatom, Foraminifera, Ca Mau Peninsula, Mangrove swamps, Environmental change, Human impacts

INTRODUCTION

Diatom and foraminifera have been used as the significant indicators for paleo-ecology, sedimentary environment and stratigraphical correlation in Quaternary [1, 6, 7]. Recently diatom and foraminifera are useful for studying sedimentary environment, relative sea- level changes in the Pleistocene, Holocene and environmental changes due to human impacts specially in the coastal zone and mangroves [4, 5, 8, 9]. Together with lithological features, sedimentary structure and absolute ^{14}C dating, diatom, foraminifera and molluscs contribute considerably to identify sedimentary environments related to Late Pleistocene-Holocene sea-level change in the Mekong River Delta (MRD) [2, 3, 7]. Diatom and foraminifera have many species ranging from fresh to saline and brackish to saline environments respectively, thus a compilation of both microfossils is necessary and significant for investigating the change of sedimentary environments. In this report, diatom and foraminifera assemblages from boreholes and surface sediments are used as indicators of environmental change in Camau Peninsula particularly in mangrove swamp area.

This work was supported by the Natural Science Council of Vietnam. This was part of a collaborative project between the Sub-Institute of Geography, Vietnamese Academy of Science and Technology, and the Department of Geography, Nagoya University Japan.

STUDY AREA

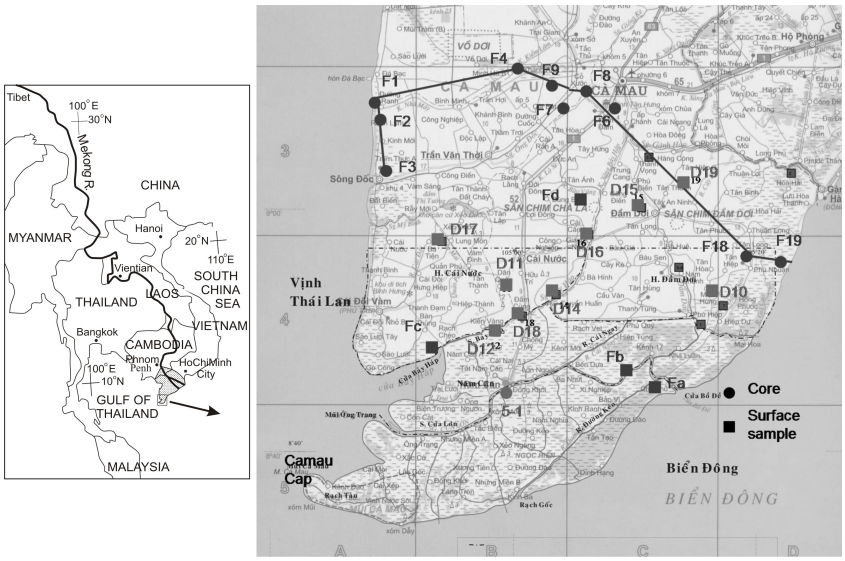

Fig. 1. Camau Peninsula in Mekong River Delta and location of cores and samples

Camau Peninsula is located in the southwestern part of the Mekong River Delta (MRD) (Fig.1). It is a flat and low plain criss-crossed by a system of rivers and tidal inlets. Mangrove swamp is a dominant landform of coastal zone at Ca Mau Peninsula where well developed mangrove forest has occupied an area

of over 90 km long and 25 km wide in the southern and southeastern. This area is subjected by two tidal regimes, semi-diurnal and diurnal tides with mean tidal ranges of 2.5-3.2 m and 0.5-1.0 m in the East and West Seas, respectively. Major longshore current patterns are induced by the monsoon regimes. Mean surface salinities are normal for sea water, around 28-30 ‰ during the winter and increases to more than 33 ‰ during the summer.

Camau Peninsular plain, a deltaic margin of the MRD, has been evolved since the last 3000 year by a tide- dominated delta progradation. Holocene sediments are characterized by the thick pro-delta/shelf mud facies, delta front mud facies, sub- to intertidal flat and marsh or mangrove swamp mud facies. The tide-dominated delta is characterized by mangrove on the subaerial delta plain.

METHOD AND MATERIAL

Environmental changes were clarified by the changes of diatom and foraminifera species from 11 core and 13 surfacial samples. Foraminifera changes were studied from 10 cores and 4 surfacial samples and diatom from 1 core and 9 surfacial samples (Fig. 1). The 9 localities taken surfacial samples, 30 to 45cm thick, were ranged from recent coast to the inland. Each surfacial samples were collected in detail with 4-5cm thick in each sample (Tab. 1, 2). The core samples were split out and described. Diatoms and foraminifera were identified and counted under optical microscope. Based on ecological spectra, these diatoms are grouped into five ecological groups, namely marine plankton, marine-brackish, brackish, fresh-brackish and fresh water. Foraminifera are grouped into calcareous and agglutinated foraminifera. Moreover, there are planktonic and benthonic foraminifera belonging to brackish species, inner and outer sublittoral and ocean sublittoral species.

Table 1. Percentage of diatom ecological group

Samples	Depth (cm)	Diatom ecological group (%)					
		A	B	C	D	E	F
D12	5	38.8	16.1	20.8	3.1	16.9	4.3
	10	39.6	12.3	29.9	1.6	14.4	2.1
	15	44.4	15.9	21.6	0.9	13.4	3.9
	20	53.3	10.9	21.8	1.2	9.1	3.6
	25	48.6	15.9	24.5	3.4	4.8	2.9
	30	40.6	12.1	34.0	2.7	7.0	3.5
D18	5	34.2	19.8	19.5	6.6	17.5	2.3
	7	33.8	24.6	18.3	5.0	15.8	2.5
	10	34.9	23.1	22.0	2.0	15.3	2.7
	14	39.5	27.5	19.5	1.0	10.5	2.0
	18	35.6	19.2	21.2	4.8	16.3	2.9
	22	35.8	18.9	25.2	1.7	16.9	1.7
	26	32.4	20.3	28.5	2.7	13.7	2.3
	30	32.9	22.8	25.1	1.4	14.6	3.2
D14	4	19.8	12.8	29.1	2.6	32.6	3.1
	7	21.7	29.7	18.9	3.8	23.1	2.8
	10	26.4	21.5	22.1	1.8	24.5	3.7
	13	30.5	22.1	18.8	1.9	23.9	2.8
	16	31.7	21.3	19.7	1.1	22.4	3.8
	20	30.3	20.6	21.3	3.2	21.3	3.2
	24	30.7	19.6	18.4	1.8	27.0	2.5
	25	29.4	26.5	14.7	1.2	25.3	2.9
	30	28.2	27.3	19.3	2.1	19.7	3.4
D16	4	20.0	19.6	23.5	9.1	25.7	2.2
	8	23.9	15.5	32.4	5.5	19.3	3.4
	12	19.9	22.9	27.9	8.0	18.9	2.5
	14	23.6	20.9	28.0	8.9	15.6	3.1
	17	21.4	26.2	27.0	5.6	16.7	3.2

A: Marine plankton B: Marine-brackish C: Brackish water
D: Fresh-brackish E: Fresh water F: unknown

Table 2. Percentage of diatom ecological group

Samples	Depth (cm)	Diatom ecological group (%)					
		A	B	C	D	E	F
D10	5	23.9	47.0	9.5	1.1	14.4	4.2
	10	25.0	42.9	18.7	1.2	10.3	2.0
	15	23.5	40.1	17.4	2.8	13.8	2.4
	20	21.7	48.3	15.0	2.8	8.3	3.9
	25	24.0	43.5	18.8	1.9	7.8	3.9
	30	24.7	41.9	19.5	4.7	6.0	3.3
	35	12.9	53.5	12.3	5.2	13.5	2.6
	40	23.6	38.5	19.9	6.2	9.9	1.9
	45	36.2	32.2	24.3	1.3	3.9	2.0
D17	4	25.5	25.5	23.4	1.3	22.1	2.1
	8	28.6	26.2	20.2	1.6	20.2	3.2
	10	27.0	24.6	16.4	4.5	23.8	3.7
	13	26.4	21.8	18.4	4.0	26.4	2.9
	19	24.7	22.0	17.3	7.1	26.3	2.7
	20	23.0	20.4	21.9	8.0	24.5	2.2
	24	26.2	21.5	18.2	7.0	24.3	2.8
	29	26.4	24.0	17.8	3.8	25.0	2.9
	28	25.8	24.0	18.8	4.8	24.0	2.6
D15	5	4.8	4.8	13.3	3.3	71.9	1.9
	10	2.2	5.7	15.9	4.0	68.3	4.0
	15	3.2	13.0	11.3	6.5	62.3	3.6
	18	9.4	17.7	14.3	2.3	53.2	3.0
	20	13.2	19.4	28.7	3.9	31.8	3.1
	30	5.7	16.5	22.8	6.3	46.2	2.5
D19	4	4.7	4.7	13.2	3.3	71.2	2.8
	8	2.2	6.2	16.0	4.0	68.9	2.7
	12	3.4	11.0	11.8	6.8	65.0	2.1
	15	8.0	14.7	15.1	2.4	56.2	3.6
	18	7.6	17.4	25.7	3.5	42.4	3.5
	22	6.0	10.6	23.8	6.6	49.7	3.3
	25	4.1	30.0	6.0	6.9	49.3	3.7
	28	8.2	20.1	17.9	6.0	44.0	3.7
D11	5	2.7	8.7	3.8	6.5	76.4	1.9
	10	2.5	10.2	5.5	3.0	75.4	3.4
	15	2.2	24.9	4.3	3.6	62.1	2.9
	20	3.2	40.1	4.7	5.4	43.7	2.9
	29	9.9	30.4	14.9	5.0	36.6	3.1

(See table 1 for legend)

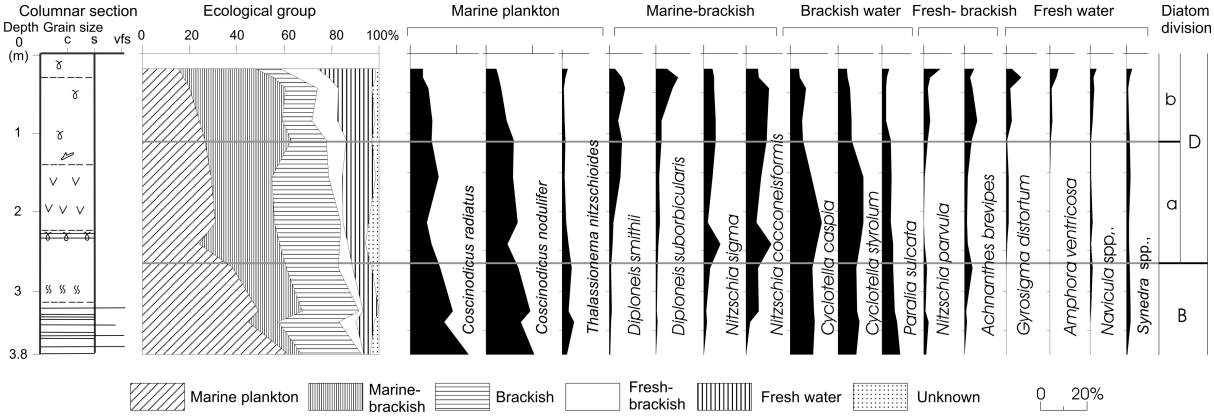

Fig. 2. Diatom division of core 5-1

RESULTS AND DISCUSSION

1. Diatom division

The stratigraphical change of diatom flora in 5-1 core is divided into two diatom divisions, namely B and D in ascending order (Fig. 2).

- B division (3.8 to -2.6 m) is characterized by the predominance of marine planktonic and brackish water species. It is composed of 38,1-61,8% marine planktonic, 21,9-25,9% brackish and 5,5-22,5% marine- brackish water groups. *Coscinodicus radiatus, C. nodulifer* and *Thalassionema nitzschioides* in marine planktonic species are common. *Cyclotella caspia*, *C. styrolum* and *Paralia sulcata* occur with low

frequency. This indicates a habitat under marine-brackish water.

- D division (2.6 to 0 m) is divided into 2 sub-divisions, namebly Da and Db.

The Da (2.6 to 1.1m) is characterized by marine- brackish, marine planktonic and brackish water groups. It is composed of 25,2-36,2% marine- brackish, 24,0-30,6% marine planktonic and 15,0-27,9% brackish water groups. The marine- brackish and fresh water species are increase from the lower to upper parts of this sub-division. Moreover the marine planktonic group is decreased considerably in comparison with the B division. *Coscinodicus radiatus*, *C. nodulifer* of marine planktonic, *Cyclotella caspia*, *C. styrolum* of brackish are common. *Diploneis smithii, Nitzschia cocconeisformis, N. sigma*, *N. granulata* of marine- brackish and *paralia sulcata* of brackish water groups occur with low frequency. This indicates a habitat under brackish water.

The Db (1.1 to 0m) is characterized by the intermixture of 32,3-40,4% marine- brackish, 14,3-24,3% fresh water 15,1-19,8% marine planktonic species. It shows that marine planktonic and brackish water species are decrease, but a remarkble increase of manine- brackish and fresh water groups in comparison with the below Da sub-division. *Diploneis smithii*, *Diploneis suborbicularis*, *Nitzschia sigma* and *Nitzschia cocconeisformis* of marine- brackish, and *Coscinodicus radiatus*, *C. nodulifer* of marine planktonic are common. *Cyclotella caspia* và *C. styrolum* of brackish water and *Gyrosigma distortum*, *Synedra* sp., *Amphora ventricosa*, *Navicula* spp., of fresh water groups occur with low frequency. This indicates a habitat under brackish water.

2. Foraminifera division

Based on foraminifera study at the cores, there are 3 foraminifera groups and namely brackish swamp, coastal disturbed and cosatal calm brackish [2]. The brackish swamp group is characterized by *Trochammina* spp., *Discorbis* spp., *Ammotium salsum* and *Arenoparella mexicana*. The coastal disturbed group is representative of *Elphidium advenum, Parrellina hispidula, Triloculina tricarinata* and *T*. sp. The cosatal calm brackish group is characterized by *Ammonia beccarii* and *Quinqueloculina seminulum*, *Pararotalia sp., and Bolivina* spp.

3. Depositional environments

Based on lithological, sedimentological characteristics, diatom divisions depositional environments of the 5-1 core (Fig. 2) are discussed as follows:

- Shallow marine/pro-delta environment

This deposit is 1.3m thick mainly consisting of dark- grey sandy silt at the 5-1 core and commonly found about 6-8m thick in this area and dated 3,7 ky. BP., [7]. Parallel laminae and discontinue parallel laminae are common. Mud content ranges from 90-95%, very fine to fine sandy layers are common at the lower part. Shell fragments, plant fragments and bioturbation scattered throughout the facies. This facies corresponds to the diatom division B and characterized by the predominance of marine planktonic and brackish water species. *Coscinodicus radiatus, C. nodulifer* and *Thalassionema nitzschioides* in marine planktonic species are common. *Cyclotella caspia*, *C. styrolum* and *Paralia sulcata* occur with low frequency. Moreover, data of foraminifera show that shallow marine foraminifera species with hyaline calcareous forms are representative of *Asterorotalia pulchella, Ammonia beccari, Elphidium advenum, Pararotalia niponica and Bolivina* spp., [2]. This indicates deposits were formed in a shallow marine and/ pro-delta environment.

- Sub- to inter- tidal flat environment

This environment is about 1.5 m thick and consisting of laminated dark gray mud. Parallel laminae are characteristic at the lower part. Bioturbation decreases and shell fragment is sparse, but organic materials become abundant, especially, with a thickness of 0.5-0.8m. It is corresponded to the diatom sub-division Da and characterized by marine- brackish, marine planktonic and brackish water groups. The marine-brackish and fresh water species are increase from the lower to upper parts of this sub-division, and clearly decreased of marine planktonic group in comparison with the below shallow marine/pro-delta environment. *Coscinodiscus radiatus, C. nodulifer* of marine planktonic and *Cyclotella styrolum, C. caspia* of brackish water are common, *Nitzschia granulata* and *N. cocconeisformis of* marine-brackish diatom species occur with low frequency. Moreover, data of foraminifera from another cores show that coastal disturbed and coastal calm brackish environments are common [2]. Foraminifera species are representative of *Ammonia* spp., *Quinqueloculina* spp*., Nonion* sp., Elphidium advenum, Parrelina hispidula (Fig. 3). It is considered

as a sub- to inter- tidal flat environment.

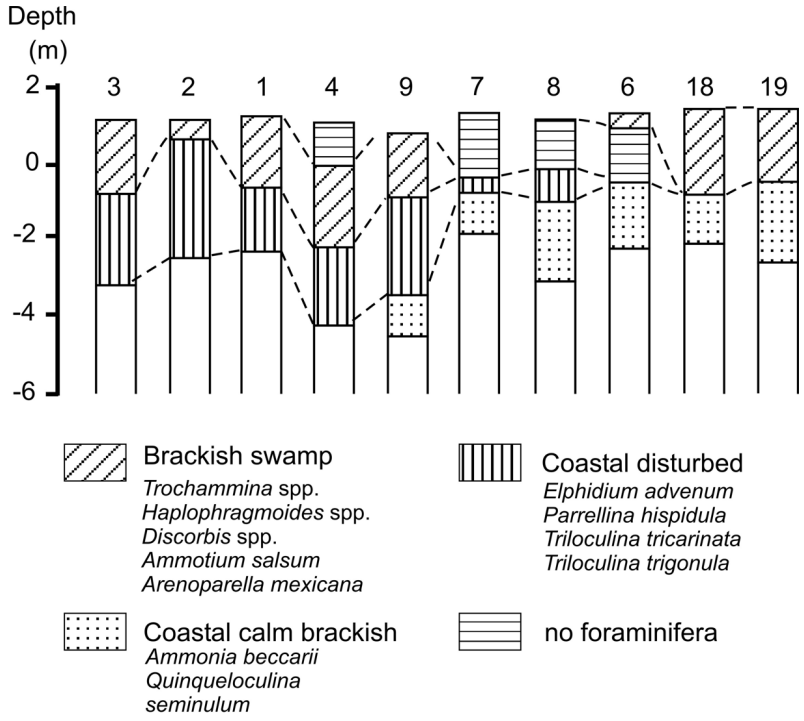

Fig. 3. Cross section with foraminiferal assemblage change

- *Mangrove swamp environment*

This environment is about 1 m thick and composed of grayish brown clayey silt to clay with rich organic matters and mica flakes. It is characterized by discontinous parallel laminae, rootless and especially color laminae. There is an increase of brackish and fresh water diatom groups, meanwhile a consederable decrease of marine planktonic and marine- brackish water groups. *Diploneis smithii*, *D. suborbicularis*, *Nitzschia sigma* and *Nitzschia cocconeisformis* of marine- brackish, and *Coscinodicus radiatus*, *C. nodulifer* of marine planktonic are common. Moreover brackish water agglutinated foraminifera species considerably increase and representative of *Miliammina* sp., *Trochammina inflata*, *Jadammina macrescens,* and *Haplophragmoides wilberti* [2]. This indicates a mangrove swamp environment.

4. Recent environmental changes

Based on ditailed studies of diatom species from surfacial samples, there is considerable change of diatom ecological groups. Distribution of diatom ecological groups taken from D12, D18, D14 and D16 indicates a change from recent coast to the inland. Marine planktonic group decreases, brackish and fresh water group increase remarkbly. Marine planktonic group gradually decreases from 39- 48% to 20- 23% at the D12, D18, D14 and D16 samples. Meanwhile brackish water group increases obviously from 20- 24% to 23- 32%, then fresh water group increases from 5- 17% to 16- 25% at the above mentioned samples. Moreover, marine- brackish water group also increases from 10- 16% to 23- 32% (Tab. 1). This indicates more marine influence near the coastline in comparison with the inland localities.

The localities of D10 and D17 are shrimp ponds, and D15, D19 and D11 are paddy fields. These localities were mangrove swamp, but under different land-uses the environments have been changed. Data of diatom ecological groups at these samples could be a good indicator of environmental changes by human impacts. Marine planktonic and marine- brackish water groups are abandant and ranging from 20- 36% and 20- 53% respectively. It indicates a high salinity with brackish environment that similar the mangrove swamp environment. In the contrast, fresh water group is dominant and range from 31 to 76% at D15, D19 and D11, meanwhile marine planktonic group is very low, about 2- 10% and marie- brackish water group ranges from 4- 24% and 20- 40% at the upper and lower parts respectively (Tab. 2).

Data of foraminifera study from localities at Fa, Fb, Fc, Fd (Fig. 1) indicate that in the surface sediments, the dominant species are the agglutinated forms and representative of *Trochammina inflate, Trochammina amnicola, Arenoparrella asiatica, Miliammina fusca* and some hyaline calcareous forms

such as *Elphidium* cf. *Incertum, Ammonia turgida.* Low density and dominance of agglutinated species of surface sediments indicate the impact of deforestation and extension of acid sulfate soils, the influence of organic matter in shrimp ponds, and the impact of pollution in a tidal channel [3].

CONCLUSIONS

The change of diatom and foraminifera assemblages in sediments from cores and surface samples indicated the changes of depositional environmental in late Holocene and recent environments in mangrove swamps in Camau Peninsula. Sub- to intertidal flat mud facies are characterized by predominance of marine-brackish diatom species with representative of *Nitzschia granulata* and *N. cocconeisformis*; brackish species including *Cyclotella caspia*, *C. Styrolum.* Foraminifera species are representative of *Ammonia* spp., *Quinqueloculina* spp*., Nonion* sp. Mangrove swamp sediments are characterized by predominance of marine-brackish, fresh-brackish diatom species with repesentative of *Diploneis smithii, D. suborbicularis, N. cocconeisformis, N. parvula, Achnanthes brevipes*. Moreover brackish water agglutinated foraminifera species considerably increase and representative of *Miliammina* sp., *Trochammina inflata*, *Jadammina macrescens,* and *Haplophragmoides wilberti*.

In recent environment, the distribution and change of diatom and foraminifera assemblages indicate the change of environment due to both natural characteristics and recent human impacts. Diatom assemblages show variation of salinity from coastline to inland or dilution by shrimp farming. The increase of agglutinated foraminifera species also indicate the impacts of deforestation or pollution channel water.

Further research on distribution and change of diatom and foraminifera should be carried out to help assessing environment impacts due to increasing human activities or natural conditions

References

1. Barbosa C. F., Scott D. B., Seoane J. C. S. and Turcq B. J., 2005. Foraminiferal zonations as base lines forquaternary sea-level fluctuations in south-southeast Brazilian mangroves and marshes. The Journal of Foraminiferal Research, v. 35, no. 1, 22-43
2. Bui, T.L., Debenay, J. P., Pagès, J., 1994. Holocene Foraminifera in the Camau Peninsula (Southern Viet Nam). Hydrobiologie Tropicale, Paris 27, 23-31.
3. Bui, T.L., Debenay, J. P., 2005. Foraminifera, environmental bioindicators in the highly impacted environments of the Mekong delta. Hydrobiologia, 548, 75-83.
4. Debenay, J-P., Guiral D., Parra, M., 2002. Ecological factors acting on the microfauna in mangrove swamps. The case of foraminiferal assemblages in French Guiana. Estuarine, Coastal and Shelf Science 55, 509-533
5. Debenay, J. P., Guillou, J. J., 2002. Ecological transitions indicated by foraminiferal assemblages in paralic environments. Estuaries, v.25, no.6A, 1107- 1120.
6. Horton B.P., Zong Y., Hillier C., Engelhart S., 2006. Diatoms from Indonesian mangroves and their suitability as sea-level indicators for tropical environments. Marine Micropaleontology 63/3-4, 155-168
7. Nguyen, V.L. and Ta, T.K.O., 2004. Latest Pleistocene- Holocene sedimentary environments of Ca Mau area. Journal of Earth Science, 26/2, 170- 180 (in Vietnamese with English abstract)
8. Sylvestre, F., et al., 2004. Modern diatom distribution in mangrove swamps from the Kaw Estuary (French Guiana). Marine Geology, 208/2-4, 281-293
9. Vance D. J, Culver S. J., Corbett D. R., and Buzas M., 2006. Foraminifera in the Albemarle estuarine system, North Carolina: distribution and recent environmental change. Journal of Foraminiferal Research, v.36, no.1, 15–33.

The Mangrove-Shrimp System in The Mekong Delta, Vietnam: Present Status, Researches, and Conservation

Bùi Thị Nga[1] , Huỳnh Quốc Tịnh[1]

[1] *Department of Environmental Sciences, College of Environment & Natural Resources, Can Tho University*

Abstract

The mangrove-shrimp system is popularly practiced in the coastal provinces in the Mekong Delta. Although the average shrimp production is low, this system is of special interest in view of sustainability of aquaculture. Extension of shrimp farming in mangrove areas occurs at a rapid rate, shrimp production has leveled off in recent years, as many aquaculture farms have either collapsed or experienced declining yields, for instance, extensive farms produced 100-400 $kg.ha^{-1}.y^{-1}$ in 1996, and 80-250 $kg.ha^{-1}.y^{-1}$ in 2000. There have been many researches of mangrove-shrimp system: aquatic ecology, nutrient cycles, soil characteristics, and socio-economic dimensions, however little is known of the knowledge of system level processes for controlling the mangrove-shrimp system.

There is the main challenge between the mangrove forest protection and the sustainable development of mangrove-shrimp system. Therefore, the expansion of mangrove-shrimp farming should pay special attention to improve aquaculture activities. To enhance sustainable shrimp production within the mangrove-shrimp system, research is needed on the key processes of ecological factors controlling pond production that is not only effective conservation of the mangrove-shrimp farming but also support local decision-maker in sustainable development of coastal area in the Mekong delta.

Keywords: Mangrove–shrimp system, ecological factor, coastal zone, sustainability

1. INTRODUCTION

Mangroves are the coastal equivalent of tropical forests. They protect the coasts from erosion caused by hurricanes that periodically scourge these tropical zones. The most common uses of mangroves and their ecosystems are extraction of firewood, material for housing, and more importantly, they serve as spawning, nursery and feeding grounds (figure 1) for many commercially important species of prawn and fish (Rasolofo, 1997; Slim et al., 1997). Recent studies also reported that mangroves enhance the biomass of coral reef fish communities (Mumby et al., 2004). Hambrey demonstrated that 1 ha of mangrove forest may support 100-1000 $kg.yr^{-1}$ of marine fish and shrimp catch. Therefore, fish production is believed to be dependent on mangrove areas, and the dependence of many penaeid shrimp species on mangroves has also been shown (Christensen, 1978; Barbier, 2000). In fact, the decline in mangrove areas in the Mekong delta certainly had an impact on the decrease in coastal fisheries production over the last decades (Graaf and Xuan, 1998).

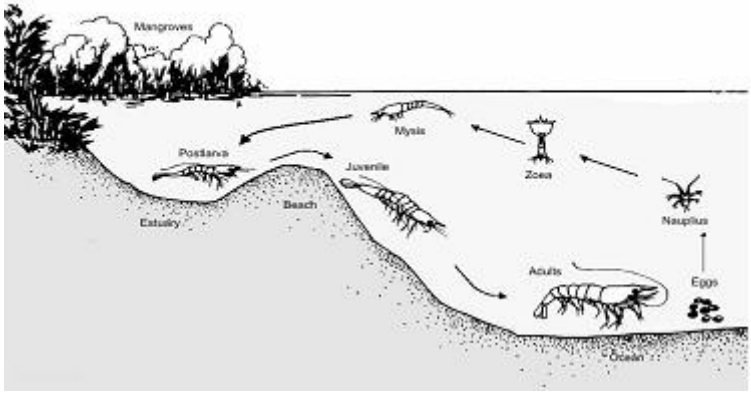

Figure 1. The life cycle of penaeid shrimps in relation to their habitat (B.T. Nga, 2004)

Figure 2. The mangrove-shrimp system in the Camau province, Vietnam

2. MANGROVE-SHRIMP SYSTEM AND THEIR EFFECTS

The Mekong delta of Vietnam is well known as a region rich in aquatic resources. Fisheries and aquaculture are very diversified practices in terms of scales and intensifications, and the coastal area shrimp culture is the major aquaculture practice, particularly the shrimp-mangrove systems were popular in most coastal provinces in the Mekong delta. In 1997, shrimp farming occupied 186,000 ha, representing extensive, improved extensive, semi-intensive and shrimp-rice culture systems (Christensen et al., 2002). The mangrove-shrimp extensive system produced 100-400 $kg.ha^{-1}.y^{-1}$ in 1996 (Johnston et al., 2000), and 80-250 $kg.ha^{-1}.y^{-1}$ in 2000 (Ministry of Fisheries, 2001). The mangrove-shrimp culture system is characterized by mangrove stands (in Vietnam mainly *Rhizophora apiculata* Blume 1827), surrounded by ditches in which shrimps are cultured and harvested regularly (figure 2).

Mangrove leaves fallen in ditches seem likely to have positive effects on shrimp production. First of all they supply nutrients (nitrogen and phosphorus), thus enhancing algal production (Roijackers and Nga, 2002). Leaves function also as a direct and indirect food source for all kinds of animals, including shrimps. The phosphorus and nitrogen concentration in decomposing leaves increased significantly during the de-

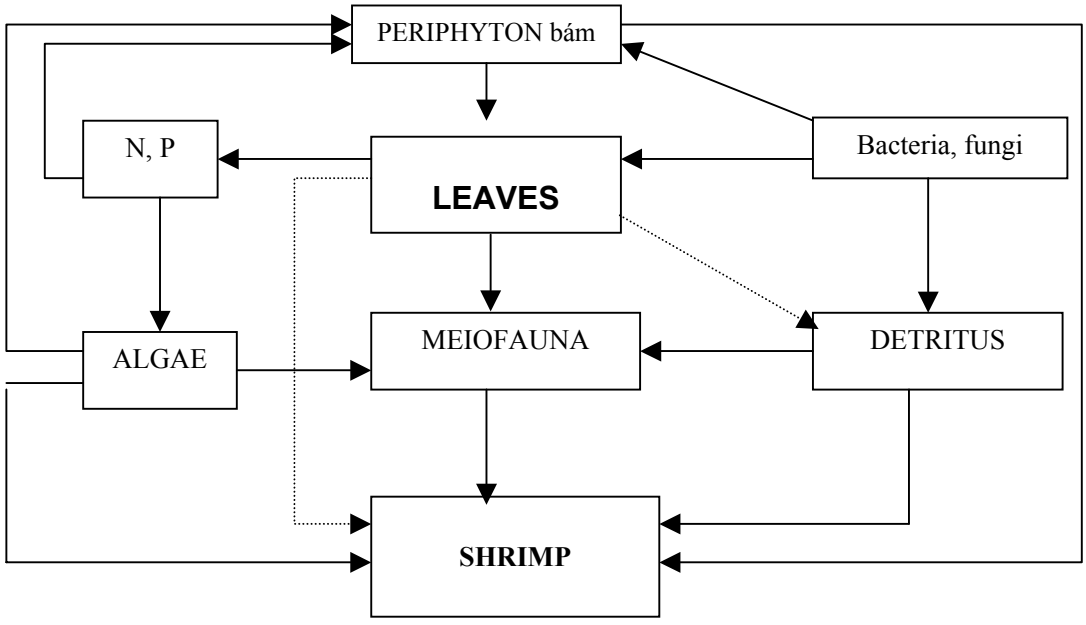

Figure 3.The detritus-based food web in mangrove-shrimp system in Camau province, Vietnam.

composition period (B.T. Nga and Roijackers 2006a). This could result in a higher food quality, thus making it more attractive to aquatic organisms (B.T. Nga et al., 2006b). This was reported by Zhou (2001) reported that meiofauna colonization on mangrove leaves varied over the decaying time: no colonization in the early stages of decomposition (1-10 days), followed by a transitional period (10-30 days) and, finally, a high colonization in the later stages (30-60 days). This suggests that such meiofauna can utilize not only periphyton but also bacteria, invertebrates and organic matter developing during leaf litter decomposition, and thus becoming themselves also a prime food source for other aquatic animals in mangrove-shrimp systems, especially for shrimps. In fact, the decomposition mangrove leaves is the crucial proccess that supplied a useful food and nutrients e.i. nitrogen and phosphorus tothe aquatic organisms, particularly shrimps as well as the detritus-based food web in the mangrove-shrimp system (figure 3).

Nutrients are released or absorbed during decomposition is the net result of mineralization and the import and export of nutrients through animal activity, translocation in fungal and abiotic processes (O'Connell, 1988). Furthermore, through the decomposition process nitrogen and phosphorus may become available to sediments where these nutrients will be absorbed by *Rhizophora apiculata* (Steinke et al., 1993; Lu & Lin, 1990).

3. STATUS OF MANGROVE-SHRIMP FARMING SYSTEM

The remaining area of mangroves in Camau and Baclieu Provinces is not known accurately, but is probably in the vicinity of 50,000 ha or less (Hong and San 1993). In the Mekong Delta, the mangrove-shrimp farming system has been practiced popularly in Camau peninsular (Nga et al, 2005). The size of farm varies 4-8 ha of mangrove forest, which farmers are required to manage for wood and fuel production. However, financial returns to farmers from aquaculture are much higher than those from mangrove forestry. Hence, most farmers are keen to expand their ponds into areas presently set aside for forestry (Lewis et al, 2003).

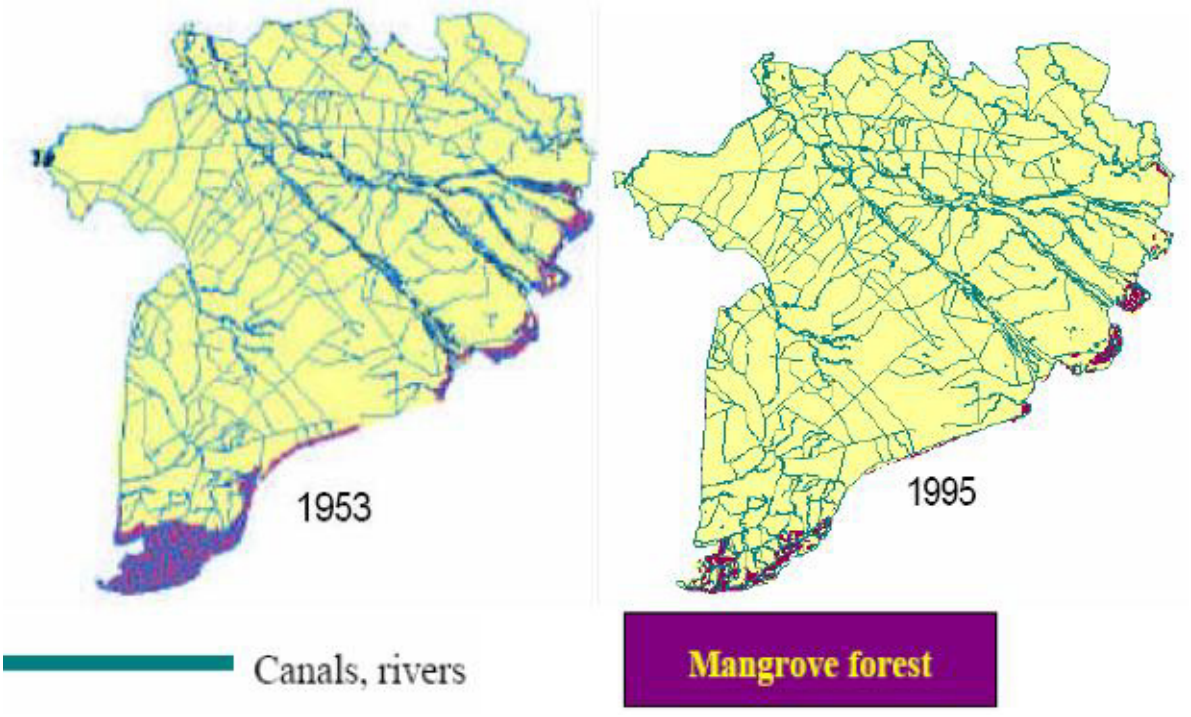

Figure 4. Mangrove clearance for shrimp farming and other activities from 1953 to 1995 in the Mekong delta

Aquaculture development in Camau Province which is the largest mangrove-shrimp area in Mekong Delta, has had a significant impact on the hydrology of mangrove areas. Many of the mangroves stands are surrounded by levee banks, or situated in areas where tidal access is hindered. In farms, where mangroves are enclosed within a levee, normal tidal flooding and flushing is prevented by constant water level in the pond. Farmers reported shrimp yields decrease when mangroves reaching of 8-10 years old. This is attributed by farmers to a lack of light from the ponds through shading of the mangrove canopies. On the other

hand, mangrove leaves have a very high tannin level, and a more likely explanation is that the decomposition of litterfall into the pond could be a relatively high level of tannin, particularly near the bottom where shrimp usually living. Regardless of the mechanisms involved, most farmers respond to the decline in pond production by cutting back the mangroves along the edge of the pond.

It is clear from the foregoing that extensive mangrove farming systems present a number of environmental and production problems, and that they require management compromises to be made that are not optimal for either shrimp culture or mangroves. These problems will become even more serious as farmers shift from extensive culture of wild shrimp to improved extensive and semi-intensive culture of *Penaeus monodon* in response to government policy for the aquaculture sector, and to socio-economic pressures (Clough et al, 2002a).

The risk of shrimp mortality from disease and poor water quality is a major factor affecting income security for farmers. The risk of mortality from disease and other causes can be reduced, and income security improved, by the adoption of better pond design and management practices. Income security would also be improved dramatically by diversification of the cultured species including mud crabs (Lewis et al, 2003). Recently, farmers gradually change from mangrove-shrimp farming system to others which diversify cultural species such as: mangrove-shrimp-crab (*Scylla species)*, mangrove-shrimp-crab-blooded cockle (*Anadara granosa*) (figure 5). The development of the farm system was rapidly and highly in 1998. The reasons are low income from mangrove-traditional farm, not enough income from mangrove-crab monoculture farm, high risk from mangrove-shrimp monoculture, and especially from new comers who came and bought from failed old farmers in 1997 (Minh et al, 2001).

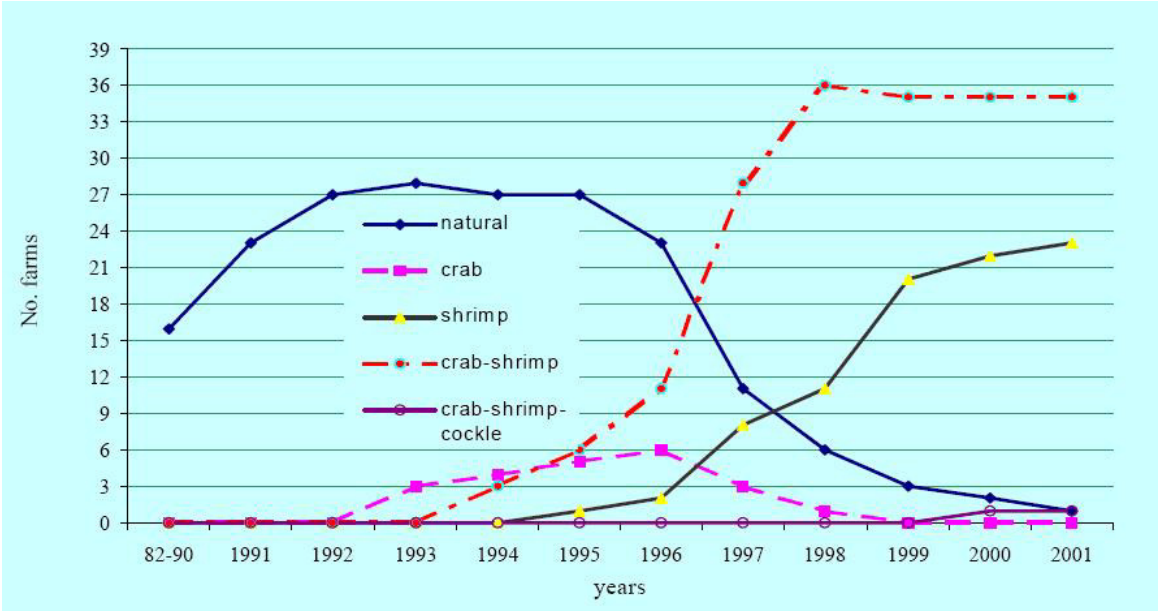

Figure 5. The dynamics of aquaculture development in mangrove area (adopted from Minh et al, 2001)

4. RESEARCHES AND CONSERVATIONS

The recent studies on species classification, tree growth, succession, silviculture, forest utilization, aquatic ecology, nutrient cycles, soil characteristics, biodiversity of associated animal in the system, and socio-economic dimensions, and litter fall of mangroves, relationship between environmental factors and mangrove structure have been carried out in Vietnam (e.g. Nam and Thuy, 1997; Clough et al., 2000b; Loi et al., 2002; N.T. Phuong 2004; B.T Nga et al, 2005; T. T. Nga et al., 2005, H. Q. Tinh, 2007). However, the ecosystem level processes for controlling the mangrove – shrimp system are still not clearly yet.

At the present, the monoculture of tree species, which have high economic value, and water management in mangrove-shrimp system not only reduce the forest's quality but also the system's biodiversity. Therefore, the expansion of mangrove-shrimp farming should pay specially attention to improve aquaculture activities. Moreover, we found the main challenge between the mangrove forest protection and the sustainable development of mangrove-shrimp system in the coastal areas in the Mekong Delta.

To enhance sustainable shrimp production within the mangrove-shrimp system, research is needed on the key processes of ecological factors controlling pond production that is not only more effective conser-

vation of the mangrove-shrimp farming but also support local decision-maker in sustainable management of coastal area in the Mekong delta.

References

B.T.Nga (2004), Penaeus monodon post-larvae and their interaction with *Rhizophora apiculata*. Ph.D thesis, Wageningen University, The Netherlands.

B.T. Nga, H.Q.Tinh, D.T. Tam, M. Scheffer, and R. Roijackers (2005), Young mangrove stands produce a large and high quality litter input to aquatic system in Camau province, Vietnam. Wetland Ecology and Management 13: 569-576.

B.T.Nga, R Roijackers, T.T. Nghia, V.N.Ut, M. Scheffer, 2006b. Efects of decomposing *Rhizophora apiculata* leaves on larvae of the shrimp *Penaeus monodon*. International Aquaculture 14: 467-477

B.T.Nga, R. Roijackers, 2006a. Effects of decomposition and nutrient release of *Rhizophora apiculata* leaves on the mangrove-shrimp systems in the Camau province, Vietnam. Selected papers of the workshop on the fourth Internatiọnnal symposium on southeast Asian Water Environment Thailand: 49-58.

B.T.Nga, R. Roijackers, T.T.Nghia, 2007. Effects of feed amendments on shrimp-mangrove systems in the Mekong Delta, Vietnam. Selected papers for oral presentation of the Summit on Ecological Sustainability: Challenges and opportunities for 21st- century Ecology in Beijing, China.

Barbier, E, B., 2000. Valuing the environment as input: review of applications to mangrove-fishery linkages. Ecol. Economics 35: 47-61.

Christensen, B. 1978. Biomass and primary production of *Rhizophora apiculata* in a mangrove in southern Thailand. Aquatic Botany 4: 43-52. Barbier, E, B., 2000. Valuing the environment as input: review of applications to mangrove-fishery linkages. Ecol. Economics 35: 47-61.

Christensen, S. M., Macintosh, D. J. and Phuong, N. T., 2002. Enhancing income opportunities in mangrove-aquaculture systems by introducing semi-intensive Mudcrab aquaculture, preliminary studies. Selected papers of the worshop on Integrated Management of Coastal Resources in the Mekong Delta, Vietnam: 73-83.

Clough, B., D. Johnston, T.T. Xuan, M.J. Phillips, 2002a. Silvofishery Farming Systems in Ca Mau Province, Vietnam. Report prepared under the World Bank, NACA, WWF and FAO Consortium Program on Shrimp Farming and the Environment. Work in Progress for Public Discussion. Published by the Consortium. 70 pages.

Clough, B., Tan, D.T., Phuong, D.X. and Buu, D.C. 2000b. Canopy leaf area index and litter fall in stands of the Mangrove Rhizophora apiculata of different age in the Mekong Delta, Vietnam. Aquatic Botany 66: 311-320.

Graaf, G.J. and Xuan, T.T. 1998. Extensive Shrimp Farming, Mangrove Clearance and Marine Fisheries in the Southern Provinces of Vietnam. Mangroves and Salt Marshes 2: 159–166.

H.Q. Tinh, 2007. Relationship between Environmental Factors and Mangrove Structure at Mui Ca Mau National Park, Vietnam. Faculty of the Graduate School, University of Philippines Los Baños in Partial Fulfillment of the Requirement for Degree of Master of Science (Environmental science).

Hambrey, J., 1996. Comparative economics of land use options in mangrove. Aquaculture Asia 1, 2: 10-14.

Hong, P. N. and San, H.T. 1993. Mangroves of Vietnam. IUCN Wetlands Programme. Bangkok Thailand, 1-173.

Johnston D., Trong N. V., Tuan T. T. and Xuan T. T. 2000. Shrimp seed recruitment in mixed shrimp and mangrove forestry farms in Ca Mau province, Southern Viet Nam. Aquaculture, 184: 89-104.

Lewis, R.R. III, M.J. Phillips, B. Clough and D.J.Macintosh, 2003. Thematic Review on Coastal Wetland Habitats and Shrimp Aquaculture. Report prepared under the World Bank, NACA, WWF and FAO Consortium Program on Shrimp Farming and the Environment. Work in Progress for Public Discussion. Published by the Consortium. 81 pages.

Loi, L.T., Tri, L.Q. and Tee, J. 2002. Biomass of Rhizophora apiculata and soil characteristics in the coastal area of Camau province, Mekong Delta, Vietnam. Selected papers of the worshop on Integrated Management of Coastal Resources in the Mekong Delta, Vietnam: 65-70.

Minh,T.H., Yakupitiyage, A. and Macintosh, D.J. 2001. Management of the Integrated Mangrove-Aquaculture Farming Systems in the Mekong Delta of Vietnam. ITCZM Monograph No. 1: 1-24.

Ministry of Fisheries, 2001. Report on the Fisheries development in the Mekong Delta and its development plan for the period from 2001-2005: 49 pp.

N. T. Phuong, T. H. Minh and N.A. Tuan, 2004. Overview of *Penaeus monodon* Culture Models in Mekong Delta. College of Aquaculture, Cantho University, Vietnam.

Nam, V.N. and Thuy, N.S. 1997. The biomass of a *Rhizophora apiculata* plantation in Can Gio district, Ho Chi Minh city. Proceeding of National workshop on the relationship between mangrove reforestation and coastal aquaculture in Vietnam, CRES-ACTMANG, Hanoi.

O'Connell, A.M.,1988. Nutrients dynamics in decomposing litter in karri (*Eucalyptus diversicolor*) forest of South-western Australia. J. Ecol. 76: 1186-1203.

Rasolofo, M.V., 1997. Use of mangroves by traditional fishermen in Madagascar. Mangroves and Salt Marshes 1: 243-253.

Roijackers R. and Nga B. T., 2002. Aquatic ecological studies in a mangrove-shrimp system at the Thanh Phu state farm, Ben Tre province, Viet Nam. Selected papers of the workshop on Integrated Management of Coastal Resources in the Mekong Delta, Vietnam: 85-94.

Slim, F.J., Hemminga, M.A., Ochieng, C., Jannink, N.T., Cocheret de la Moriniere, E. and van der Velde, G., 1997. Leaf litter removal by the snail *Terebralia palustris* (Linnaeus) and sesarmid crabs in an East African mangrove forest (Gazi Bay, Kenya). J. Exp. mar. Biol. and Ecol. 215: 35-48

T.T.Nga, E.C. Ashton, H.Q. Tinh, V.N. Thao, 2005. Mangrove Productivity Compared Inside And Outside Of Mixed Integrated Mangrove-Shrimp Farms In Ca Mau, Vietnam. International Journal of Ecology and Environmental Sciences No 31(3): 157-162.

Zitzen (1999), Water quality exchange in a sluice gate controlled extensive mangrove-cum-shrimp system at the Thanh Phu, Ben tre province, Viet Nam. Msc. Thesis at Wagenningen University, The Netherlands

Mangrove Community Institutional Development: Experience of Pred Nai, Trat, Thailand[1]

Somying Soontornwong, Tanongsak Janthong

Thailand Collaborative Country Support Program, RECOFTC

Abstract

Trat province contains the second largest mangrove forest area in Thailand. Much of it had been deforested during the 1980s because of the establishment of shrimp farms, heavily promoted in the national government's social and economic plan at the time. The Pred Nai Mangrove Conservation and Development Group, a local community organization, was formed in 1986 to campaign against local forest deforestation and to develop a sustainable system for the management of mangrove and marine resources. Over the course of twenty years, the group has developed strong forest management institutions through a participatory approach that seeks to involve a diverse range of community actors, particularly poorer households. They have also established good working relationships with government agents and, with RECOFTC's support, have reached out to neighboring villages to establish a provincial Mangrove Network that has linked up with regional and national forestry networks. Pred Nai's success in collaborating with government and non-government agencies and networking with other forest communities serves as a valuable case study in participatory CBNRM from which other forest communities and practitioners can learn.

Key words: Equity, participatory process, community rights, natural resource access, community organization institutional development and networking.

INTRODUCTION: AN OVERVIEW OF PRED NAI MANGROVE COMMUNITY

Pred Nai village is located in the Mueang district of Trat province, Thailand. The total village area of 2,367 *rai* (379 hectares[2]) comprises residential properties, public lands and agricultural lands. To the east of the community lie the Para commercial rubber plantation and fruit orchards of durian, rambutan, pineapple, and pomelo. To the west are fish and crab cultivation farms, and beyond these are mangroves.

The total population of Pred Nai is 601 persons, distributed among 137 households. Most of the community members are Buddhist, while some are Muslim. Fruit orchards and rubber plantations form the basis of most villager livelihoods, but residents are also involved in other forms of agriculture as well as fisheries and daily wage labor. While some households manage shrimp and fish farms, most families harvest fishery products from the mangrove forest.

The mangrove forest in this region covers an area of approximately 10,430 *rai* (1,669 hectares). 12 main and 6 minor canals provide access routes into the forest. There are also 15,000 *rai* (2,400 hectares) of coastal conservation area in the region. While much of the mangroves and coastline became degraded in the 1980s due to the establishment of shrimp farms, many areas of forest have since been rehabilitated due to local community efforts.

Pred Nai residents utilize the mangrove forest primarily in the collection of timber and non-timber forest products (NTFPs). Mangrove trees provide a variety of wood products, such as cucumber wood stakes; however timber extraction has declined since the community campaigned against logging for wood stakes in 1995. Non-timber products consist primarily of foodstuffs; mollusks, wild vegetables, samae crab or

[1] Informantion in this paper is primarily drawn from the following three reports: 1) Improving Rural Livelihood Through CBNRM: A Case of Self-organization in Community mangrove Management in Thailand by Somying Soontornowng, 2005. 2) Community Profile: Pred Nai, ThCCSP, 2007. 3) Focus group discussion of Pred Nai Mangrove Conservation and Development Group in June 2007.

[2] 1 hectare (ha) is equal to 6.25 *rai*.

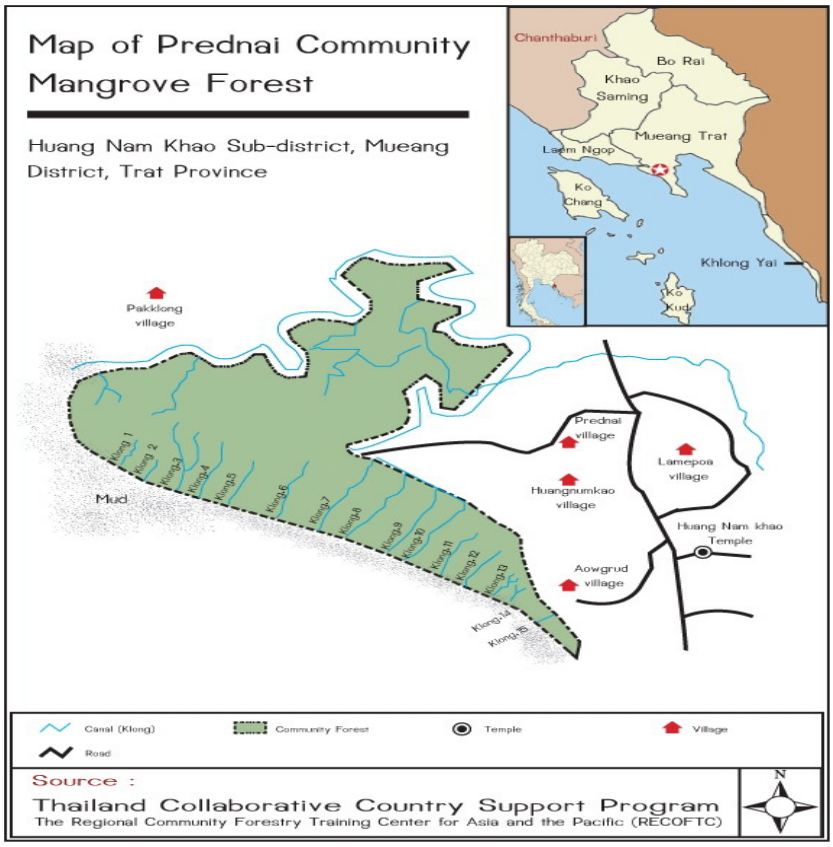

Map 1: Thailand and the Pred Nai Mangrove Community

grapsoil crab (*Metapographus* species), mud crab (*Scalla serra*), and both brackish water and marine fish are harvested for both household consumption and commercial sale. These are mostly sold onto middlemen as either fresh or processed products and are both a primary or secondary source of income for both community members as well as outsiders.

TWENTY YEARS EXPERIENCE: THE PRED NAI MANGROVE CONSERVATION AND DEVELOPMENT GROUP

Shrimp aquaculture flourished in the 1980s, and the local economy became quite dependant on it as a source of income. However, the industry collapsed between the years 1990 and 1996, and falling prices caused a dramatic increase in the debt of local villagers. During this period, villagers noticed an increase in the degradation of the mangrove ecosystem and a scarcity of other marine products due to shrimp farming practices and the extraction of wood for charcoal production. The Pred Nai Mangrove Conservation and Development Group was first organized in 1986 to develop a sustainable system for the management of mangroves and marine resources. This group has worked to successfully involve a diverse group of actors, both within and outside the community, in the sustainable management of the local mangrove forest.

The Pred Nai Mangrove Conservation and Development Group is currently comprised of a sixteen-member managing committee. This includes 1 chairperson, 2 vice-chairs, 1 secretary, and 6 sub-groups composed of 2 members each. Four of these subgroups are

each tasked with monitoring a particular forest zone, while the remaining two provide eco-tours and home-stay services for village visitors. The committee also has a seven-member advisory group.

The group has three primary objectives: 1) the conservation and restoration of the mangrove forest for the regeneration of aquatic resources; 2) preventing exploitation of local natural resources by outsiders; and 3) the development of the community and the mangrove forest for future generations. Members of the group's managing committee also have a very strong sense of ownership regarding the mangrove forest and are currently campaigning to have the area legally recognized as a community forest. The group is also working to ensure that landless villagers in Pred Nai (an estimated 20-30% of total households) have greater equity and access to the mangrove resources (RECOFTC/ThCCSP Report 2003).

To organize the local community, the Pred Nai Mangrove Conservation and Development Group initially drew upon the strength of local traditions and village elders such as Phra Subin Pyuto,[3] a respected monk. The group began inviting everyone to collaborate using the village savings group fund as a base for meetings and discussion. These gatherings led to the initiation of a management plan that sought to increase planting in the mangrove area and to allow some sections to naturally regenerate. Government agencies and other supporting organizations, such as the Social Investment Fund (SIF), the Thailand Research Fund and the Education Institute, also stepped in to support the community in its conservation efforts.

The Community Mangrove Forest Management Movement[4]

Period	Situation and activities
1983	- Mangrove forestland is cleared to make way for extensive shrimp farms, which were introduced by outside investors and promoted by government policies.
1983-1985	- Local villagers form a group to protest against mangrove destruction. The group attempts to involve all community members to foster better understanding of the issues at stake and greater cooperation in initiating protest activities.
1986	- Politicians support the local community protests against mangrove destruction.
1986-1987	- Substantive protection measures for the mangroves are established through local collaboration and the support of government officials from the Royal Forestry Department, the Royal Thai Navy and the local police force. The investors abandon their shrimp farms. - A mangrove conservation group is established. Named the Pred Nai Mangrove Conservation and Development Group, this group consists of 6 sub-groups, four of whom are responsible for monitoring and safeguarding an assigned zone within the forest and two of whom provide eco-tour and homestay services for community visitors.
1987	- After the shrimp farm investors leave, mangrove reforestation is implemented according to local traditions and knowledge.
1999	- A mangrove community forest management plan is initiated. The process encompasses forest assessment and inventory, management zoning, the development of agreements to formulate species utilization rules in each management zone, and the development of a mangrove network with neighboring villages to improve forest management and coastline protection.
2000- 2003	- Community-initiated activities to increase fishery products include the study of the mud crab population and the establishment of a crab bank, the building of artificial reefs, and mangrove replanting. Pred Nai begins cooperating with neighboring villages in mangrove management, and Trat Conservation Network is formed.
2004-present	- Research to reduce coastline erosion is implemented. Activities include constructing bamboo fencing and artificial reefs out of used tires to keep fishing boats away from the coastline. - The Trat Conservation Network is expanded to include forest communities within the four eastern coastal provinces of Thailand (Chantaburi, Rayong, Chonburi, and Trat). - Pred Nai has by this time earned a reputation as a 'learning center' for CBNRM. Many interested outsider groups and organizations begin visiting the community to learn from its experience in resource management.

[3] Pra Subin Pyuto initiated the Savings Group in Trat Province. His idea of a savings group and strengthening civil society in rural areas has expanded and been linked with other provinces along Thailand's eastern coast.
[4] Source: Pred Nai Community Profile, ThCCSP, 2007.

The current community mangrove forest management plan drawn up by the group covers five main topics. These include: 1) forest management classification and zone; 2) guidelines on the use and collection of forest products; 3) forest protection regulations; 4) group organization and administration; and 5) the expansion of networks.

Generally, the plan offers guidelines for the protection of current forest resources, reforestation by annual planting, and a sustainable utilization and monitoring program. The monitoring program involves undertaking an inventory of the forest ecosystem and the natural resource base every 3 years. The plan also includes principles for local organization administration and development, and a networking strategy to develop collaboration on the management of marine and coastal resources with neighboring villages and other community forestry networks in the Upper Gulf of Thailand.

The management plan also details the regulations concerning the harvesting of forest products such as timber, crabs, fish, shrimp, mollusks, bees and fireflies, and other wildlife. These rules define the rights of the local community and outsiders in accessing and utilizing forest products.

Community participation has been a key principle in the process of drawing up and implementing the mangrove forest management plan. As the planning phase requires participatory data collection and group discussions between the forest users and community leaders, issues of livelihood development and user rights are taken into account in the formulation of forest regulations and management practices. Participatory management approaches also creates an opportunity for different forest user groups to learn from and share one another's experiences.

ACHIEVEMENTS OF THE COMMUNITY MANGROVE FOREST MANAGEMENT SYSTEM

Since the implementation of the mangrove community forest management plan, the following results have been achieved:

- **Mangrove and coastline areas have been significantly rehabilitated due to better protection policies and practices.** Large-scale mangrove deforestation came to an end with the prohibition of forest concessions and the curtailment of intensive shrimp farming activities. Trawlers and push nets have been banned from fishing practices in the coastline areas, which are also now protected by artificial coral reefs. Monitoring and observation exercises have demonstrated that as a result of these actions, mangrove and marine resources have significantly increased and previously absent plant and wildlife species are returning to the area. Important water bird species that have returned include the Painted stork (*Mycteria leucocephala*), the Purple coot (*Porphyris poliocephalus*), the Purple heron (*Ardea purpurea*), the Grey heron (*Ardea cinerea*), the Indian Whistling Duck (*Dendrocygna javanica*), and the Brahminy Kite (*Haliastur indus*). The presence of these species attests to the health of the forest and the ecosystem food chain. Other mangrove species that have seen a resurgence in population include the Crab-eating macaque (*Macaca fascicularis*), *kob i-ae* (a type of frog), and the clam species *Solen strictus*. (Sukwong, 2004)

- **Harvest yields of non-timber forest products have significantly increased.** One important example is that of grapsoil crabs. In 2002, collectors (between six and ten persons in total) would collect an average of 7-8 kilograms per person per night. In 2005-2006, after the implementation of the community mangrove management plan and a campaign to stop the crab harvesting during breeding season,[5] nightly harvests would yield an average of 10-15 kilograms per person per night, even with an increase in the number of collectors (now up to forty a night).

  Community leaders estimate that given the current average of nightly yields and the price of crab,[6] collectors could earn up to THB 120,000 to THB 140,000 per year. The gross value of the yearly crab harvest is estimated to be at least THB 7-8 million per year. Honey is another important NTFP sourced from the mangrove forest, as indigenous trees and plants provide primary sources of pollen for bees.

[5] This campaign's slogan was "*yud jab roy khoy jab laan*," ('Don't harvest 100 now, harvest 1,000,000 later').
[6] Crab collectors typically sell their nightly harvests to middlemen at a rate of THB 60 per kilogram.

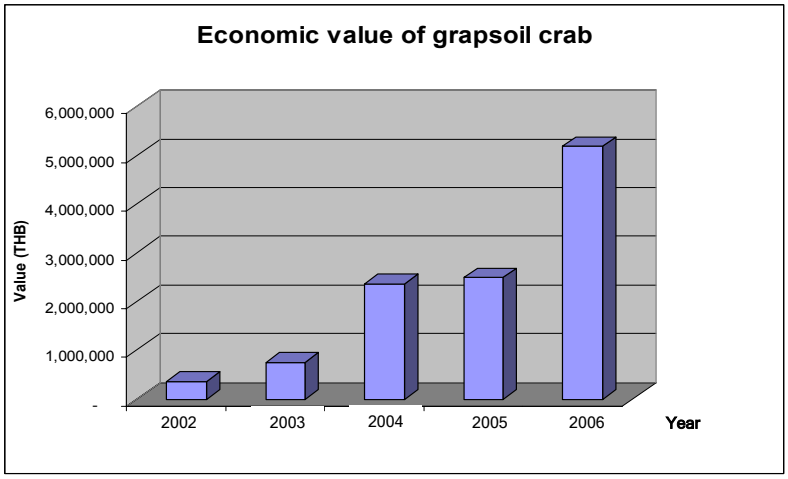

Figure 1: Economic Value of Grabsoil Crab

More than 1,000 bottles worth were harvested in 2004-2005, with a gross value of THB 100,000. (Information sourced from a discussion with community leaders in June 2007.)

- **Awareness and collaboration concerning local natural resource conservation issues has increased within Pred Nai as well as between neighboring villages.** Members of neighboring communities have demonstrated an increased sense of ownership and responsibility in the use, management, and protection of mangrove and coastline areas. For example, the Pred Nai Conservation and Development group had to work with fishermen from the neighboring village of Nong Sa-nor in order to stop the use of trawlers and push nets in fishing. This inter-community cooperation has persuaded government organizations such as the Royal Forestry Department (RFD) and the Department of Fisheries (DoF) to greater recognize community capacities to sustainably manage local resources.

STRENGTHENING LOCAL INSTITUTIONS AND INVOLVING MARGINALIZED STAKEHOLDERS

The participation of representative stakeholders from every sub-group within a community is essential for creating local resource management systems that are economically and politically equitable. In Pred Nai, the Mangrove Conservation and Development Group has worked in particular to encourage poor and marginalized households within the community to become more involved in mangrove management. However, this has proven to be a challenge. It is often difficult for poor families to find the time and effort necessary to meaningfully participate, as many often lack adequate means of production must devote more time to livelihood activities than more prosperous households. Furthermore, many poor families will often not engage in communal activities if they do not perceive any benefit from their involvement.

While many of the poorer residents of Pred Nai have limited involvement in community mangrove management at the level of primary decision-making, most still are engaged to some extent in both direct and secondary ways. Their influence is felt through participating in internal discussions and affecting decision-making at lower levels, and many contribute their time and labor to manage the mangroves.

Their actions have helped to improve their livelihoods and their political power within the community. The distribution of access and power may not yet be fully equal, but it has become more equitable.

What can be learned from Pred Nai's success in increasing the equity and participation of the poor in local resource management? Perhaps it is that factors outside of participatory processes can have a significant effect on attempts to create greater equity within local communities through CBNRM. Pred Nai is fortunate to have been positively supported in its efforts to manage its local mangroves by influential external actors such as governmental offices, educational institutes and funding agencies, and to have strong leaders who have the ability to bring together and negotiate between various actors within and outside the community.

Community groups and outside practitioners such as RECOFTC must recognize that the poor may continue to remain marginalized in community decision-making activities, even as their livelihoods improve from the rehabilitation of local resources. The internal heterogeneity of power, economic standing and personalities within individual communities presents a serious challenge to any community participation project. Facilitators are even limited in the extent to which they can promote participation to poor families, as the decision of those community members who choose not to participate must be respected. However, it is hoped that by demonstrating the advantages of full participation and creating an equitable space for different voices to be heard, non-participants will eventually be persuaded to become involved in community forest management.

COLLABORATION AND NETWORKING IN MANGROVE MANAGEMENT

Recognizing that a single community could not by themselves successfully manage and rehabilitate the entire mangrove forest area, the Pred Nai Mangrove Conservation and Development Group brought together a number of local villages in 2003 to form a local Mangrove Network. This network, supported by RECOFTC, incorporated community groups from villages who share the mangrove forest with Pred Nai. The network then expanded to include other villages in Trat province under the Natural Resource Conservation and Management Network, and in 2004 became linked with forest networks in four provinces on Thailand's eastern coastline (Chantaburi, Chonburi, Rayong

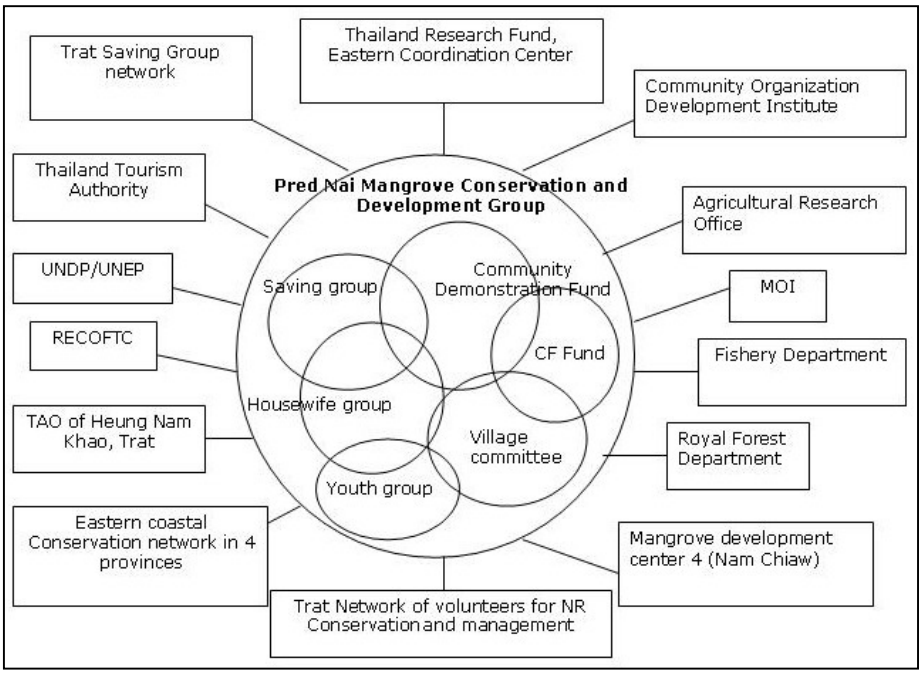

Figure 2 Strengthening Local Institutions and Involving Marginalized Stakeholders Relationship in Pred Nai

and Trat) and the Community Forestry Network of Thailand.

Collaboration between Pred Nai and different communities in local mangrove management has proven to be essential, as the mangrove forest area covers the territory of several villages and there is no clear demarcation of village boundaries nor are there any common regulations on forest utilization. At the local level, this cooperation has strengthened community knowledge and experience in resource management, and has helped to initiate new ideas and practices that respond to local needs. At regional and national levels, it has also allowed communities in Trat to link up with forest networks in other parts of Thailand and to collaborate on national forestry issues, such as the community forestry campaign and the proposal of a Community Forestry bill to the Thai Parliament.

The Pred Nai Mangrove Conservation and Development Group has also worked collaboratively with government agents and NGOs, and currently receives support and assistance from 14 organizations (both local and outsider) directly involved in forest and natural resource management (see Figure 2). These include the SIF, which provides funding for office and nature trail construction; the local, regional and national offices of the RFD, which supply seedlings for replanting and staff to monitor forest rehabilitation; the DoF and marine police, who assist in suppressing illegal fishery; the Community Development Department (CDD), which provides ongoing training and capacity building exercises in community resource management; the Thailand Collaborative Country Support Program (ThCCSP) of RECOFTC, which provides technical assistance and capacity building on participatory natural resource management; and the Provincial Agriculture Office, which supports agro-tourism development in the area.

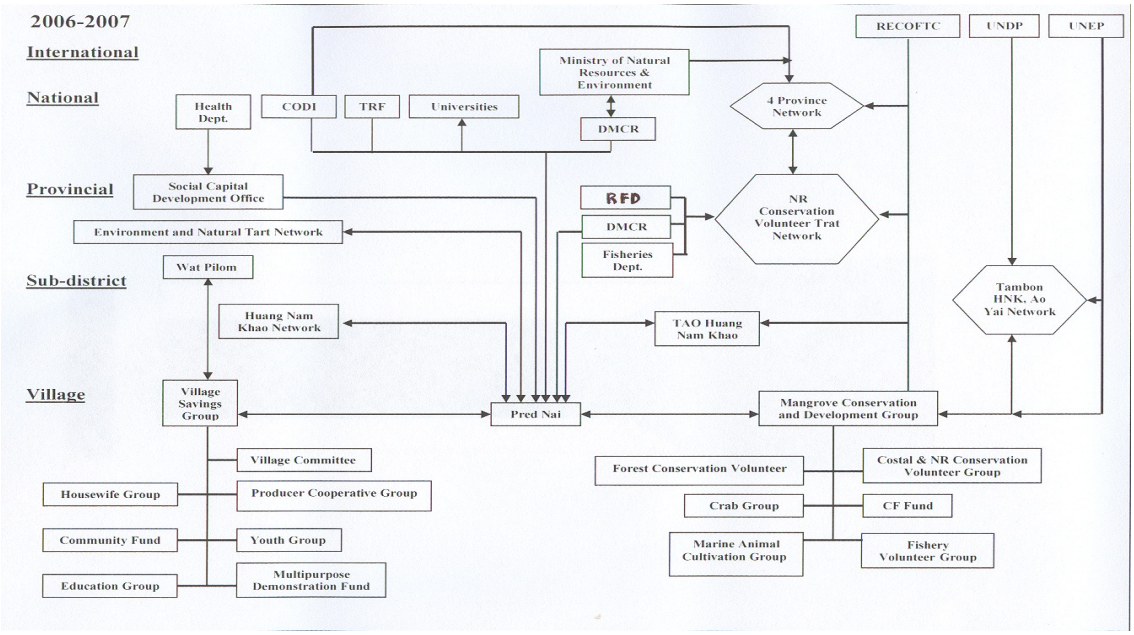

Figure 3: The linkages between community-based, outsider and government groups involved in conservation at Pred Nai[7]. Source: Jason Senyk presentation 2005.

Figure 3 illustrates how the Pred Nai Mangrove Conservation and Development Group is interlinked with different community-based groups as well as outside organizations and networks at the provincial and national level. While the group is connected to a wide spectrum of multiple stakeholders, partners and supporters, it is strong and well enough established to handle the various and sometimes competing pressures that may arise from these complex linkages and relationships. The community's experience and reputation in mangrove management has earned it a level of recognition that gives the group some leverage and greater political equity when operating at provincial and national levels.

[7] Acronyms: CODI stands for the Community Organization Development Institute, TRF stands for the Thai Research Fund, DMCR stands for the Department of Management of Coastal Resource, and TAO stands for the Tambol Administrative Organization.

Conclusions

Since its formation in 1986, the Pred Nai Mangrove Conservation and Development Group has successfully campaigned to end shrimp-farming activities that were destroying the local mangrove forest, and has used participatory approaches to develop strong institutions by which to rehabilitate, manage, and utilize this local resource base. The group has created greater opportunities for marginalized members of the community to increase their equity in community decision-making and thereby improve their livelihoods. It has also sought to actively collaborate and engage with neighboring villages, government offices, and NGOs not only to strengthen mangrove governance locally, but also to build up a regional conservation network.

Pred Nai's experience in networking and collaboration is a valuable model for community based resource management in areas where there is conflict over local resource use and management between different communities and government organizations. The community has developed a strong village network, a strong sense of identity and a willingness to put in the effort required to successfully manage local mangroves. This is considered a good base for grassroots action. While Pred Nai intends to continue expanding its forest networks to the provincial and regional levels, local conservation efforts look to be sustained as long as there are economic, environmental and cultural incentives. Indeed, the community is confident that it will be able to manage the mangroves without depending on government or outside organizational assistance in a few years time. However, current national legislation greatly restricts the rights of communities to manage their local resources. It is hoped that Pred Nai's strategy of working collaboratively with outsiders in local management planning and activities and of linking with other forest communities and networks in Thailand will change this.

Geomorphological Evolution and Mangrove Habitat Dynamics of the Northern Mekong River Delta and the Dong Nai River Delta

Kiyoshi Fujimoto[1], Masatomo Umitsu[2], Kumiko Kawase[3], Van Lap Nguyen[4], Thi Kim Oanh Ta[4], Duc Hoan Huynh[5]

[1] Faculty of Policy Studies, Nanzan University, Seto 489-0863, Japan (e-mail: kfuji@nanzan-u.ac.jp)
[2] Department of Geography, Nagoya University, Nagoya, Japan
[3] Faculty of Education, Ehime University, Matsuyama, Japan
[4] Sub-Institute of Geography, Vietnamese Academy of Science and Technology, Ho Chi Minh, Vietnam
[5] Can Gio Mangrove Protection Forest Management Board, Ho Chi Minh, Vietnam

Keywords: Mekong River Delta, Geomorphological evolution, Sea-level changes, Can Gio, Mangrove forest, Holocene

INTRODUCTION

The geomorphological evolution of the Mekong River Delta has been discussed along the main stream (Nguyen et al. 2000, Ta et al. 2001, 2002a, b), therefore there is little information in the fringing areas where the sediment input is estimated to have been relatively small. The present main mangrove forests in southern Vietnam distribute on the Ca Mau Peninsula, southern tip of the Mekong River Delta and in Can Gio on the Dong Nai River Delta. The mangrove forests formed in small sediment input areas, where *Rhizophora* sp. generally dominates, have created and maintained their habitat by accumulating mangrove peat by themselves (Fujimoto et al. 1996, 1999). Therefore, to discuss the formative processes of delta in the tropics, we need to clarify the habitat dynamics of mangrove forests as well as sedimentation processes. The mangrove peat layer also provides direct information of paleo-sealevel because its formative environment is restricted between around mean sea level and around mean high tide level (Mochida et al. 1999).

This study will discuss the geomorphological evolution and mangrove habitat dynamics in the Northern Mekong River Delta and the Dong Nai River Delta in relation to the sea-level changes during the mid to late Holocene, especially noticing the distribution of mangrove peat layers.

STUDY AREA

Study area is mainly in and around Long An Province and Ho Chi Minh City situated on the north of the Mekong River (Fig. 1). Sediment supply seems to have been relatively small because of the distance from the main stream. Therefore, marine deposits including mangrove deposits are shallowly buried and acid sulfate soil is widely distributed. On the other hand, the Dong Nai River which has a river mouth in southeastern Ho Chi Minh City has formed a small delta covered by mangrove forests. The area is called the Can Gio District. Though the mangrove forests in Can Gio were almost destroyed by herbicides sprayed by U.S. military during the Vietnam War, they have been mostly recovered by aggressive plantation by Vietnamese own effort. The about 40,000 ha of reforested mangrove forests were designated as the Mangrove Biosphere Reserve by UNESCO in 2001.

METHOD

44 hand boring data and 30 radiocarbon ages were obtained in this study. The radiocarbon ages were obtained from plant remains and were calibrated using CALIB 5.0. The geomorphological evolution, mangrove forest dynamics and sea-level changes were discussed using these data together with the existing data (Nguyen et al. 2000, Ta et al. 2001, 2002a, b).

The elevation of boring sites were estimated using SRTM data downloaded from the web site of NASA (ftp://e0srp01u.ecs.nasa.gov/srtm/) and 1:50,000 of topographical maps downloaded from the web site of the Vietnam Center and Archive of Texas Tech University (http://www.virtual.vietnam.ttu.edu/starweb/virtual/maps/servlet.starweb?path=virtual/maps/maps_new.web).

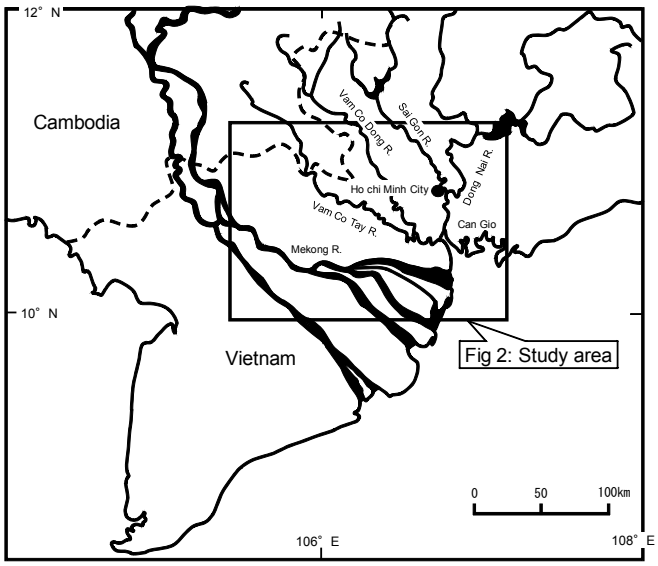

Fig. 1 Map showing the study area.

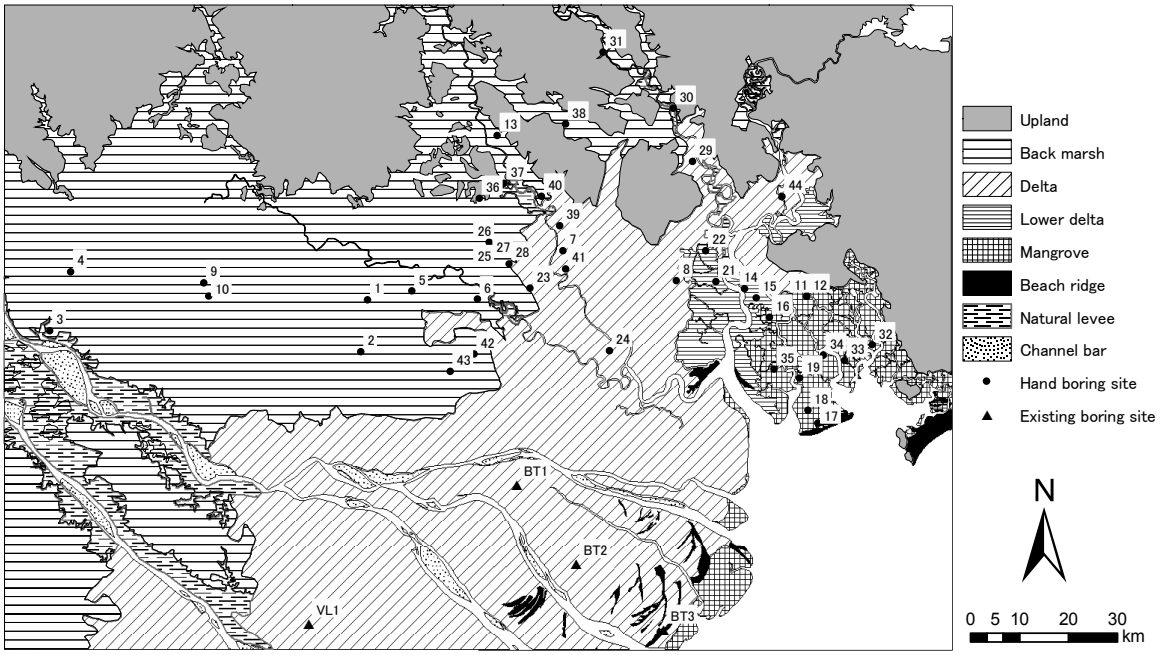

Fig. 2 Geomorphological map in the study area with boring sites.

When the estimated elevation differ between SRTM data and topographical map, the value read from topographical map was adopted because SRTM data, which is about 90 m mesh, were possibly affected by tree and building heights and were sometimes missing. The elevation based on topographical map was estimated from the values of the nearest two or three control points. When the values differ between these points, the elevation was estimated to be between the values.

The geomorphological map shown in Fig. 2 was depicted using the LANDSAT images taken in 2001 and 2002, which were downloaded from the web site of University of Maryland (http://glcfapp.umiacs.umd.edu:8080/ esdi/ index.jsp).

RESULTS AND DISCUSSION

Distribution of mangrove peat layers and their formative periods

The latitude and longitude of boring sites and their estimated elevation are shown in Table 1 and the

results of radiocarbon dating and their calibrated ages are shown in Table 2. The value in parentheses of calibrated age shows the median probability and the values are indicated in Figs. 3 and 4.

Table 1 Location of boring sites and their estimate elevation.

Site No.	Borehole No.	Area	Latitude (N)	Longitude (E)	Elevation estimated by SRTM(m)	Elevation estimated by topographical map (m)	Land use/condition
1	010303-1	VCTR	10° 37′ 17.0″	106° 05′ 12.9″	0	2	Cultivated field
2	010304-1	MR-VCTR	10° 31′ 35.2″	106° 04′ 28.3″	1	2	Cultivated field
3	010305-1	MR	10° 33′ 53.0″	105° 30′ 14.2″	5	2	Natural levee
4	010608-1	MR	10° 40′ 21.5″	105° 32′ 32.0″	2	2	Paddy field
5	020608-1	VCTR	10° 38′ 15.9″	106° 10′ 04.6″	1	2	*Melaleuca* forest
6	020608-2	VCTR	10° 37′ 22.7″	106° 17′ 17.3″	1	1-2	Paddy field
7	020608-3	VCDR	10° 42′ 42.1″	106° 26′ 42.1″	1	1	Sugarcane field
8	020608-4	DNR	10° 39′ 24.5″	106° 39′ 10.9″	2	1-2	Paddy field
9	020808-1	MR	10° 39′ 09.7″	105° 47′ 10.3″	2	2	Swamp
10	020808-2	MR	10° 37′ 41.9″	105° 47′ 43.2″	6	2	Melaleuca forest
11	040821-1	CG	10° 37′ 40.1″	106° 53′ 31.5″	3	1	Mangrove forest
12	040822-1	CG	10° 37′ 40.1″	106° 53′ 31.5″	3	1	Mangrove forest
13	040828-1	VCDR	10° 55′ 22.0″	106° 19′ 28.2″	1	1-2	Paddy field
14	050819-1	CG	10° 38′ 31.4″	106° 46′ 41.4″	1	1	Abandaned paddy field
15	050819-2	CG	10° 37′ 30.4″	106° 48′ 00.0″	1	1	Abandaned paddy field
16	050819-3	CG	10° 35′ 21.5″	106° 49′ 26.4″	2	1	Mangrove forest
17	050820-1	CG	10° 23′ 44.1″	106° 54′ 45.5″	2	2	Salt field
18	050820-2	CG	10° 25′ 08.6″	106° 53′ 40.5″	1	0-1	Mangrove scrub
19	050820-3	CG	10° 28′ 40.1″	106° 52′ 44.8″	6	1	Mangrove forest
20	050820-4	CG	10° 30′ 55.1″	106° 51′ 29.5″	7	1	Mangrove forest
21	050822-1	DNR	10° 39′ 18.3″	106° 43′ 32.5″	0	1	Paddy field
22	050822-2	DNR	10° 42′ 40.8″	106° 42′ 24.6″	2	?	Waste land
23	050823-1	VCTR/VCDR	10° 38′ 34.8″	106° 23′ 05.5″	1	1	Sugarcane field
24	050823-2	VCTR/VCDR	10° 31′ 41.7″	106° 31′ 49.4″	1	1	Paddy field
25	050824-1	VCTR/VCDR	10° 43′ 29.0″	106° 18′ 39.7″	0	1-2	Grazing land
26	050824-2	VCTR/VCDR	10° 43′ 37.1″	106° 18′ 35.3″	2	1-2	Cultivated field
27	050824-3	VCTR/VCDR	10° 41′ 51.8″	106° 18′ 41.9″	0	1	Paddy field
28	050824-4	VCTR/VCDR	10° 41′ 14.5″	106° 20′ 46.3″	1	1	Cultivated field
29	050825-1	SGR	10° 52′ 31.4″	106° 40′ 58.1″	0	2	Cultivated field
30	050825-2	SGR	10° 58′ 20.9″	106° 38′ 49.1″	2	?	Cultivated field
31	050825-3	SGR	11° 04′ 31.7″	106° 31′ 07.5″	1	?	Paddy field
32	060821-1	CG	10° 32′ 20.4″	107° 00′ 44.9″	4	1	Mangrove forest
33	060821-2	CG	10° 30′ 36.7″	106° 57′ 41.4″	2	1	Mangrove scrub
34	060821-4	CG	10° 31′ 12.1″	106° 55′ 22.1″	4	1	Mangrove forest
35	060821-5	CG	10° 29′ 39.5″	106° 49′ 56.4″	2	1	Mangrove forest
36	061005-1	VCDR	10° 48′ 34.4″	106° 17′ 16.3″	2	2-3	Paddy field
37	061005-2	VCDR	10° 50′ 05.7″	106° 20′ 13.1″	0	2	Melaleuca forest
38	061005-3	VCDR	10° 56′ 36.8″	106° 27′ 00.3″	0	1	Waste land
39	061006-1	VCDR	10° 45′ 25.5″	106° 26′ 21.5″	1	1	Sugarcane field
40	061006-2	VCDR	10° 48′ 41.1″	106° 24′ 21.6″	0	1	Paddy field
41	061006-3	VCDR	10° 40′ 40.9″	106° 26′ 59.9″	1	1	Cultivated field
42	061007-1	MR/VCTR	10° 31′ 19.8″	106° 16′ 56.3″	3	1	*Melaleuca* forest
43	061007-2	MR/VCTR	10° 29′ 32.1″	106° 14′ 03.2″	2	1	*Eucalyptus* forest
44	070118-1	DNR	10° 48′ 38.1″	106° 50′ 48.7″	0	1-2	Cultivated field

MR: Mekong River, VCTR: Vam Co Tay River, VCDR: Vam Co Dong River, DNR: Dong Nai River, SGR: Sai Gon River, CG: Can Gio

The ground elevation of alluvial plain in the study area is mostly between +1 and +2 m (Table 1). The distributional areas of mangrove peat in the Northern Mekong River Delta are located about 60 to 80 km inland from the present coastline, which are in the present backmarshes between the Mekong and the Vam Co Tay rivers and the Vam Co Dong River and Pleistocene hilly land (Figs 2 and 3). The formative age of the mangrove peat layers, which were overlain by about 1 m thick of silt or clay layer, indicated between 7000 and 6000 cal BP (Fig. 3). Mangrove peat layer younger than 6000 cal BP has not been found in the Northern Mekong River Delta though mangrove organic deposits indicating between 5400 and 4500 cal BP have been found (Sites. 4 and 28 in Fig. 3). The peat layer at Site 10 was presumed to have been formed

under freshwater swamp forest such as *Melaleuca* forest from the facies. The Pleistocene deposits were shallowly buried in the study area.

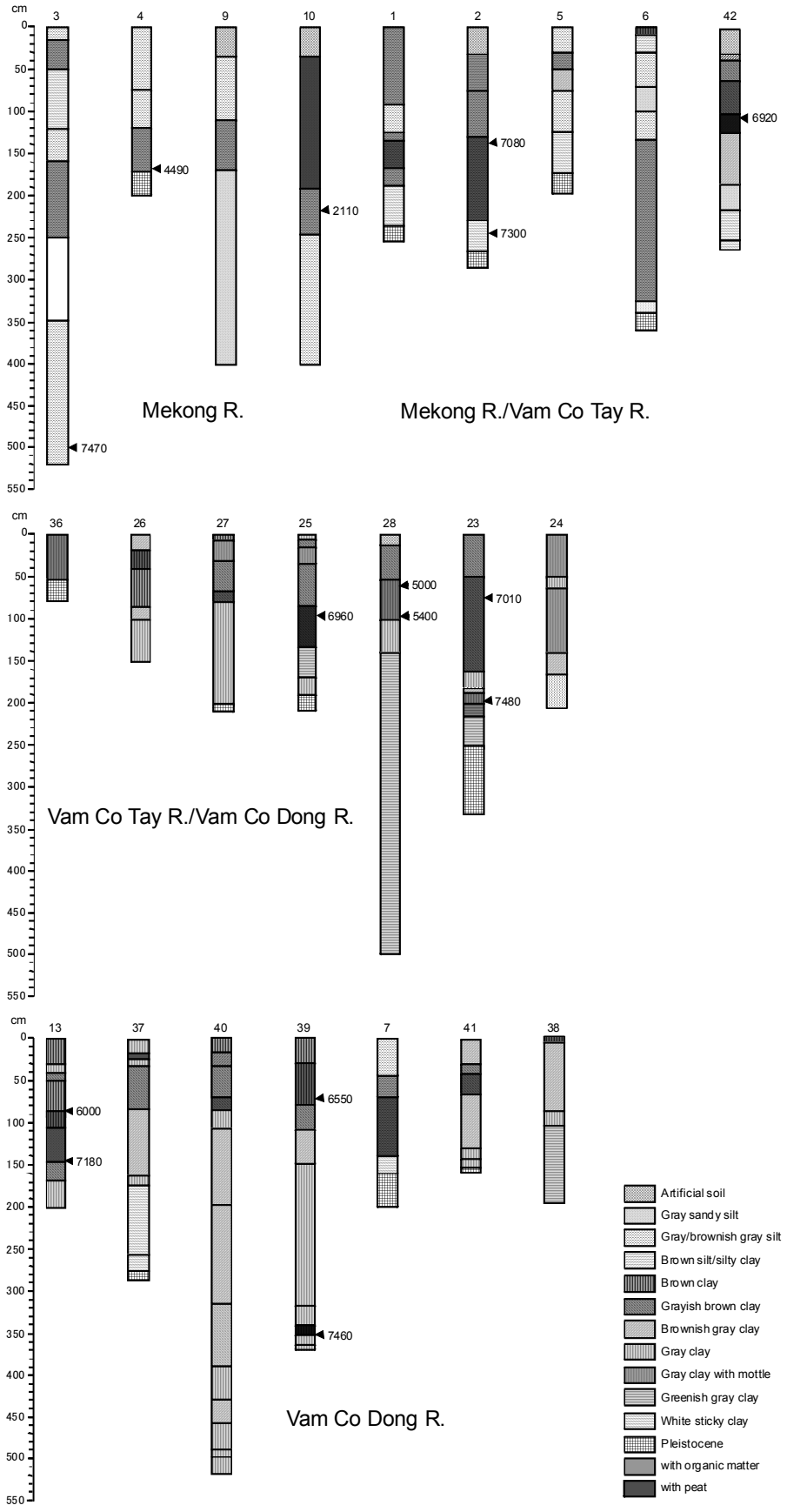

Fig.3 Boring columns in the Northern Mekong River Delta.

Table 2 Radiocarbon ages obtained from the Northern Mecong Delta and the Dong Nai River Delta

Area	Site No.	Lob.code no.	Depth (cm)	Sample	$\delta^{13}C$	Conventional age (^{14}C BP)	2σ calibrated age (cal BP)	Sampling horizon
CG	19	NUTA2-10784	176-178	wood frag.	-28±1	400±30	330-360, 430-(480)-510	upper horizon of lower tidal-flat deposit
CG	20	NUTA2-10867	83	wood frag.	-30±1	600±30	550-(600)-650	middle horizon of mangrove organic deposit
CG	16	NUTA2-10868	115	wood frag.	-30±1	1320±30	1180-1210, 1230-(1270)-1300	mangrove peat
CG	11	NUTA2-8858	70-74	wood frag.	-26±1	330±30	310-(390)-470	mangrove peat
CG	12	NUTA2-8859	143-145	wood frag.	-28±1	330±30	310-(390)-470	upper horizon of lower mangrove organic deposit
CG	32	IAAA-62134	133-141	wood frag.	-23.16±0.83	360±30	320-400, (410), 420-500	bottom horizon of mangrove peat
CG	34	IAAA-62135	146-148	wood frag.	-25.93±0.82	1790±30	1620-1670, 1680-(1720)-1820	lower horizon of mangrove peat
CG	35	IAAA-62136	125	wood frag.	-21.10±1.00	2530±40	2480-(2610)-2750	lower horizon of mangrove organic deposit
DNR	44	IAAA-70004	84	wood frag.	-28.38±0.49	5530±50	6210-6240, 6270-(6330)-6420	upper horizon of lower mangrove organic deposit
DNR	44	IAAA-63122	240	wood frag.	-25.88±0.82	6590±40	7430-(7490)-7520, 7530-7560	bottom horizon of lower mangrove organic deposit
SGR	29	NUTA2-10782	80-82	wood frag.	-31±1	5660±40	6320-(6440)-6540	upper horizon of lower tidal-flat deposit
SGR	29	NUTA2-10783	494-496	wood frag.	-29±1	6970±40	7690-(7800)-7870, 7900-7930	estuarine deposit
SGR	30	IAAA-51733	93-96	wood frag.	-28.59±0.79	4850±40	5480-5540, 5570-(5600)-5660	upper horizon of lower tidal-flat deposit
SGR	30	NU-1773	167-200	wood	-28.9	4470±80	4880-(5120)-5310	estuarine deposit
VCDR	13	NUTA2-8866	85-86	Plant frag.	-29±1	5240±40	5920-(6000)-6120, 6150-6180	top horizon of mangrove organic deposit
VCDR	13	NUTA2-9050	144	peat	-26±1	6240±30	7020-7120, 7150-(7180)-7250	bottom horizon of mangrove peat
VCDR	39	IAAA-62137	70	wood frag.	-26.76±0.87	5750±40	6450-(6550)-6650	bottom horizon of mangrove organic deposit
VCDR	39	IAAA-62138	346-353	Plant remains	-29.51±0.88	6550±40	7420-(7460)-7520, 7530-7560	estuarine deposit
VCTR/VCDR	23	NUTA2-10863	73-75	wood frag.	-25.01±0.96	6130±30	6940-(7010)-7160	upper horizon of mangrove organic deposit
VCTR/VCDR	23	IAAA-51734	195-199	wood frag.	-27.46±0.90	6580±40	7430-(7480)-7520, 7530-7560	basal mangrove organic deposit
VCTR/VCDR	25	NUTA2-10784	95-97	wood frag.	-24±1	6090±40	6850-(6960)-7160	upper horizon of mangrove peat
VCTR/VCDR	28	NUTA2-10828	57-63	wood frag.	-29±1	4420±30	4870-(5000)-5060, 5190-5220, 5230-5260	top horizon of mangrove organic deposit
VCTR/VCDR	28	NUTA2-10892	96-99	wood frag.	-29±1	4610±30	5290-5330, 5380-(5400)-5450	bottom horizon of mangrove organic deposit
MR/VCTR	42	IAAA-62139	105-110	wood frag.	-25.01±0.96	6060±50	6750-6770, 6780-(6920)-7030, 7060-7060, 7110-	upper horizon of mangrove peat
MR/VCTR	2	NUTA2-3565	138	wood frag.	-25.42	6170±30	6980-(7080)-7170	top horizon of mangrove peat
MR/VCTR	2	NUTA2-3566	244	wood frag.	-32.95	6360±40	7180-7210, 7240-(7300)-7420	upper horizon of lower tidal-flat deposit
MR	3	NUTA2-?	500	Plant remains (*Nypa*)	?	6560±40	7420-(7470)-7520, 7530-7560	estuarine deposit
MR	4	NUTA2-?	165-172	wood frag.	?	4020±40	4410-(4490)-4590, 4600-4610	bottom horizon of mangrove organic deposit overlying
MR	10	NUTA2-?	215-220	wood frag.	?	2130±40	2000-(2110)-2180, 2240-2300	middle horizon of lower mangrove organic deposit

MR: Mekong River, VCTR: Vam Co Tay River, VCDR: Vam Co Dong River, DNR: Dong Nai River, SGR: Sai Gon River, CG: Can Gio

On the Dong Nai River Delta, mangrove peat layers formed between 1700 and 400 cal BP, which were overlain by 0.5 to 1.2 m thick of clay layer, widely distribute in Can Gio (Fig. 4). The oldest age obtained from the mangrove organic layer in Can Gio indicated around 2600 cal BP at Site 35. At Site 44 located about 50 km inland from the present coastline, the peaty deposit of about 10 cm thick was found and calibrated ages indicating about 7500 cal BP and 6300 cal BP were obtained from the upper and bottom horizons of mangrove organic layer overlain by the peaty deposit, respectively. At Sites 8, 21 and 22 on the right bank of the Dong Nai River, mangrove organic layer was not found.

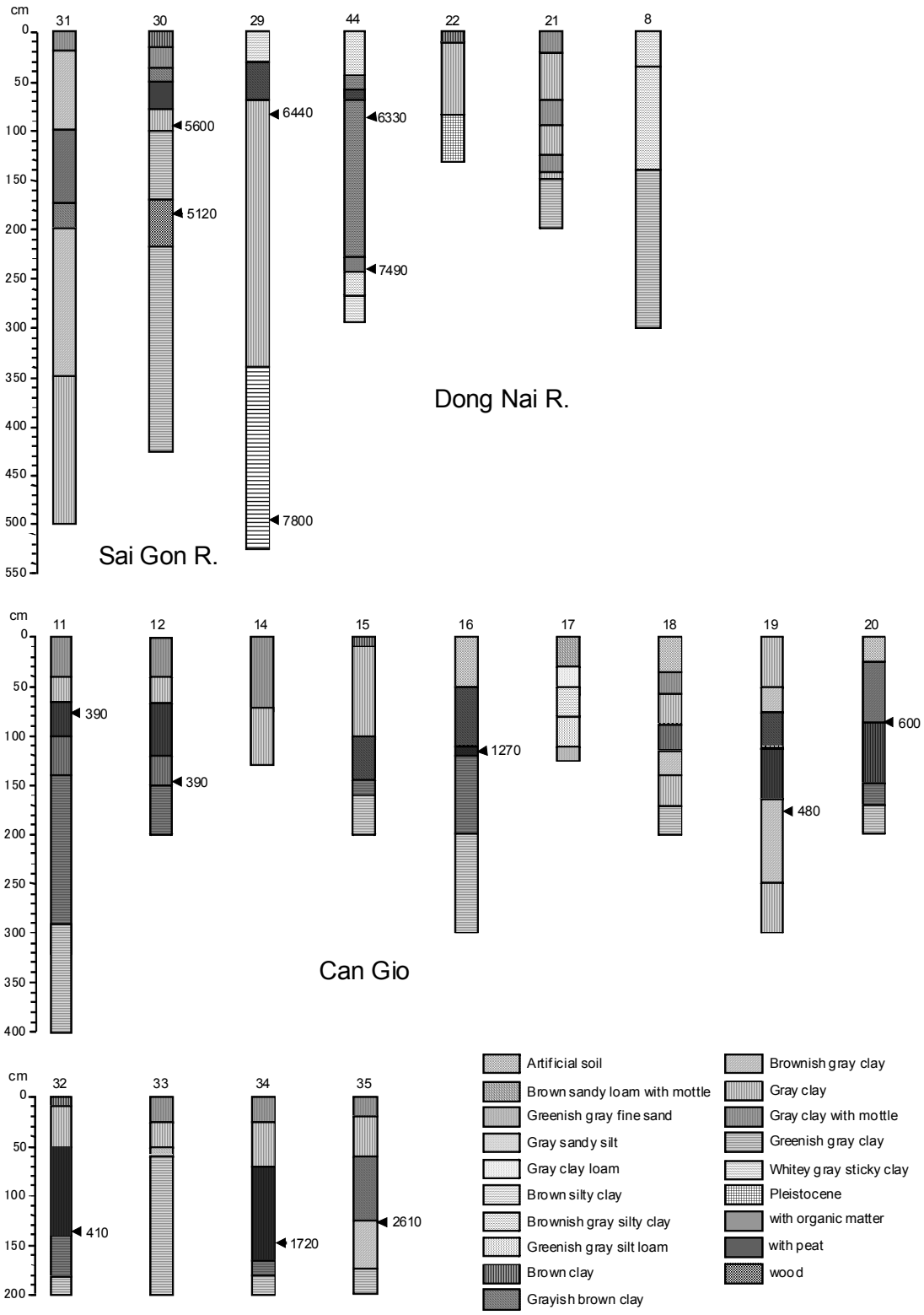

Fig.4 Boring columns in the Dong Nai River Delta.

Relative sea-level changes estimated from the heights and ages of mangrove organic deposits

Fig. 5 shows the relationship between calibrated ages obtained from mangrove organic deposits and estimated ranges of sea level. The rectangular area shows the range of estimated sea level for each calibrated age including the error for determination of sampling elevation and radiocarbon dating.

Generally, mangrove deposits are formed between around mean sea level and highest high tide level because the mangrove forests are only formed between the tidal environments. Mangrove peat layer is especially formed under *Rhizophora* forest only, whose formative tidal environment is restricted between

around mean sea level and around mean high tide level (Mochida et al. 1999). The present mean spring tidal range and mean neap tidal rage in Can Gio are 370 cm and 310 cm, respectively (Japanese Coast Guard 2005). Supposing that the tidal range has been constant during the Holocene, the paleo-sealevel must be estimated to be 0 to 160 cm lower than sampling elevation for the samples obtained from mangrove peat and 0 to 190 cm lower for the samples obtained from other mangrove deposits. As the samples obtained from around bottom horizon of mangrove deposits including mangrove peat layer are considered to have deposited around mean sea level, the estimated sea-level range for these samples in Fig. 5 shows the error for sampling elevation only.

The estimate error for elevation of boring site is ±50 cm because the elevation data of both SRTM and topographical map are shown in meters.

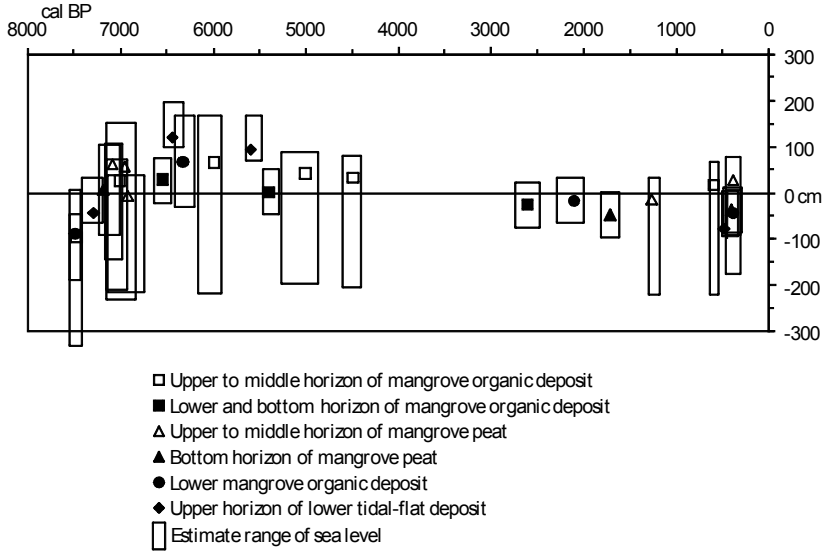

Fig. 5 Relationship between calibrated ages obtained from mangrove organic deposits and estimated ranges of sea level.

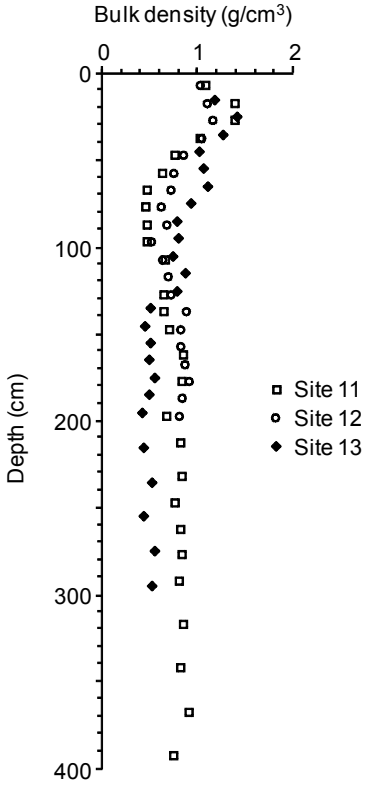

Fig. 6 Vertical distribution of bulk density for Sites 11 and 12 in Can Gio and Site 13 at about 60 km inland along the Vam Co Dong River.

The data obtained from alluvium possibly involve the effect of compaction. The effect can be inferred by comparing the values in bulk density between the samples obtained from inland, which is relatively old deposit, and coastal area, relatively new. Fig. 6 shows the vertical distribution of bulk density for Sites 11 and 12 located in Can Gio and Site 13 located about 60 km inland along the Vam Co Dong River. The bulk densities obtained from the marine clay layer below 150 cm deep overlain by mangrove organic layer at Site 13 showed relatively lower values than those at Sites 11 and 12 in Can Gio. This trend indicates that there is no significant effect of compaction in inland area. It is obviously that the data obtained from Sites 4 and 7 indicating the sea level around 4500 and 7300 cal BP, respectively, have not been affected by compaction because the samples were obtained from just above the Pleistocene deposit. The shallowly buried Pleistocene deposits seem to have attenuated the effect of compaction.

Fig. 5 shows that the sea level between 6500 and 5500 cal BP was relatively higher than present one and around 2000 cal BP was the same level as present or slightly lower. The highest sea level around 6000 cal BP was estimated to have never reached over 2 m above present one. These results correspond with the data obtained in southwestern Thailand (Fujimoto et al. 1999), but differ significantly from the data obtained in northern Vietnam by Boyd and Doan (2004), in which the sea level has been identified at 3.25 m above present one around 5500 cal BP and at 1.5 m above present one around 2000 cal BP. The evidence indicating the sea level around 4000 cal BP has not been obtained yet, when the relative high stand of sea level has been generally found in the Asia – Pacific region (e.g. Fujimoto 1990, Fujimoto et al. 1999).

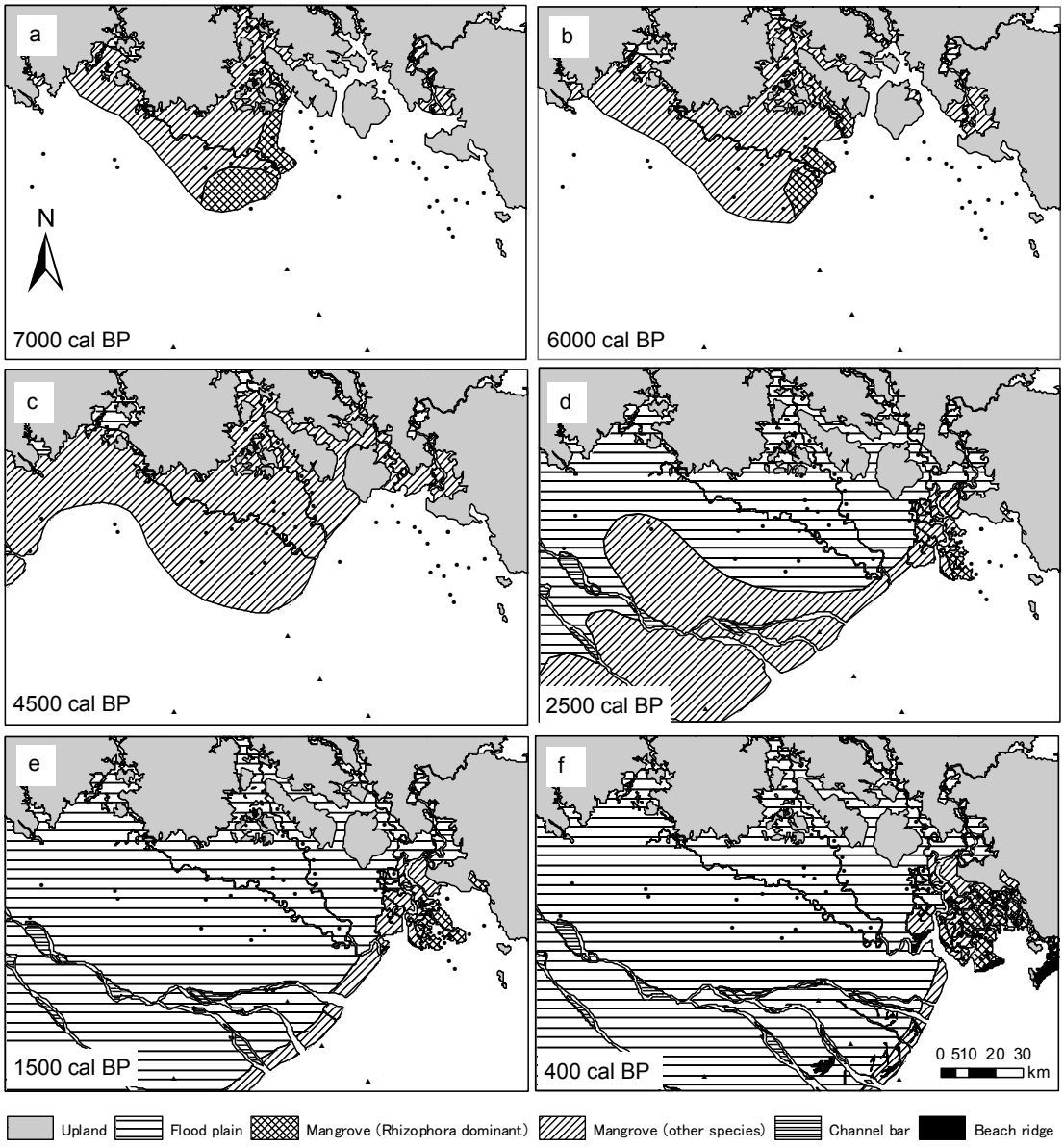

Fig. 7 Gemorphological evolution and mangrove habitat dynamics of the Northern Mekong River Delta and Dong Nai River Delta.

Geomorphological evolution of the deltas and mangrove habitat dynamics

Based on the distribution and the formative ages of mangrove peat layers, mangrove forests dominated by *Rhizophora* seem to have been formed on the delta of the Vam Co Tay and the Vam Co Dong Rivers between 7000 and 6000 cal BP, which are situated about 60 to 80 km inland from the present coastline (Figs. 7a and b). The postglacial sea-level rise almost ceased by 7000 cal BP and a lot of low islands consisting of Pleistocene deposits distributed in the shallow sea. The formation of *Rhizophora* forests started around 7000 cal BP on the tidal flats surrounding the islands and other dominant species of mangrove forests developed on the delta behind the *Rhizophora* forests, where fluvial sedimentation rapidly progressed because of the existence of shallowly submerged Pleistocene deposits. The data obtained from Sites 3 and 4 show that the delta front of the Mekong River was located at least more than 140 km inland from the present coastline around 6000 cal BP and reached there by around 4500 cal BP. Though the *Rhizophora* forests disappeared after 6000 cal BP, it is presumable that other dominant species of mangrove forests were distributed on the Vam Co Tay and the Vam Co Dong Rivers Delta and the Mekong River Delta (Fig. 7c). Around 2500 cal BP, the delta front of the Mekong River located about 40 km inland from the present coastline and the mangrove forests without *Rhizophora* distributed to about 120 km inland from the present coastline (Fig. 7d). After that, the mangrove environments changed to the freshwater environments with the sea-level fall (Fig. 7e).

On the other hand, the delta front of the Dong Nai River reached the Can Gio area by 2600 cal BP and a *Rhizophora* forest developed first on the southwestern part (Fig. 7d). The mangrove forest expanded to the northeastward with the delta formation after that and the mangrove area reached almost the same area as present one by 400 cal BP (Fig. 7f). The *Rhizophora* forest has changed to other dominant species of mangrove forest with the ground-level rise by accumulation of mangrove peat and fluvial sedimentation.

References

Boyd, W. E. and Doan, D. L. 2004. Holocene elevated sea levels on the north coast of Vietnam. *Australian Geographical Studies* 42: 77–88.

Fujimoto, K. 1990. Reexamination of Late Holocene sea-level changes in Japan. *Sci. Repts. Tohoku Univ.*, 7th Ser. (Geogr.), 40: 37-70.

Fujimoto, K., Miyagi, T., Kikuchi, T. and Kawana, T. 1996. Mangrove habitat formation and response to Holocene sea-level changes on Kosrae Island, Micronesia. *Mangrove and Salt Marshes* 1: 47-57.

Fujimoto, K., Miyagi, T., Murofushi, T., Mochida, Y., Umitsu, M., Adachi, H. and Pramojanee, P. 1999. Mangrove habitat dynamics and Holocene sea-level changes in the southwestern coast of Thailand. *TROPICS* 8: 239-235.

Japanese Coast Guard 2005. Tide table 2005 –Volume 2 Pacific Ocean and Indian Ocean. *Japan Hydrographic Association*. (in Japanese)

Mochida, Y., Fujimoto, K., Miyagi, T., Ishihara, S., Murofushi, T., Kikuchi, T. and Pramojanee, P. 1999. A phytosociological study of the mangrove vegetation in the Malay Peninsula – Special reference to the micro-topography and mangrove deposit –. *TROPICS* 8: 207-220.

Nguyen, V.L., Ta, T.K.O and Tateishi, M. 2000. Late Holocene depositional environments and coastal evolution of the Mekong River Delta, Southern Vietnam. *J. Asian Earth Sciences* 18: 427-439.

Ta, T. K. O., Nguyen, V. L., Tateishi, M., Kobayashi, I. and Saito, Y. 2001. Sedimentary facies, diatom and foraminifer assembladges in a late Pleistocene – Holocene incised-valley sequence from the Mekong River Delta, Bemtre Province, Southern Vietnam: the BT2 core. *J. Asian Earth Sciences* 20: 83-94.

Ta, T. K. O., Nguyen, V. L., Tateishi, M., Kobayashi, I., Saito, Y. and Nakamura, T. 2002a. Sediment facies and Late Holocene progradation of the Mekong River Delta in Bentre Province, southern Vietnam: an example of evolution from a tide-dominated to a tide- and wave-dominated delta. *Sedimentary Geology* 152: 313–325.

Ta, T. K. O., Nguyen, V. L., Tateishi, M., Kobayashi, I., Tanabe, S. and Saito, Y. 2002b. Holocene delta evolution and sediment discharge of the Mekong River, southern Vietnam. *Quaternary Science Reviews* 21: 1807-1819.

Geo-environment and Acid Sulfate Soils in the Lower Central Plain, Thailand

Naruekamon Janjirawuttikul, Masatomo Umitsu

Graduate School of Environmental Studies, Nagoya University, Nagoya, Japan
E-mail: naruekamon@gmail.com

Abstract

The characteristics of acid sulfate soil in the Central Plain of Thailand and its relationship with the Holocene landform evolution were studied. Landforms of the plain were classified into alluvial fan, flood plain, deltaic plain and tidal lowland. Characteristics of the surface geology in the area are generally classified into the four units. The uppermost horizon is an artificial cultivated soil. They are considered as the fluvial sediments. Sediments under the fluvial grey mud are considered as the sediment deposited in the intertidal condition with mangroves. The underlying layer is shallow marine or open bay sediment. Characteristics of acid sulfate soils, there are six soil samplings for field morphology and electrical conductivity measuring. The horizons of the profiles can grouped into five distinct characteristics; potential acid sulfate horizon, Pleistocene alluvium, non-acid sulfate horizon, actual acid sulfate horizon, and topsoil from lower to top. The yellow mottle of jarosite zone can be observed in actual acid sulfate horizon, the strongest acid condition zone in profile. The conditions of material are considered from Electrical Conductivity values, they usually sequence as marine, brackish water, and fresh water from lower part to surface. The environments of sedimentation are determined as marine is shallow marine under mangrove forest, brackish water is tidal to intertidal, and fresh water is alluvial sediments.

The largest area of acid sulfate soil is distributed in the northern part of the deltaic lowland area, and the area is the former tidal plain zone which developed towards the north of Ayutthaya in 7,000 yrs BP. Development of acid sulfate soil in the Lower Central Plain is related to the thickness of the sediments over the soft marine or shallow marine sediments. Acid sulfate soil with shallow jarosite horizon (< 50 cm) can be seen in the areas where the thickness of the intertidal or fluvial sediments is less than 2.2 m. Shallow marine under mangrove forest was started after culmination of Holocene transgression, caused area riches iron sulfide materials. Then the environment was changed to tidal to intertidal in period of sea regression. The deltaic plain was developed continuously with fluvial sediment. After drainage was introduced, soil moisture condition changed from under wet condition all the time to wet alternated with dry which caused oxidation occurred, iron sulfide (mainly pyrite) was changed to be jarosite appearing as yellow mottles and soil was extremely to very strongly acid condition.

Keywords: acid sulfate soil, Holocene landform evolution, the Central Plain of Thailand

INTRODUCTION

Acid sulfate soils naturally contain sedimentary pyrite (FeS_2) and remain environmentally benign if maintained in a saturated state under reducing conditions (McElnea et al., 2004). In a board sense, acid sulfate soils were formed especially after the last major sea level rose, within the past 10,000 years or the Holocene epoch. They commonly occur on wetlands as layers of Holocene marine mud and sands deposited in protected low-energy environments such as barrier estuaries and coastal lakes. Acid sulfate soils are formed when seawater or sulfate-rich water mixes with land sediments containing iron oxides and organic matter in a waterlogged situation, in the absence of oxygen (Department of Natural Resources and Water, 2007). Wilson (2005) stated that sea level change will affect the position of pyritic sediments in the landscape. Although there is general agreement on the timing and elevation of maximum sea level during the Holocene, there is debate over whether the fall to present sea level was a smooth decline or whether there existed a secondary still-stand period of higher sea level.

The presence of jarosite, bright–straw yellow in color, is one of the most importance features of acid sulfate soil environment. It is well established that acid sulfate soils have accumulated a substantial amount of iron in the so-called sulfuric horizon (Muhrizal et al., 2006; Soil Survey Staff, 2006). The boundary between the oxidized zone and the underlying unoxidised zone marked the depth to sulfides, and was easily distinguished in the field because of the sharp morphological contrast. The change from brownish oxidised zone to the black or dark gray unoxidised material was abrupt and easily identifiable (Martin and Terry, 2005). When cultivated, acid sulfate soils cannot be kept wet continuously because of climatic dry spells and shortages of irrigation water, surface drainage may help to remove the acidic and toxic chemicals

(formed in the dry spells) during rainy periods. Sufuric acid and soluble sulfate can move upwards by capillary action forming an actual acid sulfate soil from what was once a non-acid sulfate soil (Lin et al., 1995). Knowledge of how pyrite forms is important to variety of fields. Depth of jarosite, which is a stable characteristic of acid sulfate soil, was a reasonably reliable criterion for distinguishing between soil units at various scales in areas of acid sulfate soils having jarosite mottles in the profile, but short range variability of property was also large. The presence or absence of jarosite is useful characteristic for mapping at semi-detail and reconnaissance scales (Burrough et al., 1988).

According to many researches about marine transgression-regression during Late Pleistocene-Holocene and widespread marine and continental deposits developed in the Central Plain which have been reviewed and studies such as Jon and Nutalaya (1983), Somboon (1988), Dheeradilok and Kaewyana (1986), Sinsakul (1992), Somboon and Thiramongkol (1992), and Umitsu et al. (2002). The acid sulfate soil characteristics of this plain also described by soil scientists such as Slager et al. (1970), Vlek (1971), van Breemen (1973), Dent and Pons (1995), and Udomsri et al. (2004). Despite the importance of relation to acid sulfate and land evolution, a few papers were described. This paper is aimed to determining characteristics of acid sulfate soil in the Lower Central Plain of Thailand and its relation to the Holocene landform evolution. The study concentrates on morphology of acid sulfate soil, landforms and the paleotidal current in the Central Plain of Thailand.

METHODOLOGY

1. Study site

The study area is the Lower Central Plain. The northern boundary of the plain is delineated in the Chainat province ($15^{o}15^{/}$N, $100^{o}15^{/}$E) where the Chao Phraya River passed the monadnocks and flowed southward through the flat, low-lying plain until reaching the Gulf of Thailand at Samut Prakarn ($14^{o}30^{/}$N, $100^{o}30^{/}$E). The distance from Chainat to the Chao Phraya River mouth is about 200 km; the widest part of the plain in an east-west direction is about 180 km, and the total area is approximately 36,000 km^2. The elevation of the plain ranges from 15 m A.S.L. at Chainat to 2.5 m A.S.L at Ayutthaya and 1.5 m A.S.L. at Bangkok which is about 25 km north of the Gulf of Thailand. The southern edge of the plain is marked by a narrow strip of tidal flat, with vegetated mangrove forest, extending for 30 km along the banks of the Chao Phraya River mouth. The most cultivation in acid sulfate soil areas are used for paddy fields but recently, most of the area was converted into the salt pans and prawn farms (Sinsakul, 1997 and 2000). In the era of King Rama V, the late 19^{th} century, is regarded as a milestone in the irrigation history of Thailand. In this period, the excavation of canals as both irrigation and transport facilities expanded rapidly, until almost all of the deltaic areas were covered with high-density canals network that still exists (Hara, 2005). Land Development Department (2006) reported that acid sulfate soil occupies in the Thailand around 5,510,144 rai or 881,623 hectare, the largest region of acid sulfate soil is the Lower Central Plain. They also organized them to be three groups as acid sulfate soil with variety depth of jarosite horizon; shallow (jarosite horizon within 50 cm), moderately deep (jarosite horizon 50-100 cm), and deep (jarosite horizon deeper than 100 cm). Finally, they created acid sulfate soil distribution map as achievement (Fig 1). The distribution map was complied from soil map which soils were classified as soil series. Then the series of acid sulfate soil were grouped and classified again by considering depth of jarosite horizon. The pattern of acid sulfate soil distribution is very similar to the pattern of Qm unit in the Geological map of Thailand 1:2,500,000 in scale (Geological Survey Division, 1999). It was found that most of acid sulfate soil areas locate as the Qm unit which is defined as coastal deposits: beach, mangrove swamp, marsh and lagoon unit.

2. Methods

There are 39 represent sits for study sediment distribute around the Lower Central Plain (Fig 2A), at each site, samples were determined establish stratigraphic sequence, some shells and organic fragments were collected for radiocarbon date determination. The selecting area for acid sulfate soil investigation is Pathum Thani and Ayutthaya, the extensive distribution areas of acid sulfate soil in Thailand. The six soil samplings were drilled to average depth of 3.7 m from eastern part of the Lower Central Plain (Fig 2B). Soil borings were made using a bucket auger with quick connect extensions. Field indicators for soil are used to assist in the identification of acid sulfate soils is field pH, color, texture, organic matter accumulation, and distinctive features. Soil sample were taken, and then measured for electrical conductivity to understanding environment of sedimentation.

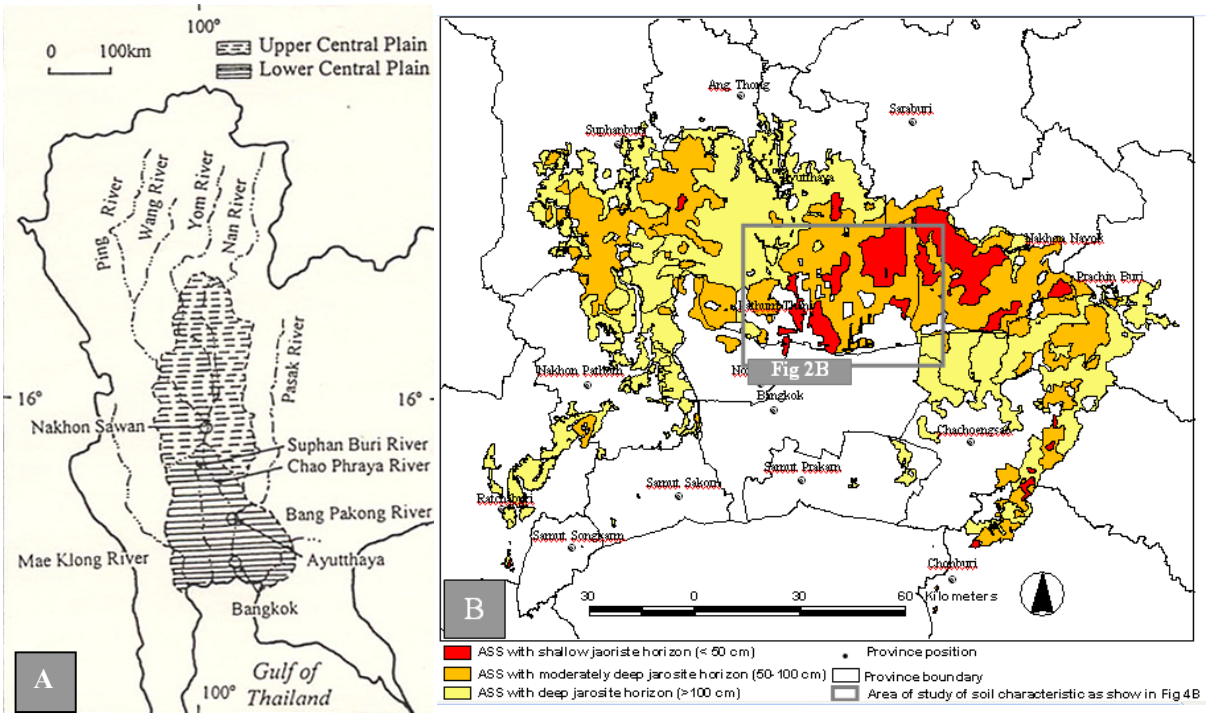

Fig 1 The boundary of the Upper and Lower Central Plain (Choowong, 2002) (A). Acid sulfate soil distribution in the Lower Central Plain of Thailand (modified after Land Development Department, 2006) (B)

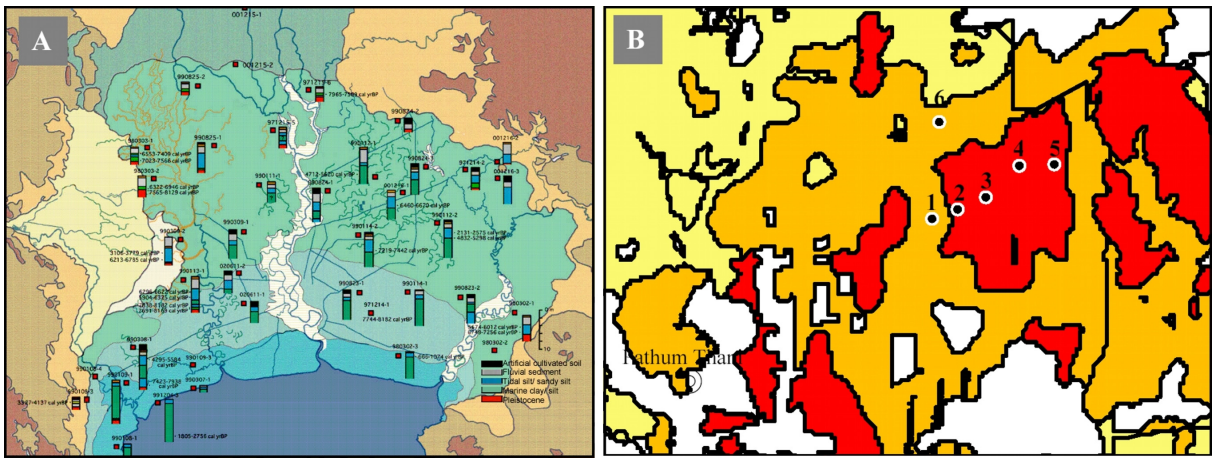

Fig 2 Geologic columns of the upper Holocene sediment at the sampling sites of geo-environment study (A) and locations of six soil sampling (B)

RESULTS

1. Geo-environmental classification of the delta

The Chao Phraya delta is located in central Thailand, and draining into the Gulf of Thailand. Geomorphologic boundaries between the Holocene alluvial surface and older surfaces are relatively clearly shown in Satellite images (Landsat TM, JERS-1, MOS-1), and it is almost along the inner limit of marine or tidal flat sediments. Landforms of the Chao Phraya Delta are classified into three regions: the deltaic floodplain in the north, the deltaic tidal plain in the central and south, and the tidal plain in the southernmost regions of the plain (Fig 3). Elevation of the tidal plain is around 1 m a.s.l., and its surface is very low and flat. Most of the region was originally lower than the high tide level, and the sediments of the region are thin tidal flat silt or clay over thick marine sediments. The deltaic tidal plain with elevations of 2-3 m, has been formed as a tidal and deltaic lowland since the Holocene high stand around 6 ka BP. The surface sediments of the region which cover the marine sediments are soft silt and mostly consist of tidal flat origin. There are few fluvial landforms and their sediments are also rare in the deltaic tidal plain. Fluvial landforms such as natural levees and flood basins develop in the deltaic floodplain. Surface sediments of the region are characterized by fluvial silt or clay that covers tidal silty sediments.

The Holocene sediments are divided into lower transgressive peaty (mangrove swamp) sediments and upper regressive deltaic sediments (Somboon, 1988; Somboon and Thiramongkol, 1992; Sinsakul, 2000). The Holocene sediments in the central plain mainly consist of silt and clay and occasionally organic matter. They are classified into four units: basal peat, marine, tidal and fluvial units from the lower to the top horizons. The basal peat is develops mainly at the depth about -5 to -10 m in the south western part, and about -5 to 0 m in the eastern and northern parts of the plain. The marine unit, so called Bangkok clay (Nutalaya, 1983), is very soft clay with occasional shell fragments and plant remains. The thickness is over 10 m in the central and southern parts, and decrease towards the plain margin. The tidal unit consists of silt, or silty clay with very thin organic rich sandy layers, and it is covered with fluvial units. Its thickness is 2-3 m in the central part, 3-5 in the marginal part, and decreases toward the south of the plain. Fluvial unit is brownish stiff clay or reddish mottled clay, silty clay with occasional plant remains. Boundary of fluvial and tidal units usually lies within 0-2 m a.s.l. Radiocarbon ages of the basal peat and mid-Holocene tidal sediments show approximate former relative sea-level. The maximum height of the sea-level was higher than 2 m above the present sea-level, and was recorded at around 6-7 ka BP (Fig 4A). Holocene transgression extended towards the region around Ayutthaya, 100 km from the present coast, and most of the Chao Phraya Delta was submerged according to the transgression. Rapid sea level rise continued until 5000 cal. yr BC (7000 cal. yr BP; 6000 yr BP) and the maximum height of the sea-level at that time was higher than 2 meters above present sea-level. (Umitsu et al., 2002). Late Holocene tidal sediments develop in the central and southern parts of the plain (4B), and they show that the plain expanded according to the retreat of tidal plain towards the south (4C).

Evolution of the Central Plain is also reported by Somboon and Thiramongkol (1992) and Tanabe et al. (2003) that the embayment of the Holocene transgression extended towards the area of Ayutthaya province, about 100 km from the present shoreline. After the maximum transgression at between 8 and 7 cal kyr BP, the delta system migrated southward into the paleo-Gulf of Ayutthaya. A large mud shoal (the Sananivate Mud Shoal) formed ear the mouth of the paleo-gulf between 7 and 3 cal kyr BP and facilitated it's infilling. As a result, the delta has prograded rapidly particularly during the last 2 kyr. The sea level approached its highest level of ca 2-4 m above MSL between 8 and 7 cal kyr BP, which is defined as MHH (calibrated from data in Sinsakul, 1992; Somboon and Thiramongkol, 1992). Most of the present delta plain was under a shallow sea known as the paleo-Gulf of Ayutthaya (Somboon and Thiramongkol, 1992).

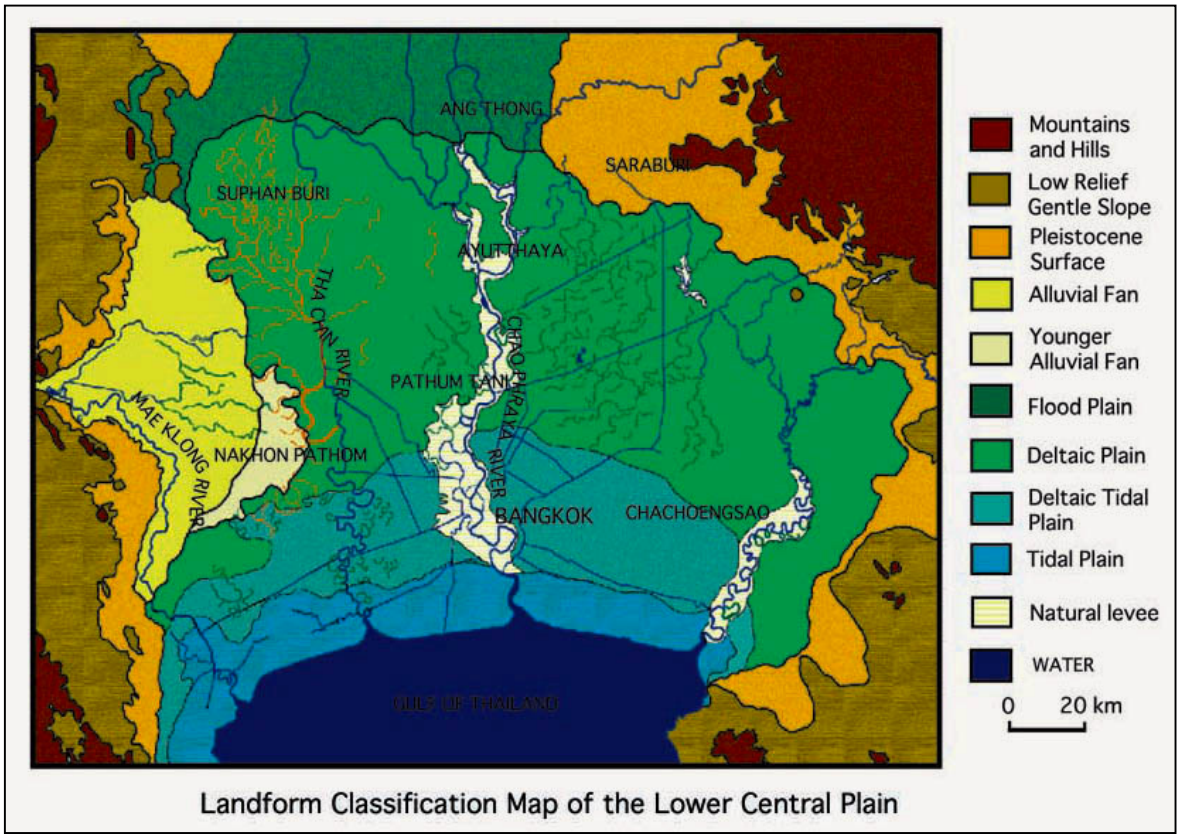

Fig 3 Landform classification map of the Lower Central Plain

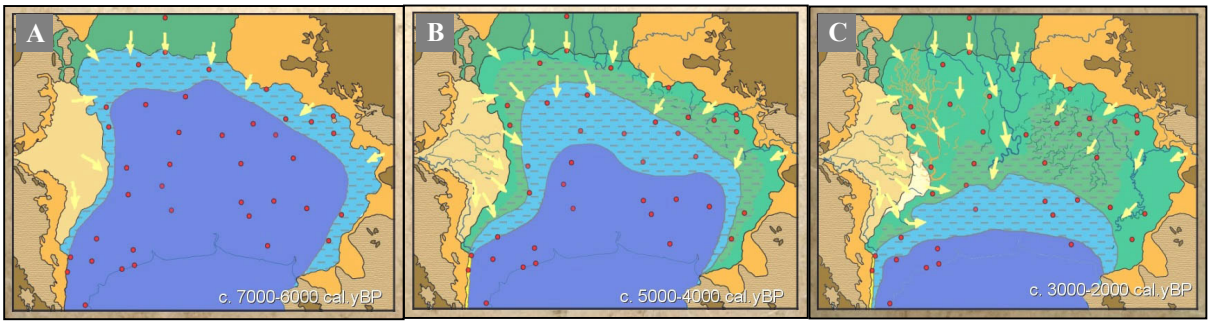

Fig 4 Holocene paleogeography of the Lower Central Plain at c. 7000-6000 cal yr BP (A), c. 5000-4000 cal yr BP (B), and c. 3000-2000 cal yr BP (C)

2. Characteristics of soils

There are six soil samplings for field morphology studying and electrical conductivity measuring. All of horizons of the profiles can grouped in to five distinct characteristics. They are potential acid sulfate horizon, Pleistocene alluvium, non-acid sulfate horizon, actual acid sulfate horizon, and topsoil from lower to top (detail is showed as Fig 5 and Table 1).

Potential acid sulfate horizon is found in the last part of soil profiles of location 1, 2, and 5, it develops mainly 220-240 cm of profiles, thickness is 80-150 cm. The color of soil are greenish gray, bluish gray, and black. The texture is silt, silty clay, silty sand, and sandy silt. The organic matter accumulates as organic materials, wood fragments, and peat. Soil reaction is ranging from neutral to strongly alkaline (filed pH is 7.0-8.5). Electrical Conductivity (EC) values show environment of sedimentation of the horizon is brackish water to marine condition. Whereas, Pleistocene alluvium is found only in location 6 at the last horizon of profile, 305-380 cm. It is light gray with red and olive iron nodules; silt with fine sand; plant fragments can

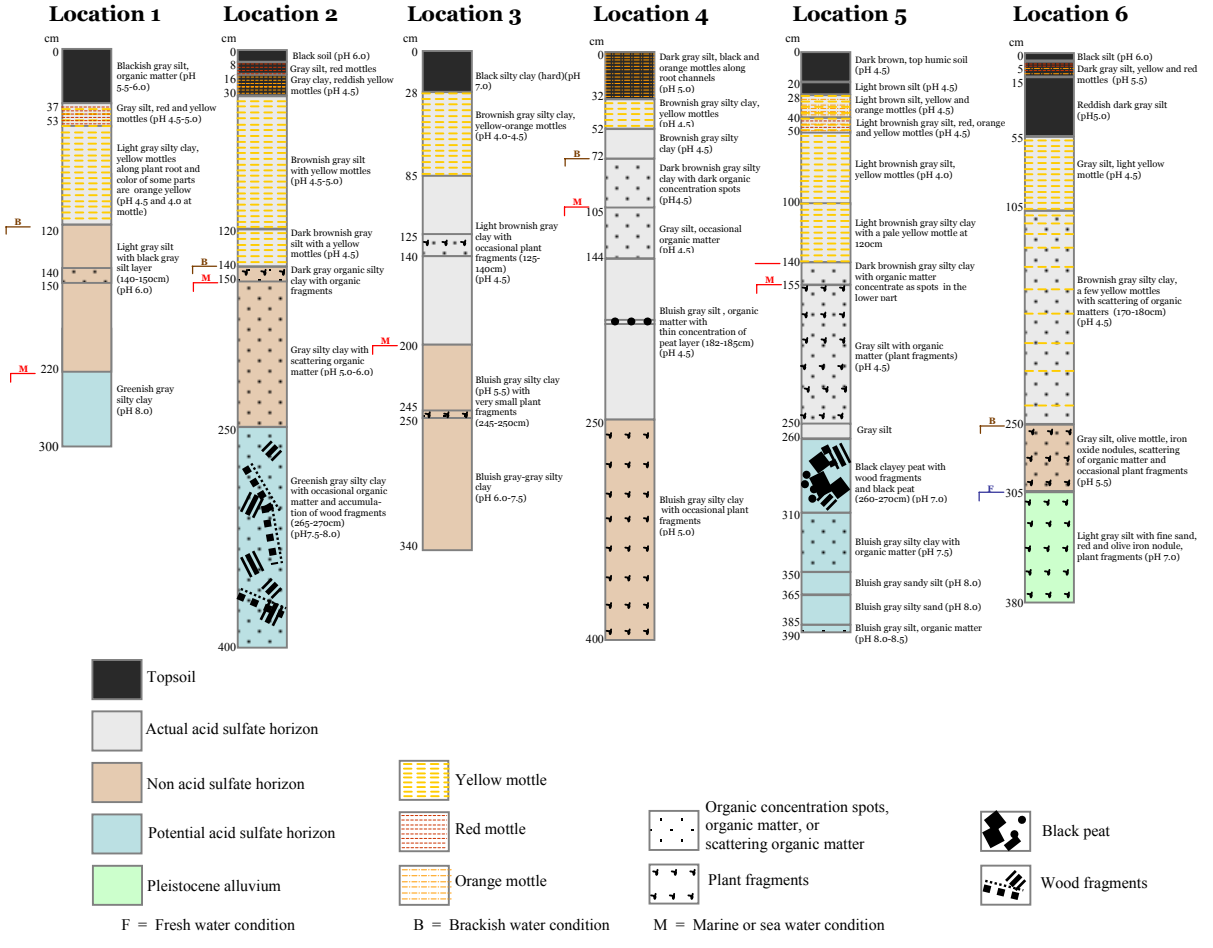

Fig 5 Soil profiles in the six locations

be suggested. The reaction is neutral (field pH is 7.0) and show that sediment deposited under fresh water condition. Non-acid sulfate horizon develops in every profile, except the profile of location 5. The horizon occurs 120-400 cm, thickness is 100-150 cm, except the profile of location 6 that has thickness only 55 cm. Color of soil is light gray to dark gray, olive mottle is found only in this of location 6. The texture is silt to silty clay with organic matter accumulation as darker area, scattering of organic materials, and small plant fragments. Soil reaction is ranging from very strongly acid to slightly alkaline (field pH is 5.0-7.5). Parent material of this horizon is considered as brackish water to marine sediments. The actual acid sulfate horizon overlies non-acid sulfate horizon, develops in 28-260 cm, thickness is 83-232 cm. The color is various shade of gray and brown with orange to red mottles and also yellow mottles of jarosite. Texture class is silt and silty clay to clay; organic matter is found in some locations as plant fragments, concentration spots, organic materials, and a very thin layer of peat concentration. Soil reaction is extremely to very strongly acid (field pH is 4.0-5.0). It is sediment mainly under fresh water condition zone of all profiles and also marine condition in lower part of location 4 and 5. The topsoil horizon develops over actual acid sulfate horizon, thickness is 28-55 cm. Color is gray to blackish gray and light to dark brown with red, yellow, orange, and black mottles; silt to clay with many of plant roots. The reaction is vary from strongly acid to neutral (field pH is 4.5-7.0). Environment of sedimentation is mainly fresh water.

Mostly the horizons of profiles sequence from lower to top is potential acid sulfate horizon, non-acid sulfate horizon, actual acid sulfate horizon, and topsoil. The Pleistocene alluvium is found as the last horizon in location 6. The non-acid sulfate horizon can be considered as transition zone of potential acid sulfate and actual acid sulfate horizons. The potential acid sulfate horizons appear only in profiles of location 1, 2, and 5, nevertheless, this horizon should found in profiles of location 3 and 4 as a horizon in lower part. Soil profiles with shallow potential acid sulfate horizon are also the profiles have thick layer of yellow mottle of jarosite, 83-112 cm and thin transition zone. This is dissimilar to profiles with very deep potential acid sulfate horizon as location 3 and 4; the profiles have thin layer of yellow mottles and thick layer of transition zone. The profile of location 6 is distinction from others; it has shallow Pleistocene alluvium, a thin non-acid sulfate and actual acid sulfate horizon but no potential acid sulfate horizon which is considered as source of acidity. It can be inferred that sulfidic material is level advanced from adjacent acid sulfate soil area as soil fluid. Thus, acid material can move both vertical and horizontal direction. To compare the two directions, flowing in vertical path as along plant roots and voids is easier due to they are connected pores. The yellow mottle of jarosite zone is the strongest acid condition zone in the profile. The appearing of jarosite and very low pH value are characteristics of acid sulfate soil. This part is actual acid sulfate horizon, occurs only in fresh water sediment. The conditions of material of profile are usually sequence as marine, brackish water, and fresh water from lower part to surface. They can be considered the environment of sedimentation by marine is shallow marine under mangrove forest, brackish water is tidal to intertidal, and fresh water is alluvial sediments.

It can be suggested different oxidation conditions in profile from characteristics of soil that topsoil and actual acid sulfate horizon has strong oxidation, the mottle appearing and very low pH values are considered as products of high stage of oxidation. While non-acid sulfate horizon has not low pH value as much as actual acid sulfate horizon and practically no mottle, these indicate oxidation occurred in this horizon as low stage and will further more develop to higher stage if meet dry periods. As another reason, it obtains low concentration of sulfidic material, small amount of acid can not change reaction of soil to extremely acid and shows accumulation of them as mottles. On the contrary, potential acid sulfate horizon that this part still being under reduction with high pH value and no mottle.

CONCLUSIONS AND DISCUSSION

Development of acid sulfate soil in the Lower Central Plain is related to the thickness of the sediments over the soft marine or shallow marine sediments. Acid sulfate soil with shallow jarosite horizon can be seen in the areas where the thickness of the intertidal or fluvial sediments is less than 2.2 m. The profiles with shallow potential acid sulfate horizon intend short distance for sulfidic material move up and accumulate as concentrate zone. Therefore, these soils have thick extremely acid with yellow mottles in profiles. Shallow marine under mangrove forest, which is the most suitable for sulfidic material (mainly pyrite) forming, was started after culmination of Holocene transgression. Then the environment was changed to tidal to intertidal in period of sea regression. The deltaic plain was developed continuously with fluvial sediment as recent condition. After drainage was introduced, soil moisture condition changed from under wet condition all the time to wet alternated with dry which caused oxidation occurred. Pyrite was moved upward from source

(potential acid sulfate soil horizon) with soil water movement and capillary action to upper part. Then pyrite was oxidized and changed to be jarosite appearing as yellow mottles in soil pores and cracks, the horizon got extremely to very strongly acid condition. Oxidation condition of acid sulfate soil in this area is relation to fluctuation of water table.

References

Burrough, PA, van Mensvoort, MEF & Bos, J 1988, 'Spatial analysis as a reconnaissance survey technique: an example from acid sulfate soil regions of the Mekong Delta, Vietnam', *Selected papers Dakar Symp. Acid sulphate soils*, 1986, Dakar, Senegal, Dost, H (ed), LIRI Publ. 44, pp. 68-89.

Choowong, M 2002, 'The Geomorphology and Assessment of Indicators of Sea-Level Changes to Study Coastal Evolution from the Gulf of Thailand', *Proceedings of the Symposium on Geology of Thailand*, 26-31 August 2002, Bangkok, Thailand.

Dent, DL & Pons, LJ 1995, 'A world perspective on acid sulphate soils', *Geoderma*, vol. 67, pp. 263-276.

Department of Natural Resources and Water 2007, '*Acid sulfate soils*', Queensland Government, viewed 5 December 2007, <www.nrm.gld.gov.au/land/ass/index.html>.

Dheeradilok, P, & Kaewyana, W 1986, 'On the Quaternary deposits of Thailand', *GEOSAE V Proceeding*, vol I, Geol Soc, Malaysia. Bulletin 19, pp. 515-532.

Geological Survey Division 1999, *Geological map of Thailand*, 1:2 500 000, Geological Survey Division, Department of Mineral Resources, Thailand.

Hara,Y, Takeuchi, K & Okubo, S 2005. 'Urbanization linked with the past agricultural landuse patterns in the urban fringe of the deltaic Asia mega-city: a case study in Bangkok', *Landscape and Urban Planning*, vol. 73, issue 1, pp. 16-28.

Jon, L, RAU & Nutalaya, P 1983, 'Geology of Bangkok Clay', *Geo. Soc. Malaysia*, Bulletin 16, December 1983, pp. 99-116.

Land Development Department 2006, '*Acid sulfate soil distribution map of Thailand*', 1:2 500 000, Land Development Department, Thailand.

Lin, C, Melville, MD & Hafer, S 1995, 'Acid sulphate soil-landscape relationships in an undrained, tide-dominated estuarine floodplain, Eastern Australia', *Catena*, vol. 24, pp. 177-194.

Martin, CR & Terry, MV 2005, 'Estimating the depth to sulphide-bearing materials in upper Cretaceous sediments in landforms of the Maryland coastal plain, *Geoderma*, vol. 126, pp. 101-116.

McElnea, AE, Ahern, CR, Manders & Smith CD 2004, 'Variability of acid sulfate soil chemistry at east Trinity remediation site, far north Queensland, Australia', paper presented to the ISCO 2004-13th International Soil Conservation Organisation Conference, Brisbane, July 2004.

Muhrizal, S, Shamshuddin, J, Fauziah, I & Husni, MAH 2006, 'Change in iron-poor acid sulfate soil upon submergence', *Geoderma*, vol. 131, pp. 110-122.

Nutalaya, P 1983, 'Geology of Bangkok clay', *Geological Society of Malaysia Bulletin*, vol. 16, pp. 99-116.

Sinsakul, S 1992, 'Evidence of Quaternary sea level changes in the coastal areas of Thailand', *A review: Journal of Southeast Asian Earth Sciences*, vol. 7, no. 1, pp. 23-37.

Sinsakul, S 1997, 'Country Report: Late Quaternary Geology of the lower Central Plain, Thailand', paper presented to International Symposium on Quaternary Environment changes in the Asia and Western Pacific Region. October 14-17, University of Tokyo, Tokyo, Japan

Sinsakul, S 2000, 'Late Quaternary geology of the Lower Central Plain, Thailand', *Journal of Asian Earth Sciences*, vol. 18, pp. 415-426.

Slager, S, Jongmans, AG, Pons, LJ 1970, 'Micromorphology of some tropical alluvial clay soils', *Journal of Soil Science*, vol. 21, no. 2, pp. 233-244.

Soil Survey Staff, 2006, '*Keys to Soil Taxonomy*, 10th edn', United States Department of Agriculture, Washington D.C., U.S.A.

Somboon, JRP 1988, Paleontological study of the recent marine sediments in the lower central plain, Thailand', *Journal of Southeast Asian Earth Sciences*, vol. 2, Nos ¾, pp. 201-210.

Somboon, JRP, & Thiramongkol, N 1992, 'Effect of Sea-level Rise on the North Coast of the Bight of Bangkok, Thailand', *Malaysian Journal of Tropical Geography*, vol. 24 (1/2), pp. 3-12.

Tanabe, S, Saito, Y, Sato, Y, Suzuki, Y, Sinsakul, S, Tiyapairach, S & Chaimanee, N 2003, 'Stratigraphy and Holocene evolution of the mud-dominated Chao Phraya delta, Thailand', *Quaternary Science Reviews*, vol. 22, pp. 789-807.

Udomsri, S, Hoontrakoon, K & Watana, S 2004, '*Characterization of Established Soil Series in the Central Plain Region of Thailand Reclassified According to Soil Taxonomy 2003*', Publ. no. 520, Office of Soil Survey and Land Use Planning, Land Development Department, Thailand.

Umitsu, M, Tiyapairach, S, Chaimanee, N & Kawase, Kumoko 2002, 'Late Holocene Sea-Level Change and Evolution of the Central Plain, Thailand', *Proceedings of the Symposium on Geology of Thailand*, 26-31 August 2002, Bangkok, Thailand.

van Breemen, N 1973, 'Soil forming processes in acid sulphate soils', *Dost, H (ed), Acid Sulphate Soils. Proc. Int. Symp.*, Wageningen, ILRI Publ. no. 128, vol. 1, pp. 66-130. Internat. Instit. for Land Reclam. and Imp., Wagenngen.

Vlek, P 1971, '*Some morphological physical and chemical aspects of acid sulphate soils in Thailand*', Report SSR-84, Bangkok, Soil Division, Department of Land Development, Thailand.

Wilson, BP 2005, 'Elevations of sulphurous layers in acid sulphate soils: what do they indicate about sea level during the Holocene in eastern Australia?', *Catena*, vol. 62, pp. 45-56.

Table 1 Characteristics of acid sulfate soils in five distinct horizons

Category	Depth/ Thickness (cm)	Matrix color	Mottle color	Texture class	Organic matter	Field pH	EC ($dS\ m^{-1}$)	Other features
Topsoil								
Location 1	0-37/ 37	Blackish gray	-	Silt	Plant roots	5.5-6.0	NA	-
Location 2	0-30/ 30	Black and gray	Red and reddish yellow	Silt and clay	Plant roots	4.5-6.0	0.36-0.42 (F)	-
Location 3	0-28/ 28	Black	-	Silty clay	Plant roots	7.0	0.37 (F)	-
Location 4	0-32/ 32	Dark gray	Black and orange	Silt	Plant roots	5.0	0.99 (B)	-
Location 5	0-28/ 28	Dark brown and light brown	-	Humic soil and silt	Plant roots	4.5	0.35 (F)	-
Location 6	0-55/ 55	Black, dark gray and reddish dark gray	Yellow and red	Silt	Plant roots	5.0-6.0	0.32-0.38 (F)	-
Actual acid sulfate soil								
Location 1	37-120/ 83	Gray and light gray	Red and yellow and orange yellow	Silt and silty clay	-	4.5-5.0	0.30-0.39 (F)	-
Location 2	30-140/ 110	Brownish gray and dark brownish gray	Yellow	Silt	-	4.5-5.0	0.41-0.47 (F)	-
Location 3	28-200/ 172	Brownish gray and light brown	Yellow-orange	Silty clay and clay	Occasional plant fragments	4.0-4.5	0.16-0.23 (F)	-
Location 4	32-250/ 218	Brownish gray, dark brownish gray, gray, and bluish gray	Yellow	Silty clay and silt	Dark organic concentration spots, occasional organic materials, concentration of peat	4.5 4.5	0.44-0.55 (F) 2.80-3.51 (M)	-
Location 5	28-260/ 232	Light brown, light brownish gray, dark brownish gray, and gray	Yellow, pale yellow, orange, and red	Silt and silty clay	Organic concentration spots and plant fragments	4.0-4.5	0.43-0.54 (F) 1.80-1.96 (M)	-
Location 6	55-250/ 195	Gray and brownish gray	Light yellow and yellow	Silt and silty clay	Concentration of organic materials	4.5	0.34-0.41 (F)	-
Non acid sulfate soil								
Location 1	120-220/ 100	Light gray and black gray	-	Silt	Darker color area	6.0	0.63 (B)	-
Location 2	140-250/ 110	Dark gray and gray	-	Silty clay	Scattering of organic materials	5.0-6.0	0.99 (B)	-
Location 3	200-340/ 140	Bluish gray -gray	-	Silty clay	Small plant fragments	5.5-7.5	1.45-1.88 (M)	-
Location 4	250-400/ 150	Bluish gray	-	Silty clay	Occasional plant fragments	5.0	4.03 (M)	
Location 6	250-305/ 55	Gray	Olive	Silt	Scattering of organic materials and occasional plant fragments	5.5	0.86-1.27 (B)	Iron oxide nodules
Potential acid sulfate soil								
Location 1	220-300/ 80	Greenish gray	-	Silty clay	-	8.0	3.93 (M)	-
Location 2	250-400/ 150	Greenish gray	-	Silty clay	Occasional organic materials and wood fragments	7.5-8.0	1.42-1.49 (M)	-
Location 5	260-390/ 130	Black, and bluish gray	-	Silt, Silty clay, sandy silt, silty sand	Peat, wood fragments, and organic materials	7.0-8.0 8.0-8.5	2.35-4.5 (M) 0.77 (B)	-
Pleistocene alluvium								
Location6	305-380/ 75	Light gray	-	Silt with fine sand	Plant fragments	7.0	0.33 (F)	Red and olive iron nodule

The Conservation Problems of Mangrove Forest in Segara Anakan – Central Java – Indonesia

Junun Sartohadi[1], Langgeng Wahyu Santosa[2], Wirastuti Widyatmanti[3]

[1] *Department of Environmental Geography, Faculty of Geography, Gadjah Mada University, Yogyakarta, E-mail: sartohadi@yahoo.com*
[2] *Department of Environmental Geography, Faculty of Geography, Gadjah Mada University, Yogyakarta, E-mail: wahyus_72@yahoo.co.id*
[3] *Diploma Program of Remote Sensing and Geographic Information System, Faculty of Geography, Gadjah Mada University, Yogyakarta, E-mail: widyatmanti@yahoo.com*

Abstract

This paper was proposed to figure out the conservation problems of mangrove forest in Indonesia with a special case in Segara Anakan, Central Java. The study area is located in the river-mouth of several rivers coming from both West Java and Central Java Provinces. As it is located in the estuary, the Segara Anakan receives a huge amount of sediment due to severe erosion in the up-streams.

To conserve the mangrove forest in Segara Anakan had several problems coming from physical, socio-cultural and political situation. The physical problem was mainly related to the high rate of sedimentation. That situation was mainly coming from the misuse of land in the up-streams. The regional autonomy era that based on the district levels had forced every district improve their economical incomes. The way of how to generate new and/or improve economical incomes were mainly based on the natural resources. In the end, the exploitation of land resources was seems excessive. The socio-cultural problems were mainly related to poverty and fisherman culture. The decrease of environmental situation of the mangrove forest both physical and biological had made the decline of fish production. In the end, the decline of fish production made the incomes of the Segara Anakan regions went down.

Comprehensive scientific research in Segara Anakan is required to formulate the comprehensive solutions. When the problems in Segara Anakan can be solved, the problems in other areas in Indonesia may be solved too. It is because the problem in Segara Anakan is one of the most complex problems compared to the other areas in Indonesia.

Key words: mangrove forest, conservation problems, Segara Anakan

INTRODUCTION

Mangrove forest is a unique ecosystem located in the coastal area, influenced by tidal but is not influenced by climatic condition (Department of Forestry - RI, 1994). Nybakken (1982) figured out that the variety of tropical coast community is dominated by some unique vegetation species or shrub with unique capability of adaptation in saline water. The mangrove ecosystem is contained 11 genus (*Avicennia, Snaeda, Laguncularia, Lumnitzera, Conocarpus, Aegicera, Aegialitis, Rhizophora, Bruguiera, Ceriops*, dan *Sonneratia*), which of each of them has pneumotafor and grows on the muddy or fine sandy soil under various water salinity.

According to Santosa-Nyoto (2001), the mangrove forest in Indonesia can be classified into 2 geographical zones, i.e., Asian Zone and Oceania Zone. Those two zones have relatively higher biotic variety than other mangrove forest in the other countries. This situation is due to the differences of natural condition on each island, even to the one on different location within one island. The combination of mangrove vegetations with their unique environments creates various ecosystems with distinctive species variety living within it.

The Zoning of Mangrove Forest

Mangrove vegetation tends to perform a zone or strip following the soil condition and the degree of water salinity. Based on that fact, the mangrove forest can be grouped into some zones, i.e., *Sonneratia and Avicennia* (seaward direction), *Rhizophora, Bruguiera, Ceriop*s, and *Nypa association.* That zone is derived from the level of mangrove resistance to wind and wave. For instance, *Sonneratia and Avicennia* sp. are

located in the high salinity water, and are well know as pioneer mangrove. On the other hand Nypa fruticans is the one of the most un-resistant mangrove to salinity (Nybakken, 1982).

Furthermore, Steenis (1985) explained that on the more consolidated material of mud deposit eventually can be found *Avecinnea marina*, whereas on the soft mud deposit is grown with *Avicennia alba.* On the rear of this zone there is *Bruguiera cylindrica* which grows collectivelly with *Rizophora apiculata, Rizophora mucronata, Bruguiera parviflora*, and *Xylocarpus granatum* (the peak of the canopy can reach 35 – 40 metre of height). The mangrove forest, which is far away from the sea, are mostly pure stand. Some zones will be different in one place to another, depend on soil and water condition in each area. In Indonesia, such as in Rambut Island Natural Conservation, it is composed of 3 zones from the sea up to the land, i.e: *Rhizophora mucronata*, *R. stylosa*, and *Scyhiphora hydrophyllcea* which associated with *Lumnittzera racemosa.* While in Cilacap, Central Java, consist of 3 zones, i.e: *Avicennia sp*. or *Sonneratia sp., Rhizophora sp*. and *Bruguiera sp*. (Santoso-Nyoto, 2001).

The Coastal Area and the Habitat of Mangrove Forest

Schimper (1998) considers that mangrove forest becomes *xerophyl* vegetation which physiologically inhabit in dry land as the result of high salinity in such swampy areas. It causes mangrove forest becoming an important point in relating coastal area and the shore. Mangrove vegetation is able to create dense forest along the shore line, which is effective enough to be a sediment, nutrient and pollutant trap. This ecosystem can also control the run off, stabilize the coastal area, expel the detritus, become a coastal demarcation conservation zone and protect the fish fries (Dahuri, *et al*., 1996). According to Steenis (1985) and Nirarita, *et al*. (1996) mangrove forest can grow within the water environment with some characteristics, i.e.:

(a) Mud soil which is combination of sandy clay with the fragment material of coral;
(b) Periodically submerged, daily or at the full moon, these can effect the composition of mangrove vegetation;
(c) Accepting enough freshwater supply from the land (river or groundwater), which can reduce the seawater salinity, affix the nutrient supply and mud;
(d) Brackish water with 2 - 22 ppm of salinity, or salty one with the salinity condition until 38 ppm.

Based on those concepts above, it can be concluded that mangrove forest grows up and develops within such transition zone between sea and land, called as coastal area, and generally is regarded as mangrove's habitat. Coastal area can be bordered from the land upward, which is area which still effected by seawater sprinkling or the sea water tidal, and from the sea downward is delimited by continental shelf (Beatly, *et al*., 1994, in Sugandhy, 1996). Based on genetic process and etymology point of view, the coastal area is a landform initiated from the sea line border, signed with the appearance of breakers zone to upland, which has landform type that is genetically still affected by the marine activity, such as coastal alluvial plain (after CERC concepts, 1984; Pethick, 1984). Coastal area is also included shore and coast. Shore is an area between shoreline with the highest average of seawater rise tide, which called as coastline. Coast is an area started from coastline which shows the highest average of rise tide to upland until to the zone that is genetically affected by marine activity, and is usually named as coastal alluvial plain (based on concept of CERC, 1984).

Coastal area as mangrove's habitat has variety of type and characteristic. However, not all of the coastal area gives chance to the mangrove for living and developing. Based on coast area classification by Shepard in King (1972) on Figure 1, mangrove has feasibility to grow and develop on the two types of coast, i.e. sub aerial depositional coast and marine depositional coast. *Sub aerial depositional coasts* is a coast shaped by direct accumulation of river sediment, glacial, wind or landslide material to the sea, which carried and deposited by the river stream to the estuary zone. These categories are included delta's formation and tidal platform. *Marine depositional coast* is a coast formed by deposition material of marine sediment in clay up to sandy size, included barrier coasts, such as: shore barrier, island barrier, spit barrier and bay, cuspate foreland, shore plain, coastal sand plain without lagoon, mud flat and salt marsh.

According to Ongkosongo, *et al.* (1986) in Mulia (1999), classified mangrove forest based on the environment condition, which can be described as below:

(1) *Mangrove in delta type*. Mangrove which grows and develops on the big river's outlet has large amount of sediment and deposited as delta. This kind of mangrove is mostly found in Indonesia, i.e.: in Sumatera (Delta of Musi, Tembilahan, and Siak), in Kalimantan (Delta of Mahakam, Tarakan, and Batu Ampar Kapuas River), also in Irian Jaya (Delta of Bintuni).

(2) *Mangrove in mud platform type* is a type of mangrove which formed along the shore edges, takes place surrounding the mountainous area with small rivers over it. The current of tide spreads the river's sediment downward to the sea, creating such plain with mud material contain (combination between clay and sand). Such condition almost can be found along the East Sumatera's shoreline, North Java's shore, West Irian Jaya's shore, and East Sulawesi's shore, especially on the big river's outlet.

(3) *Mangrove in island platform type* is a type of mangrove which grows within a small island. It arises out of the sea level when the low tidal occurred. Its material consists of land sediment or sea's carbonate sediment, such as mud sediment platform on the group of small islands in Kepulauan Seribu Jakarta.

(4) *Mangrove in shore platform type* is a kind of mangrove situated along the narrow path of shoreline. The material is composed of sand, clayed sand up to gravel. This ecosystem is usually called as fringing mangrove. This type of mangrove can be observed in East shore of Lampung, East shore of South Sumatera, and shore of North Java.

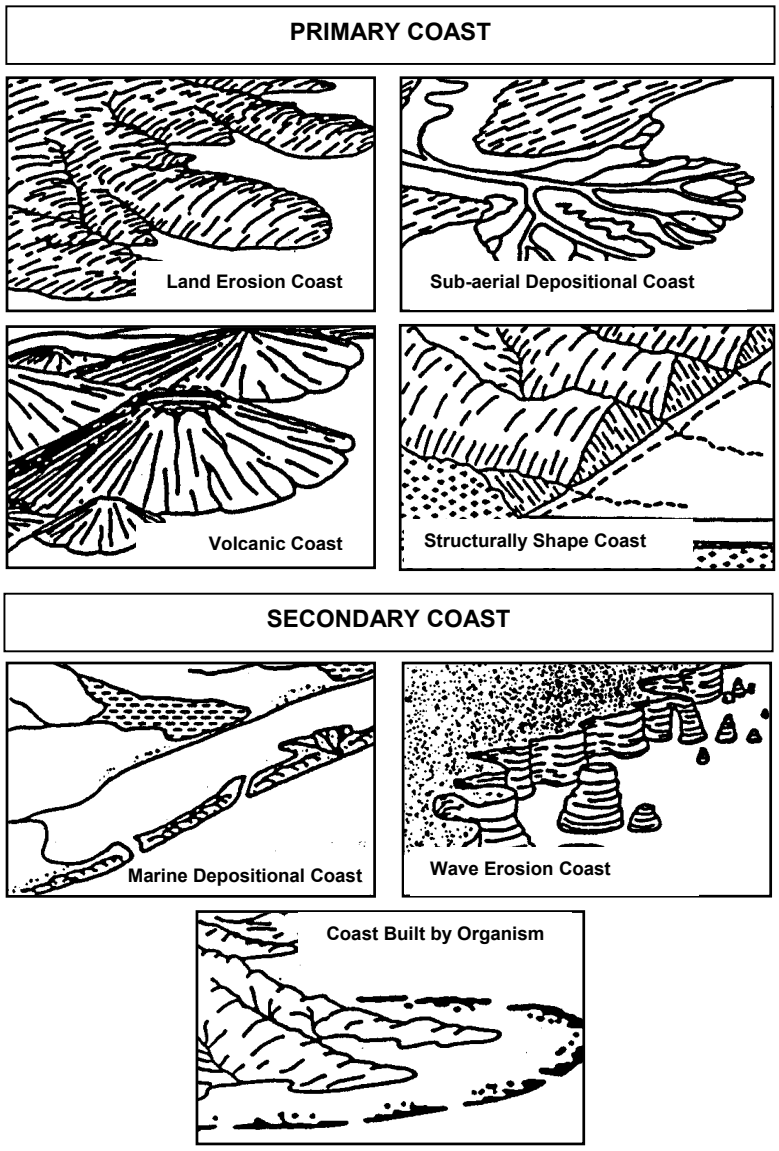

Figure 1. The Genetic Classify of Coast according to Shepard (King, 1972)

THE GEOGRAPHIC CONDITION OF MANGROVE FOREST IN COASTAL AREA OF INDONESIA

Coastal Area and Biologic Variety in Indonesia

The geographical condition of Indonesia as an island country gives numerous prospects to many coastal and sea resources. Indonesia, largely extended on the equator from 92°-141° E and 7°20'-14° S, is the biggest archipelago country in the world, and consists of 17.508 big and small islands, with 81.000 km length of shoreline and 5.8 million km^2 large of sea water. This landscape is composed of shore, ZEE territorial area of sea and continental platform, the continental slope, the ocean basin below it and air above it. Based on the size of area, followed by natural unity of earth, sea and air above it, also global position as continental margin, thus Indonesian region has the characteristics of continent. Therefore, it is apt if Indonesia is called as *Continent of Indonesian Maritime* (BMI) (Kamiso, 2000, in Puji, 2005). As an archipelago, it will certainly gives consequent to the various configurations development of coastal area, which of one of them is mangrove forest with its biologic variety.

Soemodihardjo (1993), describes that mangrove in Indonesia consists of 15 families, 18 genus, 41 species, and 116 associated species. Meanwhile, Kusmana (1993) also explains that there are at least 101 species of mangrove plants, either of specific or not-specific mangrove habitat, which consists of 47 species of trees, 5 species of bushes, 9 species of herbs and grasses, 9 species of liana, 29 species of *epiphyte*, and 2 species of *parasites.* Alikodra, *et al.*, (1990) in Kusmana (1993), reported that in mangrove forest of Cimanuk outlet and Segara Anakan Cilacap, respectively there are 23 species of water animals and 16 species of water birds, with 12 of them are categorized as migration bird. Furthermore, some species of primates exist within the mangrove forest, i.e.: *Nasalis larvatus, Macaca fascicularis, Presbytis sp.*; also kind of reptiles i.e.: *Varanus salvator*, *Lizard*, *Snake*, and *Crocodile (Crocodylus porosus).* In the same time, Kartawinata, *et al.*, (1979) in Kusmana (1993), reported as well that at least there are 90 species of sea animals which included to the habitat of mangrove forest, i.e: *Gastropoda* (50 species), *Bivalvia* (6 species), and *Crustacea* (34 species).

A Glance Condition of Mangrove Forest in Indonesia

According to some sources, the large of mangrove forest in Indonesia is quite various, i.e.: 3,177,700 Hectare (Ha) (Forestry Program Construction of Indonesia, 1973); 3,707,100 Ha (UNESCO, 1979); 4.251.011 Ha (Forestry Program Construction of Indonesia, 1982); and 4,355,553 Ha (Department of Forestry - RI, 1993). Forestry Department of Indonesia (1999) stated that the width of mangrove forest is 3,980,496 Ha, and 4,812,648 Ha is outside the forest area. Rosalina (1993) and Santoso-Nyoto (2001) also said those different with prediction of the mangrove forests is caused by the different perspective of determining the deepest border or the wide of formation or the mangrove's zoning. In case of Java Island, in 1993 there are 616.405 Ha of mangrove forest. Its value is detail provided in Table 1.

According to Department of Forestry - RI (1999), the data inventory result of damaged level of mangrove forest from 15 provinces in Indonesia showed that 2,432,418 Ha of mangrove forest is in good condition, 2.268.033 Ha inside the forest area and 164.385 Ha outside the forest area. Meanwhile, the damaged mangrove forest is 5,901,975 Ha; 1,712,462 Ha inside the forest and 4.189.513 Ha outside the forest area (Santoso-Nyoto, 2001). In the Java Island, the intact mangrove forest is 2.983,36 Ha, and however the damaged one has reached 318.364,12 Ha. Those data is described in Table 2.

Since 1992, when the Province and District Spatial Plan are approved, there is a change to the management status and the width of mangrove forest area. Based on the Regional Spatial Planning, mangrove forest is regarded as Conservation and Cultivation Area (Forestry Cultivation, Fishery and Agricultural Cultivation). Nevertheless in some region, mangrove forest area is considered as Conservation Area. This different regulation creates a contradiction with the previous policy that stated the mangrove forest is regarded as conservation forest area, wildlife reserve forest, eco-tourism forest, and production forest.

Another problem in determining the management status of the mangrove forest is, there is no yet agreement of management status criteria (conservation forest or production forest). Commonly, it is derived from management interest and another purpose in order to keep up the Region Original Income, which related to sustain the region autonomy (Santoso-Nyoto, 2001). Dealing with those conditions, thus the large and the management status should be reevaluated based on the Regional Spatial Planning Regulation of each area.

Table 1. The Large (Hectare) and the Distribution of Mangrove Forest Area each Province, Including Its Function Status and Its Large Changing Level within 1982 until 1993 in Indonesia.

No	Province	Permanent Forest Area (KHT)				Number of KHT	HPK	APL	Number of HPK & APL	Total Large with in 1993	Large of Mangrove Forest 1982[1]	Degree of Large Changing (%)
		HAS & HW	HL	HPT	HP							
1.	Aceh	750	-	41.250	6.720	48.720	5.560	47.660	54.220	102.270	54.335	+89,5
2.	North Sumatera	12.490	-	444.080	320	56.840	2.120	39.380	41.500	98.340	50.000	+33,9
3.	West Sumatera	0	0	0	0	0	3.910	940	4.850	4.850	0	Unlimited
4.	Riau	6.410	15.680	80.540	8.440	111.150	128.180	1.720	103.900	221.650	276.000	-19,9
5.	Jambi	4.800	0	0	0	4.800	0	8.650	8.650	13.450	65.000	-79,3
6.	South Sumatera	20.310	28.010	0	68.020	216.340	8.460	38.630	47.090	363.430	95.000	+86,4
7.	Bengkulu	0	0	0	0	0	522	2090	2.612	2.612	0	Unlimited
8.	Lampung	3.650	0	0	8.540	12.190	0	37.250	37.250	49.440	17.000	+190,8
9.	West Java	-	-	-	-	-	-	594.061	594.061	594.061	28.608	+1976,5
10.	Central Java	-	-	-	-	-	-	12.188	12.188	12.188	13.577	-10,23
11.	East Java	-	-	-	-	-	-	10.156	10.156	10.156	7.750	+31
12.	Bali	-	-	-	-	-	-	-	-	800	1.950	-95,5
13.	West South-East Nusa	01	0	0	0	0	0	0	0	0	3.678	-100
14.	East South-East Nusa	2.810	0	0	0	2.810	0	7.970	7.970	10.780	1.830	+489,1
15.	East Timor	0	0	0	330	330	940	3.330	4.270	4.600	0	Unlimited
16.	West Kalimantan	3.280	52.520	940	27.200	83.940	58.350	52.000	110.360	194.300	40.000	+385,8
17.	Central Kalimantan	0	2.340	0	9.380	11.270	37.920	0	37.020	48.740	10000	+387,4
18.	South Kalimantan	21.090	160	22.340	0	43.590	34.530	42.660	77.190	120.780	56.650	+81,2
19.	East Kalimantan	50.530	2.350	3.280	514.320	580.530	125.110	0	195.110	775.640	266.800	+190,7
20.	Central Sulawesi	2.600	160	2.370	790	5.920	320	31.400	31.720	37.640	0	Unlimited
21.	South-East Sulawesi	10.690	1.040	18.720	2.590	33.040	4.290	33.510	37.800	70.840	29.000	+144,3
22.	North Sulawesi	1.580	0	5.540	800	7.920	3.800	26.430	30.230	38.150	4.833	+689,4
23.	South Sulawesi	1.100	18.290	13.120	0	32.500	0	71.530	71.530	104.030	66.000	+57,6
24.	Maluku	2.650	2.130	71.880	4.040	80.710	67.630	310	58.000	148.710	100.000	+48,7
25.	West Papua “Irian Jaya”	367.240	291.470	204.380	196.480	1.059.570	257.420	0	267.420	1.325.990	2.943.000	-54,9
Total Number		**522.070**	**614.120**	**508.490**	**847.970**	**2.492.650**	**795.710**	**1.063.721**	**1.859.431**	**4.355.553**	**4.251.011**	**-**

Sources: (1) Directorate of Forestry Program Construction of Indonesia (1982); (2) Rosalina (1993) in Santoso-Nyoto (2001)
HAS = Reserve Park ; HW = Tourism Forest; HL = Protected Forest; HPT = Permanent Production Forest; HP = Limited Production Forest
HPK = Production Forest can be conserved; APL = Other land use

Table 2. The Data of the Damaged and the Rehabilitation of Mangrove Forest in Indonesia until 1999

No	Province	Intact Mangrove Forest (Hectare)			Damaged Mangrove Forest(Hectare)			The Realization of Rehabilitation (Hectare)	Explanation
		Inside the Area	Outside the Area	Inside the Area	Outside the Area	Inside the Area	Outside the Area		
1.	Aceh	-	31,530.96	31,503.96	2,442.69	312,897.69	315,340.38	800.00	
2.	North Sumatera	-	386.94	386.94	26,639.73	8,881.67	35,521.40	785.00	
3.	Riau	36,140.04	27,813.78	63,953.82	515,607.70	575,523.88	1,091,131.58	1,530.00	
4.	West Sumatera	4,850.00	-	4,850.00	-	-	-	0.00	Not inventoried yet
5.	Jambi	833.67	2461.23	3,294.90	35,869.83	224,184.28	260,054.11	330.00	
6.	Bengkulu	2610.00	-	2610.00	-	-	-	0.00	Not inventoried yet
7.	South Sumatera	247,950.63	14,881.66	262,832.29	339,928.08	444,135.28	784,064.20	1,050.00	
8.	Lampung	-	-	-	10,762.07	7,607.91	18,369.98	960.00	
9.	West Java	-	77.03	77.03	33,453.71	94,766.52	128,220.23	1,600.00	
10.	Central Java	2,906.33	-	2,906.33	16,025.34	76,669.98	92,431.69	1,684.00	
11.	Yogyakarta	-	-	-	-	-	-	0.00	Not inventoried yet
12.	East Java	-	-	-	42.22	97,669.98	97,712.20	990.00	
13.	West Kalimantan	-	-	-	143,460.75	328,905.05	472,365.80	0.00	
14.	South Kalimantan	-	-	-	76,1669.91	132,453.36	208,620.27	8.00	
15.	East Kalimantan	54,334.17	315,574.02	11,156.10	61,740.54	327,935.16	389,675.70	0.00	
16.	Central Kalimantan	31,974.30	224,135.40	256,109.70	443,025.60	1,529,451.50	1,972,477.10	0.00	
17.	North Sulawesi	38,150.00	-	38,150.00	-	-	-	0.00	Not inventoried yet
18.	Central Sulawesi	78,840.00	-	78,840.00	-	-	-	0.00	Not inventoried yet
19.	South Sulawesi	104,030.00	-	104,030.00	-	-	-	3,550.00	Not inventoried yet
20.	South-East Sulawesi	70,840.00	-	70,840.00	-	-	-	100.00	Not inventoried yet
21.	Bali	501.41	-	501.41	6,532.66	18,519.74	25,052.40	1,423.00	
22.	West South-East Nusa	2,993.23	6,302.55	9,295.78	764.04	10,174.42	10,938.46	1,020.00	
23.	East South-East Nusa	10,780.00	-	10,780.00	-	-	-	0.00	Not inventoried yet
24.	Maluku	148,710.00	-	148,710.00	-	-	-	0.00	Not inventoried yet
25.	East Timor	4,600.00	-	4,600.00	-	-	-	0.00	Not inventoried yet
26.	West Papua "Irian Jaya"	1,326,990.00	-	1,326,990.00	-	-	-	0.00	Not inventoried yet
27.	DKI Jakarta	0	0		-	-	-	0.00	Not inventoried yet
Total Number		**2,268,033.78**	**623,136.57**	**2,432,418.26**	**1,712,462.87**	**4,189,512.63**	**5,901,975.50**	**15,830.00**	

Note : The implementation of mangrove forest rehabilitation is still under try-out phase, the accomplishment will be carried out in the following year
Source : Directorate of Forestry Program Construction, Department of Forestry - RI (1982) in Santoso-Nyoto (2001)

General Root Factors of the Damaged Mangrove Forest in Indonesia

At least there are 8 main factors which causing the damaged mangrove forest in Indonesia, as described by Santoso-Nyoto (2001) below:

1. **The Basic Demand and the Shrimps Price Level**

   The conversion activity from mangrove forest into shrimp's cultivation has an extreme increase, following the peak of world shrimps demands in 1982. The competitive price of shrimps motivated the people to explore and open the mangrove forest for shrimp's pond cultivation. This condition was also triggered by the monetary crisis, which elevate the shrimp's price until Rp 150,000.00 - per kg, thus the rehabilitation of mangrove forest was hampered.

2. **Illegal exploitation of wood for charcoal raw material and firewood**

   The mangrove felling activity has been done since along time on the East Shore of Sumatra in order to obtain the charcoal, which of its production was done in traditional method (home industry). This product was supplying local demand (cooking substance) and the rest was exported to Malaysia, Singapore, Hongkong, and Taiwan through the market mechanism which is involved the *Tauke.*

   In fact, the effects of this activity has decreased the qualities of mangrove forest, such as wood potential, biomass productivity and the buffer function for the live sustainability. In East Shore of Sumatra, the wood potential is under 20 m^3 per Ha. This value is very low comparing to the wood potential of the primary forest which is more than 70 m^3 per Ha, and is 140 m^3 per Ha in West Papua (Santoso-Nyoto, 2001)

3. **The Management Failure**

   The government attention in managing the ecosystem of mangrove forest is quite low. It can be seen from the output of the entire law's product, even in forestry sector, fishery and the other. Until 1978, almost all of the government policy in mangrove management was still tend in exploitation activity. It was might be caused by the lack of knowledge of the mangrove biologics and characteristics.

   All this time, the potential of mangrove forest has been not regarded as the mainstay potential of national income. For instance, mangrove forest management of the National Forest Management Company *(Perum Perhutani)* still relies on the wood production but not on the fishery product or another environmental service. The *sylvo-fishery* approach, which has been used, is inadequate in pushing the aspect of fishery cultivation, and is lack of profit (Santosa-Nyoto, 2001)

   In autonomous era, shrimp pond cultivation has been becoming the main alternative for all of District Government or City which has coastal area, in order to raise the original region income. This condition is very endangering the environment and the people, mainly who live surrounding the coast area that depends on traditional fishery sector.

4. **The land use management authority of mangrove forest**

   The damaged mangrove forest which has occurred is caused by the poor regulation of the land use management authority in the mangrove ecosystem. For instance, a case has occurred on the shrimp's pond opening in Delta Mahakam. The authority for clearing of forest is more involved the Head of Village who gives *the Letter of Land Official Statement (Surat Keterangan Tanah = SKT)* which used by the industrialist to clear the mangrove forest. Beside that the poor watching and monitoring are has been utilized by the other sides who want to clear the mangrove forest (Santoso-Nyoto, 2001). Hence, in the future needs more regulation, control improvement and limitation for land clearing authorize, mainly for limitation or prohibition of the Head of Village to issue the SKT. This authority is only occupied by *National Land Agency (BPN)* who coordinating with the forestry and fishery sector, and accepting the civilian suggestion.

   Until today, the authority of mangrove forest management is under the Forestry Department or Forestry Service, whereas the other forest is authorized by the Local Government. Nevertheless, in the future, this authority will be determined by Local Government supported by forestry, fishery and sea field of development.

5. Original Region Income (Regional Autonomy)

Most Local Government plan the improvement of original region income derived from pond fishery cultivation. The spirit and plan of improvement has been already intensively published, but unfortunately the supporting system is very weak. Those weaknesses are:

(a) the lack of knowledge of the people about the mangrove ecosystem;
(b) there is an ambiguous environmental friendly criteria and technology indicator of pond cultivation;
(c) the Government Law or Act about fishery cultivation within the coast area hasn't been available;
(d) the local peoples do not have a role in a big scale pond cultivation;
(e) there are no guarantee from the government if the pond cultivation can damage the environment; and
(f) it has not been decided the administrative rule which related to mangrove fishery cultivation that environmental friendly.

Principally, whatever kind of local authority, in region autonomy era could not leave the principle of sustainability development, preservation of biological variety, and improvement of community involvement. Nevertheless, the mangrove forest deforestation in order to improve people's involvement and to stifle the people demand is not allowed.

6. People's perception about the mangrove ecosystem

Peoples who live in the coast area understand, feel the benefit, and know the mangrove forest function. However, because of live demand and change, there is perception changing among the peoples of the ecosystem of mangrove forest. For the peoples who depend on the ecosystem of mangrove forest, they are aware to keep the availability and the preservation of the mangrove forest. But for the new resident (from the outside of coast area), they often explore the available resources as much as possible.

Some the people in general think that the ecosystem of mangrove forest is a dirty and stinky area, mosquito's nest, snake or another hazardous animal. This reason has influenced the policy determination by the stake holder in managing the mangrove forest.

7. The poor incentive and punishment

Considering that the policy of sustainable pond cultivation is not issued yet by the government, it causes some difficultness in pond cultivation it self. This condition very considerably effects to the damaged mangrove forest in such local region. The Local Government has no something to rely on about how large the tolerable pond cultivation compared with the environmental carrying capacity, able to improve the people's welfare, and raising the original region income. According to these problems, hence the Local Government's policy is only based on the feasibility study result from the private consultant. Accordance to such financial analysis will give high benefit to the local region.

Based on that situation, incentive and sanction to the industrialist who has broken the rule will be difficult to be implemented. Commonly, the problem solving is by bargaining, even sometimes the politic interest has involved too deep in decision determination.

8. The status of the "*sedimentation land or delta*"

The big river outlet, which brings much sediment from the land, created a material accumulation area or sedimentation land which is called delta. The delta is such kind of media which appropriate for mangrove vegetations. Nevertheless, since the management approach of mangrove forest often rely on the forest land which its ruled based on official boundary, hence the mangrove forest land that situated on the outside of official boundary (delta) is frequently regarded by the local people not as a forest area. It causes the people consider to possess that delta, even among the government institution want to show their authority in holding the ownership and the managerial status of those 'land'.

THE PROBLEM AND ITS SOLUTION APPROACH OF MANGROVE FOREST IN SEGARA ANAKAN – CENTRAL JAVA

(1) The Situation and condition of Mangrove Forest in Segara Anakan

Segara Anakan, called *Kinderzee* in Dutch, is kind of lagoon or estuary water area that located nearby to the administration boundary between Central Java Province and the West Java Province, on the coastal area of Cilacap District, shown in Figure 2. Administratively, Segara Anakan area is divided into 4 villages, which are: Ujung Galang, Ujung Gagak, Klaces, and Panikel Villages, part of Kampung Laut Sub-District (Figure 3). The term of "*Kampung Laut"* is originated from the people community in Segara Anakan, which has mean village or area that situated above the sea. That name was derived from the past house model of the people at that time was stage house which situated above the Segara Anakan's water surface.

Segara Anakan water is the outlet point of several big rivers which of the upper course is located on West Java Province and Central Java Province. Citanduy River which its up stream comes from West Java is the biggest river which influences the Segara Anakan's dynamic process, beside Cimeneng River, Cikonde, and Cibeurem which it up stream come from Central Java. The semi-closed estuary condition of Segara Anakan waters is originated by the existence of Nusa Kambangan Island which has function as a barrier between this waters and the Hindia Ocean. Nevertheless, the hidrooceanography effect of Hindia Ocean still influences to the Segara Anakan waters, through the West Plawangan's and East Plawangan's outlet. This condition is the reason of that Segara Anakan estuary is famous called as Segara Anakan Lagoon. The existing of Segara Anakan waters, effected by tidal pattern from the Hindia Ocean and fresh water supplying from some big rivers, have created habitat formation as an appropriate growing place for the mangrove forest. The mangrove ecosystem in Segara Anakan is the largest in Java Island with the biologic variety inside it (LPP Mangrove, 1998, in Maarif, 2006).

Figure 2. The Location of Segara Anakan within Indonesia and Central Java Province

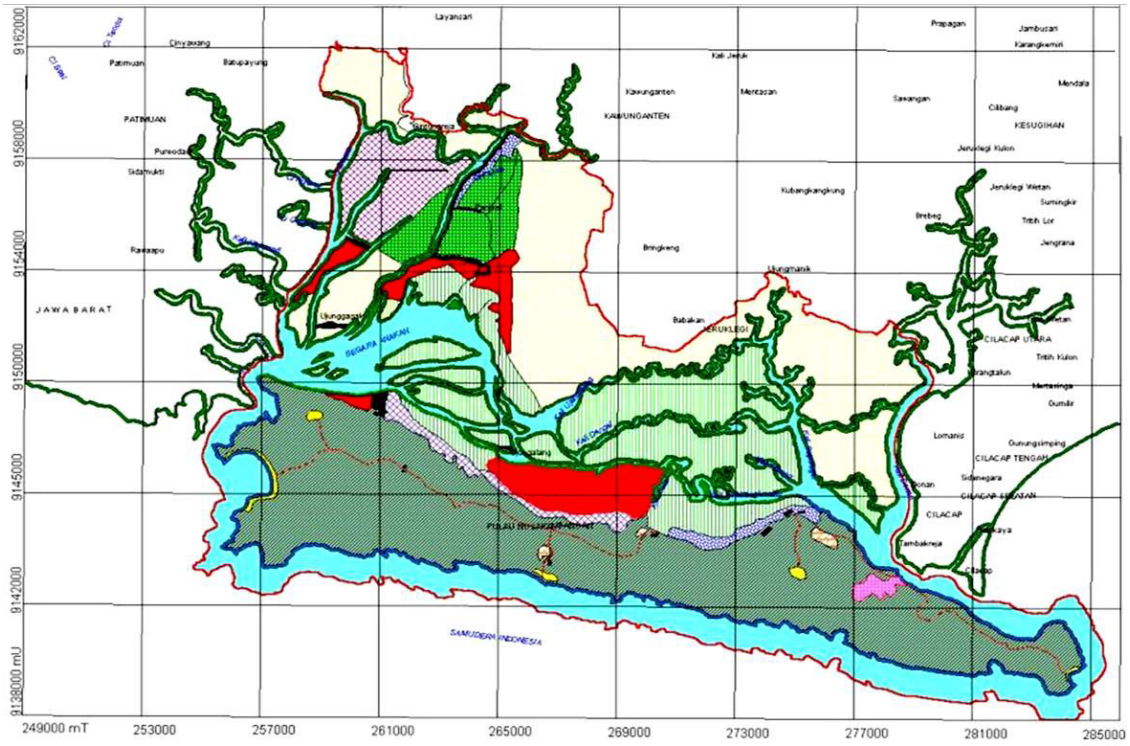

Figure 3. The Situation of Segara Anakan with its Rivers

According to Maarif (2006), Segara Anakan's Lagoon, with its unique characteristics; at least have 2 important points which has to be preserved. *First,* it is dealing with the lagoon function as spawning ground, reproduction and nursery ground, and feeding ground for any kind of biotic which are included to migratory species or settle at the lagoon area. This function really related to the mechanism of ecologic cyclic of some migratory biotic, hence it has relation with the fishery potential in the Southern part of Java coast. The availability of this function is surely depended on the waters ecosystem condition and its interaction with the mangrove forest ecosystem. *The second* essential point is dealing with the hydrology's system, considering Segara Anakan lagoon is the main outlet from some big rivers with large area of catchments. This area is included into Citanduy Watershed and Cimeneng Watershed, which are the priority area of flood controlling program in the southern part of Java. The essential value of the second point is extremely related with the erosion of hinterlands, the high sedimentation in the river, and flood which is often occur in this area.

Dealing with the first essential point, the existence of mangrove forest in Segara Anakan plays an important role to the preservation of its ecology cyclic. The area of Segara Anakan mangrove forest basically consists of some interrelated ecosystems, which are: waters area of opened lagoon, delta, salt marsh, and mangrove forest as the habitat place for many kinds of valuable flora and fauna (Purnamaji, 2006). Segara Anakan Lagoon has real contribution in improving the waters productivity of the Southern part of Java Island's coast. This lagoon has supported the coast waters productivity until more than Rp 62 billion in a year, and it will more increase following the empowerment of Segara Anakan ecosystem functionality (Purnamaji, 2006). The biological variety in the lagoon area can support the livelihood of the local people in form of brackish water fishery production. Beside that, the growing mangrove forest in this area has created habitat place and egg's laying place for numbers of migratory birds.

Mangrove forest is a complex and dynamic ecosystem which mostly grows on the tropic or sub-tropic area and also as a tidal ecosystem which has high productivity. Indonesia, as one of tropical country, is stated as the country that has the biggest area of mangrove in the world. Based on RePPProt (1985-1989), Indonesian mangrove forest reached 3.7 million hectare width meanwhile the Department of Forestry (1982-1983) predicted the mangrove forest was 4.25 million hectare. Gisen (1993) in Tomascik, *et al*., (1977) predicted that the remainder large of man-

grove forest during (1986-1990) was 2,5 million hectare. For Java Island the large of mangrove forest is described into: West Java 8,200hectare became <500 hectare, Central Java has 18,700 hectare became 13,577 hectare, and East Java has 6,900 hectare became 500 hectare (Sudiana, 2006). For the Central Java Province, that large value was concentrated in Segara Anakan Cilacap.

Based on Tomascik, *et al*., (1977) the decreasing large of mangrove forest in general is caused by the mangrove forest conversion into pond land, the declining of structure quality and forest composition of mangrove forest is caused by felling of mangrove trees for any necessity, such as charcoal industry and building material. Moreover, Sudiana (2006) affixes that watershed degradation on the part of hinterland has increased the sedimentation rate in great value downward into rivers and flowing to the coast area which the mangrove forest growth over there. Beside that, the solid waste from the city or the liquid waste from the industry which accumulated on the river's outlet, are the two main causing factors in term of damaged mangrove forest in Java. Sudiana (2006) observed the structure and the composition of mangrove forest type in Segara Anakan. The results showed that on the delta area is commonly dominated by kinds of vegetation that is able to sustain in the puddle area, such as: *Avicennia spp.*, and *Sonneratia spp.* The distribution of this mangrove reaches the edges area of Segara Anakan coast with 50-100 meter distance to the land which still affected by tidal water.

Next, there are another species, such as: *Rhizophora spp., Aegiceras sp., Ceriop sp.*, and etc. As showed in Table 3 that the species of *Avicenia spp*. is a dominant mangrove in Lebrag Block, Muara Dua area, which have harvest level 0f 200, root level of 139.6, and trees level of 237,2. It can illustrate that such species has high succession level, it means that the environmental condition is physically and chemically appropriate to the ecology characteristic of this species. Physically this area has normal tide, the salinity reaches 11‰ (medium), and the material is mud deposit. The appropriate condition for *Avicenia spp*. is in normal tide condition and has high tolerance to the high salinity (Tomlinson, 1986 in Sudiana, 2006).

For the time being, on the location of Klaces is dominated by *Avicenia spp*., *Sonneratia spp*., and *Bruguiera sp.* This condition is suitable with the environment condition which situated along the coast edges of Segara Anakan to the landward until 100 meter which still affected by the tidal and inundation. These kinds of vegetation are adaptive to salt water with variation of salinity, and the soil substrates consist of mud or sediment material. In Cikiperan, part of the land area of Segara Anakan, Ujung Alang River, is dominated by *Rhizophora mucronata,* with the important index value of trees level of 58.18, rooted level of 86.94, dan harvest level of 73.87. Such species grows well since the ecosystem existence has been old enough. Such kind species has adaptive ability on the river edges or protected area that uninfluenced by sea water tidal effect. According to De Hann (1931) in Tomascik, *et al.*, (1977), *Rhizophora mucronata* grows and develops on the last side of mangrove area, 10-30‰ of salinity, the rise tide until 20 days per month, soil substrate consist of sediment that still early compacted. Even though, on some locations can be found associated vegetation which is *Acanthus ilicifolius,* which indicate that there are has already occur high disturbance within the mangrove ecosystem and difficulties in recovering them to be natural mangrove community.

According to Management Agency of Segara Anakan (BPKSA, 2004), Segara Anakan has variety potential, as described below:

(a) Fishery potential
There are 45 species fishes with 17 among of them are migratory fish, mangrove crab, and mud crab. Cultivated pond lands are used for milkfish and Windu Shrimps which has already ruled on Segara Anakan Spatial Plan.

(b) Water Transportation Potential
Segara Anakan has an important role as regular transportation path which is connecting West Java territory with Central Java Territory in form of tourism package (PANCIMAS: Pangandaran – Cilacap – Banyumas). Beside that, the path area is also used as people's transportation for surrounding area.

Table 3. The Analysis of Mangrove Forest Vegetation in Lebrag Block (Muara Dua) Segara Anakan – Cilacap

No	Species	K	KR	F	FR	D	DR	INP
Harvest Level								
1.	*Avicenia latana*	2,6	100	0,6	100	-	-	200
Rooted Level								
1.	*Avicenia latana*	0,06	17,9	0,2	7,7	100,1	7,3	33,0
2.	*Avicenia alba*	0,14	43,6	1,0	38,5	786,3	57,5	139,6
3.	*Sonneratia caseolaris*	0,07	23,1	0,8	30,8	414,3	30,3	84,1
4.	*Rhizophora apiculata*	0,01	2,6	0,2	7,7	7,9	0,6	10,8
5.	*Aigeceras corniculatum*	0,04	12,8	0,4	15,4	58,8	4,3	32,5
Tress Level								
1.	*Avicenia alba*	0,04	85,7	1,0	71,4	2153,4	80,1	237,2
2.	*Sonneratia caseolaris*	0,01	14,3	0,4	28,6	35,8	19,9	62,8

Source: Sudiana, 2006
Note: K = Density F = Frequency D = Domination
KR = Relative density FR = Relative frequency DR = Relative domination
INP = Important Value Index = KR + FR + DR

(c) Research Potential

The existence of biological variety within Segara Anakan, Nusa Kambangan Island, and natural phenomena such as sedimentation process, are the important objects in term of scientific study and knowledge development. For the moment, there is a development plan, called as *International Tropical Marine Ecosystem Center (ITMEC),* which was initiated by Sudirman University Purwokerto, ZMT, and Bremen University.

(d) Mangrove Forest Potential

Mangrove forest area in Segara Anakan has such large area reach view to the landward. There are 26 species of mangroves which grow and develop, such as: *Avicenia alba, Sonneratia alba, Rhizophora mucronata, Bruguiera gymnorizha, Bruguiera carryophyloides, Carapa oboyata, Heritiera littoralis, Carbera manghas,* and *Carapa molluccensis.*

(e) Tourism Potential

The area of natural education tourism program of the mangrove ecosystem in Segara Anakan water can be reached through Majingklak lane (Pangandaran) to Cilacap. Natural caves within Nusa Kambangan Island, Rancababakan Beach, Nusa Kambangan coast and sea fishing are some interesting tourism objects surrounding Segara Anakan.

(2) Problems in Segara Anakan

Based on the report of BPKSA (2004), it describes that the occurring problems in Segara Anakan area can be grouped into 2 locations, which are the problem inside the lagoon and outside the lagoon. The main problem inside the lagoon is the high rate of sedimentation (1 million m^3 per year), which in one part causes the formation of delta but in the other side it causes the constriction of lagoon area. Meanwhile, the problem outside the lagoon area is permanent flood every rainy season, which can devastate the irrigated farm land until ±1000 hectare from 22,000 hectare in Sidareja, Cihaur, Cilacap region; and ±700 hectare from 5,000 hectare of farm land in Ciami region.

Sedimentation

Segara Anakan, as a location of big rivers outlet, is getting more pressure from the sedimentation from those big rivers. In accordance with ECI (1994) in Maarif (2006), the sediment that enters to Segara Anakan is 5,770,000 m^3/year, which is 5,000,000 m^3/year from Citanduy River and is 770,000 m^3/year from Cikonde River. From that amount, ±1,000,000 m^3/year is deposited in Segara Anakan waters, with 73% of the composition is the sediment from the Citanduy Rivers, 26% from Cikonde Rivers and the rest come from the small rivers.

Moreover, Maarif (2006) explains that this sedimentation rate is affected by the land use pattern and land use change in upland area, which should be used as the catchments area. The land use pattern and the conversion activity of protected areas relatively ignore the environmental conservation rule, such as deforestation and land opening for local farming within the forest area. Consequently, it accelerates the soil erosion and supplies the sediment downward to the river. The transported sediment in rivers flow will be deposited along the river path and stopped in Segara Anakan. The high rate of sedimentation in Segara Anakan's lagoon has decreased its large and depth. Satellite imagery interpretation (Landsat) (Figure 4) between 1984 – 2002, shows that there is decreasing value of sedimentation area up to 79%, from 2,906 hectare in 1984 to 600 hectare in 2005, or equal to average rate 4,39% per year (BPKSA, 2004).

The reduction of Segara Anakan's Lagoon has caused some significant problems, i.e.: decreasing of fishery productivity, deforestation of mangrove forest into pond land. In the same time, on the other side the delta formation, it has created serious social problems, i.e.: social conflict related with the ownership status of new land, the occurrence of non regular settlements, the interest collide between institute or agency, the overlapping authority in land management.

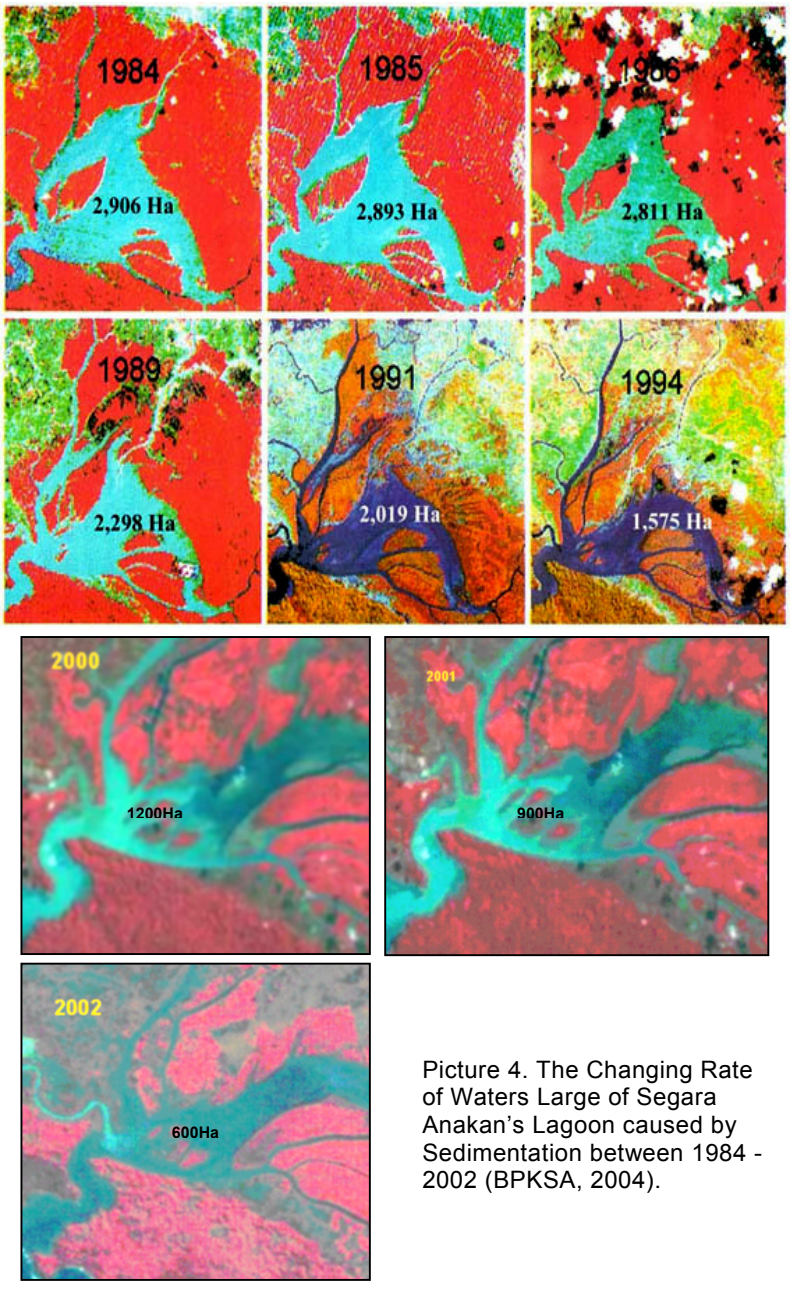

Picture 4. The Changing Rate of Waters Large of Segara Anakan's Lagoon caused by Sedimentation between 1984 - 2002 (BPKSA, 2004).

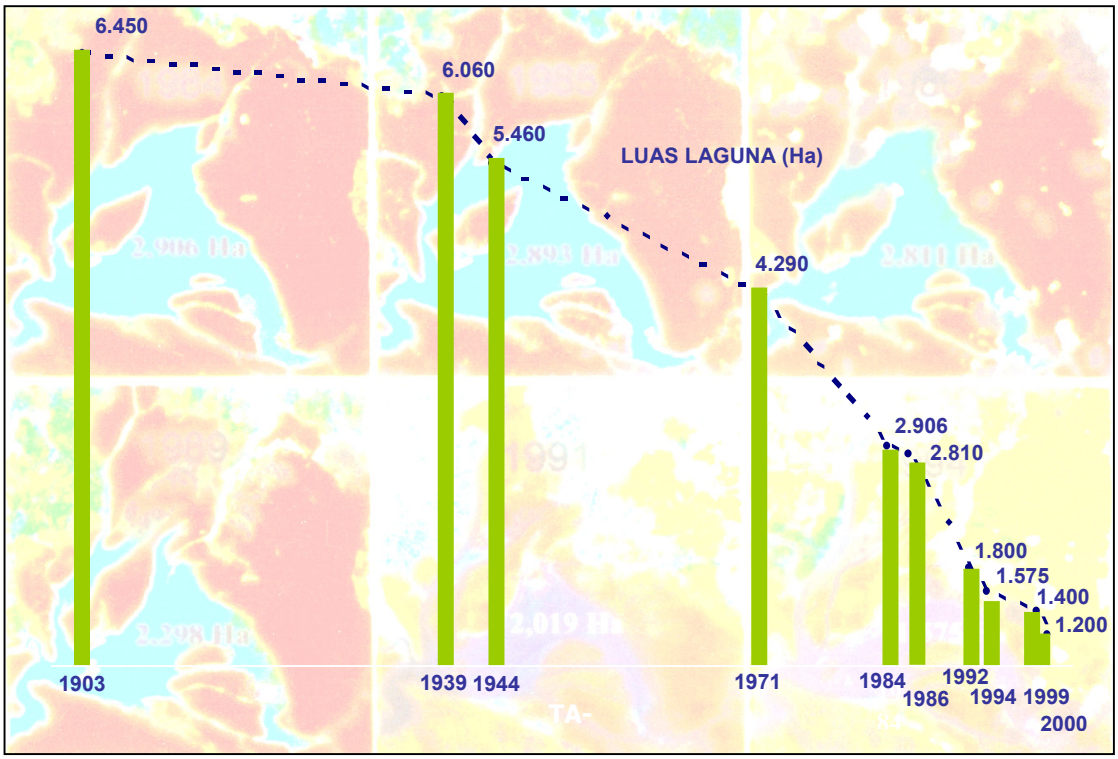

Figure 4c. The Graph of the Waters Large Changing of Segara Anakan caused by Sedimentation since 1903-2000 (BPKSA, 2004).

The Damaged Mangrove Forest

The decline of Segara Anakan's Lagoon has reduced the population and the productivity of fishery, decreasing of mangrove forest area and its biologic variety. Since the decreasing productivity of sea fishery, hence the peoples start to fell down the mangrove trees and open new lands for ponds, settlements and farming. The utilization of mangrove, wood as firewood and charcoal, has triggered the damaged mangrove forest in this area.

Even there are new floating lands (delta) occur in this area which can be as a medium for new mangrove growth, but this growing mangrove only for some certain species. Hence, it is not so significant to the damaged rate of mangrove forest in this area.

The Overlapping Authority and Institutionalism

The management of Segara Anakan Area, based on Local Rule of Cilacap Regency Number 23 year 2000, is covering Segara Anakan and Nusa Kambangan Island. In term of conservation, the management of this area is offered to such managerial agency which formed based on Local Rule of Cilacap Regency Number 28 Year 2000, which called as Management Agency of Segara Anakan Area *(Badan Pengelola Kawasan Segara Anakan = BPKSA)*. Administrative approach as guideline for determining the boundary Segara Anakan Anakan, still offers some problems in creating an integrated management, since the boundary of this area is located in the border area between West Java and Central Java (Maarif, 2006).

From sediment point of view, the upstream of Citanduy River as the main supplier of sediment material to the Segara Anakan, is located in Cakrabuana Mountainous, West Java Province, meanwhile the location of Segara Anakan is in Central Java Province as the affected area. Until today, the Nusa Kambangan Island which part of the Segara Anakan Area's managerial is authorized under Ministry of Justice and Human Rights. On the other side, the mangrove forest in this area is still under National Forest Management Company *(Perum Perhutani)*. Based on that fact, it will be difficult for BPKSA to formulate and to enroll the management program of Segara Anakan. The fuzziness of authority and the differences between physical boundaries with the administrative boundary will become constraints which is hard to be solved.

The Continuous Following Problem

Maarif (2006), considering the phenomenon within the Segara Anakan, it is true if there many site curious to its waters condition in the future. Increasing sedimentation which accelerated by the people behavior that difficult to be directed and the fuzzy authority in the management of Segara Anakan will be able to create many following problems which going to be continuous. The problems are: the more decreasing number of sea fishery potential, free tools for catching the fish to get more fish (example: *floating net*), and permanent flood every year.

The missing fishery potential in this area will affect the fishery potential of South Java Coast, mainly for shrimps and small pelagic fish. It can happen since the Lagoon of Segara Anakan acts as spawning, feeding, and nursery ground for *Crustacea* family (shrimp and crab), and another migratory species. This condition is becoming worse since the local fisherman use un- appropriate tool to the environment i.e. floating net. Based on observation result, there are 1.444 floating nets distributed on Segara Anakan Waters (Maarif, 2006). Floating net is the main tool for catching the fish by the people of Kampung Laut. It is in cone shape, looks like *trawl*, its operation work depend on the sea tidal. The size of *cod end* is 0,2 – 1 inch, hence able to catch the larva of fish and shrimp. It is clear that it will be kill the fish ecology cycle, which related to the more decreasing sea fishery productivity.

The large and the depth of Segara Anakan which is getting narrower and shallower have changed also the drainage pattern and rivers flow to this area. The changing pattern of the drainage and the flow consequently increase the time and the large of puddle area along the river, such as Cibereum River which cross Sidareja Sub-District and its surround area. When the rainy season comes, the river body can not be able to sustain all of the water, hence it will be flooded. This typical flood in this area happens in long duration. Such condition also happens in Cikonde River in Kaunganten area, Cijalu River in the territory of Pahonjean-Majenang, and Citanduy River in the territory of Lakbok and Padaherang. Many main problems and following problems within Segara Anakan have caused its lagoon waters in such complicated and critical situation. The late decision making to solve those problems will be loosing the ecology and the economy value of Segara Anakan in the future.

(3) The Solving Method Dealing with the Problems in Segara Anakan

In order to solve the problems in Segara Anakan, then there was issued such program called as *Segara Anakan Conservation and Development Project (SACDP*) year of 1997-2005. The aim of this program was to construct sustainable Segara Anakan and surrounding area, which covering environmental function protection, poverty decline, and growing the economic value of natural resources. The target of this program is improving the local institution in term to cope the management of Segara Anakan Area and the improvement of people's socio economic condition and arranging the model of integrated management of Segara Anakan Area. This Program was funded by Asian Development Bank, which grouped into 3 component, i.e.: component A (water and sediment resources), Component B (village development), and component C (Institutional).

(a) Component A is Water Resources Management and Sediment Controlling, coordinated by Citanduy – Ciwulan Banjar Project, consists of:
   - ☑ Citanduy Waterway Diversion (the plan has been postponed until this moment);
   - ☑ Cikonde or Cimeneng Waterway Diversion (done);
   - ☑ Dredging the Segara Anakan (done);
   - ☑ Normalizing the river and flood controlling (not realized yet).

(b) Component B is Village Development, coordinated by BPKSA. This program aims to improve the village facility to create people's awareness to the environment, i.e.:
   - ☑ Mangrove Forest Rehabilitation with 1.125 hectare of large and sustainable management in form of people's mangrove forest with 5.000 hectare of large;
   - ☑ Creation of Aquaculture specimen for shrimp's pond, crab, and fish, also the introduction of the salty water paddy;
   - ☑ Construction of village facility (road pavement, village office and convention hall, clean water, sanitary and water drainage);
   - ☑ Variety of courses in order to increase the people's skill as alternative livelihood;

☑ Soil Conservation and soil erosion controlling with large 5.000 hectare in Cimeneng Watershed and 3.800 hectare in Cikawung and Citanduy Sub-Catchments (has done).

(c) Component C is management and coordination (institutional), coordinated by BPKSA, i.e.:

☑ Administrative Management and village development program;

☑ Realization and Monitoring Program of environmental management and monitoring;

☑ Preparedness of cost recovery plan and monitoring of the operational-management Segara Anakan's Lagoon;

☑ People awareness program;

☑ Arrangement of ortho-photo, cadastral survey and aerial photo;

☑ Institutional strengthen, Local Rule determination and coordination.

Systematically, the management strategy of Segara Anakan's Lagoon within SACDP project is showed in Table 4, and spatially showed in Figure 5.

Table 4. The Management Strategy of Segara Anakan's Lagoon (SACDP)

Target Area	Ekosistem & Resources	Management
Catchments Area Citanduy, Cikawung and Cimeneng Watershed	Upland area: - People forest - River cliff - the Area of National Forest Management Company	Soil Conservation and Erosion Controlling
The lagoon of Segara Anakan Villages within Kampung Laut (4 villages) Mangrove Forest Area	- Sediment and large of lagoon - Lagoon fishery - Land use pattern - People's socio economic - Mangrove Forest	Civil work: ▪ Dredging, waterway diversion, and normalizing the river flow ▪ Mangrove forest rehabilitation ▪ Sustainable management of people's mangrove forest ▪ Improvement of people's economic
Hindia Ocean	Coast and sea fishery (fish and shrimp potential)	Diverting the fishing base from the Lagoon to the offshore (Ship stock for type).

Source: BPKSA, 2004

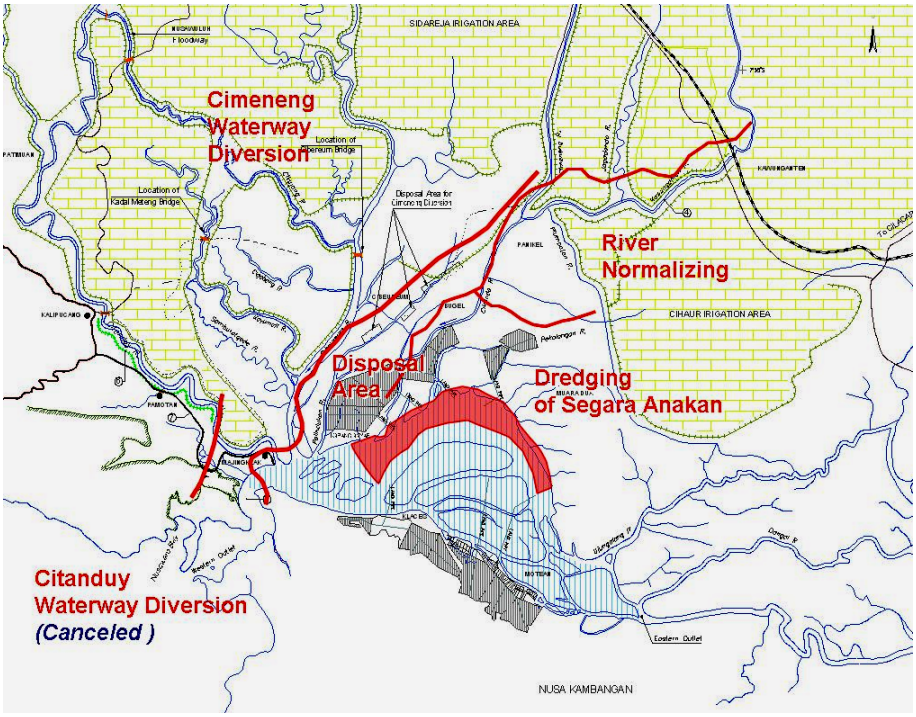

Figure 5. Implementation Area of SACDP Project for the Management of Segara Anakan Area – Cilacap

The mangrove forest management with large 5.000 hectare which cooperated with National Forest Management Company *(Perhutani)*, the solving method include: treatment of the plant, secure from illegal logging activity (cooperating with police and maritime), land use usage regulation with controlling the Spatial Plan of Segara Anakan Area and arrangement of Local Rule for the management of Segara Anakan's mangrove forest, establishment the Family's Awareness of Mangrove Forest *(Keluarga Sadar Bakau = Kadarkau)*. Moreover, the rehabilitation target of the damaged mangrove forest 1.125 hectare, with the handling action consist of forest rehabilitation based on damaged level reach 675 hectare, and the rehabilitation on the damaged pond area reach 400 hectare.

The soil conservation and soil erosion control program is directed to the upland area that consists of: 5.000 hectare of critical land from 7.440 hectare within Cimeneng Watershed, and 5.000 hectare from 15.000 hectare critical land within Cikawung Watershed. Those activities consist of: physical conservation in form of check dam, restraint dam and bamboo construction; also vegetative conservation effort i.e. agro forestry, Specimen Unit of Natural Resources Conservation, and village seed garden.

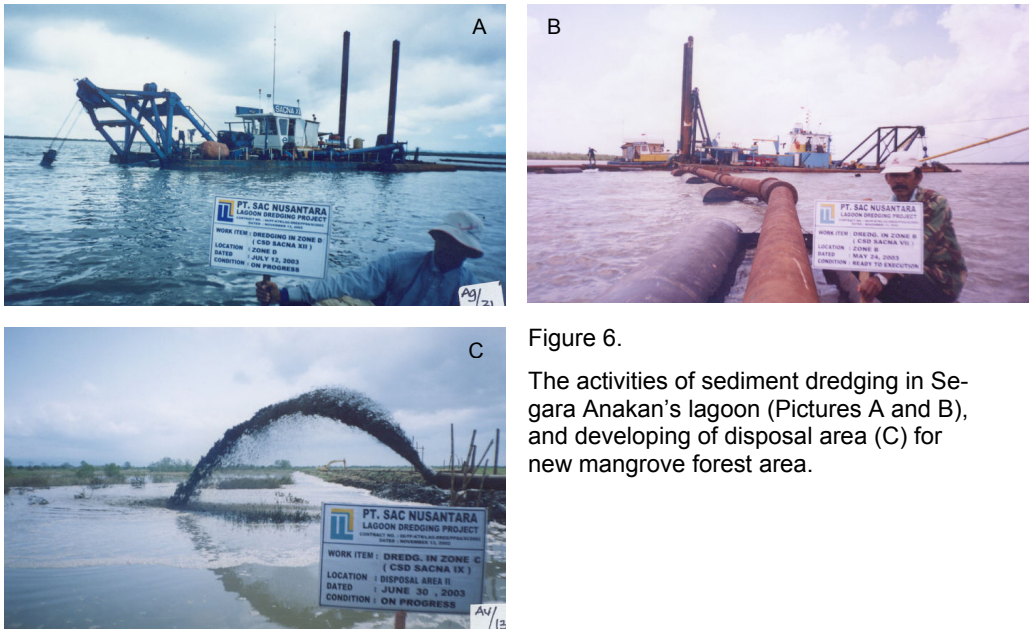

Figure 6.

The activities of sediment dredging in Segara Anakan's lagoon (Pictures A and B), and developing of disposal area (C) for new mangrove forest area.

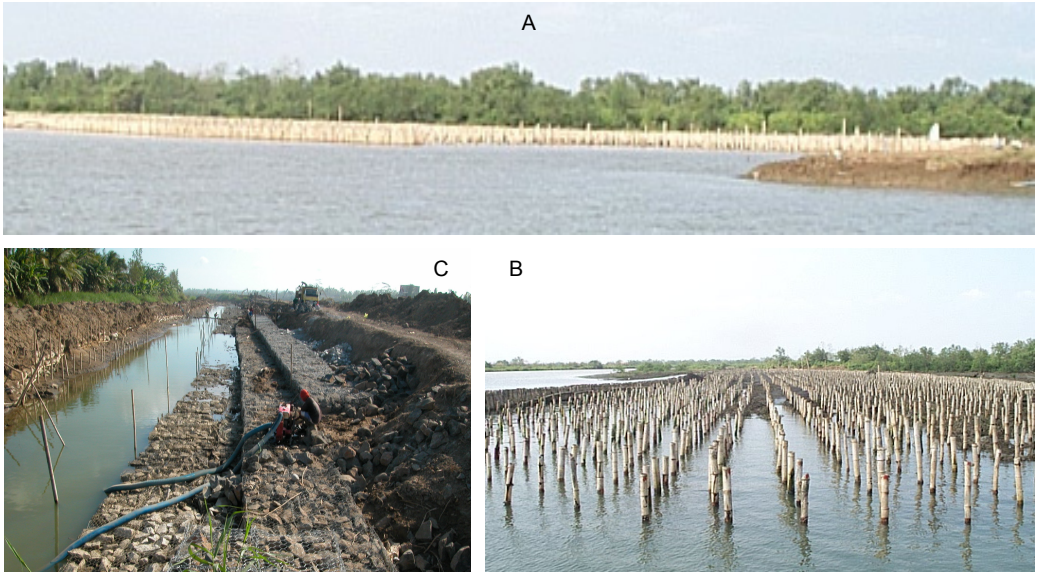

Figure 7. The activities of bamboo closer dam in Palindukan (Pictures A and B), and developing of Spill Weir Panikel.

Figure 8. The activity of vegetative rehabilitation on critical land of upland area (top pictures) and mechanic method with check dam construction (below pictures).

Figure 9. The activities of mangrove forest rehabilitation in the shallow water of Segara Anakan Area.

Figure 10. Integration between fishery and agriculture activities (top pictures), and developing of environmental facilities, i.e.: clean water facilities and road paving in Kampung Laut (below pictures).

In order to achieve good management, then it is required a better circumstance of institutional system and human resources. Therefore, the institutional strengthen, consist of:

(a) creating the people groups of environmental conservation observer, both on the upland or on the lowland area;
(b) establishing the Local Rule which dealing with the management of Segara Anakan Area;
(c) improving the people's skill through various course activities;
(d) conducting research works within Segara Anakan Area, map updating and identifying the float land (delta) on the entire area of Segara Anakan; and
(e) preparing the cost recovery plan.

Various activities of the SACDP program are showed on the following pictures below:

To continue the SACDP program year of 1997-2005, hence in 2005-2006 need to be followed up with integrated program, such as:

(a) Establishing the law product dealing with the management of Segara Anakan Area, which rules:
  - ☑ management border of Segara Anakan Area;
  - ☑ creating the organization and the framework of BPKSA;
  - ☑ management of Segara Anakan Fishery;
  - ☑ management of Segara Anakan mangrove forest; and
  - ☑ master plan of Segara Anakan Area.

(b) Plan establishment of Pacangsanak Spatial Plan (Pangandaran, Kalipucang, Segara Anakan, and Nusakambangan).

Furthermore, there are some points that must be followed up, i.e.:

(a) placement of associate NGO as mediator and facilitator of project activity implementation;
(b) socializing the law products continuously;

(c) explanation through printed medium, audio visual radio, traditional art;
(d) awaken the tradition law which was exist before in Segara Anakan Area; and
(e) making Focus Group Discussion and uniformity of conservation development vision through Participatory Rural Appraisal in each project target location.

CONCLUSION

The Initiative Management Strategy of Coastal Area in Term of Region Autonomy

Considering the fact of coastal area condition in Indonesia, and especially in Segara Anakan, the region autonomous government system should be implicated in coastal area development. In addition, the meaning of autonomous should be straightened in order to persevere with the coastal area conservation, and create concept of sustainable and environmental insight of Integrated Coastal Area Development. Here are some initiatives (hopefully it will not be only a dream to the environment observer) which is dealing with the base frame of region autonomy in the management of coastal area natural resource.

(1) It is preferable if the base implementer of region autonomy is on the province level not district or city, then the coordination function will be easier. The autonomy base should be started from the smallest community, regarding the conventional tradition law of natural resources management in coastal area and the entire environment. This tradition has been rooted since along time ago. Then, the politic interaction will be directed in heterogenic order, and there will be no ethnic conflict and "small king".
(2) The management of natural resources in coastal area must be based on an ecological oriented, and below coordination of institution which have more authority and independent. It can be executed if the region autonomy base is under province level, which has larger territory. Thus, some districts that included in one ecosystem will be easier to be organized, and will be no more overlapping authority. Furthermore, in province level, it is going to be easier to communicate with other province within one island, as in the management of bio-eco-region area, the coordination between provinces will be more efficient rather than through district or city. The act of Environment Impacts Assessment Agency in province level, and Coastal and Sea Management Agency are very important to the management of coastal area natural resources in order to establish the sustainable region autonomy and keep the environmental conservation.
(3) The authority function should be revised in term of permit issue for the management of natural resources in coastal area. Hence, it is necessary to establish kind of agency which independent, has the highest coordination function in province level, has the right to establish the management permit of the coastal area. This agency is supported with huge budget and professional and qualified man power in environment aspect. This agency will formulate the monitoring and management of coastal area and environment holistically.
(4) It is necessary to revise the environment act and to establish the special Act of the management of natural resources in coastal area which is holistically use bio-eco-region approach. This Act strike regulates the authority of BAPPEDAL and related institution, and heavy sanction for the environment ethic breaker. This is the true challenge that should be wisely discussed.
(5) All of those thinking or dreams will be impossible to be done if the bureaucrats do not keep the right ethics and norm which have been decided together. Hence, the consistency of collaboration between all related institutions should be maintained.
(6) For the community, the most important thing that has to be preserved is the local wisdom in a shape of tradition or conventional law which is related to the management of the natural resources in coastal area. It can be implemented by creating traditional community groups of environment observer, which support the management of environment founded on an agreement (coordination between Environment Management Agency and local people).

References

Abdul-Gaffar-Karim, Amirudin, Mada-Sukmajati, and Nur-Azizah, 2003, *The Problems of Local Autonomy in Indonesia*, Pustaka Pelajar, Yogyakarta *(in Indonesia language)*

BPKSA, 2004, The Status of Segara Anakan's Lagoon Quality and Management Strategies, *Report Progress of SACDP*, Cilacap

CERC, 1984, *Shore Protection Manual,* Vol. II, Department of the Army, U.S. Army Corp of Engineers, Washington D.C.

Dahuri R., J. Rais, A. Ginting, and M.J. Sitepu, 1996, *Sustainable Management of Coastal and Sea Resources,* PT. Pradnya Paramita, Jakarta *(in Indonesia language)*

Department of Ocean and Fishery, Republic of Indonesia, 2002, Decision Letter of Minister of Ocean and Fishery, Number: KEP. 10/MEN/2002*, Guide to Sustainable Planning and Management of Coastal Area*, Jakarta *(in Indonesia language)*

Eko-Rudianto, 2005, Sustainable Management of Coastal Area, *Proceeding*: *Seminar on Coastal Ecosystem for Social Prosperity*. Faculty of Geografi Gadjah Mada University, Yogyakarta *(in Indonesia language)*

Ministry of Environmental, Republic of Indonesia, 2003, *Guide Book of Sustainable Coast and Sea Program*, Jakarta *(in Indonesia language)*

King, 1972, *Shores and Coasts*, Edward Arnold Publishing, London

Kusmana C., 1993, *Survey Method to Vegetation,* IPB Press, Bogor *(in Indonesia language)*

LPP Mangrove, 1998, The Frame of Mangrove Forest Management System in Segara Anakan Area, *Progress Report*, Cilacap *(in Indonesia language)*

Maarif I.H., 2006, Segara Anakan: Not Anymore for Sea of Fish Children, *Alami: the Journal of Water, Land, Environment, and Disaster Mitigation*, Vol 11 No.3, BPPT, Jakarta *(in Indonesia language)*

MacKinnon K., Hatta G., Halim H., and Mangalik A., 1996, *The Ecology of Indonesia*, Vol III, Dalhousie University, Periplus Ltd.

Nybakken J.W., 1982, *Sea Biology: Ecological Approach*, Gramedia, Jakarta *(in Indonesia language)*

Pethick, J., 1989, *Introduction to Coastal Geomorphology*, Edward Arnold, London

Puji-Hardati, 2005, the Potency of Coastal Ecosystem and Fishermen Activities, *Proceeding: Seminar on Coastal Ecosystem for Social Prosperity*, Faculty of Geografi Gadjah Mada University, Yogyakarta *(in Indonesia language)*

Purnamaji S., 2006, Solving Problems of Segara Anakan Area after SACDP, *Alami: the Journal of Water, Land, Environment, and Disaster Mitigation*, Vol 11 No.3, BPPT, Jakarta *(in Indonesia language)*

Santoso-Nyoto, 2001, Potency of Mangrove Resource and Its Problems in Indonesia, *Seminar on Potency and Exploitation of National Natural Resources to Support Regional Autonomy*, Jakarta *(in Indonesia language)*

Siregar S.B., 1996, Coastal Sustainable Management: the National Defense Approach and Marine Defense, *Training Module on Sustainable Management of Coastal Area,* Research Institute, Indonesia University, Jakarta *(in Indonesia language)*

Steenis C.G.G. Van, 1985, *Flora Malesiana*, Published under the Auspecies of the Kebun Raya Bogor, Botanic Garden of Indonesia

Sudiana N., 2006, Structure and Composition of Mangrove Forest Types in Segara Anakan Cilacap, *Alami: the Journal of Water, Land, Environment, and Disaster Mitigation*, Vol 11 No.3, BPPT, Jakarta *(in Indonesia language)*

Sugandhy, A., 1996, the Strategy of Coastal and Ocean Management, *Training Module on Sustainable Management of Coastal Area,* Research Institute, Indonesia University, Jakarta *(in Indonesia language)*

Sunarto, 2000, Polygenetic and Dynamic Equilibrium as a Paradigm in Coastal Ecosystem Management, *Proceeding: Seminar on Coastal Ecosystem for Social Prosperity*, Faculty of Geografi Gadjah Mada University, Yogyakarta *(in Indonesia language)*

Tomascik T., Anmarie Janice Mah, Anugerah Nontji, and M. Kasim Moosa, 1977, *The Ecology of the Indonesian Seas,* Part II, Periplus Edition (HK) Ltd, Singapore

An Adaptive Microwave Radiometry Technology for the Monitoring Forest Ecosystems and Cpastal Zones

Mkrtchyan F. A., Krapivin V. F., Golovachev S. P.

Institute of Radioengineering & Electronics, RAS
Address:1 Vvedensky Sq., Fryazino, Moscow reg., 141190 Russia
Tel.: 7+495+7855639+1202, Fax: 7+096+5649060, E-mail: ferd@ms.ire.rssi.ru

Abstract

Forest ecosystems and coastal zones are one of the important objects of geoinfomational monitoring. Knowledge of microwave attenuation properties of forests and coastal zones is needed in this respect since attenuation values and their dependence on frequency and biometrical features afford a basis for microwave remote sensing retrieving algorithms.

One of perspective approach to the solution of the problems arising here is GIMS-technology(GIMS = GIS + model).The basic scheme of collection and processing of the information in geoinformation monitoring system(GIMS) recognizes that effective monitoring researched object is possible at complex use of methods of simulation modeling, collection and processing of the information.

From the position of system analysis, the system of collection and processing of the information in geoinformation monitoring represents the structure uniting the computers of various classes, databases and the advanced problem-oriented software. Creation of such system demands the development of formalized description of the information flows and unique methodology of its processing.

Development of GIMS requires the decision of a set of problems related to the formation of data measurements flows to be solved. The problem of monitoring forest ecosystems and coastal zones using the remote sensing measurements is one of important among them. Various algorithms of the theory of images recognition, statistical decisions and cluster analysis are used to solve this problem.
The feature of remote measurements is information acquisition, when the data of measurements, acquired during tracing of flying system along routes of survey, are directed to input of the processing system. As result the two dimensional image of investigated object is registered. Statistical model of spottiness for investigated space is one of models for this image.

In real conditions, the study of spots, the acquiring of their statistical characteristics and their using in a problem of detection is enough a complex problem. It is necessary to develop the criteria allowing the distinguishing the spots from other phenomena. For example, it is necessary to determine such threshold the exceeding of which is the spot indicator. Also it is necessary to develop model presentation of processes of spots detection.Realization of GIMS-technology will result in the creation of regional and global maps of forest and coastal systems radiative characteristics and characteristics of electromagnetic waves attenuation by forest covers and coastal zones based on created database, a priori information and modeling in conditions of limited closure of Earth surface by satellite microwave survey.

MODELLING THE FOREST ECOSYSTEMS

The forest ecological system is an important constituent of the global continuum of the soil-plant formations on the Earth. Therefore the development of the models that would describe the forest dynamics is a principal stage of the synthesis of the global model. Of course, the importance of the models of the forest ecosystems is greater, since forest resources and their use affect the economic potentials of the regions.

Many authors describe the dynamics of total biomass of an individual plant in the form of a logistic equation:

$$dB/dt = k(B_{\lim} - B)B,$$

where B is the biomass, $B_{\lim}$ is the threshold amount of biomass, k is the coefficient reflecting the effect of the environmental factors and the plant's type on its growth.

To describe the dynamics of the tree growth, the simplest functions are often used, such as Terazaki's equation $B = a\exp(-b/t)$, Koller's function $B = ax^b c^{-ct}$, approximation by Korsun' and Bakman $B = a\exp(b\ln t$

+ $c\ln^2 t$), etc. Bichele *et al.* (1980) were first to propose a more complicated model of the tree growth described by the system of ordinary differential equations:

$$dB_j = K_\Phi - k_R R_j - V_j + K_M ,$$

where $K_\Phi = k_F \sum_{i=1}^{4} \alpha_{ij} \Phi_i$; $K_M = M \sum_{i=1}^{4} \beta_{ij}$; B_j is the biomass of individual organs of a plant (j =1,2,3,4), M is the dry biomass of the whole plant; Φ_i is an amount of carbon dioxide assimilated during 24 hours by the i-th organ of the plant ($k_F \Phi_I$ is an equivalent dry biomass, k_F is the coefficient of equivalence); R_i is an amount of carbon dioxide emitted during 24 hours by the i – th organ of the plant ($k_R R_i$ is an equivalent dry biomass, k_R is the coefficient of equivalency); V_i is the dry biomass of part of the i-th organ; α_{ij} is the share of "fresh" assimilates created during 24 hours in the i-th organ of the plant, moving during the same period of time into the j-th organ of the plant; β_{ij} is the exchange of "old" assimilates during 24 hours between the i-th and j-th organs, per gram of dry biomass of the whole plant; K_Φ is an increment of biomass due to photosynthesis and re-distribution of fresh assimilates; K_M is an increment connected with the re-distribution of old assimilates; $k_R R_j$ is the biomass expenditure on respiration..

Of course, the coefficients of the model described above are functions of the environmental parameters. An account of the effect of the environment on the dynamics of the tree growth is realized, as a rule, within the principle of the Libikh limiting factors. Among the factors of the environment are PAR, carbon dioxide, temperature, humidity, as well as mineral salts in the soil. By the principle of limiting factors, a plant grows until the "resources" of some factor reach the limit. An introduction of this principle is connected with many uncertainties, and therefore in concrete situations it must be tested with the use of experimental estimates.

More developed models of the tree growth instead of a set of empirical parameters whose uncertainties are often a great barrier to practical application of the models, include the functional dependences of the elements of the tree growth on the environmental factors. Among the most widespread and often applied is the Libikh criterion consisting in that the growth of a plant is confined to an element, whose concentration is at a minimum. By this criterion a plant or its organs grow until the resources of some element, for instance, photosynthetically active radiation (PAR), moisture, temperature, carbon dioxide, nutritious salts are exhausted. There are other criteria testifying to a weighed influence of all environmental factors, these weights are characteristic indicators of the plant type.

The process of tree growing can be presented as a result of interaction of three processes of growth: change of the leaf (needle) mass, growth of the trunk, and development of the root system. Denote the biomass of the canopy, trunk, and roots of the tree as $x1$, $x2$, and $x3$, respectively. Then the balance equations of a tree model is written as

$$x_i(t+\Delta t) = x_i(t)+\varepsilon_i(t)\{R_x - T_x\}\Delta t, \ (i=1,2,3),$$

where Δt is the characteristic time step, R_x is the gross productivity of a tree due to photosynthesis, T_x is the biomass expenditure on respiration, ε_i is the share of new biomass moving into the biomass of the i-th organ of the tree. The ε_i parameters are the functions of time as well as other parameters of the environment. Following the principle of maximum survival, a supposition can be made that the principle of maximum primary productivity is valid:

$$\tilde{Y}^*(t+\Delta t) = \max_{\{\varepsilon_i(t)\}} Y\left\{x_i(t) + \varepsilon_i(t) Y\left[x_i(t), E(t,\varphi,\lambda), C_A, T_A\right]\Delta t, E, C_A, T_A\right\}$$

One of the important limiting factors of the tree growth is water, the movement of which in the soil and the tree body determines the dynamics of the tree biomass change. Following Kirilenko (1990), denote the soil as a homogeneous porous layer $[0,z_g]$, where z_g is the depth of ground water. Introduce notations: W - relative soil moisture (kg H_2O/m^3/[kg soil/m^3], ρ - water density, ρ_s – volume density of soil. Introduce a system of coordinates (x,y,z), where the z–axis is directed down from the soil surface (z=0). Then the movement of water through the soil can be described by Darsi's 3-D equation:

$$V=-K[\nabla(\Phi_s - \rho g z)]/(\rho g), \qquad (1)$$

where $V(t,x,y,z)$ is the rate of water flow, K (t,x,y,z) is the hydraulic conductivity of water, g is the gravity acceleration, Φ (t,x,y,z) is the water potential of soil.

The equation of the soil moisture dynamics is

$$\partial W/\partial t = -(\rho/\rho_s)(f+\mathrm{div}V) \quad (2)$$

where $f(t,x,y,z)$ is the sink function.

Dependences of the water potential of soil and its hydraulic conductivity on soil moisture is written as

$$K = K_s^* W^m, \qquad \Phi_s = \Phi_s^* W^{-n}$$

where

$$K_s^* = K_{FM} W_{FM}^{-m}, \qquad \Phi_s^* = \Phi_{MG} W_{MG}^n, \qquad m = 2n+1,$$

W_{FM} is the total water capacity of soil, K_{FM} is the soil conductivity corresponding to total water capacity, m and n are constants.

The system of equations (1) and (2), with assumed notations, is re-written as:

$$\partial\omega/\partial t = (-\rho/\rho_s)[(K_{FM}/W_{FM})\,\mathrm{div}\{\mu\,\omega^n\nabla\omega + i\,\omega^n\} + f/W_{FM},$$
$$V = K_{FM}(\mu\omega^n\nabla\omega + i\,\omega^n),$$

Where $\omega = n\Phi_{FM}/(\rho g)$, i is the unit vector directed along the z-axis.

In the case of homogeneous processes in the plane (x,y) the problem is simplified:

$$\partial\omega/\partial t = (-\rho/\rho_s)[(K_{FM}/W_{FM})\partial/\partial z\{\mu\,\omega^n\partial\omega/\partial z + \omega^n\} + f(t,z)/W_{FM},$$
$$V(t,z) = K_{FM}(\mu\omega^n\partial\omega/\partial z + \omega^n)$$

Boundary and initial conditions are given in the form:

$$\omega(t,z_g)=1,\ V(t,0)=P(t)-e(t),\ \omega(t_0,z_g)=\omega^0(z),$$

where $P(t)$ is precipitation intensity, $e(t)$ is the intensity of evaporation off the soil surface, $\omega^0(z)$ is the initial soil moisture.

The f function describes the intensity of water absoption by a tree's root system:

$$f(t,z) = \xi_0[\Phi_s(t,z) - \psi_0(t)]ds/dt,$$

where $\xi_0 = \xi_k\sigma_0$ is the conductivity of water entry to the root system, $\xi_k = r_k^{-1}$ is the specific conductivity of water entry to the root, r_k is the specific resistance of water entry to the root, σ_0 is the general area of the sucking roots of the tree per unit soil surface area ($\sigma_0 = \beta_k m_k$), m_k is the mass of roots beneath unit soil area, β_k is an empirical constant, ψ_0 is the water potential within the root system, $s(z)$ is the function of the vertical distribution of the root system [$s(0)=0$, $s(z_0)=1$].

To complete the synthesis of the tree's water regime, parameterize the processes of water flow in the plant and transpiration. Assume that from the root system the water flows by the trunk to canopy (branches, leaves) and then evaporated into the atmosphere. Divide the above ground part of the tree of the height H into n equal layers: $H=n\Delta z$. Across the boundaries of the i-th layer the water moves due to the difference between water potentials ψ_i and ψ_{i-1} overcoming the resistance of the xylem vessels:

$$r_{ks}^*(z) = \left(S_{ks}^*(z)\xi_{ks}\right)^{-1},$$

where ξ_{ks} is the specific conductivity of the xylem, S_{ks}^* is the cross-section of the tree at a height z. As a result, with the area of the cross-section supposed to be vertically constant, we obtain the following formula to describe the rate of water flow in the trunk across the i-th layer:

$$v_{i-1,i}^* = -\xi_{ks}S_{ks}^*\Delta z^{-1}\left(\psi_i - \psi_{i-1} + \rho g\Delta z\right)$$

According to Kirilenko (1990), the intensity of transpiration from the i-th layer can be described with the formula:

$$\gamma_i^* = \frac{d^i}{r_L^i}S_L^{*i}$$

where d^i is the deficit of saturation of an absolute air humidity in the atmosphere, S_L^{*i} is the leaf area of the i-th layer, $r_L^i = r_{st}^i + r_a$, r_{dt}^i is the stomatal resistance, r_a is the air boundary layer resistance.

To complete the description of the model after Kirilenko (1990), consider a standing wood of the density ρ_F. The model equations are written as

$$d^2\varphi / d\eta = Uv(\eta)\varphi(\eta),\ \eta \in [0,\alpha]; \tag{3}$$

the boundary conditions are

$$\begin{cases} \varphi'_0 = & -\left[G(\tilde{\varphi}_s - \varphi_0) + F\right] \\ \varphi'_\alpha = & -F \end{cases},\ d\varphi/d\eta = -F \text{ for } \eta \in [\alpha,1]; \tag{4}$$

At $\varphi_0 \le 0$, a system of equations (3) and (4) becomes:

$$\begin{cases} \dfrac{d\varphi}{d\eta} = & -F \\ \varphi_0 = & \tilde{\varphi}_s \end{cases}$$

with the following notations: $\eta = z/H$, $\varphi(\eta)=1+\psi(\eta H)/\psi^*$, ψ^* is the leaf's water potential, $1/D_1$ is a minimum mouth resistance, $U=Hr_{ks}D_1 d\beta m_L / \psi^*$, $F=\rho gH/\psi^*$, $G=Hr_{ks}\xi_0$, $\alpha=a/H$, β is the leaf index, $h=-z$,

$$a = \begin{cases} H, & \psi(H) \ge \psi^*, \\ h, & \psi(h) = -\psi^*, \quad \psi(H) < -\psi^* < \psi(0), \\ 0, & \psi(0) \le -\psi^* \end{cases}$$

ESTIMATION OF RISK IN THE MONITORING REGIME

A decision on the level of potential risk of possible change in the environment can be made on the basis of analysis of pre-history of such events and using the methods of prediction of natural events. As a rule, methods of assessing the risk is based on statistical processing of data on parameters of the processes whose interaction can initiate undesirable changes in the environmental characteristics. For instance, when assessing the risk of human health from the environmental pollution, to make a serious decision, a certain level of the informative description of the territory is needed:

- multi-year observations of concentration of chemical elements with their indicated allocation and characteristics;
- data on hydrology of the territory and synoptic characteristics;
- assessment of ecological consequences of pollution and their impact on human health;
- characteristics of the state of protective constructions and the level of development and technical equipment of services for monitoring, prevention and meeting extreme situations.

An efficiency of the systems of risk assessment depends on the form and kind of the applied procedure of decision making (Krapivin and Varotsos, 2007). Most informative is a combination of prediction procedures with the environmental monitoring regime, which can foresee situations of decision making in a real time mode on the basis of information accumulation before the decision was made or from analysis of database fragments without time reference. Statistical analysis of several events that follow the functioning of the monitoring system can be carried out by numerous methods whose applicability in each case is determined by a totality of probabilistic parameters that characterize the phenomenon under study. However, non-stationarity and parametric uncertainty in situations when each observation requires much effort and expense make one seek new methods of decision making on the basis of observation data fragmentary both in time and in space.

With development of alternative methods of making statistical decisions, the problem of finding objective estimates of the perimeters of processes taking place in the environment has been substantiated anew. It is possible to consider and compare two approaches to this problem: classical approach based on a-priori restricted number of observations, and successive analysis based on the procedure of step-by-step

decision making. Development of computer technologies makes it possible to realize both approaches in the form of a single system of making statistical decisions.

The classical procedure of making statistical decisions by the Neumann-Pearson method is based on n measurements fixed beforehand and taken from a-priori assumptions of the probabilistic character of a set of observations $X = \{x_1 , \dots , x_n \}$. Accepting hypotheses H_0 or H_1 is based on drawing the boundary of an optimal critical area E_1 in the form of a hyper-surface

$$L_n = L_n(x_1 , \dots , x_n) = f_{a\,1}(x_1 , \dots , x_n) / f_{a\,0}(x_1 , \dots , x_n) = C \tag{5}$$

where $f(x_1,\cdots,x_n) = \prod_{i=1}^{n} f(x_i)$, $f_a(x)$ is the density of probabilities distribution for the variable x with an unknown parameter a ; C is the constant magnitude chosen under condition that E_1 have a certain level of error of the first kind α .

Relationship (5) called the probability coefficient serves as a key to the final choice between the hypotheses:

1) If $L_n \le C$ then the hypothesis H_0 is accepted;
2) If $L_n > C$ then the hypothesis H_1 is accepted.

The content and semantic load of hypotheses H_0 and H_1 depend on a concrete problem. In real experiments, based on a sample $\{x_i\}$, an empirical and then continuous distribution $F(X) = f(x)$, but with an assumption of uncertainty of one or several values of the parameters. As a rule, based on one of the goodness-of-fit tests, a concrete form of distribution is chosen, and its parameters are evaluated from measured values $\{x_i\}$.

The Neumann-Pearson methods and sequential analysis make it possible to construct operative characteristics for decision making without concretization of the type of density $f_a(x)$. Consider the case of a homogeneous independent sample, when samples values x_i ($i = 1 , \dots , n$) are independent realizations of the same random variable ξ with density $f_{a\,0}(x)$ for hypothesis H_0 and density $f_{a\,1}(x)$ for hypothesis H_1. The parameter a of a true density $f_a(x)$ can differ from a_0 or a_1. It is shown that there are the following relationship for errors of first or second kind (α and β):

$$\alpha \approx \exp[-0.5\{(E_{a\,1}\xi - E_{a\,0}\,\xi)\,(D_{a\,0}\,\xi)^{-1/2}\}^2 n],$$
$$\beta \approx \exp[-0.5\{(E_{a\,1}\xi - E_{a\,0}\,\xi)\,(D_{a\,1}\,\xi)^{-1/2}\}^2 n],$$

where

$$E_a\xi = \int_{-\infty}^{\infty} \ln [f_{a\,1}(x) / f_{a\,0}(x)]\, f_a(x)\, dx ,$$

$$D_a\xi = \int_{-\infty}^{\infty} \{\ln [f_{a\,1}(x) / f_{a\,0}(x)]\}^2 f_a(x)\, dx - (E_a\,\xi)^2 ,$$

In the case of successive procedure, an operative characteristic is as follows:

$$L(a) \approx [A^{h(a)} - 1\,] / [A^{h(a)} - B^{h(a}\,)$$

where $h(a)$ is the root of equation:

$$\int_{-\infty}^{\infty} \left[f_{a1}(x) / f_{a0}(x)\right]^{h(a)} f_a(x)\, dx = 1 ,$$

A and B are two thresholds for the likelihood coefficient $L_n(x)$, for which the following estimates are valid:

$$B \approx \beta / (1-\alpha), \quad A \approx (1-\beta) / \alpha,$$

In accordance with this, like in the classical algorithm, $L(a_0) = 1-\alpha$, $L(a_1) = \beta$. Hence, an average number of observations in the sequential analysis can be evaluated:

$$E_a\,\nu = [(1-\alpha)\ln[\beta/(1-\alpha)] + \alpha \ln[(1-\beta)/\alpha]\,/E_{a0}\,\xi, \quad \text{for } a=a_0; \tag{6}$$
$$E_a\nu = [\beta \ln[\beta/(1-\alpha)] + (1-\beta)\ln[(1-\beta)/\alpha]\,/E_{a\,1}\xi, \quad \text{for } a=a_1 .$$

With $a = a_*$, when $E_{a*}\xi = 0$ and $E_{a*}\xi^2 > 0$ we have

$$E_{a*}\nu \approx [- \ln[\beta/(1-\alpha)]\ln[(1-\beta)/\alpha]/E_{a*}\xi^2 \quad (7)$$

According to (6) and (7), in the sequential procedure the number of observations for making a decision is a random variable ν, whose average value $E_a\nu$ can be greater or smaller than n. To judge about possible ν values, it is necessary to know the distribution $P\{\nu = n\} = P_a$, for which the following expression is valid:

$$E_a\nu \cdot P_a(n) = W_c(y) = c^{1/2} y^{-3/2} (2\pi)^{-1/2} \exp[-0.5c(y+y^{-1}-2)], \quad (8)$$

where

$$0 \le y \le n\,|E_a\xi| < \infty,\ c = K\,|E_a\xi|\,/\,D_a\xi = (E_a\nu)^2 / D_a\nu > 0,\ D\nu = K\,D_a\xi\,/(E_a\xi)^3,\ E\nu = K / E\xi,$$

$$K = \begin{cases} \ln A \text{ for } E_a\xi > 0, \\ \ln B \text{ for } E_a\xi < 0 \end{cases}$$

The distribution function (5.11) in Russian literature was called the Wald distribution:

$$W_c(x) = (c/2\pi)^{1/2} \int_0^x z^{-3/2} \exp\left[-0.5c\left(z + z^{-1} - 2\right)\right] dz \quad (9)$$

The Wald's distribution universality follows from its duality with respect to the normal distribution:

$$W_c(x) = \Phi[(x-1)(c/x)^{1/2}] + \Phi[-(x+1)(c/x)^{1/2}] \exp\{2c\}, \quad (10)$$

where $\Phi(x) = 1/(2\pi) \int_{-\infty}^{x} \exp\{-t^2/2\}\,dt.$

Note that if $|E_a\xi|$ and $|D_a\xi|$ are small compared to $\ln A$ and $\ln B$, then the distribution of a relative variable $\nu/E_a\nu$ determined from expression (8), will approximate the real distribution of this magnitude, even if ξ is distributed not following the normal law.

Theoretical constructions concerning universality of the distribution (9) are important for a general assessment of the efficiency of the sequential procedure of decision making. However, these constructions are not important in practical application of the Wald distribution. Therefore synthesis of the system of automated decision making as a GIMS unit has been accomplished with correlation (10) left out of account. It has been done in connection with the fact that in fact, it often happens that the number of observations turns out to be small and the effect of asymptotic normality is not realized. The resulting situation is resolved by making a decision either following the procedure of the evolutionary algorithm (Krapivin and Varotsos, 2008) or in accordance with the Mkrtchian algorithm (Mkrtchian, 1982).

REMOTE MONITORING OF THE SOIL-PLANT FORMATIONS

The remote sensing technology is an important way to map the soil-plant formations and to solve many applied problems of the landscape ecology. Recent achievements in this field are closely connected with the air- and space-borne systems, which can promptly provide information about the spatial structure of the Earth covers with a high resolution both in space and in time (Schmidt and Skidmore, 2003). The resolving characteristics depend on the applied instruments and on measurement principles. The instruments operating in the optical region are developed best. In this case the remotely obtained images of the Earth covers are in the form of photographs. On their basis the characteristic features of the surface are identified and various versions of the image of the vegetation elements are derived. Here evident progress has been made due to the use of hyperspectral sensors with a high spectral resolution (<10 nm). The hyperspectral sensors cover the spectral region 400-2500 nm. The spectral image of the vegetation cover depends on the biochemical composition of vegetation, characteristics of foliage, concentration of pigments, canopy structure and many other parameters. Here of importance is the development of methods to recognize the types of plants from their absorption and reflection of light. The main problems of spectral analysis appear because in many cases the optical images of the geological formations and vegetation covers are alike. Due to their biochemical composition, the living plants often demonstrate the overlapping features of the electromag-

netic waves absorption. There is also a multiple scattering of waves within the canopy, which raises their capabilities to absorb and reflect. However, the concentration of pigments, the biochemical composition, characteristics of foliage and canopy structure change from one type of plants to another. This is an object of analysis in order to understand which biophysical and biochemical characteristics are responsible for differences in the spectral images of the types of plants and soils (Painter *et al*., 2003; Kondratyev *et al*., 2006).

Wetlands are important elements of the Earth cover. Their monitoring provides the control of the natural cycle of biogenic elements, which is of principal importance for raising the accuracy of the estimates of the greenhouse effect and protecting the biospheric water resources. The increasing anthropogenic impact on wetlands due to tourism and cattle grazing causes changes of the vegetation cover, and depending on the totality of loads (pollution, rise of sea-level, climate change, extraction of minerals, etc.), these territories change their role in the global biogeochemical cycles.

Schmidt and Skidmore (2003) analyzed possibilities to identify 27 types of plants on the coastal saline lands on the southern side of the island Schiermonnkoog (53°29'N, 6°15'E), which is a part of the Dutch Waddenzee ecosystem. The structure of the Dutch saltmarshes vegetation cover is simple. These are mainly grasses, sedges, rushes and herbs. Here and there some types of bushes can be seen. The canopy never exceeds 1.5 m being located, on the average, at the height 25 cm. Use of the traditional method of identification of two hypotheses made it possible to demonstrate that of 351 possible pairs of the types of the covers, the probability of recognition within 740-1820 nm constituted 83%, and within 1970-2450 nm – 77%. There were local maxima of the probability of correct recognition of the types of plants: 84% at 404 nm, 81.4% at 501 nm. 80.9% at 579 nm, 82.9% at 628 nm. These maxima are explained by the absorbing features of most soil-plant formations on the coastal saline lands.

Thus the use of hyperspectral sensors enables one due to increased spectral resolution, to raise the probability of identification of the types of vegetation covers similar in their characteristics. The statistically significant distances between medians of the spectral classes provide a reliable spatial differentiation of these classes, which gives an efficient algorithm of recognition of the types of the Earth cover by their optical images.

The remote monitoring of the soil-plant formations is aimed at assessing the biological productivity, understanding interactions in the "soil-plant-atmosphere" system, calculating the biomes' dynamics, modelling the biogeochemical cycles with a consideration of the role of vegetation, managing the vegetation resources. The radar methods in solving these problems have been well developed (Krapivin *et al.*, 2006).

The Earth covers are characterized by a great variety of landscapes differing in the types of soils, special features of the water-salt and temperature regimes, the character of tilling the surface layer on agricultural lands, the type of vegetation cover, special features of the local macro-relief. The soil includes solid particles, ground water (ground solution) and air. Solid particles consist of mineral and organic substances (mineral soils): particles larger than 3mm – the stony part of the soil; particles from 0.01 to 1 mm – the "physical sand"; particles smaller that 0.01 mm – the "physical clay". The soil-forming minerals consist mainly of oxides SiO_2 and Al_2O_3. The content of organic substances (mainly humus) varies in such soils from 1 to 10% by weight. These circumstances, in the synthesis of the system of the Earth covers monitoring, necessitate the choice of information channels of the radar monitoring. Numerous and multi-year studies in this field made it possible to determine the most efficient wavelength regions for many types of vegetation cover and soils. The agricultural systems, forests and arid zones have been well studied.

Perspective directions in the radar monitoring of forest are the control of the hydrological regime of soil under forest and study of dynamics of the afforestation process in the region of clearings and forest fires. These problems are solved by using the decimetric range in which the canopy is transparent for electromagnetic waves of the microwave region and hence, the soil can be sounded down to ground waters.

The possibility of inventory of the tree-bush vegetation from the data of radar sensing is based on the connection of the coefficients of backscattering of microwave waves with the structure and dielectric properties of plants. Use of radar means in the monitoring of forests together with remote measurements in the visible and IR regions is explained by possibilities to obtain additional information. The main task of the space-borne radars in monitoring the forest is the global mapping of vegetation the scale of which is determined by the ecological and economic needs of a given region.

Recent achievements in the field of remote studies of the forest-bush vegetation became possible due to a combination of the observation means using various wavelength regions. For instance, the radar AN/APQ-96 in the IR region classifies the types of vegetation covers, the synthetic-aperture radar "Goodyear" has a resolution of 10-15 m and permits to recognize the types of soil-plant formations, the multi-channel radar SAR-580 with the resolution about 2 m identifies coniferous and deciduous forests and

bushes. A combination of the optical range with the SHF-region (3 cm, 5 cm, 10 cm, 23 cm) makes it possible to classify the states of regeneration of the burnt forest. It is seen in radio-images that the dead forest areas have a low reflectivity. This is connected with a strong absorption of radio waves of the 10-cm range in the stems of dead trees. Radio-images obtained at cross-polarization make it possible to identify images of the restored and mature forest. The dead wood images are usually darker compared to those of clearings.

The fire-protection of forests is one of the directions of development of the remote monitoring of the state of vegetation covers. The current space- and air-borne remote monitoring systems of the type JERS-1 and NOAA/AVHRR permit to solve the following problems:

- prompt assessment of the degree of the forest fire-risk;
- mapping the water-saturation of the territories in putting out large-scale forest fires;
- mapping the outlines of forest fires through the smoke layer and forest stand canopy;
- estimation of the energetic parameters of the fire;
- assessment of the post-fire state of forests.

Studies of the thermal emission of natural layers of the forest inflammable material (lichen, moss, dry grass, dead fir needles, brushwood) enables one to derive a technique to identify the forest fire parameters when measuring the thermal emission in the centimeter range of electromagnetic waves. Spectral distributions of this range clearly show the front and the rear of the fire as well as the burnt part of the forest. A comparison of brightness temperatures at different wavelengths has shown that radiant emittance of forest fires increases with decreasing wavelength and depends on the character of the fire. Spectra of brightness temperatures for various elements of the forest fire provide a reliable classification of its elements.

The GIMS synthesis to control the forest fire risk over large territories necessitates the development of applied models describing the increasing fire risk of the forests. Of course, these models are based on knowledge of the dependence of thermal emission intensity of an element of the forest landscape on its moisture content. Observations show that an increasing fire risk of the layers of the forest inflammable materials causes changes in the statistical characteristics of the fields of SHF emission of forests. In particular, this dependence can be presented as

$$T_J = \kappa(\lambda,w) T_S \, (1 - exp\{- \alpha(\lambda,w\} \, h) + T_{JS} \, exp\{- \alpha(\lambda,w\} \, h),$$

where κ and α are coefficients of emission and absorption, respectively, w is the moisture content of the environment, h is the thickness of the emitting layer, T_S is the soil temperature, T_{JS} is the soil brightness temperature. Yakimov (1996) proposed the following rule of solution based on calculation of mathematical expectation M^* and standard deviation σ^* to record T_J of the forest site in the range 2.25 cm. The M^* value is compared with the threshold value $d = 7.2514\sigma^* + 249.876$: if $M^* \geq d$ then the site of the forest is characterized by the middle or higher fire risk; if $M^* < d$ then the fire risk of this site is low. This model should be supplemented with the model of forest fire, for instance, the model that describes a forest fire as a running wave, that is, as a self-maintaining process of local energy release in the active environment.

The millimeter range (1÷10 mm, 30÷300 GHz) is also promising in solving the problem of diagnostics of the Earth covers. As shown by numerous experimental studies, an addition to the monitoring system of the channels of the millimeter range makes it possible to raise the accuracy of classification of the soil-plant formations with roughness and small formations clearly identified. It is especially important in conditions of the anthropogenic landscape.

The soil moisture is divided into solid-bound, loose-bound and free. The bound moisture is water absorbed by the surface of soil particles in the form of a film up to 6-8 molecular layers thick. The volume of bound moisture in a soil layer is determined by the type of soil and varies widely from 2-3% for sand to 30-40% for clay and loess (Shutko, 1987). The bound water is inaccessible for plants and does not affect the salt regime of soils. Therefore the monitoring system should identify the types of moisture in soils for these types to be considered in the models.

The soil moisture is expressed in percentage of the weight of dry soils. The radiation models of moistening different types of soils taking into account soil density, its temperature and salinity, have been studied in detail. In solving this problem, wavelengths 2.25 cm, 18 cm and 30 cm turned out to be most informative. The model of radio-thermal emission of the Earth cover in conditions of non-uniformly moistened surface layer is based on the vertical gradient of the dielectric permeability coefficient $\varepsilon \cong (1 + 0.5\rho_s)^2$. The ε parameter is an informational indicator of the changing soil moisture. With the growing soil moisture the ε value increases first slowly, if the soil was dry, then more rapidly. A weak dependence of ε at the stage of

initial moistening is explained by that the bound moisture is characterized by a low dielectric permeability. Diverse experimental dependences of ε on the types of soils and volumes of moistening have been discussed by Shutko (1987). The base of knowledge and an application of GIMS-technology permit to solve the problem of diagnostics of the water content W_s in the soil layer. Essentially, the problem is reduced to the retrieval of the function $W_s(z)$ for which the values $W_{si} = W_s(z_i)$ are known, being measured either remotely of in-situ, and if it meets the conditions:

$$\left.\partial W_S / \partial z\right|_{z=0} \le C, \quad 0 \le W_S(z) \le K_S(z), \tag{11}$$

where $K_s(z)$ is the prescribed function. The measurement errors follow the known law of distribution.

Practice has shown that regardless of the climatic zone, for an adequately accurate retrieval of the vertical profile of humidity in a 1-m layer, it is necessary to use microwave radiometers 10 cm and 30 cm to measure the surface layer humidity (W_{s2}) and 100 cm to measure (W_{s3}). Then an approximation $W^*_s(z) = az^3 + bz^2 + cz + d$ is assumed, whose unknown coefficients are found traditionally from the condition of minimum functional of mean square deviation:

$$\sum_{i=1}^{3} [W_S(z_i) - W_S^*(z_i)]^2 = \min .$$

Here it is necessary to observe the limitations (11).

This approach makes it possible from the data of microwave radiometric measurements, for instance, from the flying laboratory, to measure the water supply in a 1-m soil layer over large territories with an error not exceeding 0.03 g/cm^3 for the vegetation biomass < 2 kg/m^2 and with an error of 0.07 g/cm^3 for the biomass >2 kg/m^2.

Knowledge of the function $W_s(z)$ enables one to use the model of the water supply over the territory to retrieve the dynamic characteristics of soils and other elements of water balance as functions of geophysical and ecological parameters. An important specification of such a model is an experimental estimate of the upper soil layer thickness, at the lower boundary of which, from the estimates in Shutko (1987), in 6 days after rain or after watering the capillary bonds get broken. The characteristic thickness of this over-dried layer varies within 3-5 cm.

The choice of an optimal range of electromagnetic emission and the synthesis, on this basis, of an efficient method to measure the moisture content in soils require an additional study of conditions of the formation of the emission fields in the system "atmosphere-soil-plant". Direct measurements should be combined with the use of the data processing algorithms that include the models. An example of successful application of two algorithms to retrieve the soil moisture parameters differing in the sets of input data is given in Frate *et al*. (2003). The algorithms are based on the neural network and meant for processing the remote radar measurements in *L*-range at two polarizations without preliminary information about the parameters of vegetation cover and surface roughness.

The monitoring of soils moisture is closely connected with the problem of their salinity (Metternicht and Zinck, 2003). On a global scale, this process is recorded over 995 Mha soils, with 77 Mha being salted most, of which 58% referring to the irrigated territories. Therefore knowledge of only moisture content in a soil without data on its state is insufficient for reliable model estimates of the vegetation cover productivity and, as a result, for estimation of the capacity of the surface sink of CO_2. Finally, there is one more circumstance connected with the monitoring of soil moisture. The concept of GIMS-technology suggests that to estimate the soil moisture, one can use a respectively adjusted model of the territorial hydrological regime (Kondratyev *et al*., 2006), if the estimate of water content in snow cover serves as its input information (Magagi and Bernier, 2003).

EXPERT SYSTEM TO IDENTIFY THE SPOTS OF POLLUTANTS ON THE WATER SURFACE

The problem of detection and identification of the pollution spots on the water surface, especially of oil spills, is being solved by many scientists. The recently developed technology of an adaptive identification of the environmental elements from measurements in the visible spectral region permits to synthesize an expert system for an adaptive identification of the environmental parameters (ESAIEP). The system's structure includes a compact multi-channel spectropolarimeter (MSP), information interface with computer (IIC), computer software (STW), and extending database (EDB). The STW realizes a number of algorithms

to process the data fluxes from MSP and provides service functions of visualization and control of the regime of measurements. The EDB consists of the sets of standard spectral images of the spots of pollutants represented by points in the multi-dimensional vector space of indicators, pre-calculated on the basis of learning samples.

The principle of the ESAIEP functioning is based on fixation of changes of the light flux at the MSP output and their transformation into a digital code. Further processing of these data with respect to their efficiency is determined by the STW composition containing various algorithms of recognition of 2D objects. The adaptability of the recognition procedure is determined by the level of accumulated knowledge about special features of intensity fluctuations and polarizing properties of the light reflected from the water surface. The STW includes the means that make it possible, in case of uncertain identification of the pollution spot, to make an expert decision based on the visual analysis of its spectral image. This procedure is realized in the mode of dialogue with ESAIEP, and if decision is made, the operator can fix it in the database in the form of a standard for subsequent situations of an appearance of similar spots.

The principal scheme of the STW unit providing the procedure of identification is some transformation Φ. The light intensity ξ^i_j recorded at the time moment t_i in the channel λ_j is evaluated by the algorithm Φ where two hypotheses H_0 and H_1 are identified. The ESAIEP operator determines initial data $\mathbf{v}_i$, α and β and decides of which parameters $\mathbf{u}_i = (u_1,...,u_r)$ will be calculated from measurements of $\{\xi^j_i\}$. The service unit IIC makes it possible to form vector $\mathbf{u}_i$ from statistical characteristics of the series $\{\xi^j_i\}$ or to use direct measurements. A-priori information characterizes the type of distribution $f_a(\mathbf{u}_i)$. The function

$$L_i = \sum_{i=1}^{\varnothing} \psi_j = f_{a1}(\mathbf{u}^j_i) / f_{a0}(\mathbf{u}^j_i)$$

is compared with its ultimate values $L_{i,min}$ and $L_{i,max}$ At the first stage, these values are chosen arbitrarily, but then they change till reaching a maximum accurate recognition of the hypotheses H_0 and H_1. We have $L_{i,min} \to L^*_{i,min}$ and $L_{i,max} \to L^*_{i,max}$. The values $L^*_{i,min}$ and $L^*_{i,max}$ are memorized in EDB.

After the learning procedure, the functioning of the expert system is limited only by the volume of measurements fixed by the operator, proceeding from statistical reliability and the real-time regime. The operator has two possibilities to regulate this regime, establishing the volume of the series $\{\xi^j_i\}$ or fixing the time of their accumulation. Usually the latter characteristic equal to 1 *s* is chosen. The operator is combined with the ESAIEP units through the man-machine interface IIC, which provides the selective control of operations in all units.

In the presence of the oil film on the water surface the system analyzes its thickness, age, source and geometry. In this case most informative are series of measurements at wavelengths 398 nm, 439 *nm* and 480 nm. In the case of dissolved or suspended components in the water the system estimates their concentration and from the data in EDB on the hydrodynamic parameters of the water body, it calculates their spatial distribution using the methods of 2D images processing.

References

Bichele I., Moldau X., and Ross Yu. (1980). *A sub-model of the distribution of assimilates and of the growth of plants in conditions of water deficit*. Preprint, No. A-5, The Tartu Astrophysical Observatory, Tartu, 22 pp. [in Russian].

Frate F.D., Ferrazzoli P., and Schiavon G. (2003). Retrieving soil moisture and agricultural variables by microwave radiometry using neural networks. *Remote Sensing of Environment*, **84**(2), 214-233.

Kirilenko A. P. (1990). *Numerical modeling of the production process and of the water cycle of the forest ecosystems*. Ph. D. Theses, Computing Center of RAS, Moscow, 151 pp. [in Russian].

Kondratyev K.Ya., Krapivin V.F., and Varotsos C.A. (2006). Natural Disasters as Interactive Components of Global Ecodynamics. Springer/Praxis, Chichester, UK, 579 pp.

Krapivin V.F. and Varotsos C.A. (2007). Globalization and Sustainable Development: Environmental Agendas. Springer/Praxis, Chichester, UK, 304 pp.

Krapivin V.F. and Varotsos C.A. (2008). Biogeochemical Cycles in Globalization and Sustainable Development. Springer/Praxis, Chichester, UK, 565 pp.

Krapivin V.F., Shutko A.M., Chukhlantsev A.A., Golovachev S.P., and Phillips G.W. (2006). GIMS-based method for vegetation microwave monitoring. *Environmental Modelling and Software,* **21**, 330-345.

Magagi R. and Bernier M. (2003). Optimal conditions for wet snow detection using RADARSAT SAR data. *Remote Sensing of Environment*, **84**(2), 221-233.

Metternicht G.I. and Zinck J.A. (2003). Remote sensing of soil salinity: potentials and constraints. *Remote Sensing of Environment*, **85**(1), 1-20.

Mkrtchian F. A. (1982). *An Optimal Recognition of Signals and Monitoring Problems.* Science Publ., Moscow, 185 pp. [in Russian].

Painter T.H., Dozier J., Davis R.E., and Green R.O. (2003). Retrieval of subpixel snow-covered area and grain size from imaging spectrometer data. *Remote Sensing of Environment*, **85**(1), 64-77.

Schmidt K.S. and Skidmore A.K. (2003). Spectral discrimination of vegetation types in a coastal wetland. *Remote Sensing of Environment*, **85**, 92-108.

Shutko A.M. (1987). *Microwave radiometry of the water surface and soils*. Science Publ., Moscow, 190 pp. [in Russian].

Yakimov S.P. (1996). *Algorithms for the assessment of forest fire dangerous by the remote sensing data*. Ph.D. Theses, State Technical Univ., Krasnoyarsk, 155 pp. [in Russian].

Coastline Change in Ben Tre Province, Mekong River Delta

Ngo Thi Phuong Uyen[1], Nguyen Van Lap[2], Ta Thi Kim Oanh[2]

[1] Faculty of Geology, University of Natural Sciences of Ho Chi Minh City,
227 Nguyen Van Cu St., 5 Dist., Ho Chi Minh City, Vietnam
e-mail: ntpuyen@hcmuns.edu.vn
[2] Sub-Institute of Geography, Vietnamese Academy of Science and Technology,
1 Mac Dinh Chi St., Ho Chi Minh City, Vietnam
e-mail: sedlap@hcm.vnn.vn

Aabstact

Coastal zone is an area where the land-sea interactions are quite intense. In Vietnam, coastline in Mekong River Delta has been changed in recent time. This has been studied about coastline changes in Ben Tre province, Mekong River Delta. The Ben Tre coastline has been affected by erosion and deposition processes in different places both at the shore areas and the river mouths. Information about these changes is necessary for using land and managing natural resources effectively.

This study has been based on multi-temporal remote sensing data, materials of geology, hydrometeorology, land-use documents. There are 4 scene Landsat images from 1972 to 2004. These images were corrected and digitized to obtain information about coastline in each stage. They were overlaid together to see the changes of coastline. Then, based on referencing involved materials and field researches to identify factors affected the coastline changes.

As a result, between 1972 and 2004, coastline in Ben Tre province was extended with deposits such as 2.5 km wide at Thoi Loi (Binh Dai), Thanh Hai (Thanh Phu) and 1.2 km wide Ba Lai river mouth (Ba Tri). But it was eroded about 1.0 km wide at Thua Duc (Binh Dai) and Con Loi (Thanh Phu). Its erosion and deposition has been impacted by Northeast-Southwest waves and long-shore current.

INTRODUCTION

Coastal zone is an area where the land-sea interactions are quite intense. Coastline, the physical land-water boundary, has been changed through time and occurring more and more in recent time. These changes have been influenced by several natural dynamic processes and growing of population and socio-economic activities in the coastal zone. Infomations of coastline changes, especially erosion-accretion trends is actually necessary to coastal scientists and coastal managers.

Applications of satellite remote sensing and GIS technologies in detecting, mapping and measuring changes in coastal zone are increasingly being accepted as an operational tool in recent years (Pham, *et al.,* 2004; Alesheikh, *et al*., 2007). The reflectance characteristics of water, land and vegetation are different between visible spectral and infrared spectral. So, optical satellite data which are multi-spectral, multi-temporal advantages can be used to detect effectively changes of coastline. In Vietnam, coastline in Mekong River Delta (MRD) has been changed rapidly. This study aims at detection of coastline changes in Ben Tre Province located on the lower delta plain of MRD using Landsat satellite data.

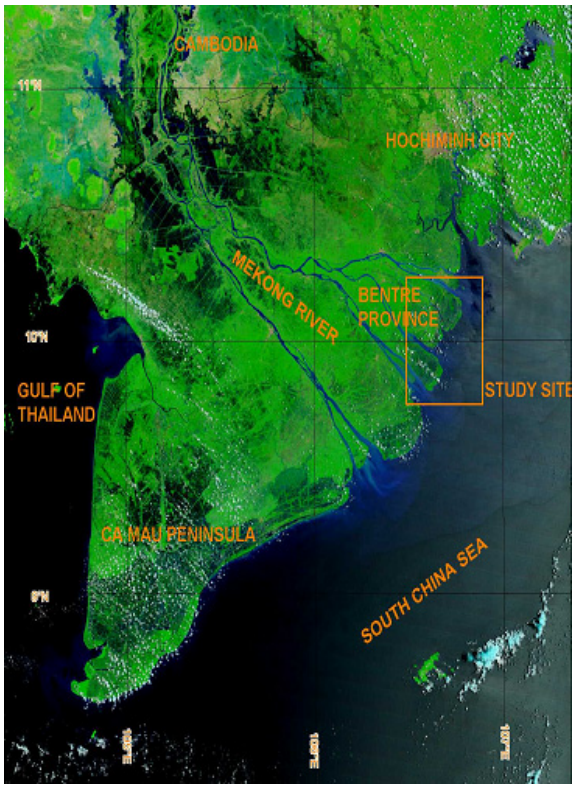

Fig. 1. Location of study site
(*image from http://visible earth.nasa.gov*)

STUDY SITE

Ben Tre Province is in the coastal plain of the MRD and located among active distributaries of the Mekong River system (Fig. 1). The climate of Ben Tre Province is subtropical and influenced by monsoon. There are two seasons in year: the wet season from May to October and the dry season from November to April of following year. The wind direction is West to Southwest in wet season and East to Northeast in dry season. The speed of East-Northeast wind in dry season is stronger than the West-Southwest wind. This may cause sea level of this area higher than in wet season. The study area is influenced the semi-diurnal tide. The mean tidal range is 2.5 – 3 m and the maximum tidal range is 3.5 – 4 m. The terrain of this area is really plain with mean elevation about 0.8 - 1 meter. This area contains numerous beach ridges indicated former positions of shoreline during the delta progradation. The MRD evolution is from 5000yr. BP. to present during late Holocene (Nguyen et al, 2000). The coastal sediment environment changed from tide-dominated initial to tide-wave-dominated since last 3000yr. (Ta et al, 2002) The progadation rate was decreased from 17 – 18m/y initially during 5300yr. to 3500yr. BP to 13 – 14m/y during the last 3500yr. (Nguyen et al, 2003).

MATERIALS AND METHODS

The study has been based on multi-temporal remote sensing data. There are 4 scenes of Landsat mutlti-spectral images from 1972 to 2004 used (some features in table 1 and 2)

Table 1. Landsat Instrument Bands. IR = infrared; NIR = near infrared; SWIR = short wavelength infrared; TIR = thermal infrared (long wavelength); and µm = micron or micrometer

Band	MSS	TM	ETM+
1		0.45-0.52 µm blue	0.45-0.52 µm blue
2		0.52-0.6 µm green	0.53-0.61 µm green
3		0.63-0.69 µm red	0.63-0.69 µm red
4	0.5-0.6 µm green	0.76-0.9 µm NIR	0.75-0.9 µm NIR
5	0.6-0.7 µm red	1.55-1.75 µm SWIR	1.55-1.75 µm SWIR
6	0.7-0.8 µm IR	10.4-12.5 µm TIR	10.4-12.5 µm TIR
7	0.8-1.1 µm IR	2.08-2.35 µm SWIR	2.1-2.35 µm SWIR
8			0.52-0.9 µm panchromatic

Table 2. Landsat images used in the study

Landsat sensor	Date (mm.dd.yy)	Bands used	Spatial resolution (m)
MSS	12.15.72	4, 5, 6, 7	80
TM	01.16.89	2, 3, 4, 5	30
TM	02.21.96	2, 3, 4	30
ETM+	01.18.04	2, 3, 4, 5	30

There are many methods extracting coastline used Landsat multi-spectral images. The coastline can be extracted from a single near infrared band image. These are relied on reflectance differences between water and land. Reflectance of water is very low (nearly equal zero) in near infrared bands (IR or NIR), reflectance of land cover is contrary, higher than water. As a result, water and land can be distinguished separately. But this method just attains at high accuracy in the coastland with less vegetation because the high reflectance of vegetation in near infrared band makes less certain on coastline extracted, especially in mangrove marsh areas. In addition, as to coastal zone areas in Mekong River Delta with extremely low terrain slope and strongly influenced tide, the coastline extracted by using satellite image may attain at less accuracy. For this reason, the study combined remote sensing technologies with image interpretation and field investigation for coastline mapping.

These imageries were all processed. Three scenes (1972, 1989 and 2004) of digital image were processed such as: threshold histograms, making band ratio image, finally, true color composite images were

made (Fig. 2., 3., 5.). On these images, the boundary between land and water can clearly separated. But on the scene in 1996 is just a false color composite image from 234 band (Fig. 4.), so the coastline was extracted by interpretation on image. All of the images were corrected in UTM projection (WGS 84). Field points were mark by GPS Garmin III Plus in UTM projection (WGS 84) too. These images were digitized using GIS software to obtain the coastline in each stage and overlaid together to see the changes of coastline from 1972 to 2004.

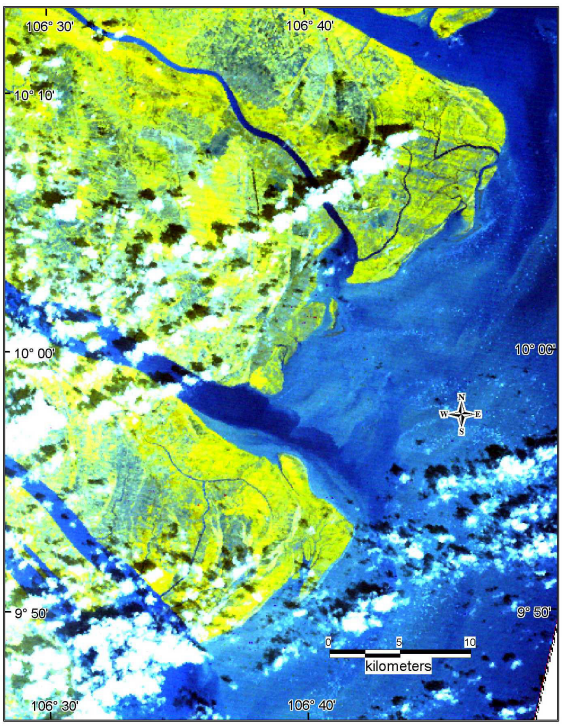

Fig. 2. Composite image in Dec, 1972

Fig. 3. Composite image in Jan, 1989

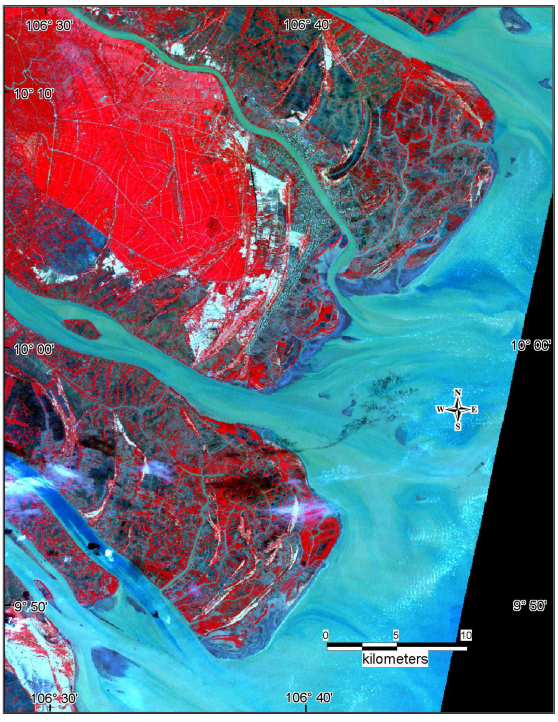

Fig. 4. Composite image in Feb, 1996

Fig. 5. Composite image in Jan, 2004

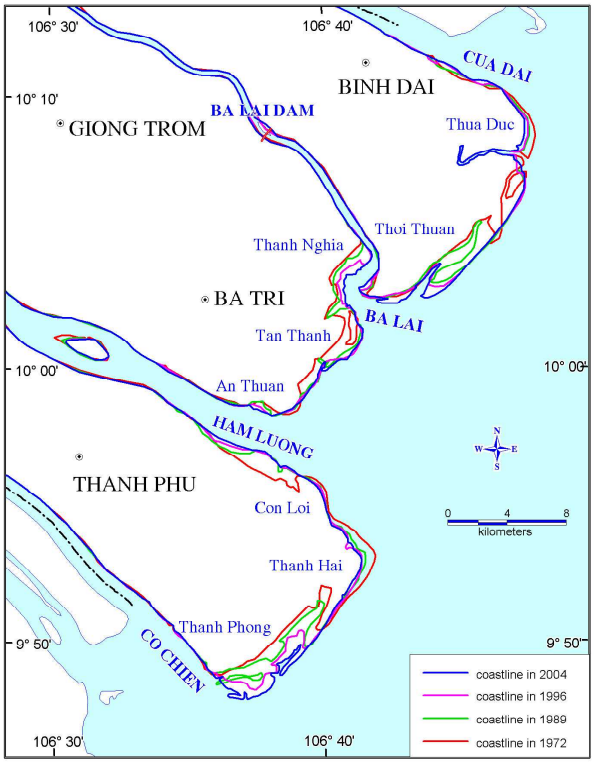

Fig. 6. Map of coastline in Ben Tre Province

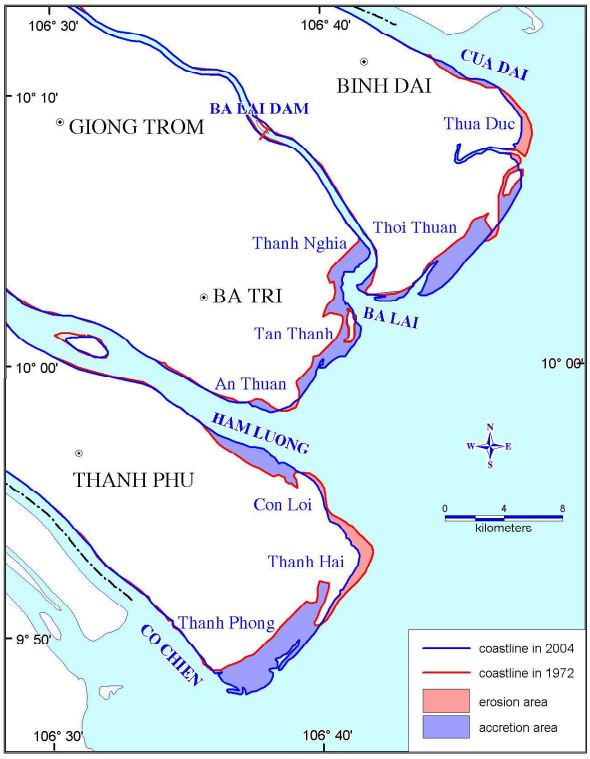

Fig. 7. Map of erosion-accretion coastland in Ben Tre Province

RESULTS

As a result, changes of coastline in Ben Tre Province were shown in Fig. 6. From 1972 to 2004, coastline in Ben Tre province was moved back toward the land at Thua Duc (Binh Dai district) at an approximate rate of 10-20m/y; at Con Loi – Thanh Hai (Thanh Phu district) the rate is 10-30m/y. Contrary, the coastline was encroached toward the sea at the approximate rate of 20-40m/y at Thoi Loi (Binh Dai district) and Ba Lai river mouth (Ba Tri district); 40-70m/y at Thanh Phong (Thanh Phu district).

Using GIS technologies, erosion and deposition areas were defined and illustrated in Fig. 7. The erosion areas were approximately estimated about 4.5 square kilometers at Binh Dai district; 1.5 square kilometers at Ba Tri district and 8.3 square kilometers at Thanh Phu district. The accretion areas were about 15.5 square kilometers at Binh Dai district; 13.5 square kilometers at Ba Tri district and 24.3 square kilometers at Thanh Phu district. The accretion areas are located on the Southwest side; the erosion areas are sited on the Northeast side.

DISCUSSION

Base on the result above, the erosion and deposition in this area indicated that the coastland in this area has been impacted by waves and long-shore current dominated direction from Northeast to Southwest in South China Sea. Sediments almost sandy silt has been transported along coast with the same direction. Researches on sedimentary environment of the MRD in recent year showed less and less in progadation rate of the MRD. In addition, global climate change, population growth, human socio-economic activities increase have been impacting on the coastal zone more and more. The coastal zone therefore has been threatening by various environmental hazards. It is necessary to assess all influenced factors to the coastal zone. The study showed clearly the tendency, located sites and estimated the erosion – accretion areas in study area; despite the source of image data was not synchronic (the scene in 1996 is only a composite image). Due to the study used combined methods, the accuracy of the extracted coastline was difficulty estimated (approximately 1 – 2 pixels). The result of this study is considered premise to next researches in the coastal zone.

Reference

Alesheikh, A.A., Ghorbanali, A., Nouri, N., (2007). Coastline change detection using remote sensing. *Int. J. Environ. Sci. Tech*., 4 (1), 61-66.

Coleman J. M. (1982). *Processes of Deposition and Models for Exploration*. International Human Resources Development Corporation, Boston, 124p.

Elizabeth H. Boak and Ian L. Turner (2005). Shoreline Definition and Detection: A Review. *Journal of Coastal Research*, 21(4), 688-703.

Nguyen, V. L., Ta, T. K. O., Tateishi, M. (2000). Late Holocence depositional environments and coastal evolution of Mekong River Delta, Southern Vietnam. *Journal of Asian Earth Science* 18, 427 – 439.

Nguyen, V. L., Ta, T. K. O. (2003). Sediment facies and Late Holocene evolution of The Mekong River Delta in Ben Tre Province. *Journal of Science and Technology Development*, National University of Ho Chi Minh City; Vol 6-9 &10, 86 – 95.

Nguyen, V. L., Ta, T. K. O. (2005). Holocene evolution of The Mekong River Delta and human impacts. International Conference on Deltas (Mekong Venue): Geological Modeling and Management. HCMC, Vietnam.

Pham, B. V., Lam, D. N., Pham, T. M. T. (2004). Using remote sensing to study shoreline change in South of Vietnam. Fundamental research on earth sciences serve the socio-economic sustainable development in South Vietnam. HCMC, Vietnam. Dec 20.

Ta, T. K. O., Nguyen, V. L. (2002). Late Pleistocene – Holocene sediment and Mekong River Delta progadation in Ben Tre Province. *Journal of Earth Sciences*, Hanoi, Vietnam, 24 (2), 103 – 110.

Umitsu M., Nguyen V. L., Ta T. K. O. Late Holocene Landform Evolution of The Mekong River Delta, Vietnam. Final Conference Project IGCP 437, Puglia 2003.

Vu, V. V. (2005). History and development of Holocene geomorphological structure of the lower delta plain, Mekong River Delta. International Conference on Deltas (Mekong Venue): Geological Modeling and Management. HCMC, Vietnam.

PART III

PATTAYA CONFERENCE
ON
COASTAL EROSION

3 - 4 November 2007

Coastal Erosion of Vietnam: Status State and Reasons

Vu Van Phai, Nguyen Hieu, Vu Le Phuong

Faculty of Geography, Hanoi University of Sciences, VNU

Abstract

Vietnamese shoreline is about 3,500 km in long stretching from Mong Cai in the North to Ha Tien in the South and about 2/3 of which made by unconsolidated sediments such as sands and silts. At present, almost shoreline is occurring erosion with a different velocity. Some parts of Red River delta (in Haihau District, Namdinh prov.) and MeKong River delta (in Baclieu and Camau prov.) coasts are being eroded with velocity of 5-10 m/year. This even occurs on the islands (Vinh Thuc, Quan Lan, Ngoc Vung, Con Son, Phu Quoc,…). Thus, it is possible to say that the shoreline erosion is now a dominant geomorphologic process and one kind of natural hazards on the coast of Vietnam.

The main reason of the shoreline erosion is the increase of wave energy influenced by some agencies: 1) tropical cyclones and typhoons with strong wind (average about 4-5 times per year); 2) sea-level rise (about four decades ago, the sea-level rise along the coast of Vietnam is 2.15mm/year in Hai Phong, 1.198 mm/year in Danang, 0,957 mm/year in Quinhon and 3.203 in Vungtau); 3) human activities damaged mangroves for aquaculture pools on low coastal zone (in period 1985-2005 the mangrove area lost 183,724 ha) and coral reefs (at present, there is only 1% of the coral reefs in good condition with cover of 75% and more than 30% -with cover less than 25%; Tran Ngoc Cuong, 2006) and constructed the dams and reservoirs on river basins.

1. INTRODUCTION

Vietnamese shoreline is about 3,500 km in long stretching from Mong Cai in the North to Ha Tien in the South and about 2/3 of which made by unconsolidated sediments such as sands and silts. There are about $41.5x10^6$ (53% of total population of Vietnam) live in coastal zone at less than ten metres elevation [8]. Human settlements including cities such as Halong, Haiphong, Vinh, Donghoi, Hue, Danang, Quinhon, Nhatrang, Phanthiet, HoChiMinh city and so on are in this area, which provide many resources, but also expose residents to various hazards (tropical cyclones, sea-level rise, coastal erosion, ...).

The coastal erosion of Vietnam has occured for long time. It may be in begining of the XX century. At that time, the coastal erosion only occured in some places as Haihau (the Red River Delta) and Bode (the Mekong River delta). But from 1990 up to now, the coastal erosion has occured and occuring in many parts made by sandy or silty sediments. In a few decades, there are a lot of researching results on the coastal erosion in Vietnam [3,4,5,9,10,11,12,13,14,15]. However, this is complex phenomena and alway change over time and space. It is possible to say that at present, almost coastline of Vietnam is eroding with diffirent velocity from a few metters to ten metters or more per year. The status state and the main reason of the coastal erosion of Vietnam as well as some affacted factors on them will be representing in this paper.

2. THE COASTAL EROSION OF VIETNAM: STATUS STATE

At present, Vietnam has 28 Provinces and Cities with 53% of total population located along the coast. Coast of Vietnam has made by many geological structures with the different directions (NE-WS, NW-SE, submeridian), ages (from Paleozoi to Cenozoi) and rocks including solid (igneous, sedimentary) and unconsolidated (gravel, sand and silt-clay). However, almost of the modern coastline of Vietnam (about 2/3 of total strenght, i.e. 2,500 km) made by unconsolidated sediments. The results of study on the coastal erosion of Vietnam representing in this paper based on the geomorphological maps of the coastal area of Vietnam (from 0 to 30 m deep) at the scale 1/500,000 having mapping by ourself in 2001 [11] and at the scale 1/100,000 (from Tuyhoa to Vungtau) in 2006 [15] and the other authors.

As well as through the World, the coastal erosion in Vietnam is increasing day by day both the length and intensity, especially on the low coastal land made by unconsolidated sediments (sand, silt-clay) (table 1).

Table 1. The number of eroded shoreline sections has been increasing through time in Vietnam

Periods	Number of sections
Before 1949	13
From 1950 to 1969	14
From 1970 to 1979	18
From 1980 to 1989	95
From 1989 to 2000	157
From 2001 up to now	Almost the shoreline is eroding

At least 2/3 total length of the shoreline (about 1,500 km) is beeing eroded (Fig. 1). Some sections have been eroded for very long time, such as Haihau shoreline in the Red River delta (Fig. 2) and Bode shoreline in the Mekong delta (Fig. 3). Whereas, on some other sections, the erosive phenomena have paused and changing by accretion. For example, some sections of Thaibinh province in the Red River delta was eroded in 1960's and 1980's and now being accreted.

The velocity of the coastal erosion in Vietnam is also different in both spaces and time (table 2). However, it will be decreased throughout the time (e.g. velocity of the coastal erosion in Haihau District, Namdinh Prov. was about 34.7 m/year from 1905 to 1927, 18.7 m/year from 1928 to 1966).

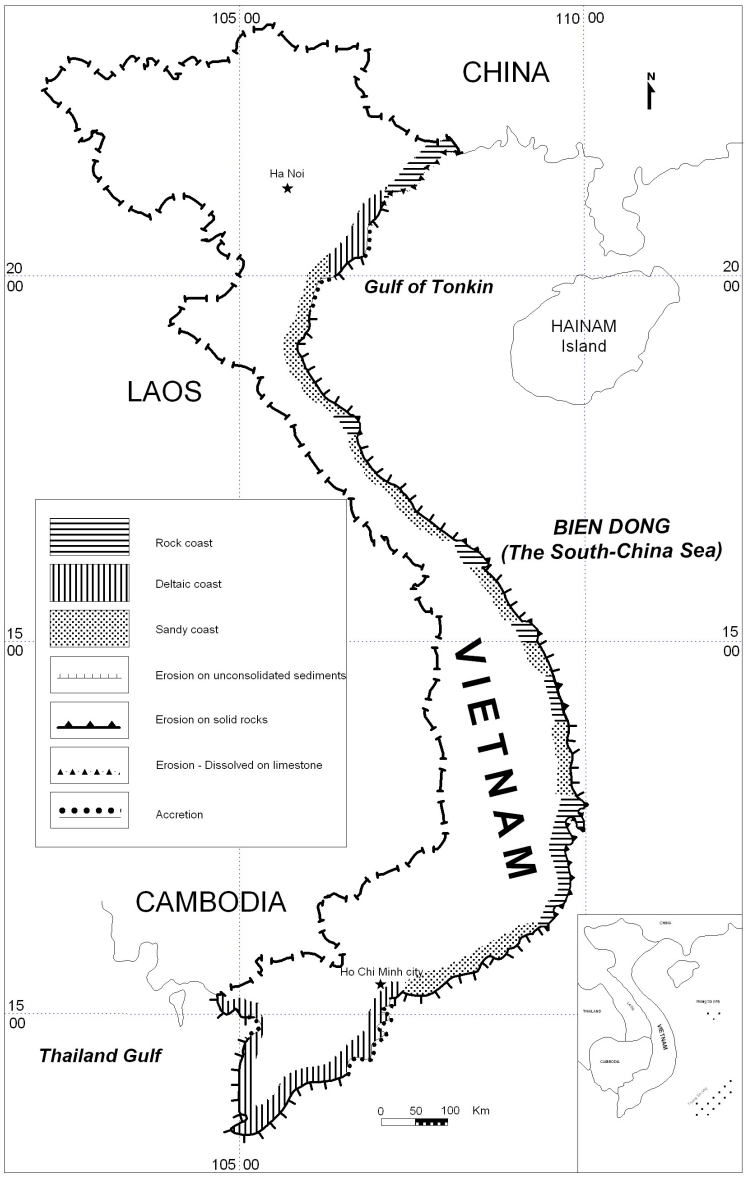

Figure 1. Distribution of erosion and accretion on the shoreline of Vietnam

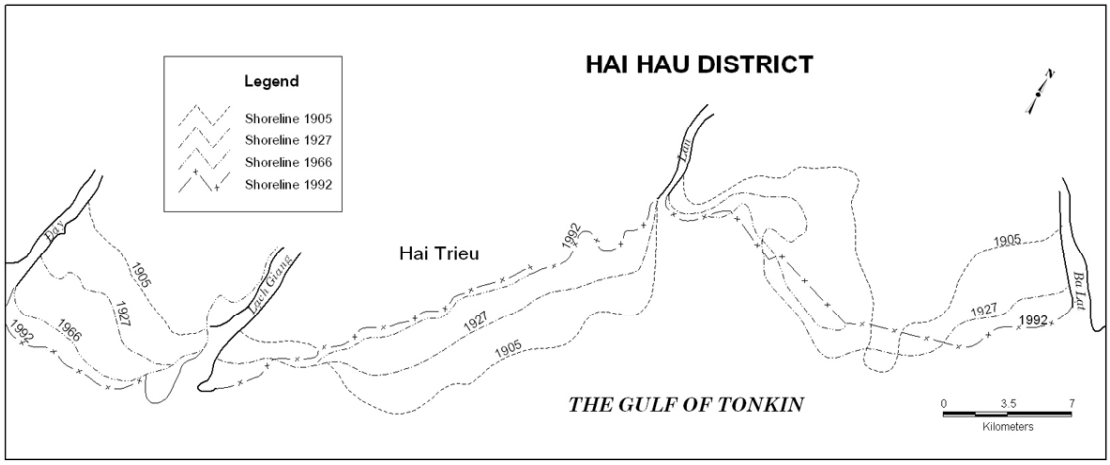

Figure 2. The change of shoreline position in Haihau district (Namdinh province) period 1905-1992 [5]

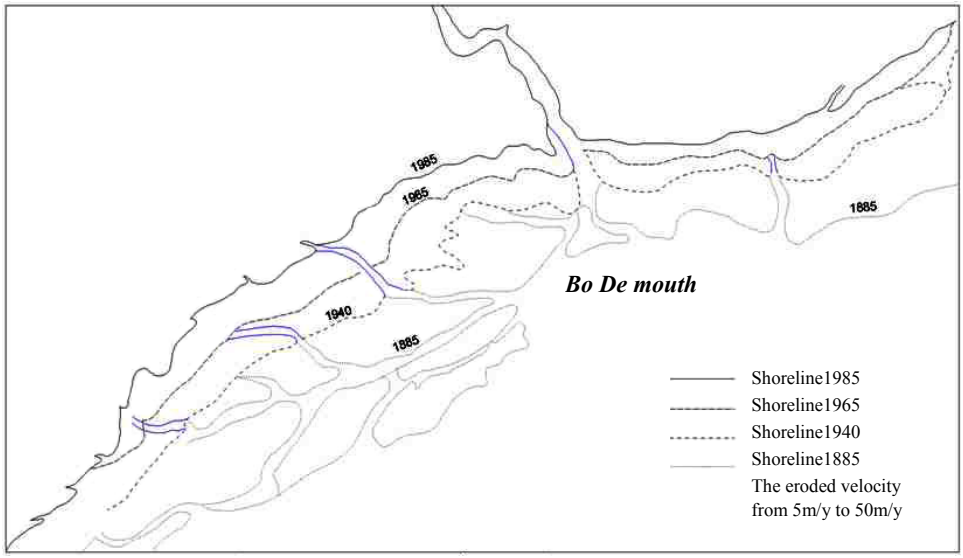

Figure 3. The change of shoreline position in Bo De mouth and adjacent areas
(Document of Me Kong Delta General Investigation Program, Code 60-02)

3. THE COASTAL EROSION OF VIETNAM: MAJOR REASON AND INFLUENTIAL FACTORS

3.1. The main reason

The main reason of coastal erosion in Vietnam is an increseased wave energy. Both theory and reality determine that the wave energy is the main factor which shapes and modifies coastline by eroding, transporting and depositing sedments. The wave energy depends on its height and length according to the formula: $E = 1/8\rho g h^2 \lambda$, where ρ- the density of the water; h- the wave height; λ – the wave length and g- gravitational acceleration. The wave height and length is alway changed depending upon a wind velocity. On the other hand, the wave energy attacked the beaches even depends on the steep of the beach profiel. The results of investigation in the few decades in Vietnam found that the wave energy is increasing more and more. It is possible to give an average significant wave height in off-shore of the Red River delta for the example (table 3).

3.2. Some major factors effect on an increased wave

There are a lot of the factors effect on the increased wave attack on the coast causing the coastal erosion. According to Bird E. [1], some 21 factors have been identified as having initiated or accelerated

beach erosion. However, in the paper, just three most important factors is represented, includes the increased tropical cyclones and depressions; sea-level rise and human activities

a) Increased tropical cyclones

In a few decades, an annual average number of the tropical cyclones and depressions attacked on the coast of Vietnam has been increasing. Matsumoto J. and Shoji H. [7] found that there were 218 cyclones attacked on Vietnam in period 1951- 2000 (fig.4). Based on this statistical data , it is possible to show that the average annual number of the tropical cyclones increases in each astronomic cycle of 19 years as below:

- 1951-1969: there were 67 the tropical cyclones, i.e. 3.5 cyclones per year
- 1970-1978: there were 90 the tropical cyclones, i.e. 4.7 cyclones per year
- 1979-2000: there were 59 the tropical cyclones (only in 12 years), i.e. 5.0 cyclones per year. If adding the period from 2001-2007, an average annual value of the tropical cyclones attacked on Vietnam is more than 5.0 per year.

b) Sea-level rise

The study results of sea-level change along the coast of Vietnam show that, the sea level has increased for the period 1957-1994 with the different velocity as below:

- At Hondau station (Haiphong City): 2.150 mm/year
- At Danang station (Danang City): 1.198 mm/year
- At Quinhon station (Quinhon City, Binhdinh Prov.): 0.957 mm/year
- At Vungtau station (Vungtau City, Baria-Vungtau Prov.): 3.203 mm/year

Table 2. Velocity of the coastal erosion on some sections in Vietnam

Sections	Period		Velocity (m/year)
	From	To	
Haitrieu (Haihau, Namdinh)	1905	1991	31.2
Quangcu-Bacson (Samson, Thanhhoa)	1976	1991	41.0
Nghiyen (Nghiloc, Nghean)	1982	1991	162.2
Xuanlien (Nghixuan, Hatinh)	1989	1991	150.0
Quangphuc (Quangtrach, Quangbinh)	1976	1991	32.0
North of Thuanan (Thuathien-Hue)	1965	2005	15.0
Dienduong (Dienban, Quangnam)	1975	1995	120.2
North of Cua Dai (Hoian, Quangnam)	1972	1993	62.8
South of Nuocman lagoon (Ducpho, Quangngai)	1962	1993	32.2
Noth of Nhonly (Hoainhon, Binhdinh)	1970	1991	40.0
Xuantho (Dongxuan, Phuyen)	1980	1992	100.0
Camthinh Dong (Camranh, Khanhhoa)	1988	1993	104.0
South of Phuocdinh (Tuyphuoc, Ninhthuan)	1975	1993	84.0
Phuocthe (Tuyphong, Binhthuan)	1972	1993	38.1
Phuochai (Datdo, Baria-Vungtau)	1972	1992	50.0
South of Canthanh (Cangio, HCM city)	1970	1991	21.9
Tanthanh (Gocongdong, Tiengiang)	1968	1991	56.0
North of Thanhhai (Thanhphu, Bentre)	1983	1992	91.0
Hiepthanh (Duyenhai, Travinh)	1982	1992	100.0
Danthanh (Duyenhai, Travinh)	1982	1992	102.0
Donghai (Duyenhai, Travinh)	1956	1992	83.0
North of Ganhhao (Giarai, Baclieu)	1976	1991	193.0
South of Ganhhao (Damdoi, Camau)	1945	1991	100.0

Table 3. The average significant wave height in offshore of the Red River delta period 1976-1995 [5]

Direction	NE	ENE	E	ESE	SE	SSE	S	SSW
Interval of the **height**	**0.3 -0.9 m**							
The significant heigth (m)	0.65	0.65	0.68	0.52	0.61	0.64	0.62	0.56
Wave period (s)	4.88	5.34	5.71	5.09	5.35	5.47	4.97	4.61
Time (day)	33.41	8.04	20.76	6.82	7.16	2.42	14.55	2.86
Interval of the height				**1,0-1.5 m**				
The significant heigth (m)	1.26	1.24	1.25	1.19	1.19	1.23	1.31	1.29
Wave period (s)	6.00	7.00	7.00	6.55	7.29	7.44	6.56	6.39
Time (day)	29.92	4.89	7.68	3.66	7.41	4.05	11.39	2.41
Interval of the height				**1.6-1.8 m**				
The significant heigth (m)	1.70	1.60	1.70	1.80	1.80	1.80	1.70	1.70
Wave period (s)	7.00	7.00	8.00	7.00	8.00	8.00	7.00	7.00
Time (day)	13.30	2.17	2.82	0.51	2.38	1.75	8.64	0.41
Interval of the height				**1.9-2.2 m**				
The significant heigth (m)	2.09	1.97	2.00	2.00	2.10	2.10	2.13	1.91
Wave period (s)	6.00	7.00	7.00	6.55	7.29	7.44	6.56	6.39
Time (day)	10.42	2.04	2.53	0.26	1.75	2.17	14.83	1.32
Interval of the height				**2.3-2.8 m**				
The significant heigth (m)	2.48	2.51	2.60	2.32	2.50	2.50	2.69	2.42
Wave period (s)	7.88	9.00	9.00	8.00	9.00	9.00	8.96	8.00
Time (day)	4.68	0.68	1.51	0.41	1.22	2.01	7.82	0.62
Interval of the height				**≥ 2.9 m**				
The significant heigth (m)	3.21	3.53	3.97	3.26	3.67	3.89	3.55	3.39
Wave period (s)	8.15	9.54	10.34	9.17	10.51	10.47	9.28	8.60
Time (day)	4.92	0.54	0.50	0.24	1.50	5.39	4.86	0.13
Total of time	**96.95**	**18.36**	**35.80**	**11.90**	**21.42**	**17.79**	**62.09**	**7.75**

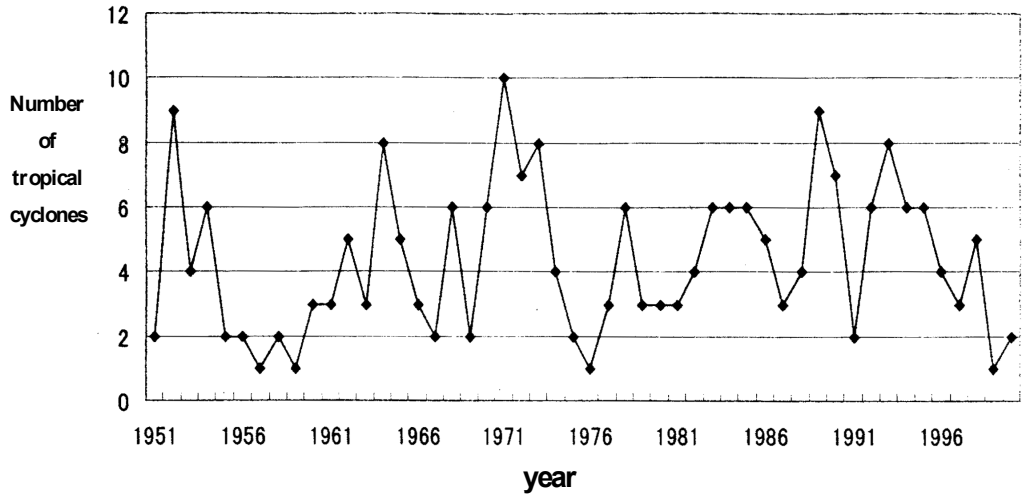

Figure 4. Inter-annual variation of the annual total number of th tropical cyclones approaching Vietnam for the period 1951-2000 [7]

In almost cases, when the relative sea level rises, the steep of the beaches also increases and the wave energy attacked on the beaches will be more intensive, and the coastal erosion is more serious, especially on the beaches made by unconsolidated sediments. This is only appropriate to an emerged coastline that is

almost of the Center of Vietnam (from Thanhhoa to Baria-Vungtau prov.). However, the coastal erosion does not occur on the shorelines where the steep of the beaches is small such as shoreline in Ganhrai bay (Baria-Vungtau Prov. and HCM city). In this case, the shoreline is submerged. This is one of the reasons leading a increased frequency of flooding by high tides in many parts of HCM city in two decades. So that, Kosmynin V.N. et al. [6] have divided into four variances as below:

- A passive submerge of the low elevation coastal zone when the steep of the beach is less than 0.0001 (the shoreline move landward);
- The erosion of the upper part of the coastal area happens when its steep is about 0.001 and forming a modern barrier by the eroded materials.
- The barriers will connect with the coast when its steep is about 0.01;
- The erosion of the beaches forms the cliff when its steep is bigger than 0.01 (case of Bruun effect).

c) Human activities

The human activities, both on river basins (e.g. construction of dams and reservoirs or the basin planning etc.) and the shoreline (s.g. the high concentration of settlements, industries, transport facilities, recreational developments, beach mining for placer deposits or constructional materials, deforestation, reclamation, constructing engineering for coastal protection, etc.) lead on the increased or decreased wave energy attack by means of diminution of sedimentary supply or damage of the nature-coastal protections. For example, after building Hoabinh Dam in 1990, the sedimentary loads of the Red River system is only about 60% comparing with a its former value (at Hanoi hydrological Station); or the beach mining for placer deposits (such as ilmenite) takes place in Quangxuong (Thanhhoa Prov.), Vinhthai (Vinhlinh distr., Quangtri prov.), Thuanan (Phuloc distr., Thuathien-Hue prov.), Hamtan (Binhthuan prov., etc). Both two above cases lead on a deficit of the beach sediments.

On the other hand, mangroves and coral reefs are the good coastal protections. However, at present, both the mangroves and the coral reefs have damaging for an economic development. According to Tran Ngoc Cuong [2], the mangrove area of Vietnam lost 183,724 ha in period 1985-2005 because of damaging for aquiculture.

The coastal erosion of Vietnam is the serious hazard to low coastal land and coastal ecosystems, especially during cyclones. For example, there were about 400 ha (including both cultivated land and housing) lost by erosion in Haihau coast. In addition, some cultivated lands and aquiculture ponds have been buried under sediments moving from the beaches by breaking through the foredunes in the Center of Vietnam. So that, if it would like to keep a coast-agricultural ecosystem as well as the settlements, industries and other eco-social areas, at first, we should be prevented the shoreline from eroding. Besides, the coastal erosion also damaged settlements, cities and industrial and tourism areas. It is possible to list some typical places. They are Thuanan tourism area in 1999; Doson (Haiphong) after cyclone number 2, May, 2005; Haihau (Namdinh) after cyclon number 7, October, 2005; or in the end of 2005, many houses in Hunglong and Duclong (Phanthiet city, Binhthuan Prov.) were damaged by the coastal erosion and 60 houses in Lienhuong (Tuyphong Dist., Binhthuan Prov.) were also damaged in this time.

4. CONCLUSIONS

Based on the above mentions, it is possible to bring out some conclusions as below:

1. The coastal erosion is very seriously occured on the almost of Vietnam and will be increasing in next years. The velocity of the coastal erosion is very different in the spacial and temporal scales. Besides of the erosion, some coastal lowland zones has been submerged by the sea-level rise. Both two above cases lead on loss of the land.
2. The main reason of the coastal erosion of Vietnam is an increase in the wave energy attacking on the beaches and shoreline. There are three most important factors influencing on this increase, including the increase of the Tropical cyclones approaching Vietnam, sea-level rise and human activities. The sea-level rise causes not only increasing of beach steep, but also submerging of the low elevation coastal zone.
3. There are the large area of the coastal low land as well as the coastal ecosystems lossed by erosion. These have limiting an economic development and causing a negative effect on the human psychology.

So, it is necessary to predict the general tendency of the coastal erosion of Vietnam relating to sea-level rise in next years for the strategic planning and management of the coastal zone.

References

1. Bird E., 2000. *Coastal geomorphology: Introduction*. John Wiley & Sons, Chichester, New York, Singapore, Toronto, p. 317.
2. Tran Ngoc Cuong, 2006. Wetland management for sustainable fisheried development in Vietnam. In *"National Workshop Proceedings on Sustainable fisheried development in Vietnam: Issues and approaches"*. Hai Phong, pp.121-127 (in Vietnamese with abstract in English).
3. Fumihiko Imamura and Dang Van To, 1997. Flood and typhoon disasters in Vietnam in the half century since 1950. *Natural hazards,* No 15, Kluwer Academic Publishers, Netherland, pp. 71-87.
4. Haruyama Sh., Le Quoc Doanh, Le Khanh Phon, Vu Van Phai, Hori K., Tanabe S. and Saito Y., 2001. Geomorphology of the Red River Delta and their fluvial process of geomorphologic development, Northern Vietnam. In *"Long climate change and the environment change of the lower Red River Delta"*, Agricul. Publ. House, Hanoi, pp.71-92.
5. Nguyen Manh Hung, Pham Van Ninh, 2005. Present research state of eroding coastline of Haihau beach. In "Marine resources and environment", Scientific and Techniccal Publishing House, Hanoi, pp. 200-211 (in Vietnamese with abstract in English)
6. Kosmynin V. N., Lukianova X. A., Maev E. G., Myslivesh V. I., Nikiforov L. G., 1990. Study on marine morpho-litho-genesis in Department of Geomorphology and Paleogeography of Faculty of Geography, MGU. In "*The exogenous morpho-genesis in different types of natural environment*", Moscow, pp. 8-16 (in Russian).
7. Matsumoto J. and Shoji H., 2003. Seasonal and annual variations of tropical cyclone approaching Vietnam. In "*Environmental change and evaluation of natural environment in the Red River Delta*". University of Tokyo Press, Tokyo, Japan, pp. 7-60.
8. McGranahan G., Balk D. and Anderson B., 2006. Low coastal zone settlements. *Tiempo-Bullentin on climate and development*, No-59, pp. 23-26.
9. Nguyen Thanh Nga (Ed.) et al., 1995. "*Status state and reasons of the coastal erosion of Vietnam. Proposing the scientific solution for protection and exploitation"*. Report of National Program, Code KT-03-14, Hanoi, p.184. (in Vietnamese).
10. Vu Van Phai, 1996. Actual situation of the erosion and accretion on the coast of Vietnam. *Journal of Science, Special Issue on Gegraphy*, VNU, Hanoi, pp. 67-71.
11. Vu Van Phai (Ed.), Dang Van Bao, Nguyen Hieu, 2001. *Mapping Geomorphology of the coastal area (0-30 metre deep) of Vietnam at the scale 1/500,000*. Department of Geology and Minerals of Vietnam, Hanoi, p.116 (in Vietnamese)
12. Vu Van Phai, Nguyen Hoan, Nguyen Hieu, 2002. Geomorphological evolution of the Balat mouth area in the recent period. *Journal of Science*, T.XVIII, No2, VNU, Hanoi, pp. 44-53 (in Vietnamese with abstract in English).
13. Vu Van Phai, Nguyen Hieu, Hoang Thi Van, Nguyen Bieu, Dao Manh Tien, 2004. Some results of geomorphologic study of present coastal area in Vietnam. *Journal of Science*, T.XX, No4AP, VNU, Hanoi, pp. 44-54 (in Vietnamese with abstract in English).
14. Vu Van Phai, Hoang Thi Van, Vu Tuan Anh, 2006. The coastal erosion and environmental management in Vietnam. *Proceedings – the Second Conference on Geography of Vietnam*, Hanoi, pp. 126-134 (in Vietnamese with abstract in English).
15. Vu Van Phai (Ed.), Nguyen Hieu, Vu Tuan Anh, Hoang Thi Van and Nguyen Thi Thu Thuy 2006. *Investigation on geology, minerals, environmental and hazardous geology of the coastal area (0-30 metre deep) of the South of the Center of Vietnam at the scale 1/100,000: Part II-Geomorphology.* Department of Geology and Minerals of Vietnam, Hanoi, p.160 (in Vietnamese)

Assessment on the Effects of Sea-level Rising and River Activity to Changing in the Coastal Zone of the Red River Delta by Using Remote Sensing and GIS

Nguyen Ngoc Thach, Tran Nghi, Nguyen Hieu, Pham Ngoc Hai, Nguyen thi Thu Hien

Centre for applied of RS and GIS, HaNoi University of Science, VietNam National University. Viet Nam, National University, Ha Noi. www.cargis.org. 84-4 85571178, mobile 0913032680.

Abstract

There were 5 cycles in the forming of Quaternary formation corresponding with 5 cycles of regression and 5 cycles of transgression alternatively. At the moment, the present sea level belongs to the 5th transgression cycle that began about 500 to 1000 years ago,belong the end of regression in Late Holocene. In present time, sea level rise in Eastern Sea of Vietnam reaches 2mm/year. Due to the lack of tectonic data during 1978 – 1997, this result was obtained without concerning to tectonic movement. Obviously along coastal zone of Viet Nam, causing for coastal line erosion taking in many places from South to North. Vietnam is a narrow and longitude land, located parallel with the North-South direction with many rivers running perpendicularly to sea. Along central part of Viet Nam, river basins are very short and steep sloping.

During rainy season, river current with very high volume and solid matter concentration runs to sea through the river mouths. Each year, there are about from 6 to 10 storms. Tidal regime is various along shoreline from regions to region. Therefore, effecting between inland water and sea water at river mouth area is very complicated during the year. At some portion, race of erosion range from 10-80 meters per year and sedimentation phenomena also different with this speed at other portions. This situation is a great problem for environmental protection and suitable development in the Red river delta costal zone.

To determine speed and scale of coastal change at each main portion of coastal line, Remote sensing and Geographical Information system have been applied for creating map and getting of statistic information about erosion, sedimentation and related information as mangrove and land use change.

Coastal zone of Red river basin is a typical case studied aspect for the above situation. During developed process since Oligocene, coastal line of the delta have been many change and developed in to sea direction, formed many old sand dunes locating parallel with existing coastal line direction.

By using GIS data from 1926 and RS data of Landsat and Spot from 1975 up to present, stages of coastal change can be clearly determined and mapped. Reasons to change of the Red River delta coastal line depending to the general condition of sea-level rise but also due to new tectonic movement locally at each major portion. This report presents methodology and results from the study and also proposes suggestions for coastal line protection and suitable development.

1. HISTORY AND TENDENCY OF THE SEA LEVEL RISE IN THE WORLD AND IN VIET NAM

1.1. Sea level change in the world

Sea level fluctuation is affected strongly by changing of climate which is controlled by the earth's orbit, slant of the earth's axis and oscillation of the earth's axis (Milankovitch). The earth was developed by geological events that sketched in long time ago but it was controlled mainly by climate change. Since Cambrian (542 million years BP) to present, the earth experienced two biggest glaciations that were in 250 millions and 200.000 to 125.000 BP. The sea level were higher than present (+30->+400m), especially in Ordovic – Silur period and Carbon, Kreta period (Fig.1A). In 1962, Fairbridge divided period of sea level rise into 4 parts since 400.000 BP to present (Fig.1B).

Since 100.000BP to present, in general, sea level was low because of Wurm glaciations but in earlier time it was still higher (+25->+30m) and in late of this period, firstly sea level reached +10m after that felt down to +2m->+5m (Fig. 1C).

- From 24.000 BP to now, the sea level had raised rapidly. The highest point occurred in the period between 6.000 to 7.000BP.
- In 1880 to 2000, sea level raised regularly from -1mm in 1890 to -20mm in 2000.

Generally, in long term as geological time, sea level fluctuated up and down by changing of each period, but in short term as recent times, it is still raising regularly. In Quaternary period there were 4 glacial periods namely Wurm, Riss, Mindel and Gunz between them occurred 3 interglacial periods (Gunz - Mindel, Mindel - Riss, Riss - Wurm)-fig, 1 B.

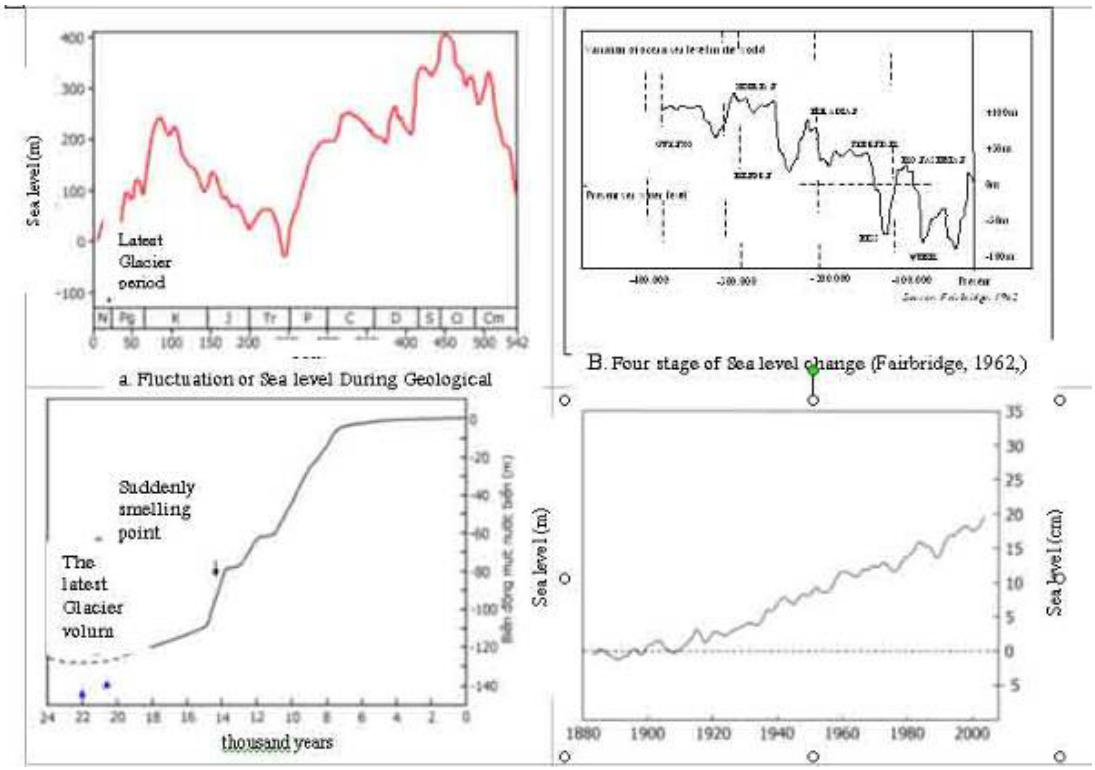

Fig 1. History of global sea level change by timing (*www.globalwarmingart.com*)

1.2. Sea level change in Vietnam

Vietnam is situated in Indochina peninsular and possessed over 3000km coastline that strength from the North to the South. In Quaternary, this area was affected strongly by sea level activities. The sea level change has occurred in 5 cycles during Quaternary with 5 alternative phases of regression transgression (Tran Nghi, 1990s).

In late Pleistocene, the latest glacier occurred synonymous with sea level was lower (about - 110m), this phenomenon was caused by lowering the ocean bottom (absolute drawdown). However, the climate change during this time has caused the glacial and interglacial periods.

The last transgression after Wurm glacier started from 17.000 - 18.000 years ago. At the beginning, the rate of the transgression was rather fast. From 6000 - 7000 years BP, the sea level has rather slower increased. Finally, the sea level has reached maximum transgression for 6000 years BP.

According to the measured data at Hon Dau station and analysis available data collected in past 30 years, the rate of sea level Eastern Sea of Vietnam reached to approximately 2mm/year and in Red River and MeKong river delta is nearly 2-3mm/year (fig 5). This data is corresponding to the average data of the world's sea level change.

Basing on analysis available data collected for the past 30 years, the average rate of sea level rise in two bigger deltas (Red River and Mekong River) is about 2 - 3mm/year. It is corresponding to the mean world's sea level change (fig 2).

1.3. Effecting of Sea level change in the Red River coastal zone

1.3.1. Shore line erosion

The study on erosion along the coastal line has showed the shoreline erosion has taken place in almost areas along the coast, although with different rate and intensity. Intensive erosion took place along the coast of Red River delta and MeKong River delta in the south. The most stable shore lines are Mong Cai - Hon Gai, from Hai Phong to Thanh Hoa of the Red river costal line in the northern part.

Results of studies shown that at present time, more than 240 areas along the coastline of Vietnam are under erosion. The erosion is taking place in almost different types of shorelines structure such as rocky

shoreline, shoreline compressed of gravel, sand, silt and clay... However, intensive erosion has taken place in shoreline area composed of sandy materials. In these areas, the erosion is still going on after the prevention measures have been implemented (such as dyke, masonry, plantation...)

The erosion coast of more than 1km in length hold 50% the total areas (>120 areas), while in 20% of the total area (50 areas) the shoreline has moved towards the mainland more than 500m (Fig3,4).

In term of erosion rate, the erosion of shoreline can be divided into following groups slowly (<5m/year) and very intensive (>30m/year). Thus, in 1992 along the coast, there were 78 locations (≈32%), where the erosion took place with the intensive and very intensive rate. The recent study of the Hai Phong Institute of Oceanography showed that in the Northern part of Vietnam (from Mong Cai to Hau Loc – Thanh Hoa Province). Length of the erosion coast reaches 114km with average rate 6.0m/year in 51 locations (Table 1).

In general**,** race of erosion is mainly related to sea current changing and sea level rising but in some position such as estuary region of Hai Phong, rising of sea level is still related to new tectonic activity with rise down race about 1mm per year in average.

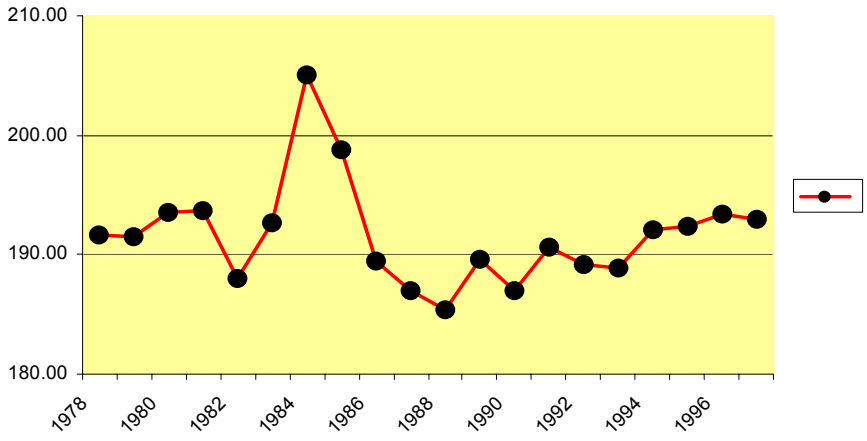

Fig 2. The principal component of sea level variation at Hon Dau station

Table 1. Number of Eroded locations, their length and average rate (Racing 1990 - 2000)

No	Area/Location	Length of erosion (m)	Rate of erosion (m/year)	Number of Eroded Location
I.	Mong Cai - Cua Luc			
	Sub Total	44565	3.1	
1.	Tien Toi	4000	5.3	30
2.	Quang Phong	2200	7.0	
3.	Thon Dong (NW)	1380	8.0	
II.	Cua Luc - Do Son			
	Sub total	43920	4.4	
1	Dinh Vu	3000	8.6	15
2	South Cat Hai	6400	12.9	
2	Phu Long	3300	9.6	
III.	Do Son - Ba Lat			
	Sub total	2700	9.1	
1.	Thuy Xuan	1800	10	3
2.	Dong Long	400	10	
IV.	Ba Lat - Lach Truong			
	Sub total	22.750	14.3	
1.	Hai Hau	17.200	14.5	
2.	Nghia Phuc	550	11.8	3
3.	Hau Loc	5000	13.9	
Total		113.930	6.0	51

Fig . Coastal line erosion and **SPOT-4 image** of the Cat Hai island (Hai Phong Province)

Fig 3. Picture of Coastal line errosion at Ba Lat area

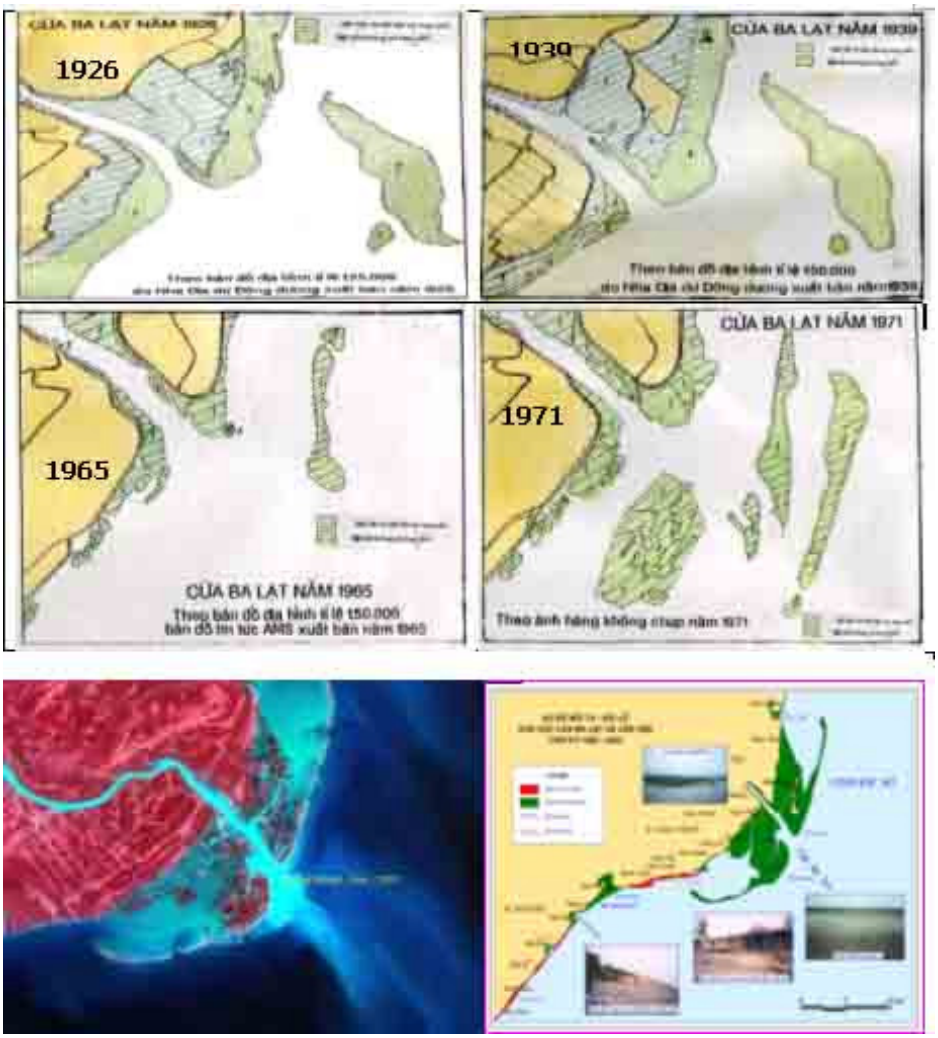

Fig.4. Typical picture of coastal erosion at the Thai Binh-Centre part of the Red river coastal

7.3. Coastal zone change at Quang Ninh area:

- Shore line change: At the Quang Ninh coastal zone, comparing of three shore lines of 1965, 1989 and 2003, some major characteristics were forseen as follow (fig5):
  - In general, these coastal lines are similar at the hard rock area (limestone)
  - In some place, shore line changed with high speed due to artificial activities such as: expanding area for tourist activities, urbanization, aquaculture, seaport and industrial construction

Fig 5. Shore line change at the Ha Long bay area

7.2. Sea floor change:

Changing is very complicated with various conditions in front of Cua Luc-Bai Chay. Due to erosion from inland and the process of expanding the HaLong city to the sea direction, sedimentation deposited with high speed from 30-35 up to 40-50mm/year. At the Bai Tu Long, sedimentation deposits with low speed of 2-4mm/year. Eroded sea floor has been occurred at the area between Ha Long and Cat Ba Island with high speed from 6-8mm up to 18-20mm/ year. Generally, sea floor of the Ha Long Bay area is rising with speed ~1,1mm/ year in average due to the main reason is artificial activities (fig 7).

Main reasons for changing are artificial activities such as: fill up tidal flats for urbanization, wash material erosion by coal exploitation and effecting of high speed tidal current (fig 6).

Fig 6. Coal mining and urbanization and tourist activities at the Ha Long coastal zone area

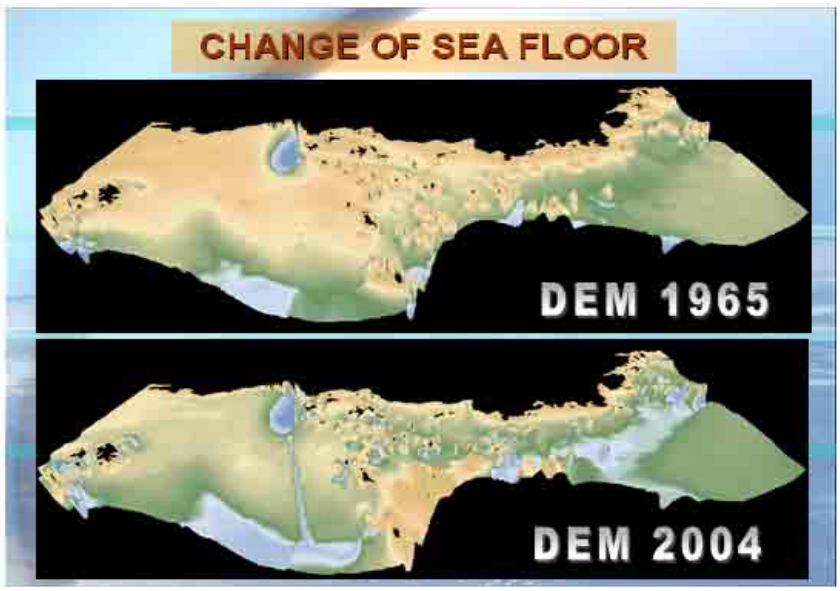

Fig 7. Sea floor deep between two dates 1965-2004

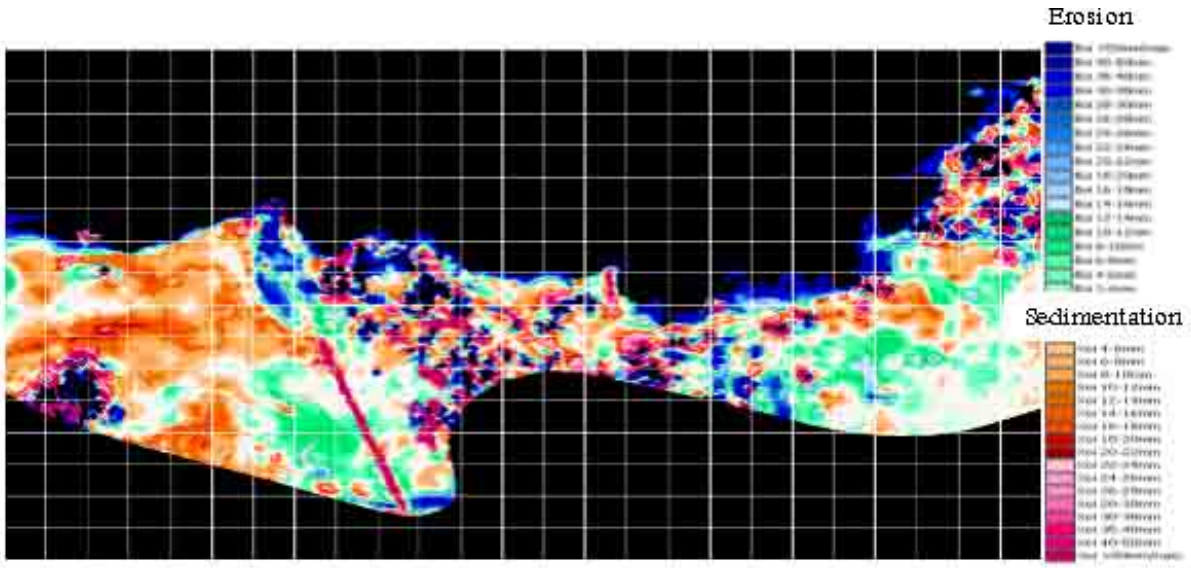

Fig 8. Sea floor change at Ha Long bay area

1.3.2. Salinity intrusion

Integrating Geophysic and Remote sensing methods, results shown that salinity is strongly happened along coastal zone of Red river delta, perpendicular to shore line with direction from sea to inland. Boundary of saline 0.5 % is differenced during two seasons (dry and wet). In some places, the saline direction is increasing along fault direction (Fig. 9) or turning by river bank.

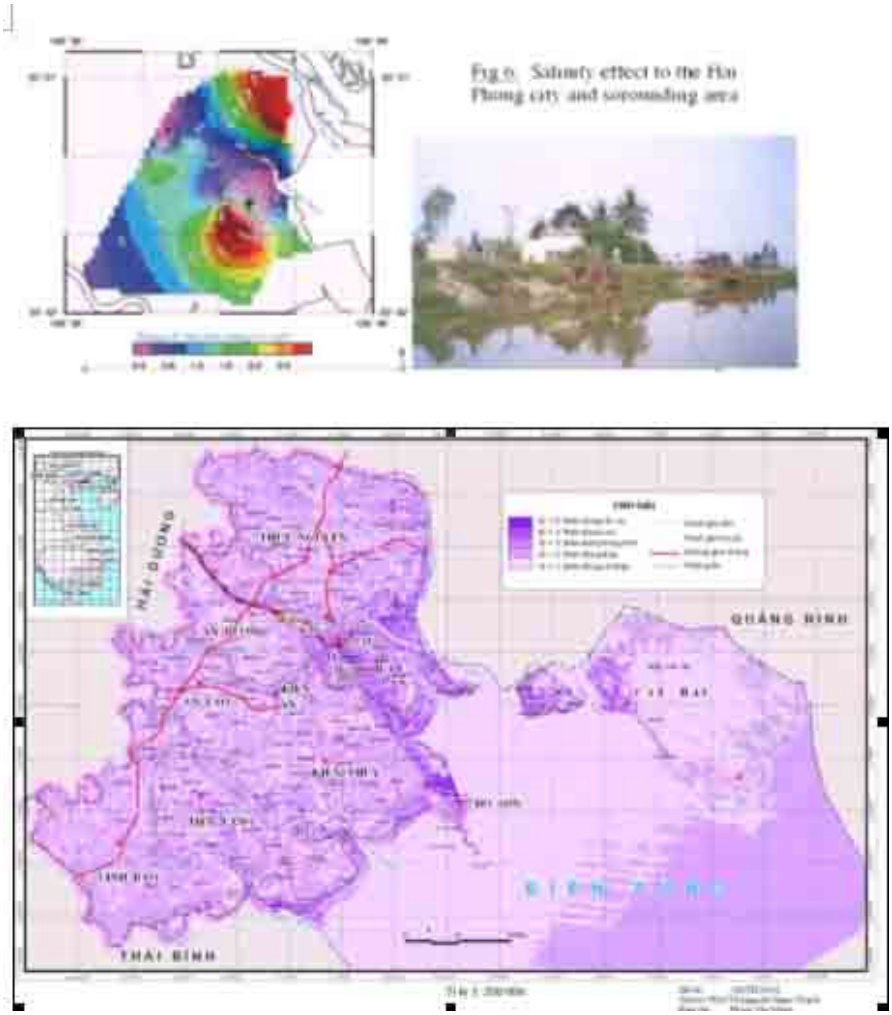

Fig.9. Salinity map in dry season extracted from Landsat image

1.3.3. Expecting for future impact of sea level rise in Vietnam

Basing on the study results of IPCC during 1990 - 1992, the fluctuation of sea level will be increased from 3 – 10 times in comparison with present value.

According to the IPCC Scenario, the sea level rise in the world was happened as follows:

Basing on the CSIRO's scenario (1992), the tendency of sea level rise in the next decades of the South East Asian region as follows:

Tab 2. Forecast sea level rise for Southeast Asia

Year	Amount of Sea Level Rise (ΔH)		
	Low case	Medium case	High case
2010	3	9	15
2070	15	45	90

According to EPA (10/1995), the sea level in all over the world will reaches approximate 15cm in 2030 and 34cm in 2100 but with 10% probability it will increase 30cm in 2050 and 70cm in 2100.

In Viet Nam: The proposed rates of sea level rise according to CSIRO's (1992) as well as IPCC's (1990, 1992) scenario are as follow:

Tab 3. Rate of sea level rise in Southeast Asian by the year of 2100

Sea level in 1990		Amount of sea level rise (cm)					
		2000	2010	2030	2050	2070	2100
The same rate as past period	Ho (Average value)	2-3	4-6	8-12	12-18	16-24	22-33
High rate according to CSIRO' scenario	Ho (High value)	6-9	12-18	24-36	36-54	48-72	66-99

Note: The figure must be calibrated with geo - dynamic condition and the rate of water withdrawn in a big city.

In the coastal zone of Viet Nam, the expected rate of sea level rise will be 30cm/year (low case) and about 100cm (high use) in the year of 2100. However, the process of sea level rise will be gradually taken place with average rate of 6 - 10 cm per decade.

2. SEA LEVEL RISE AND RELATED GEOHARZARDS

2.1. Determination of Flooding Area

According to the CSIRO's scenario, by the year to 2100, the flooding area in the Red river delta will reach 330000 ha comprising about 172000 ha of rice field; 30000 ha of residential area; 19000 of salt production field and 97000 ha of land of other use. The percentage of flooded area per total area of some provinces in coastal zone of Northern part of Vietnam is shown in table 5. By simulation, total submerged area of the Red River Delta is approximately 3184.14 km^2 (21.57% of total the Red River delta area).

Tab 4. Amount of flooding area in the year of 2100 (1m height of sea level rise in the Red River Delta (Nguyen Ngoc Thuy, 1995)

No	Province	Amount of flooded Area	
		Area (km^2)	% of total area
1	Hai Phong	581,67	3,86
2	Thai Binh	1602,26	10,72
3	Nam Ha	823,21	5,39
4	Thanh Hoa	177,81	1,60

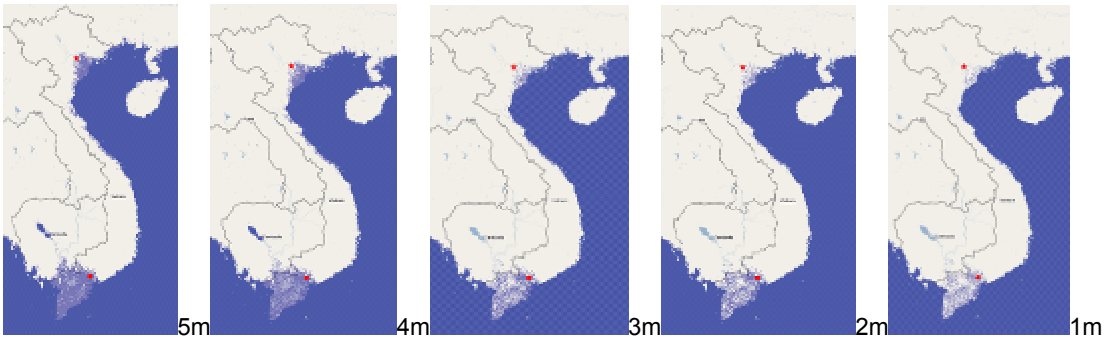

Fig 10. Influences of sea level rise on coast line and Red River delta, MeKong river delta in Vietnam by height of water (Dam Q.M, Hung D.N, 2007)

2.2. Disappearance of beaches

Increasing in sea level would result in more severe wave erosion of dunes and beaches. As results from offshore sediment transportation, flatter offshore beach profile has been created. Finally, this result would be a diminishment of local beach environments as sand sediments are transported offshore beyond the depth at which they participate in seasonal onshore - offshore sediment cycles (fig 11)

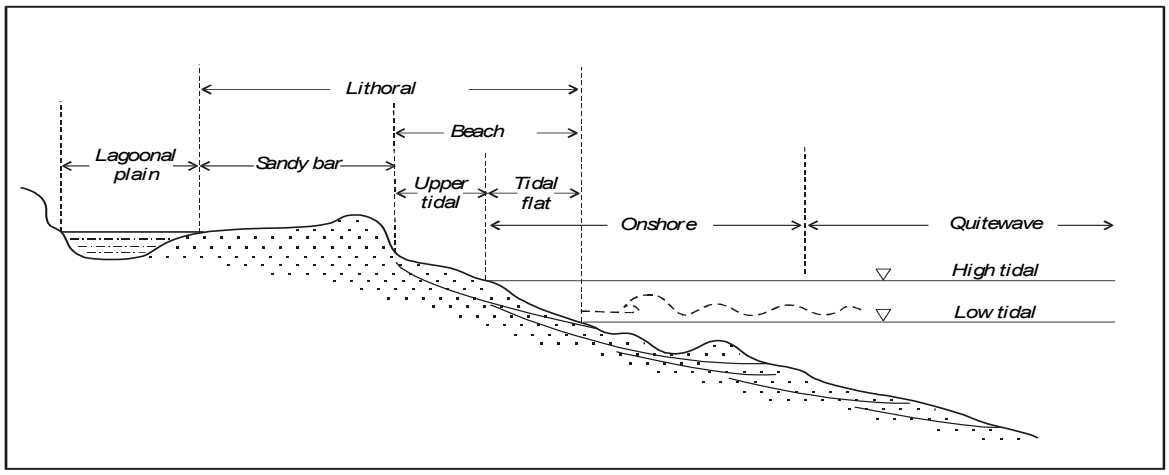

Fig 11. Sedimentary Section of Shoreline

Based on the high scenario (1m sea level rise), almost beaches along the coast such as: Bai Chay, Do Son, Sam Son will be submerged in sea water.

2.3. Salt – water intrusion

The boundary between fresh and brackish water in aquifers will have major adverse impact on coastal population centers, which often rely on groundwater for drinking water. Secondly, a salt water wedge of bottom marine water will intrude a greater distance upstream in estuaries. The end result will be an inland intrusion of marine or brackish water zone. On the effect of salt water intrusion in 1m sea level rise, the following city, town and region will bear server affect: Hai Phong city, Diem Dien port, Thai Thuy, Tien Hai towns, Con market (Nam Dinh province), etc. (Fig 12)

The salt intrusion in the Central VietNam has made difficulty for drinking production in Hai Phong, Quang Ninh.

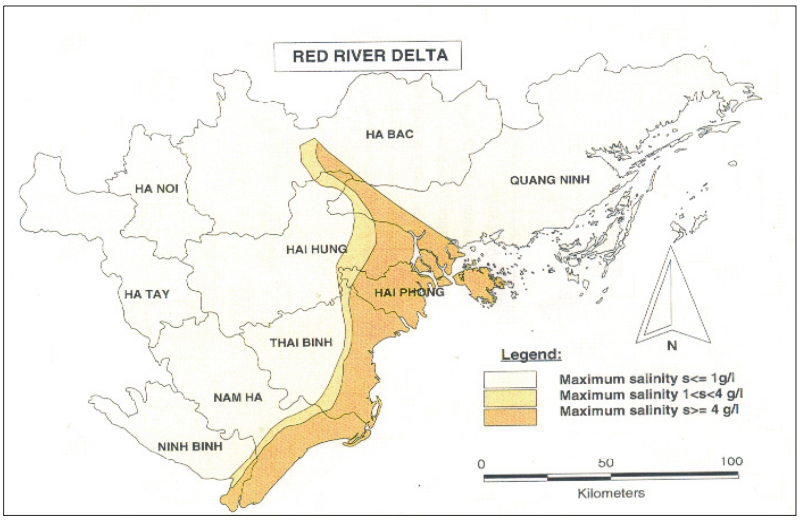

Fig 12. Schema of salinity in coastal zone of Red River Delta (Vietnam VA study, 1996)

2.3. Expecting the impact of sea level rise in Vietnam

With 1 m sea level rise without no protective measure the following impact will be taken place:

a. The impact is not limited to a narrow coastal zone, but will be more serious further in land.
b. About 40.000 km^2 will be flooding annually.
c. About 1700 km^2 (60% total coastal wetlands) will be affected and threatened by sea level rise, especially Minh Hai and Vung Tau - Ho Chi Minh city as well as Xuan Thuy mangrove area because of sea dyke and shrimp ponds ...
e. Additional pumping station and dyke raising will cost at least 2,4 billion USD.
f. About 17 billion of capital value will be lost by the annual flooding (comprising 80% of year GDP)

In short, people habitats and capital investment in the low-lying area in Vietnam are presently at high risk. The impacts of sea level rise will make more pressing situation. Appropriate measures need national and international co-operation.

CONCLUSION & RECOMMENDATION

a. Main characteristic of sea level change in Viet Nam generally and especially in the Red river coastal zone

1. The sea level rise in Vietnam has tendency to increase with average rate of 2 mm/year.
2. Sea level rise makes completely influence to coastal zone causing change shore line (erosion, accretion), filling river channel salinization etc ...
3. Erosion and accretion along the sea coast of Vietnam have strongly occurred in different types of geological formation as the result of sea-land or river-sea interaction. The high accretion has occurred in two main deltas: Red river delta and Mekong river delta. Sustainable development on land use and mangrove must be paid in the first priority attention. Erosion has been occurred along coast line, but the strongest erosion has taken place in Bach Dang estuary, Hai Hau shore line (in the North), Central Vietnam,; Ho Tau, Rach Goc (in the South)..
4. Erosion has seriously caused problems such as destroying civil construction and infrastructure,losses due to increased beach and foreshore erosion, salinization increasing particularly in Bach Dang estuary.

b. Proposed integrated coastal zone management

Integrated coastal zone management (ICZM) will help to resolve coastal development issues such as habitat loss, quality of terrestrial and aquatic coastal ecosystem, hydrological changes, responses or adaptation to sea level rise and other effect of global change.

c. Implementation of ICZM

1) Legal and organization implementation:

There are some needs in legal and organizations implementation like applying legislation governing specially activity and development in coastal zone, or better understanding coastal and coordination of effects and increasing low degree consensus and solution of lower authority level.

2) Increasing the capital spent on coastal zone defenses in order to improve safely level in coastal zone for people and infrastructure and industrialization.

3) Improve and built new pumping station and sea dyke protection. Beside of this, we develop social activities in the following activities such as development of mangrove forest, aquaculture (braking shrimp growing), growing sedge met plantation for reducing salinization.

4). Proposed measures for prevention of hazard in certain areas as in plantation in sand dune area along coast line, or prohibit sand exploitation in sand beach or strengthening sea dyke system by concrete reinforcement (minimum wide: 8 m, depth of foundation: 10 m and slope 1:1 towards sea; flooded and salinized area subjected to be changed for aquaculture development; areas which is richer in heavy metals (ilmenite placer) must be exploited before erosion occurring.

5) Training in required to improve knowledge of coastal zone processes and coastal zone protection methods. In fact, the high level of organizational ability, awareness and motivation among coastal authority and specialist presents authority for good implementation.

References

1. Dinh Van Huy & Tran Duc Thanh, 1994. Coastline development in Hai Phong - Quang Yen region in Holocene through studying old sand bars. Jour Natural Resources and Sea Environment, Vol. 2, pp. 61 - 65. HaNoi.
2. Dinh Van Thuan et al, 1996. Problem on the World's ocean water level fluctuation and transgression and regression in Quaternary in VietNam. Geology and Natural Resources. Institute of Geology. Vol. 2, pp. 269 - 273. Ha Noi
3. Do Van Thu, 1985. Late Pleistocene transgression in BacBo plain. New Discovery in Archeology in 1985, pp. 17 - 18. HaNoi.
4. Ha Quang Hai, 1996. Characteristics of Quaternary stratigraphy and Geomorphology of Eastern part of South VietNam. Ph.D. Thesis. HaNoi.
5. Hoang Dinh Minh & Dang Van Bat, 1989. Teh sea terraces in VietNam. International seminar on Quaternary Geology and Human survival. Abstr. p. 46. HaNoi.
6. Dam Quang Minh, Dinh Nho Hung, 2007. Impact of sea level raise to Vietnam.
7. Hoang Ngoc Ky, 1991. Correlation of marine transgression and regression during Quaternary period in VietNam territory. 2nd Conf. of Geol., Indochina, Procc. Vol. I, pp. 97 - 102. HaNoi
8. Le Duc An, 1980. Is the Holocene transgression transformed suddenly? Jour. of Geological Mapping, No. 47, pp.69 - 71. HaNoi
9. Tran Nghi, Ngo Quang Toan. Characteristics of Sedimentary cycle's Quaternary geological evolution of VietNam. International seminar on Quaternary Geology and human survival, 7 - 13 Octorber 1989, Ha Noi.
10. TranNghi & Nguyen Bieu, 1995. Some thought in the correlation of Quaternary Geology of mainland and continental parts of Viet Nam. Procc. of Research works on Sea Geology - Geographics, pp.86 - 98. Ha Noi.
11. The impact of El NiNo and La NiNa on Southeast Asian. Workshop report, 2000. HaNoi
12. Consequences of Sea Level Change during the Holocene in the Pacific Basin. Jour of coastal research, Vol 14. No. 1. 1998
13. Patrick D. Nunn. Sea level changes over the past 1000 years in the Pacific. Vol 14. No. 1. 1998.
14. Ying Wang. Sea level changes, human impacts and coastal responses in China. Vol 14. No. 1. 1998
15. Final report of Vietnam Coastal Zone Vulnerability Assessment, 1996. Ministry of Foreign Affaire of Government of the Netherlands.

The Changes of Coastline During the Period 1934 to 2006 in Kulonprogo District, Yogyakarta, Indonesia

Junun Sartohadi, Rino Cahyadi Srijaya Giyanto, Wirastuti Widyadmanti, Suratman Woro Suprodjo

Faculty of Geography, Gadjah Mada University, Indonesia

Abstract

The objectives of this research are: to study the coastline changes from 1934 to 2006 based on map reading and field topographic measurement, and to evaluate the geomorphological processes in the coastal area as a consequence of the environmental changes both in up-land and low-land in the study area and nearby.

This research is carried out based on map measurement. The old topographic map made by the Royal Topographic Survey of the Netherlands, is registered on the new topographic map made by the Indonesian Surveying and Mapping Bureau (BAKOSURTANAL), to identify the coastline change from 1934 to 1992. The coastline change from 1992 to 2006 is derived from field topographic measurement using RTK-GPS (Real Time Kinematics Global Positioning Systems) and topographic map.

The results of the study show that the coastline in Kulonprogo District has been shifted toward inland. It is predicted happened as results of the complex interaction of several environmental factors, such as the decrease of material support from Merapi Volcano, sand material removal in the study area caused by human activities, and coastal erosion.

Keywords: Coastline Changes, Geomorphological Processes, Coastal Erosion

INTRODUCTION

Indonesia is very prominent as an archipelagic country which has more than 81,000 km shoreline and about 17,000 islands. Among those islands, there are 5 big islands inhabited by Indonesian people, i.e. Kalimantan, Sulawesi, Irian, Sumatra, and Java. Especially Java Island has the highest population, which more than 60% of the total population in this country. Most of the big city in Java is located in the coastal area, such as Jakarta, Surabaya, Semarang, Jepara, and Rembang.

Coastal area of Java Island can be divided into two areas, those are north coast and south coast. Those areas have some distinctions, concerning to physical characteristics, potency of resources and ecosystem, and also the environmental pressure and human activities.

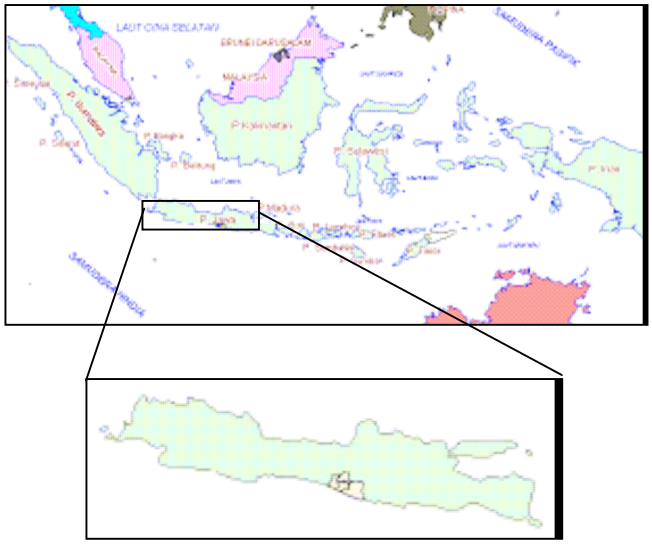

Figure 1. Java Island

The coastal areas have potential values to be developed to improve the regional development process. However, there are various problems happened in coastal area generally, which were landuse changes, seawater intrusion, coastal abrasion and accretion which bothering the human activities in coastal area.

South Java coastal area formerly was mountain block that faulted and sank below sea level. This is one of the long processes of Java first geo-anticlines that happen in Miocene, 6 million years BC (Bemmelen, 1949). Geo-anticlines was formed by tectonic activities and resulting North Serayu Mountain in Central Java. 2 million years after first geo-anticlines, the second process resulting South Serayu Mountain. This process had been working until period of third geo-anticlines which was started in the end of Pliocene and in the beginning of Pleistocene.

Entering the quarter geological time, volcanic activities increased and erupted continuously. As the result, quaternary alluvium sediment was transported and piled up this region. Fertile land was formed and by the time, many people come and build up the area of Yogyakarta.

II. SEDIMENTATION PHASE

Sedimentation phase has close relationship with geomorphological processes, because all the materials in the coastal area originally come from upland area, which were volcanic origin: Merapi and Sumbing Vol-

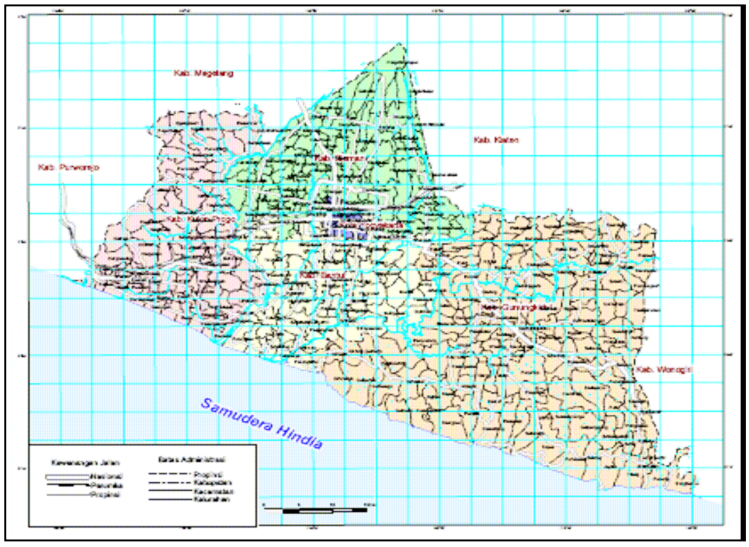

Figure 2. Special Province of Yogyakarta, Indonesia

Topographic Map of Kulonprogo 1934
(Royal Topographic Survey of Netherlands)

Topographic Map of Kulonprogo 1992
(Bakosurtanal Indonesia)

Figure 3. Comparison between Topographic Map 1934 and 1992

Figure 4. Image Wrapping Method

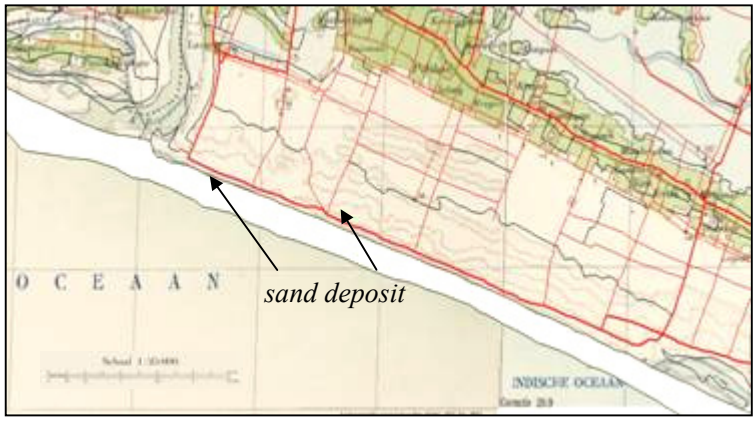

Figure 5. Sand Deposit 1934-1992

cano. The Royal Topographic Survey of Netherlands have made Topographic Map year of 1934, which is used as a base map to identify the process in the Kulonprogo coastal area.

Image wrapping method applied to rectify the topographic map year of 1934 (Royal Topographic Survey of Netherlands) with the Topographic map year of 1992 (Bakosurtanal Indonesia).

Comparing to Topographic Map from Indonesian Surveying and Mapping Bureau (BAKOSURTANAL) year of 1992, the coastline is shifted outward inland, and the landuse pattern moved regularly to the coastline.

Along the coastline of Kulonprogo of 22.04 kilometers length, there is approximately 200 – 300 meters deposit outward inland. If these sand materials have 3 meters height, it means that more than 12 millions cubic meters of sand sediment deposited in the coastline of Kulonprogo District, and complexity geomorphological processes caused this phenomenon.

The geomorphological processes in Kulonprogo coastal area are being done by fluvial, aeolian, and marine origin, such as river deposition, coastal erosion, and windblown deposition. Coastal sedimentation processes is caused by wind and sea waves (Trihatmojo, 2000). Winds generate sea waves and it shift along the shoreline transporting the sediment. The windblown has generated very specific landform in this area; it

Figure 6. IKONOS Image of Kulonprogo Coastal Area (left) and Sandunes in Kulonprogo (right)

forms sand-dunes in the coastal area. As the result, this coastal area is delineated into 3 parts: old, mature and young beach ridges, and between this beach ridges there are swales.

The swale sometimes filled up by water and generates swamp or lagoon if there is a marine process. The old beach ridge has gentle slope with some undulating dunes. The mature one has almost flat slope and some part consist of big sandunes. The young one has marine origin as dominant process very active sedimentation and erosion processes shifting each others. Lithological composition of young beach ridge consist of sand, whereas old beach ridge is sand combined with gravel and clay. In 3 meters depth founded sand beach deposition, and lagoon deposit in 3-3.6 meters depth.

III. INTERPRETATION RESULT

By the time, the development is increasing rapidly, and the human activities expand widely. During period 1934 to 1992, the coastline shifted outward inland, Data from Directorate of Jogjakarta Public Works showed that transportation materials from Merapi and Kulonprogo hilly areas to the coastline, were transported by the river roughly 220.000 mP^{3P}/years before year 1992, with grain size 0.2 – 0.4 mm and the erosion rate 0.5 mm/year.

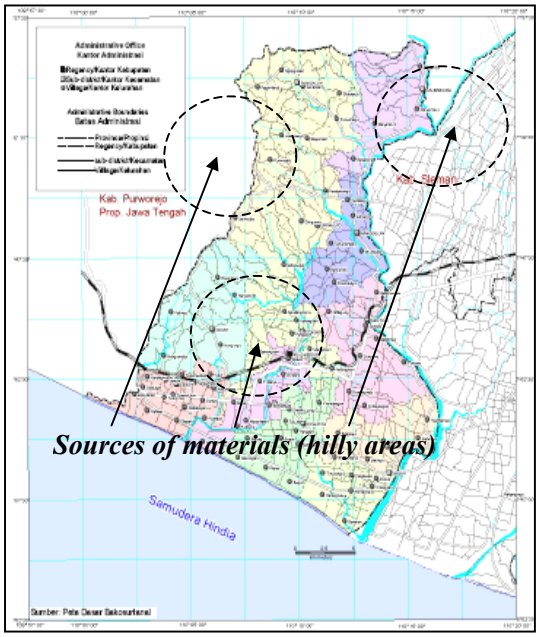

Figure 7. Zone of Erosion in the Hilly Areas of Kulonprogo

Using CERC (1982) formula explained by Yuwono (1999) as showed below, sand deposit transported along the coastline by long shore current.

$$Q = p.0{,}79.10P^{6P}.HP^{2P}.Co.(KB_{rbrB})P^{2P}.Sin(\alpha B_{brB}).Cos(\alpha B_{brB})$$

where :

Q = sediment transport (mP^{3P}/year)
P = longshore current probability (%)
H = significant waves height (m)
Co = waves velocity in deep sea (m/det)
Krbr = refraction coefficient in breaker zone
αB_{brB} = waves angle against coastline in breaker zone

From the formula, it is calculated that QB_{westB} direction 480.000 mP^{3P}/year and QB_{eastB} direction 405.000 mP^{3P}/year, so QB_{nettB} 75.000 mP^{3P}/year to the west direction. The sediment transport in the coastline was getting thicker to the western part of the river mouth. This process happen while the east monsoon moved to the west on May till October, thus in this period the sand material have maximum deposited in the coastline because the river discharge situated in the lowest level.

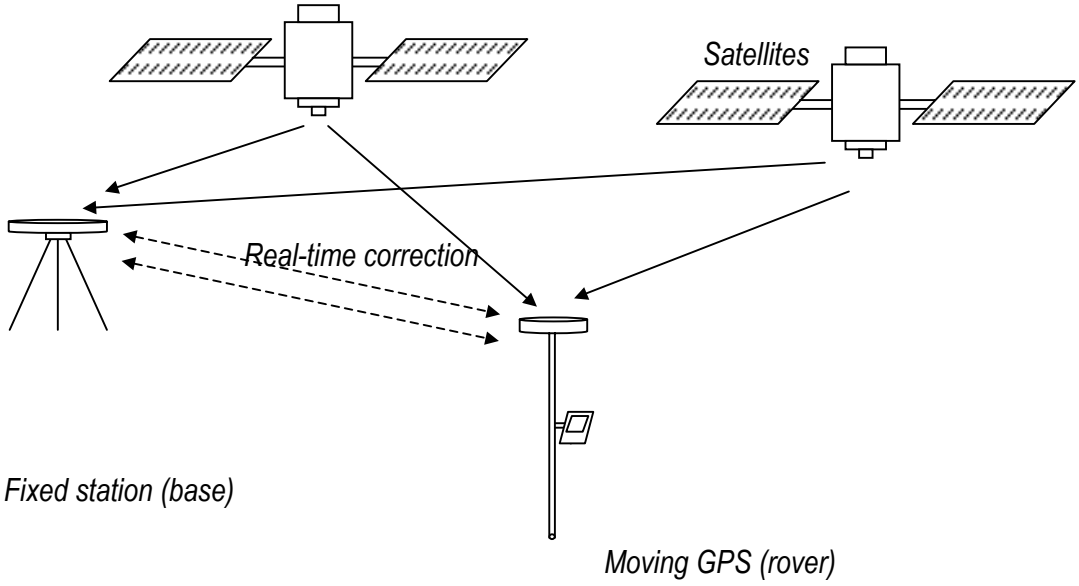

Figure 8. DGPS with Real-Time Kinematics System

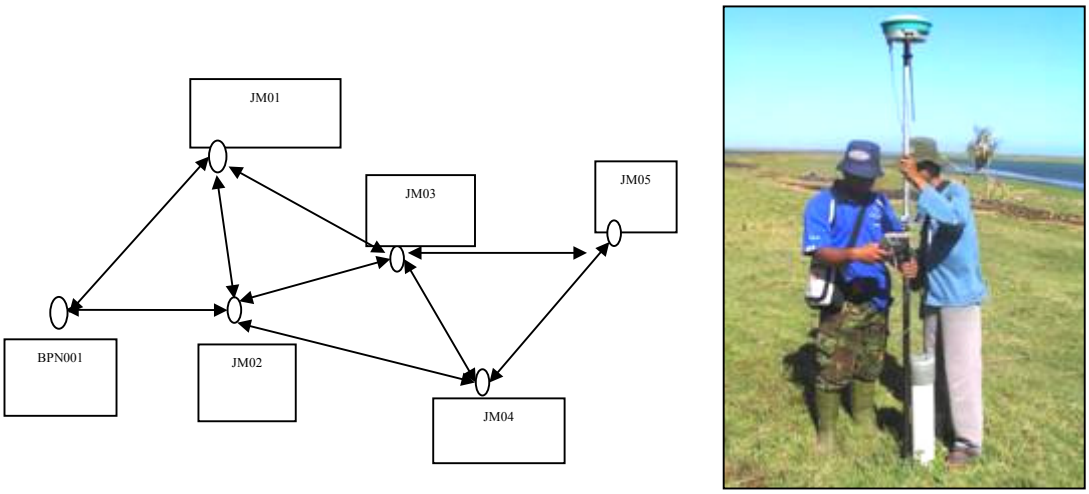

Figure 9. Base point sketch (left) and Point Measurements using Rover-GPS (right)

IV. FIELDWORK MEASUREMENT

Fieldwork measurement was done on May till July 2006 in order to study the coastline changes using Differential Global Positioning System (DGPS), one of the recent technologies to measure the land topography in accurate value, 1cm error for X and Y coordinate, and 10cm errors for Z coordinate. The system that used in this research was Real-Time Kinematics (RTK), with 1 DGPS as a Base Station and 1 DGPS as a rover. This research took 6 base points as fixed station (geodetic control point) and corrected with close polygon calculation to reduce the RMS errors.

From the figure above, the sand deposit by topographic map year of 1992 were eroded by sea waves. Considering the tidal data from Hydro-Oceanography Department of the Indonesian Navy, the waves around Indonesia raise continuously time by time. Furthermore, the sedimentation rates decrease rapidly because the sediment transport by the river getting lower.

Sediment transport decreased because the government implemented Check-Dam at many rivers from Merapi and at Kulonprogo hilly areas to reduce the discharge velocity considering flood hazard. Land degradation in the upland caused river discharge getting higher in the rainy season as almost precipitation become surface flows and some times made Flood disaster, e.g. flash flood and inundation. More than 15 dam build-up and help the sand materials from Merapi and Kulonprogo hilly areas only transport in small scale, as they are hold up by the dams.

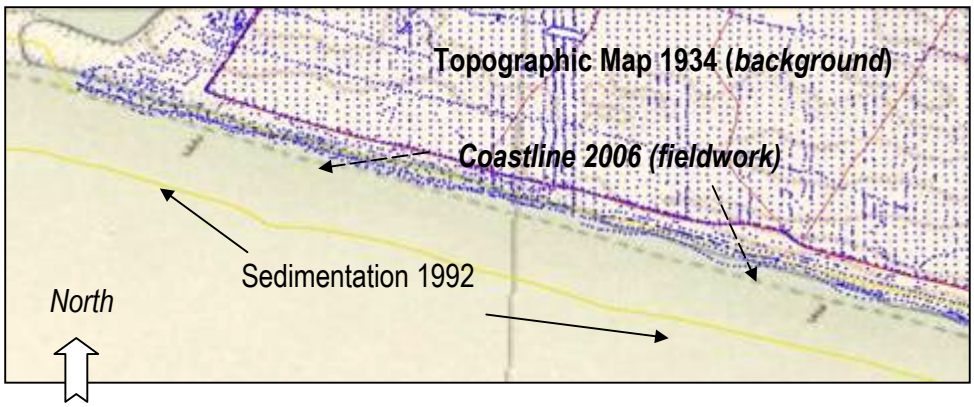

Figure 10. Comparison between Sand Sediment 1992 and Field Measurements (2006)

Figure 11. Embankment in Coastal Area (left) and Trash in coast (right)

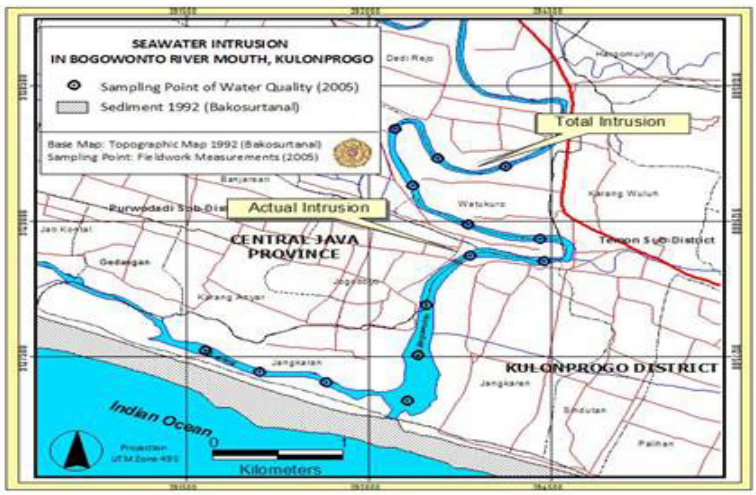

Figure 12. Seawater Intrusion into Bogowonto River, Kulonprogo District (Giyanto, 2005)

Furthermore, sand mining in these rivers increasing rapidly. Legal and illegal miners exploit the materials along the river. As the consequences, original material from the volcano decreased. These processes rearrange the ecosystem stability. The sea waves of the Indian Ocean becoming unbreakable and now, the coastline was shifted toward inland, in many places the coast eroded by the waves.

Embankment is also applied by the local government to reduce the abrasion rate; however abrasion level is still high. Another impact is trash from river sediment transported along the coastal area, which is contaminating the beach. It is causing tourism object area become uncomfortable and polluted. Moreover, the impact of sea water level increase is sea water intrusion into river and coastal area. Giyanto (2005) explained about seawater intrusion as negative effects following the coastal erosion. Seawater intrusion made fresh water of river body and aquifer changed into brackish water; it can not be consumed again.

Mathematical Equation of Research Variables

Relationship between EC with Cl⁻ contents $y = 29{,}202\,x + 258{,}76$ y = electric conductivity (µs/cm); x = Cl⁻ contents (ppm)	**Relationship between Sea wave's velocities with Intrusion Lengths** $y = -2{,}648\,x + 4{,}73$ y = sea wave's velocity (m/sec); x = seawater intrusion from river mouth (km)
Relationship between Tidal with Intrusion Lenghts $y = 0{,}9847\,x - 0{,}7409$ y = tidal height (m); x = seawater intrusion from river mouth (km)	**Relationship between River Discharge Velocity with Intrusion Lengths** $y = 0{,}4869\,x - 4{,}2247$ y = river discharge velocity (m/sec); x = seawater intrusion from river mouth (km)

Figure 13. Mathematical Equation of Research Variables (Giyanto, 2005)

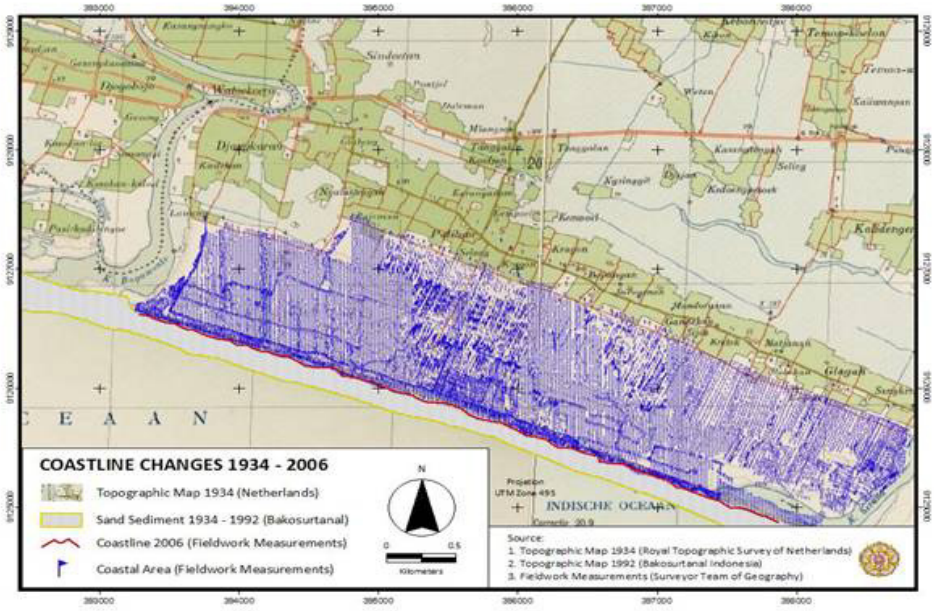

Figure 14. Coastline Changes 1934 – 2006

14 sampling point took to identify the seawater intrusion into Bogowonto River. Because of the coastal erosion increasing, the sea waves can flow directly passed the river mouth. Sediment 1992 has completely misplaced and aquifer in the coastal area faced the intrusion problems. Actual intrusion (by the sea waves) reaches 2 kilometers far from the river mouth, and the total intrusion (accumulated in a day) was 4.5 kilometers far from the river mouth. The table below shows the relationship between sea wave's velocity, river discharge velocity, and tidal flat due to seawater intrusion.

V. CONCLUSION

The sedimentation rate 1934 – 1992 approximately is 5 m/year (300 meters in 58 years). This has been happened from hundreds years ago, since volcanic and denudational activities transported materials to the lowland area. But now the abrasion rate 1992 – 2006 was 15 m/year (200 meters in 14 years). It is showed about environmental changes in the ecosystem, indicated the unbalanced cycle. Because of the human activities, environmental disregarded as important factors in human life.

Seawater intrusion also happens in the last 10 years and increase continuously. River discharge decreases on dry season, in this time the intrusion rate getting higher. On July 2005, seawater intrusion reached 4.79 kilometers to the river body from the river, now it would be higher because the local government plans to make a harbor. The river mouth opened as entry point to the harbor. Additionally, for the next development project the local government working together with foreign investor to conduct sand mining in the coastal area. If these things happen, the environmental changes is getting worst and ecosystem is depressing and cause environmental degradation. In the other hand, on rainy season river discharge increased rapidly and made flood disaster also in the lowland area; include flood inundation in the coastal area. So, all of these problems should be solved and environmental management applied comprehensively in Kulonprogo district.

Based on that indication, coastal ecosystem should be managed together, not only done by the government; nevertheless the society must join in the action plans, hence some recommendation with high priority:

1. Comprehensive Regional Planning; providing suitable zonation based on land capability, e.g. conservation zone, preservation zone, and intensive utilization zone in whole area, included upland and coastal region, and working together with other district because environmental was not limits by the administrative boundary.
2. Pollution Controlling and land degradation prevention.
3. Mining Controlling in upland and coastal area.
4. Managing fish catchments area to increase economic condition of the people who lived in coastal area, so they didn't make any destruction in the coastal region using economic excuse.
5. Community-base development to improve the social capacity.
6. Law enforcements to prevent the coastal ecosystem in stability condition.

References

Bemmelen, R.W.van. 1970. *The Geology of Indonesia vol 1.a*. The Hague Government Printing Office. Netherland.

Bhatt, J.J. 1978. *Oceanography : Exploring the Planet Ocean*. D van Nostrand Company. New York.

Ritter, D.F. 1986. *Process in Geomorphology.* 2nd Edition. Southern Illinois University. Carbondale, USA.

Triatmodjo, B. 2000. Study of Sedimentation in Coastline of South Central Java. *Technical Forum.* 24PthP Edition No.3. Page 440-451. Faculty of Engineering UGM. Yogyakarta.

Giyanto, R.C.S. 2005. *Study of Seawater Intrusion into Bogowonto River, Kulonprogo Daerah Istimewa Yogyakarta.* Faculty of Geography UGM. Yogyakarta.

Verstappen, H. th. 2000. *Outline of the Geomorphology of Indonesia*. International Institute for Aerospace Survey and Earth Sciences. Enschede. The Netherlands.

Strahler, Alan and Arthur Strahler. 1997. *Physical Geography : Science and Systems of the Human Environment.* 4PthP Edition. John Wiley & Sons Inc. New York.

Suprodjo, S.W. 1988. *Geomorphological Mapping of Daerah Istimewa Yogyakarta.* Faculty of Geography UGM. Yogyakarta.

Surjono, S.S, dan Sikandarrumidi. 2001. Morphodynamics of Bogowonto River in Congot Beach, Kulonprogo. *Technical Forum.* 25th Edition Nr.3, Page 25 Nr.2. Faculty of Engineering UGM. Yogyakarta.

Tuin, Van der. 1991. *Guidelines on The Study Of Seawater Intrusion Into Rivers*. UNESCO. France.

Yuwono, N. 1999. Study of Sedimentation in the River Mouth in South Coast of Central Java. *Technical Forum.* 23rd Edition No.3. Hal 296-308. Fakultas Teknik UGM. Yogyakarta.

Identification of Coastal Area Damage Using Remote Sensing and GIS in Parangtritis, Yogyakarta

Rino Cahyadi Srijaya Giyanto, Langgeng Wahyu Santosa, Junun Sartohadi, Suratman Woro Suprodjo

Faculty of Geography, Gadjah Mada University Yogyakarta, Indonesia

Abstract

On July 17th, 2006 Tsunami waves was generated by the earthquake at 15:19 Local Time (UTC +7) with a 7.7 magnitude of Richter scale in the southern part of West Java and shifted to the east. As the result, the southern part of coastal area in Java was damaged by tsunami. This paper presents the usage of Remote Sensing and GIS on Disaster Impact Mapping on coastal area. Located in Parangtritis Coast, this research has objectives: (1) to identify tsunami impact and its characteristics in Parangtritis, (2) to examine the relationship of coastal morphology and tsunami impact, (3) to identify the elements of Tsunami risk.

By using IKONOS and Aerial Photographs combined with field database, 1-4 meters Tsunami Run-up height were observed at Parangtritis Coast and distributed irregularly. Building and houses are clustered using IKONOS image to determinate the building vulnerability level. Differential Global Positioning System (DGPS) with Real-Time Kinematics (RTK) Method is used as a tool for topographic measuring in very detailed scale to create the DEM, and to develop building characteristics (e.g. materials, stories, building types) for identifying elements at tsunami risk.

This research has three result. First, 18% area was destroyed in the last Tsunami on 2006. Second, a close relationship of the coastal morphology and Tsunami impact shown that the lowland area has highly destructed caused by tsunami because it was crushed on the first place. This research also prove that sand-dunes have important role as a natural barrier that act as water breaker. Detailed DEM illustrated the Tsunami waves were stopped in the undulating slope. Third, 8 building clusters were classified with different building characteristics and slope condition. It is concluded from calculation that 75% of total areas were classified into highly vulnerable, 10% has medium vulnerable, and 15% low vulnerable due to Tsunami Disaster, respectively.

Keywords: Tsunami, Coastal Morphology, Tsunami Impact, Elements at Tsunami Risk.

I. INTRODUCTION

Human lives in present day are very vulnerable in facing natural disaster. The disaster happen because of the natural processes both of endogenic (earthquake, volcanic eruption, tsunami) and exogenic processes (flood, landslide, drought, or meteoric). Increasing population and the unpredictable disaster have made risk higher in term of losses. Nowadays the development in Remote Sensing and Geographic Information System can be used for reducing and monitoring the disaster. For this reason, preparation of the disaster risk management is required in order to minimize disaster impact to human life.

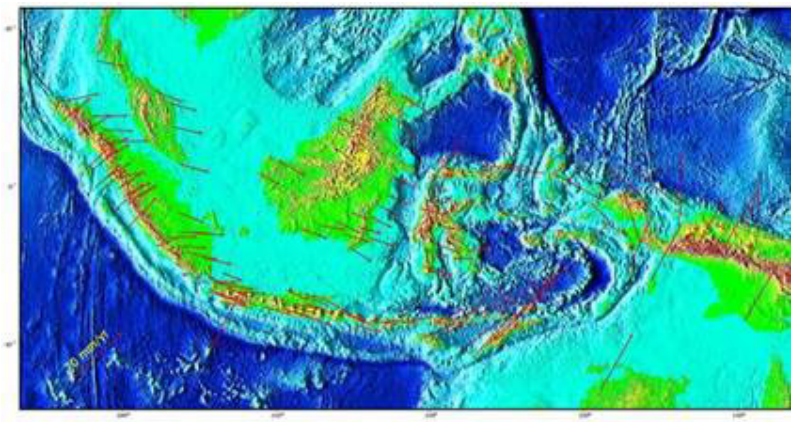

Figure 1. Present day Horizontal Plate Movement in Indonesia (Source: USGS, 2006)

Indonesia is one of the most vulnerable areas due to natural disaster, because it is closed to the collision area of the three main tectonic plates in the world. As the result, this area is situated on the subduction and obduction zone coincidently. In figure 1 below shown about horizontal plate movement in present day.

Although an infrequent disaster, tsunamis have recorded as the destructive disaster that made great losses of life and extensive damage area. The largest tsunami disaster was made by Krakatau Volcano in 1883, which documented more than 38 meters height of the waves and 2.5 kilometers trough inland both of Java and Sumatra island. The second one was happen in the year of 2004 that caused by big earthquake (9.1 in Scale Richter) and recorded as the biggest earthquake since 1900 (NGDC, 2007). This earthquake generates tsunami waves more than 30 meters height and put in 4 kilometers inland, destructing all buildings and houses.

Java Island due to tectonic setting is very vulnerable to Tsunami disaster. According to the catalogue of tsunamis in the Indian Ocean, 80% of the tsunamis are from Sunda arc region, where on an average, tsunamis are generated once in three years in different scale events (Rastogi, 2006). The Java island took place in the outer arc of volcanic belt, which the same situation with Aceh. In the year of 2006, July 17th, the tsunami happens in the southern part of West Java which shifted to the east. The impact was all the southern part of coastal zone in Java affected by the tsunami. Learning from the natural phenomenon, tsunami disaster can happen again based on the tectonic setting and plate movements. In earthquake prone areas, some epicenter which take place in deep sea, are very potential to generate tsunami waves. On the way of preventing the impact to human life, research should be conducted to reduce the impact of the future tsunami disasters.

Remote Sensing Approaches for coastal morphology were developing rapidly in the last 2 years. Based on the Landsat ETM (*Enhanced Thematic Mapper*) and DEM (*Digital Elevation Model*) data derived from SRTM (*Shuttle Radar Topography Mission*), the coastal area spatial information has been processed in order to represent the coastal morphology. Digital Image Processing methods is used to produce hill shade, slope, minimum and maximum curvature maps based on SRTM DEM, to contribute the detection of morphologic traces.

For tsunami disaster prevention, remote sensing can be used to generate tsunami hazard map. On a regional scale, the areas of potential tsunami risk will be determined by an integration of Remote Sensing data, geologic and seismotectonic data, and also topographic data. The data that can be used for this application are Landsat ETM, SRTM, and ASTER for generating image based GIS and combined with another thematic maps. These also include the seismic data record, large-scale geomorphological analysis, detailed DEM and high resolution remote sensing data such as IKONOS or Quickbird for analyzing the elements at risk shown in figure 2 below.

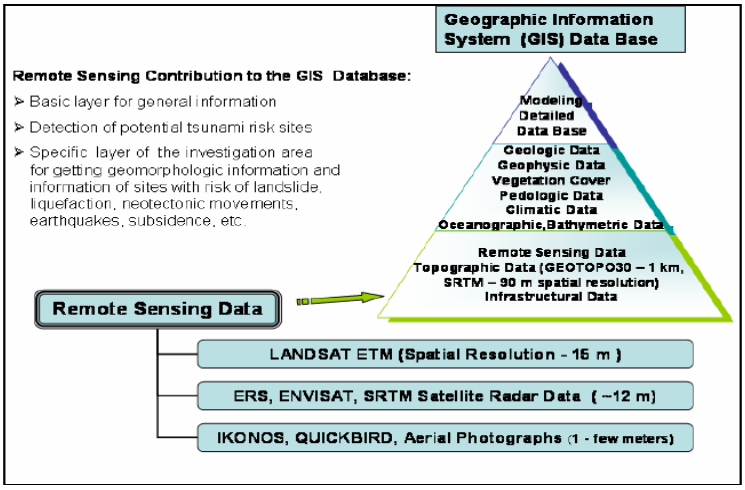

Figure 2. Remote Sensing Contribution Application (Willige, 2006)

II. STUDY AREA

Tsunami occurrences in South Coast of Yogyakarta area are relatively rare recorded comparing with other places in Indonesia. However, even in small number of events, Tsunami always made huge destruction if happen in certain area. Detailed data about the morphological of the South Coast of Yogyakarta area is ur-

gently needed in terms of mitigation of the Tsunami as every beach has their own morphological characteristics.

This study takes location in South Coast of Yogyakarta, which had tsunami occurred on 17th July 2006. Whole apart of South Coast of Yogyakarta have many differences in the morphology. Lowland coast, with flat topography found in half of South Java coast, is mostly inhabited; and the others which have less population are rocky coast with steep relief. It is about more than 80 hectares of coastal area located in prone areas due to Tsunami Disaster. Parangtritis Beach is sandy beach bounded by the cliff on the east, and is dominated by settlements that represent built-up area.

South Coast of Yogyakarta area formerly was mountain block that faulted and sank below sea level. This is one of the longest processes of Java first geo-anticlines that happened in Miocene, 6 million years BC (Bemmelen, 1949). Geo-anticlines was formed by tectonic activities and resulting North Serayu Mountain in Central Java. Two million years after first geo-anticlines, the second process created South Serayu Mountain. This process worked until third geo-anticlines which started in the end of Pliocene and beginning of Pleistocene.

Figure 3. Java Island; inset: Study area (Source: Google Earth, 2006)

The geomorphological processes occurred in this area are fluvial, aeolian, and marine origin, such as river deposition, coastal erosion, and windblown deposition. Coastal sedimentation process caused by wind and sea waves (Trihatmojo, 2000). Winds generate sea waves and it shifted along the shoreline which transported the sediment. It also generates specific landform and forms sand-dunes in the coastal area. Sand-dunes have specific requirements to develop. Those are humid area with high speed windblown and open coastal area. In Parangtritis beach, it found some dunes that formed more than 15 meters height and specific shape, like barchans so it is called with barchans dunes.

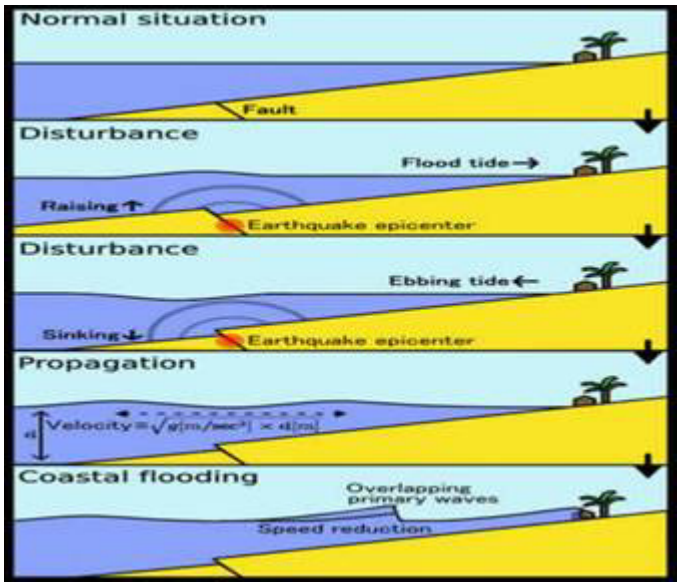

Figure 4. Tsunami generation (Web Tsunami, 2007)

III. TSUNAMI GENERATION

Tsunami is a series of large waves of extremely long wavelength and period usually generated by a violent, undersea disturbance activity near the coast or at the ocean floor (Bernard, 2005). "Tsunamis are disasters that can be generated in all of the world's oceans, inland seas, and in any large body of water. Each region of the world appears to have its own cycle of frequency and pattern in generating tsunamis that range in size from small to the large and highly destructive events" (Carayannis, 2007). Most tsunamis occur in the Pacific Ocean, Indian Ocean and its marginal seas. The reason is that covers more than one-third of the earth's surface and is surrounded by a series of mountain chains, deep-ocean trenches and island arcs called the "ring of fire" - where most earthquakes occur.

Tsunamis are generated by shallow earthquakes all around the subduction zone, but those from earthquakes in the tropical region tend to be modest in size. Even some tsunamis were generated by the volcanic eruption, undersea landslides, or human induced activity but these were very rare. This is the reason that tsunami are primarily associated with earthquake in oceanic and coastal regions, particularly in specific areas, such as plate boundaries (Meijde, 2004). In detail see figure 4.

III. TSUNAMI DISASTER JULY 17th, 2006

On July 17th, 2006 there was a Tsunami waves occurred in the South Coast of Yogyakarta Area and destructed the coastal area of West Java, Central Java, and DIY Province. More than 600 people died and hundreds of houses were completely damaged. Run-up generation recorded in various heights, from 3 – 5 meters and in some places more than 5 meters. The impacts of the Tsunami depend on the how far Tsunami can move directly inland.

Figure 5. IKONOS Image of Batu Hiu Village; Before and After Tsunami (UNOSAT, 2006)

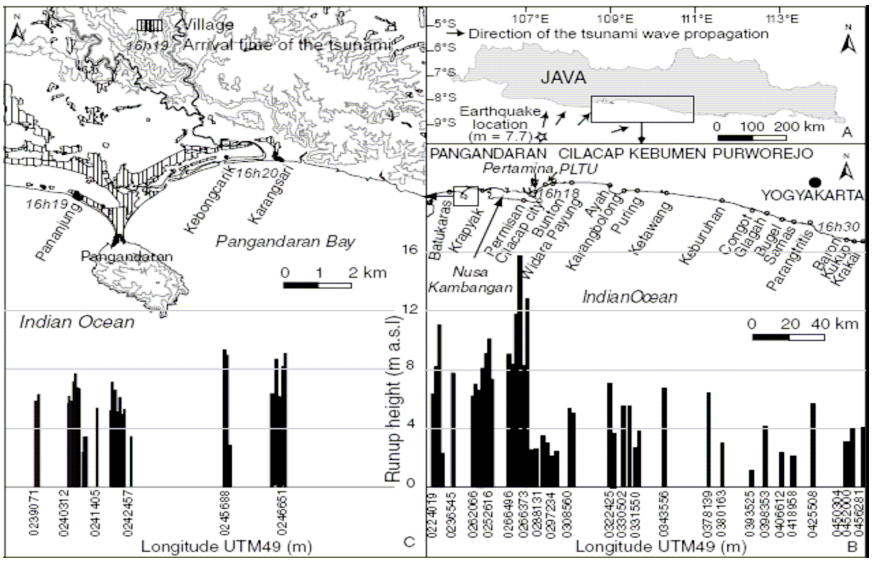

Figure 6. Tsunami 17th July 2006 Run-up Measurements (Lavigne, et.al, 2006)

In figure 5 above shows IKONOS image of Batu Hiu before and after the 17th July 2006 tsunami events. The debris materials in the coastal area indicating that the tsunami waves reached approximately 300 meters toward inland.

IV. TSUNAMI IMPACT MAPPING

Aerial Photographs and ASTER images used as preliminary interpretation to study general landuse in the research area. From these images, landuse were classified in scale 1:25.000. Landuse is human induced activities to land. In general, land-use classification are included agricultural land, barren land, swamp, and settlements. Number of people in study area is 36.100 people with the population density of 700 people/km^2, and the growth rate of 0.13% per year. Main occupation of local people is tourism services in Parangtritis, where is a famous tourism object with it's great panoramic.

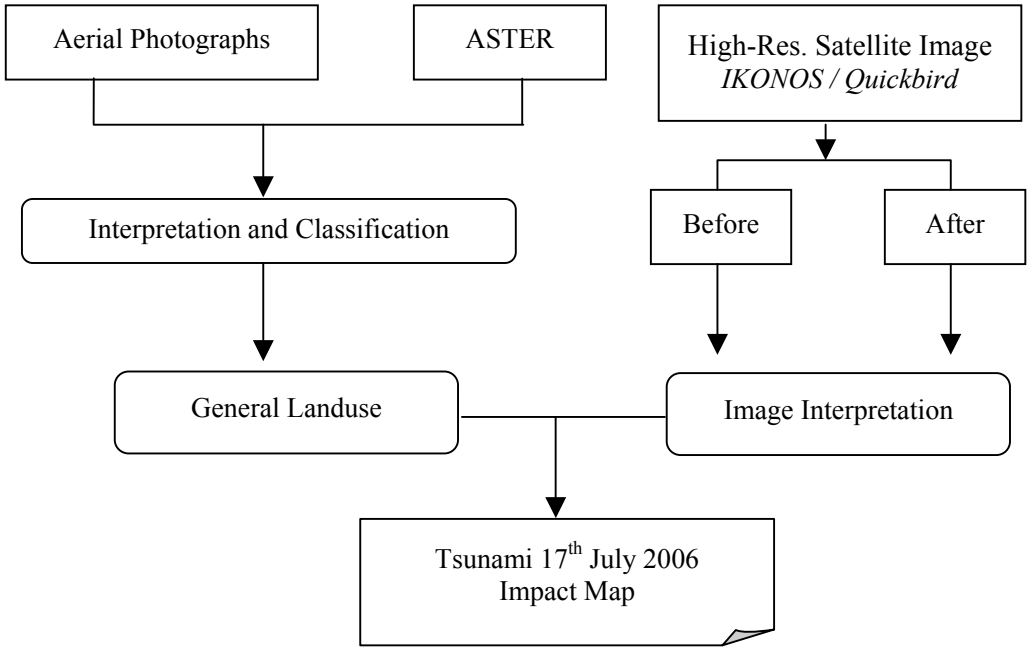

Figure 7. Framework of Tsunami Impact Mapping

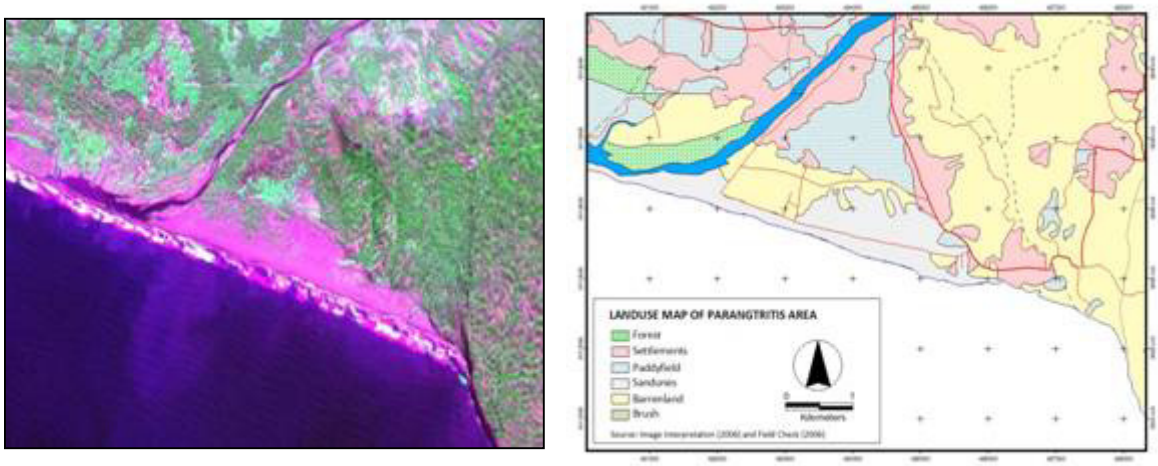

Figure 8. ASTER Band 231 Parangtritis Coastal Area and Landuse Map from Aster Images and Field check

Using IKONOS image interpretation, the impact map of Tsunami disaster showed below:

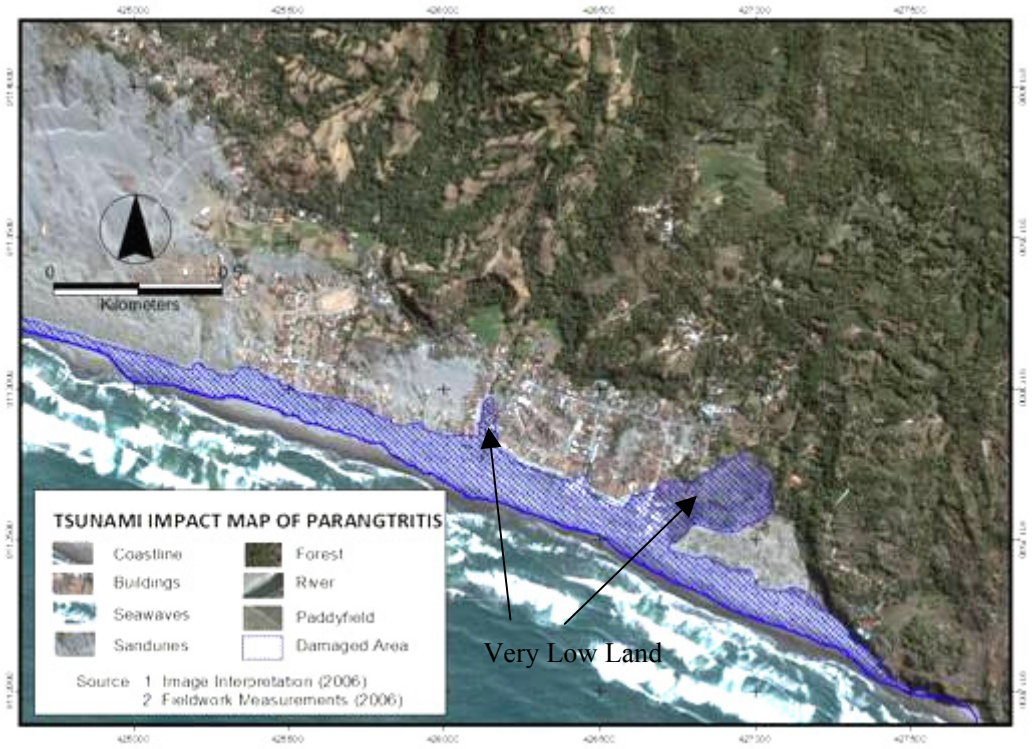

Figure 9. Tsunami Impact Map of Parangtritis

From the damage level showed the differences, 18% of the area was completely damage. The coastal morphology plays an important role in different scale of destruction; therefore doing fieldwork measurement using Differential Global Positioning System (DGPS) and sand trap was prepared in this area in order to study the coastal morphology. DGPS is one of the recent technologies to measure the land topography in accurate value, 1cm error for X and Y coordinate, and 10cm errors for Z coordinate. The system that used in this research was Real-Time Kinematics (RTK), with 1 DGPS as a Base Station and 1 DGPS as a rover. This measurement was done based on the damage area of Tsunami Disaster. DEM result from point height calculated with elements at Tsunami Risk, therefore the vulnerability level can be identified as a combination between field database and remote sensing techniques.

V. VULNERABILITY OF ELEMENTS AT TSUNAMI RISK

Eight building clustered classified using IKONOS and field database consist of: number of houses, building materials, number of stories, and interview with the people perception about the last Tsunami risk and disaster.

Three main cluster showed the type of building. First is rattan buildings, used as small shop sells food and souvenirs, non permanent and located <25 meters from coastline. Second is bricks material and permanent buildings, used as restaurant and home stay, mostly found in this area and located <500 meters from the coastline. The last is concrete material, 2 stories building and used as hotel and restaurant, located <500 meters from the coastline. From the historical Tsunami database (NGDC, 2007), tsunami in south coast of Java included DIY has been occurred 4 times in the last 200 years. It means that the frequency of tsunami occurrences approximately 1 in 50 years. In view of the run-up database by Lavige et.al (2006), the last Tsunami July 17th 2006 in Parangtritis reaches 4 – 6 meters height and less than 1 minute to destruct the Parangtritis area.

Tsunami waves occurred directly to the low land area and stopped in the swale. In some parts, these waves pass the coastline and moved toward inland until 300 meters far to the small channel and paddy field. Local people said that the waves travel very fast and inundated in the low part. More than 45 small shop and 10 houses completely damaged by the Tsunami. From the fieldwork measurements, slope condition in Parangtritis area have various value, in the eastern part very flat with 0 – 8 %, in the middle 0 – 15 % and in the western part have some places that the slope were >15%.

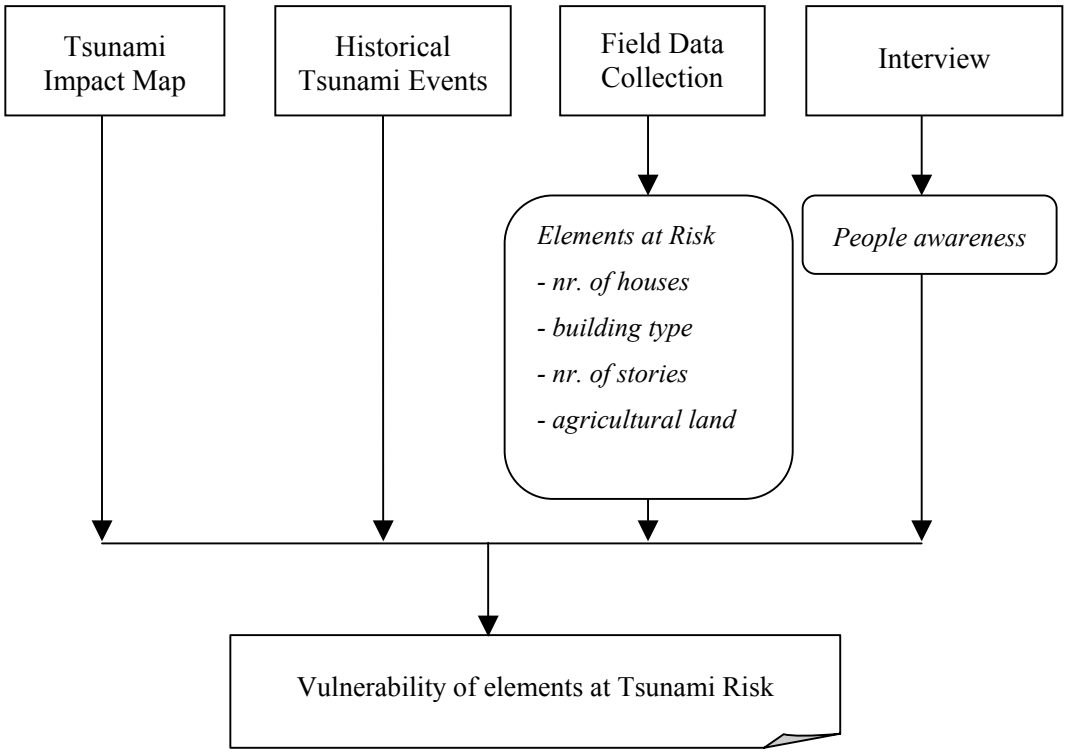

Figure 11. Framework to Identify of Elements at Tsunami Risk

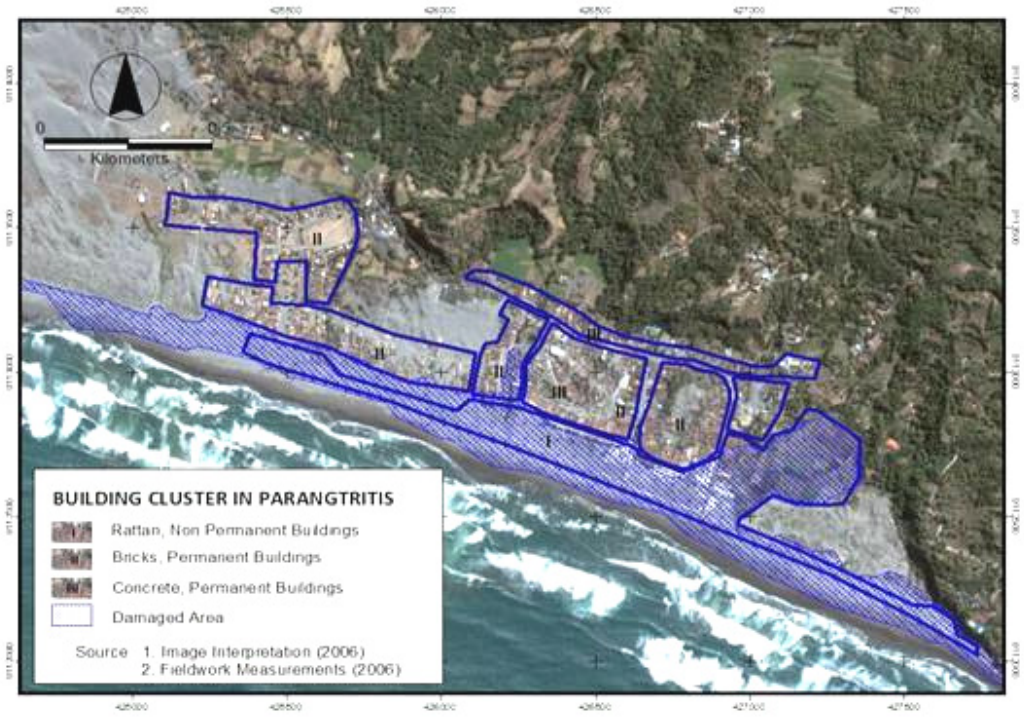

Figure 12. Building Cluster in Parangtritis

Learning from last disaster, the tsunami shattered out when bumping the swale and sandunes. Naturally, this landform unit being a tsunami wall and keep people safely. But the local people and the government develop this area irregularly, and as the result, 18% area destructed by the tsunami because it is built in the very low land area. Vulnerability of the elements at Tsunami Risk should consider about topography, slope steepness, population density, the building material, and also distance from the coastline, because Parangtritis as a tourism object located less than 500 meters far from the coastline.

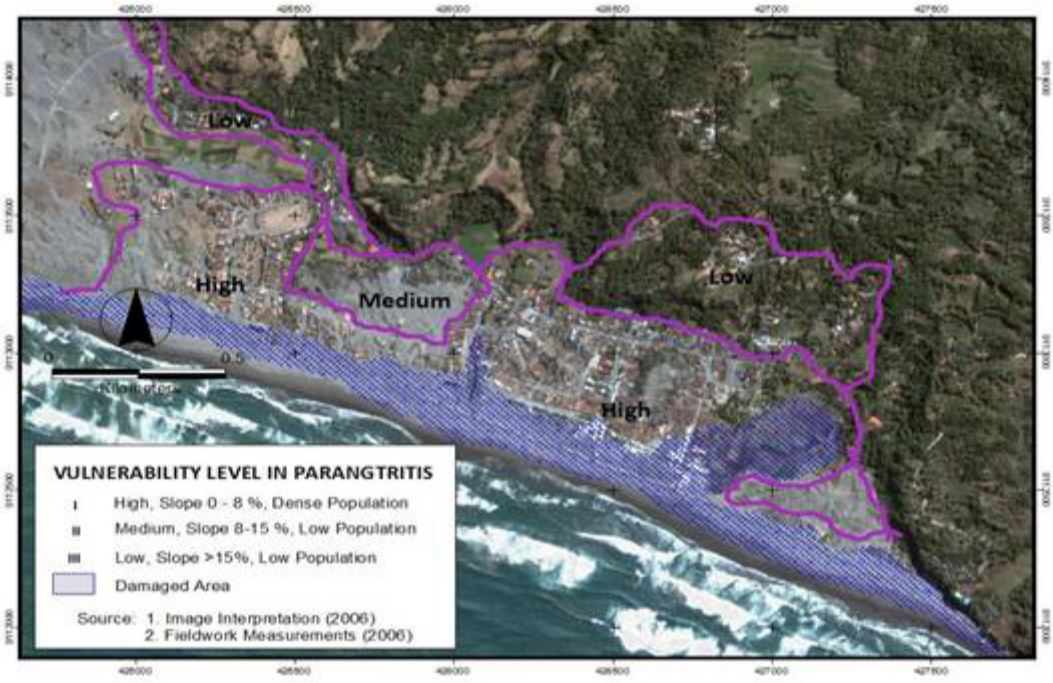

Figure 13. Vulnerability Level in Parangtritis.

More than 75 % area was classified into high vulnerable level because the slope was 0 – 8 %, dense population and only less than 500 meters far from the coastline. If the Tsunami happens again like Tsunami in Aceh with more than 25 meters height of run-up, this area will completely damage. Some part classified into medium level because it has big sandunes and covered the building behind, but still has to consider the refraction of the Tsunami waves if the waves were bumping the hills. And only 15 % area classified into low vulnerability level because it is located in upside of the coast, and is more than 30 meter altitude with low population density. The vulnerability can be showed as below.

VI. CONCLUSION

Based on the tourism objects, the local governments tend to develop the coast. The build up area attract more people to come and live for better condition. Beside that, the coastal areas were well-known as traditional fishery industries. As a consequence of this enticement, there are a significant growth of population and buildings. If tsunami disaster occurred, those cause elements of risk become higher. From this study, the used of Remote Sensing was very helpful to map the Tsunami impact and to calculate the losses. It is also able to reduce the impact in the future, by combining remote sensing with field and historical disaster database as a comprehensive methodology comparing with the old techniques. The calculation using remote sensing data shows 18% areas have completely damaged and 75% areas were highly vulnerable from the Tsunami disaster, considering the last events, historical tsunami database, distance from the coastline, topographic measurements, and landform unit identification.

Figure 14. Sandunes and Swale as Water Breaker in Parangtritis Coastal Area

Sandunes and Swale are playing important role as water breaker, and the government should preserve this unique landform in natural condition. The damage level in the last tsunami was very high because the local people built the small shop and building nearby the coastline. Furthermore, people perception about risk must be developed by socializing disaster and evacuation or emergency plans. Those have to be prepared in better ways because in this area only 15% area where is located in low vulnerable and is 10 % in medium vulnerable. The rest region is high vulnerable due to the Tsunami disaster. People and Government should working together to formulate prevention, mitigation, action plans, and also rehabilitation followed by reconstruction if the Tsunami disaster turns out. The community based disaster management should be improved.

References

Anonymous, 2006. Tsunami Damage to Terrestrial Coastal Ecosystems. Guidelines and Methodology for Rapid Field Assessment. The World Conservation Union (IUCN).

Bemmelen, R.W.van. 1970. *The Geology of Indonesia vol 1.a*. The Hague Government Printing Office. Netherland.

Lavigne, F., C. Gomez, M. Gifo, P. Wassmer, C. Hoebreck, D. Mardiatno, J. Prioyono, and R. Paris (2007), Field Observations of the 17 July 2006 Tsunami in Java, *Natural Hazard and Earth System Science*, 7(1), 177 - 183.

Nadim, F. and Thomas Glade (2006), On Tsunami Risk Assessment for the West Coast of Thailand, *Paper 28*, 2006 ECI Conference on Geohazards, Lillehammer, Norway.

NERC (2000). The Tsunami Risk Project. Coventry University and University College London. United Kingdom. *http://www.nerc-bas.ac.uk/tsunami-risks/*

Paine, Michael P. (1999), Asteroid Impacts: The Extra Hazard Due To Tsunami, *Science of Tsunami Hazards*, 17(3), 155-166.

Papadopoulos, G.A. and Th. Dermentzopoulos (1998), A Tsunami Risk Management Pilot Study in Heraklion, Crete, *Natural Hazards*, 18(2), 91-118.

Verstappen, H. th. 2000. *Outline of the Geomorphology of Indonesia*. International Institute for Aerospace Survey and Earth Sciences. Enschede. The Netherlands.

Walters, R.A. and James Goff (2003), Assessing Tsunami Hazard Along The New Zealand Coast, *Science of Tsunami Hazards*, 21(3), 137-153.

Willige, 2006. Tsunami Risk Site Detection on Greece. Scientific Journal. Technical University of Berlin, Institute of Applied Geosciences. Germany.

Website:

Google Earth Pro; [IKONOS and Quickbird] High Resolution Imagery Data
http://www.search.com/reference/Coast ; [Web Coast] Definition and image
http://www.answers.com/topic/tsunami?cat=technology; [Web Tsunami] Definition
http://www.ngdc.noaa.gov; spatial data source of tsunami events database
http://unosat.web.cern.ch/unosat/; spatial data source of tsunami impact
http://www.nws.noaa.gov/om/brochures/tsunami.htm; [Tsunami] the Great Waves

Effects of Pore Water Pressure on Scour – in Case of Local Scour Due to Runup Tsunami –

Tomoaki Nakamura[1], Norimi Mizutani[2], Yasuki Kuramitsu[3]

[1] *Ph.D. Student (JSPS Research Fellow), Dept. of Civil Eng., Nagoya University, Furo-cho, Chikusa-ku, Nagoya 464-8603, Japan. tnakamura@nagoya-u.jp*
[2] *Professor, Dept. of Civil Eng., Nagoya University, Furo-cho, Chikusa-ku, Nagoya 464-8603, Japan. mizutani@civil.nagoya-u.ac.jp*
[3] *NTT West Corp., 3-15, Bamba-cho, Chuo-ku, Osaka 540-8511, Japan. kuramitsu@nagoya-u.jp*

Abstract

Large-scale sediment transport due to the 2004 Indian Ocean Tsunami resulted in substantial erosion and scour around many structures. In this paper, we investigated tsunami-induced local scour around a land-based structure with a square cross-section on a sand foundation with both hydraulic model experiments and numerical simulations capable of computing interactions between tsunami waves and sand beds composed of nonlinear materials. In the hydraulic model experiments, we found that local scour holes around the seaward corner of the structure could be reproduced, and the maximum final scour depth at the seaward corner of the structure was sensitive to the relative incident tsunami wave height and the relative embedded depth of the structure. In the numerical simulations, we revealed that the tsunami-induced local scour around the seaward corner of the structure could be evaluated with not only flow velocity on the sand foundation but also effective stress inside the surface layer of the foundation because the effective stress acting on the foundation significantly affected restricting force between sand particles.

1. INTRODUCTION

At 7:58 a.m. local time on December 26, 2004, the Sumatra-Andaman Earthquake occurred with an epicenter under the Indian Ocean near the west coast of Sumatra, Indonesia, and then a series of lethal tsunamis called the 2004 Indian Ocean Tsunami unfortunately struck coastal areas of India, Indonesia, Sri Lanka, Thailand and other countries along the Indian Ocean, killing a large number of people and destroying many public and private structures. The tsunami waves also caused large-scale sediment transport, resulting in substantial erosion and scour around a large number of structures. For example, Borrero et al. (2005) reported a scour hole with approximately 5.0 m in width and 1.5 m in depth around the seaward corner of a schoolhouse in Kalapakkom, India. As suggested by Tonkin et al. (2003), such tsunami scour seems to have a different mechanism from a steady current and consistent short-wave field, and hence the following studies have so far been done to investigate tsunami-induced local scour around coastal structures. Uda et al. (1987) revealed with hydraulic model experiments that the collapse of a vertical seawall due to tsunami waves depended mainly on the topography of a reclaimed area and toe scouring caused by tsunami backwash, and Noguchi et al. (1997) found in laboratory experiments that a standing vortex due to tsunami downrush resulted in a scour hole in front of a seawall. Kato et al. (2000, 2001) and Tonkin et al. (2003) conducted large-scale hydraulic model experiments on tsunami-induced local scour around a cylindrical structure on a flat beach, and clarified that sediment substrate greatly affected a scouring mechanism around the onshore side of the structure. Nakamura et al. (2007) performed both hydraulic model experiments and numerical simulations to investigate local scour around a land-based square structure due to a runup tsunami wave; however, there still remained several problems in the adopted simulation model, e.g., the employment of Hooke's law enabled us not to apply this numerical model to nonlinear materials such as sand beds close to liquefaction.

The purpose of this study is to investigate tsunami-induced local scour around a land-based structure with a square cross-section on a sand foundation with hydraulic model experiments and improved numerical simulations capable of computing interactions between tsunami waves and sand beds composed of nonlinear materials. In the hydraulic model experiments, we try to reproduce similar scour holes to actual ones observed in field surveys (Borrero et al., 2005), and clarify the link between a final scouring form on the sand foundation and the profiles of incident tsunami waves as well as the dimensions of the square structure. In the numerical simulations, we treat not only flow velocity on the sand foundation but also effective stress inside the surface layer of the foundation, and reveal their effects on tsunami-induced local

scour around the square structure.

2. HYDRAULIC MODEL EXPERIMENTS

In this work, we performed hydraulic model experiments by using a 30.0 m long, 0.7 m wide and 0.9 m high wave flume with a piston-type wave generator (maximum stroke: 1.50 m) at the Department of Civil Engineering, Nagoya University. We set a wave absorbing beach at the most onshore side of the wave flume to prevent an incident tsunami wave from reflecting back. As illustrated in Figure 1, we first placed a 0.19 m high impermeable rigid bed with the seaward slope of 1/10 in front of the beach, and then installed an impermeable seawall (crown width: 0.03 m; height: 0.15 m; seaward slope: 1/0.2) and backfilling sand (length: 1.0 m; height: 0.15 m; density of sand particles: $2.65\times10^{3}\,\mathrm{kg/m^{3}}$; median grain size of the sand particles: $d_{50}=2.0\times10^{-4}\,\mathrm{m}$) on the impermeable bed. After that, we fixed the upper part of a wooden square structure (width: $B=0.14\,\mathrm{cm}$) with the embedded depth d to the wave flume at 0.28 m landward from the rear face of the seawall.

As an incident tsunami wave, we adopted one solitary wave with three still water depths h_o (26.5, 29.0 and 31.5 cm) and six incident wave heights H_o ($H_o/h_o \approx 0.2$, 0.3, 0.4, 0.5, 0.6 and 0.7). We also set four patterns of embedded depth of the square structure d, i.e., $d=$ 0.0, 1.0, 3.0 and 5.0 cm. We therefore conducted a total of 72 experimental cases. In each run, we measured water surface fluctuation η in front of the seawall and dynamic pore water pressure p_e inside the sand foundation with three capacitance-type wave gages (KENEK: CHT6-40) and eight pore water pressure gages (KYOWA: BP-500GRS, BPR-A-50KPS), whose positions are illustrated in Figure 1. In addition, we recorded the deformation of a runup solitary wave with a digital video camera (SONY: DCR-PC110). After each experimental run, we measured a surface profile of the reclaimed area around the square structure with a contact-type bottom profiler (KENEK: WHT-60).

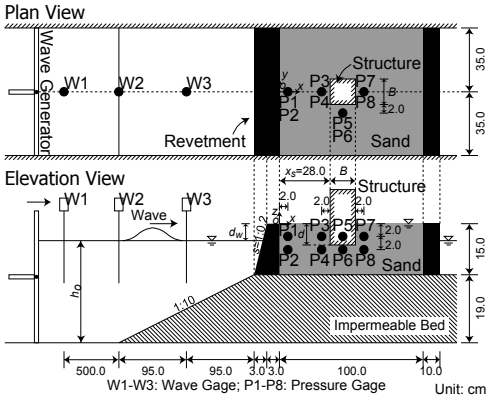

Figure 1. Schematic figure of a wave flume and positions of wave and pressure gages

3. EXPERIMENTAL RESULTS AND DISCUSSIONS

As shown in Photo 1, we could reproduce tsunami-induced scour holes around the seaward corner of the structure in the hydraulic model experiments, whose forms were very similar to actual ones due to the 2004 Indian Ocean Tsunami (Borrero et al., 2005). We note in Photo 1 that d_w is the freeboard height, i.e., the seawall height from the still water level, as illustrated in Figure 1. Moreover, a runup tsunami wave eroded backfilling sand particles even under the offshore side of the structure for the small embedded depth of the structure d such as Photo 1(b), and a narrow gap therefore appeared under the structure.

Figure 2 describes the final scour depth z_{sf} on the sand foundation, in which the positive and negative z_{sf} represent erosion and deposition, respectively, and no contour lines exist in the vicinity of the structure because of the size of the contact-type bottom profiler. As shown in Figure 2, the erosion occurred just behind the seawall and also around the seaward corner of the structure, while the deposition occurred at the onshore side of the structure. In addition, we confirmed that the maximum final scour depth $z_{sf}^{\max}$ was located at the seaward corner of the structure in all experimental cases.

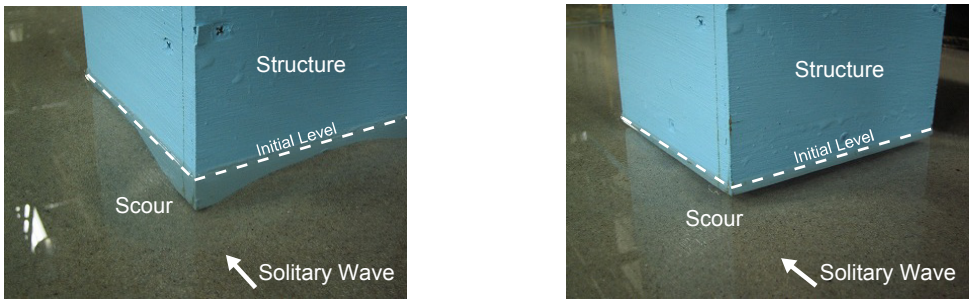

(a) $(2H_o - d_w)/B = 2.50$, $h_o/B = 2.25$, $d/d_{50} = 150.0$ (b) $(2H_o - d_w)/B = 2.04$, $h_o/B = 2.25$, $d/d_{50} = 50.0$

Photo 1. Examples of a scour hole around the seaward corner of the structure

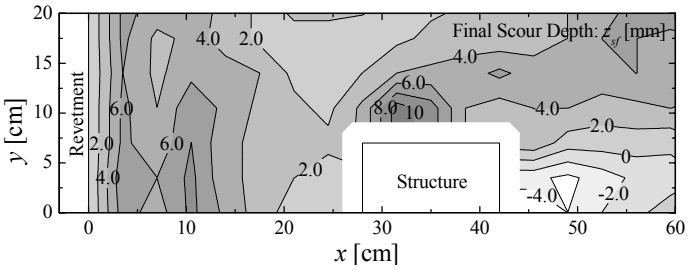

(a) $(2H_o - d_w)/B = 3.37$, $h_o/B = 2.25$, $d/d_{50} = 50.0$

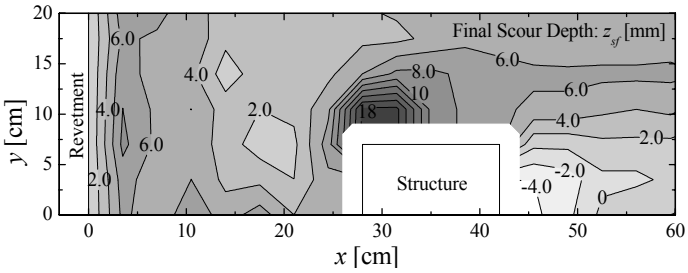

(b) $(2H_o - d_w)/B = 2.96$, $h_o/B = 2.25$, $d/d_{50} = 150.0$

Figure 2. Final scour depth z_{sf} on the sand foundation

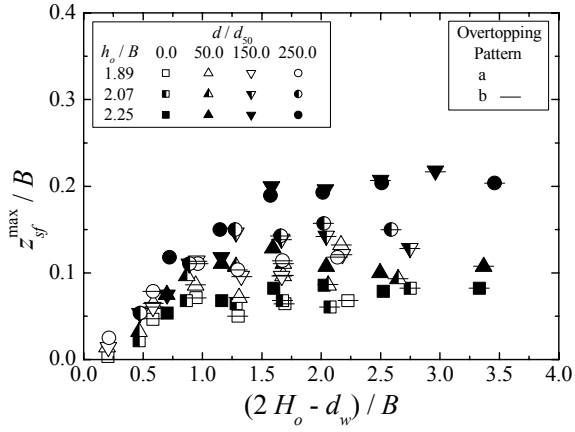

Figure 3. Maximum final scour depth z_{sf}^{max}

Figure 3 indicates the nondimensional maximum final scour depth z_{sf}^{max}/B, in which the overtopping pattern was classified following Noguchi et al. (1997), i.e., the pattern A is an overflowing wave without breaking, while the pattern B is an overtopping wave with a plunging breaker above the seawall. As plotted

in Figure 3, $z_{sf}^{\max}/B$ increases with the relative incident tsunami wave height $(2H_o - d_w)/B$. However, an increase rate of $z_{sf}^{\max}/B$ gradually decreases with an increase in $(2H_o - d_w)/B$, and finally becomes nearly constant for $(2H_o - d_w)/B > 1.5$. Furthermore, $z_{sf}^{\max}/B$ increases with the relative embedded depth of the structure d/d_{50}, which was a similar tendency to tsunami scour on a sand substrate at the landward side of a cylindrical structure (Kato et al., 2001).

4. NUMERICAL SIMULATION

Nakamura et al. (2007) developed a simulation model capable of computing wave-seabed interactions, which consisted of two numerical submodels: one was a numerical wave tank based on the VOF (Volume Of Fluid) method for air-water two-phase flow (hereafter referred to as "VOF-based submodel"); and the other was a soil-water coupled FEM (Finite Element Model) for sand beds (hereafter referred to as "FEM-based submodel"). We here modified a turbulence model in the VOF-based submodel and a constitutive equation of sand beds in the FEM-based submodel to improve the computational accuracy of wave-seabed interactions. In this section, we provide a brief explanation of each submodel.

Governing equations in the VOF-based submodel were composed of a continuity equation, modified Navier-Stokes equations and an advection equation of the VOF function. As explained above, we adopted the large eddy simulation (LES) based on the dynamic two-parameter mixed model (DTM; Salvetti and Banerjee, 1995) instead of the dynamic mixed model (Zang et al., 1993); hence, the modified Navier-Stokes equations incorporated the turbulent stress based on the DTM, laminar and turbulent resistance force due to porous media (Mizutani et al., 1996), surface tension force based on the CSF (Continuum Surface Force) model (Brackbill et al., 1992) and wave generation source of Kawasaki (1999). To improve the tracking accuracy of air-water interfaces, this submodel also employed the MARS (Multi-interface Advection and Reconstruction Solver) of Kunugi (2000).

The FEM-based submodel was a three-dimensional FEM based on the u-p approximation of the Biot equations. This submodel employed the constitutive equation of Hooke's law for isotropic elastic materials nonresistant to tensile force, so-called no-tension isotropic elastic materials, instead of the linear Hooke law. To improve the computational stability of spatial discretization, we applied twenty-node quadratic and eight-node linear isoparametric brick elements to sand skeleton displacement u and pore water pressure p, respectively. In addition, we adopted a one-way technique proposed by Mizutani et al. (1998) as a coupling calculation between the VOF-based and FEM-based submodels.

5. NUMERICAL RESULTS AND DISCUSSIONS

In the hydraulic model experiments, we observed that runup tsunami deformation around the square structure were nearly symmetric with respect to the x-z plane of $y = 0$, and we consequently analyzed only a half side of the experimental setup to reduce the computational cost. Figure 4 illustrates a schematic of a numerical wave tank. We adopted non-uniform orthogonal staggered meshes in the VOF-based submodel, whose dimensions were 1.0 x 1.0 x 1.0 cm within the foundation, for the additional reduction of the computational cost. In the FEM-based submodel, we used isoparametric brick elements with one to six times the size of the abovementioned staggered meshes. In this study, we set all physical parameters at the same values as those of the previous work (Nakamura et al., 2007).

To confirm the computational accuracy of the simulation model, Figure 5 shows a comparison of water surface fluctuation η in front of the seawall and excess pore water pressure p_e within the sand foundation, in which the circles represent experimental data, and the solid and broken lines represent numerical results computed with the VOF-based and FEM-based submodels, respectively. As shown in Figure 5, there is a small difference in phase between the experimental and numerical results of p_e, and the computed p_e slightly underestimates the corresponding measured data at the offshore and onshore sides of the structure (P3, P4, P7 and P8). Judging from Figure 5, the numerical results are, however, in good agreement with the experimental ones in both η and p_e, and we hence confirmed that the numerical model could reproduce not only the deformation of a runup tsunami due to the square structure but also tsunami-induced dynamic response of the sand foundation.

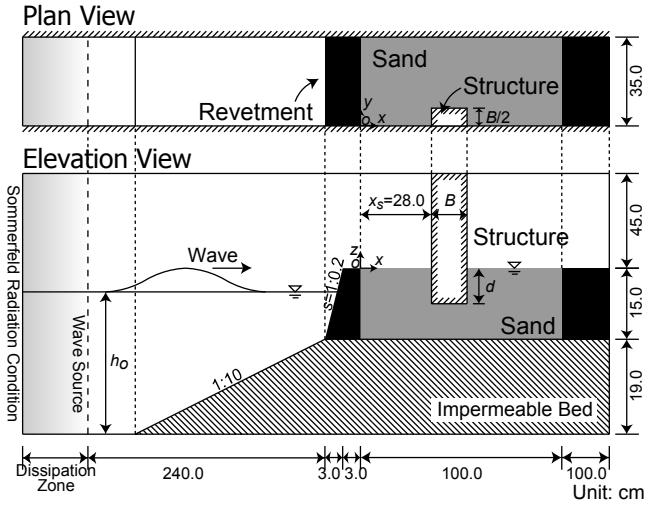

Figure 4. Schematic figure of a numerical wave tank

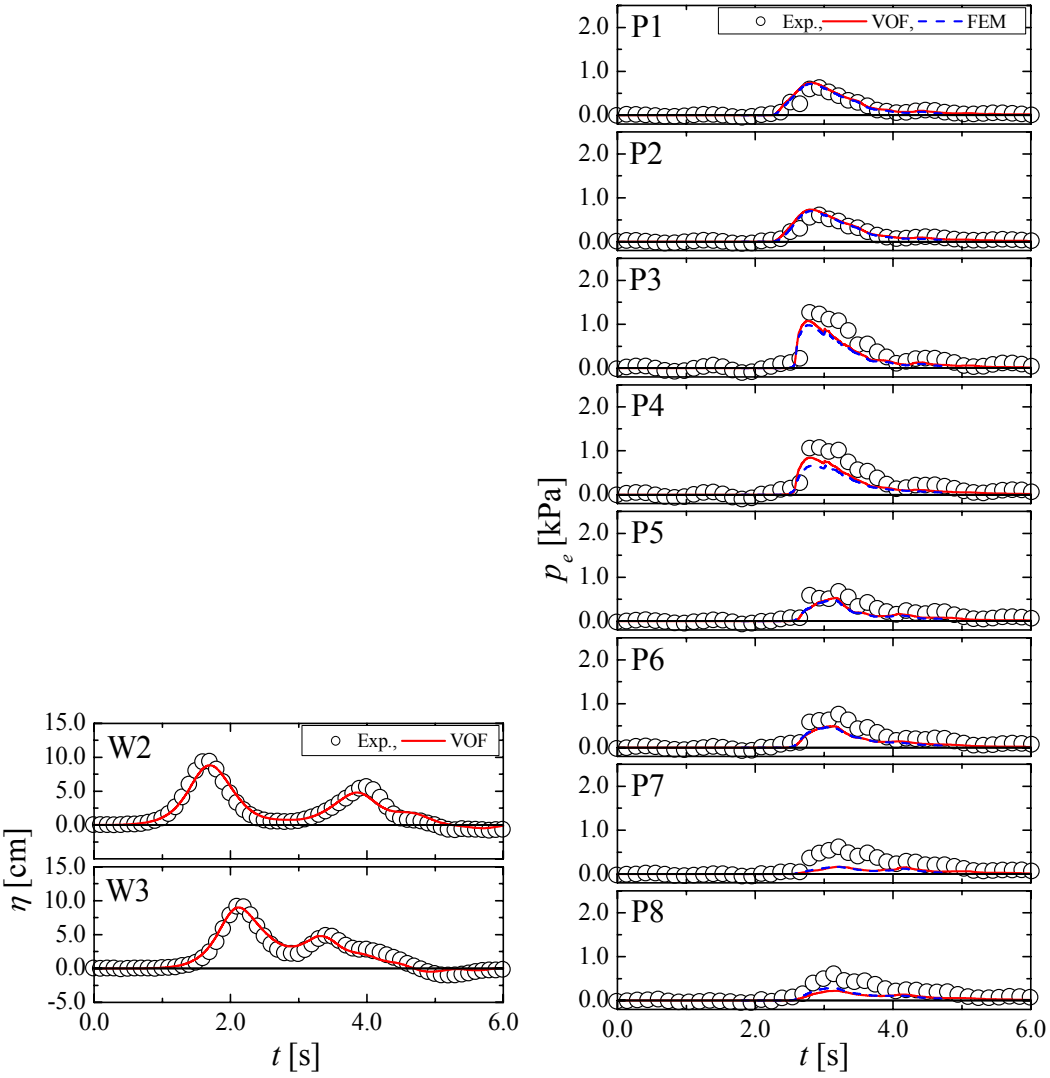

(a) Water surface fluctuation η (b) Excess pore water pressure p_e

Figure 5. Comparison between measured and computed results for $(2H_o - d_w)/B = 1.16$, $h_o/B = 2.25$, $d/d_{50} = 0.0$

In this work, we first focused on flow velocity on the surface of the foundation to investigate mechanisms of tsunami local scour around the square structure. Figure 6 shows the time integration of a tangential flow velocity gradient $v_{i,i}^{\mathrm{sum}}$ on the foundation:

$$v_{i,i}^{\mathrm{sum}} = \sum_{\mathrm{Time}} \frac{\partial v_i}{\partial x_i} \Delta t = \sum_{\mathrm{Time}} \left(\frac{\partial u}{\partial x} + \frac{\partial v}{\partial y} \right) \Delta t \,, \tag{1}$$

where u and v are the tangential flow velocities at the height of $z = 5.0 \times 10^{-3}\,\mathrm{m}$ in the x and y directions, respectively; and Δt is the time increment adopted in the numerical simulations. Since the nondimensional bed load transport rate is assumed to be proportional to the Shields number to the power of 1.5, the bed load transport rate can be expressed as a function of flow velocity on the surface of the foundation; hence, positive and negative $v_{i,i}^{\mathrm{sum}}$ represent erosion and deposition, respectively. As indicated in Figure 6, a positive $v_{i,i}^{\mathrm{sum}}$ region appeared around the seaward corner of the structure, while a negative $v_{i,i}^{\mathrm{sum}}$ region occurred at the onshore side of the structure. For this reason, the foundation was eroded near the seaward corner of the structure, and suspended sand was deposited at the landward side of the structure, as shown in the measured topographic changes (Figure 2). However, another positive $v_{i,i}^{\mathrm{sum}}$ region occurred around the landward corner of the structure, and we hence concluded that tsunami scour in the vicinity of the structure could not be evaluated with only tangential flow velocity on the surface of the foundation.

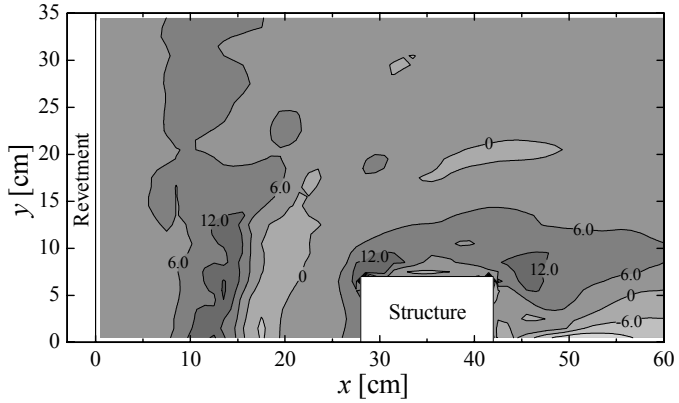

(a) $(2H_o - d_w)/B = 1.59$, $h_o/B = 2.25$, $d/d_{50} = 50.0$

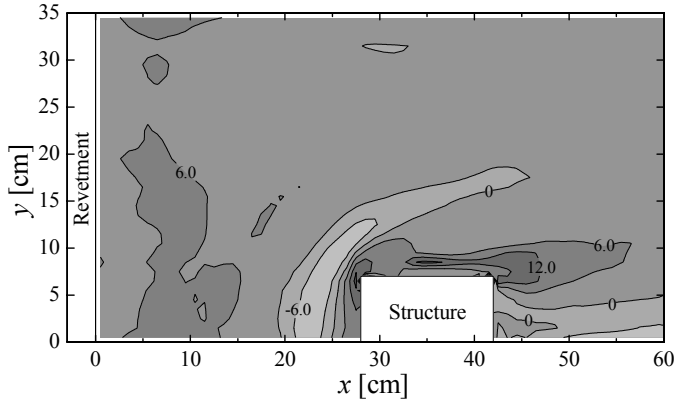

(b) $(2H_o - d_w)/B = 1.15$, $h_o/B = 2.25$, $d/d_{50} = 250.0$

Figure 6. Time integration of the tangential flow velocity gradient $v_{i,i}^{\mathrm{sum}}$ on the foundation

To evaluate effective stress acting on the surface layer of the sand foundation, we adopted the following relative mean effective stress ratio (hereafter referred to as "RMESR"):

$$\mathrm{RMESR} = 1.0 - \frac{\sigma'_m}{\sigma'_{m0}}, \tag{2}$$

where σ'_m is the mean effective stress at the depth of $z = -5.0\times10^{-3}\,\mathrm{m}$; and σ'_{m0} is the initial value of σ'_m, and the RMESR becomes unity when liquefaction occurs. Figure 7 shows the time histories of the computed Shields number and RMESR, in which the Point A was located just behind the seawall (dotted lines; $x = 5.5\,\mathrm{cm}$, $y = 3.5\,\mathrm{cm}$); the Point B at the seaward side of the structure (dashed-dotted lines; $x = 23.5\,\mathrm{cm}$, $y = 3.5\,\mathrm{cm}$); the Point C at the seaward corner of the structure (solid lines; $x = 28.5\,\mathrm{cm}$, $y = 7.5\,\mathrm{cm}$); and the Point D at the landward side of the structure (broken lines; $x = 46.5\,\mathrm{cm}$, $y = 3.5\,\mathrm{cm}$). In Figure 7, we defined the beginning time of the numerical simulation as 0.0 s. As indicated in Figure 7, the RMESR first built up sharply, and then the foundation was locally liquefied (RMESR = 1.0) at the seaward corner of the structure (Point C; solid lines); hence, the aforementioned increase of the RMESR led to a decrease in restricting force between sand particles around the seaward corner of the structure. After that, the large nondimensional shear stress (Shields number) due to a runup tsunami wave acted on the sand foundation at the Point C during the increase in the RMESR. As a result, the foundation was easily scoured in the vicinity of the Point C, and a scour hole such as Photo 1 finally appeared around the seaward corner of the structure. To evaluate tsunami-induced local scour around the land-based square structure, we consequently revealed that it was necessary to use not only tangential flow velocity on the sand foundation but also effective stress acting on the surface layer of the foundation.

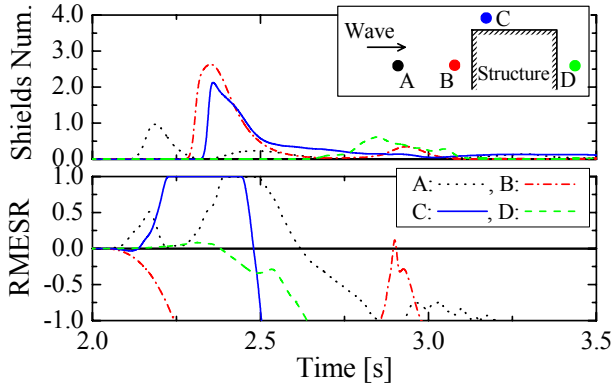

(a) $(2H_o - d_w)/B = 1.58$, $h_o/B = 2.25$, $d/d_{50} = 150.0$

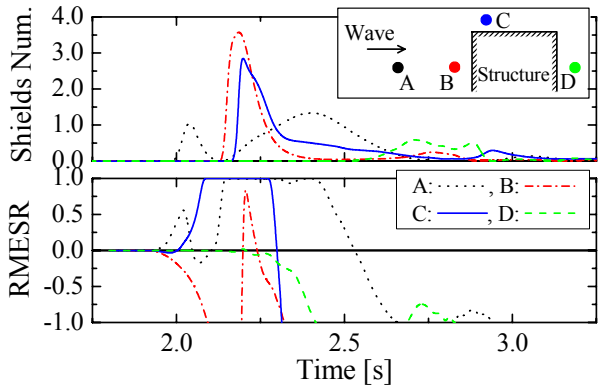

(b) $(2H_o - d_w)/B = 2.01$, $h_o/B = 2.25$, $d/d_{50} = 250.0$

Figure 7. Time histories of the Shields number on the sand foundation and relative mean effective stress ratio (RMESR) inside the surface layer of the foundation

6. CONCLUDING REMARKS

In this study, we investigated local scour around a land-based structure with a square cross-section on a sand foundation due to a runup solitary wave by conducting both hydraulic model experiments and numerical simulations. The numerical simulation model was improved to compute dynamic interactions between tsunami waves and sand beds composed of nonlinear materials. In the hydraulic model experiments, tsunami-induced scour holes could be reproduced around the seaward corner of the structure, and the maximum final scour depth at the seaward corner of the structure was affected by the relative incident tsunami wave height and the relative embedded depth of the structure. In the numerical simulations, it was revealed that tsunami scour around the seaward corner of the structure could be evaluated with not only tangential flow velocity on the sand foundation but also effective stress within the surface layer of the foundation since the effective stress acting on the foundation significantly affected restricting force between sand particles.

Acknowledgments

This work was partly supported by a Grant-in-Aid for JSPS Research Fellow (No. 19623) offered by the Japanese Ministry of Education, Culture, Sports, Science and Technology (MEXT). The authors greatly appreciate the financial support.

References

Borrero, J., Yeh, H., Peterson, C., Chadha, R. K., Latha, G. and Katada, T. (2005). "Learning from earthquakes: the great Sumatra earthquake and Indian Ocean tsunami of December 26, 2004," *EERI Special Earthquake Report*, March 2005.

Brackbill, J. U., Kothe, D. B. and Zemach, C. (1992). "A continuum method for modeling surface tension," *J. Comp. Phys.*, Vol. 100, pp. 335-354.

Kato, F., Sato, S. and Yeh, H. (2000). "Large-scale experiment of dynamic response of sand bed around a cylinder due to tsunami," *Proc., 27th Int. Conf. Coastal Eng.*, ASCE, Sydney, Australia, pp. 1848-1859.

Kato, F., Tonkin, S., Yeh, H., Sato, S. and Torii, K. (2001). "The grain-size effects on scour around a cylinder due to tsunami run-up," *Proc., Int. Tsunami Symposium 2001*, Seattle, Washington, pp. 905-917.

Kawasaki, K. (1999). "Numerical simulation of breaking and post-breaking wave deformation process around a submerged breakwater," *Coastal Eng. J.*, JSCE, Vol. 41, No. 3-4, pp. 201-223.

Kunugi, T. (2000). "MARS for multiphase calculation," *CFD J.*, Vol. 9, No. 1, IX-563.

Mizutani, N., McDougal, W. G. and Mostafa, A. M. (1996). "BEM-FEM combined analysis of nonlinear interaction between wave and submerged breakwater," *Proc., 25th Int. Conf. Coastal Eng.*, ASCE, Orlando, Florida, pp. 2377-2390.

Mizutani, N., Mostafa, A. M. and Iwata, K. (1998). "Nonlinear regular wave, submerged breakwater and seabed dynamic interaction," *Coastal Eng.*, Vol. 33, pp. 177-202.

Nakamura, T., Mizutani, N. and Kuramitsu, Y. (2007). "Local scour around a square structure due to runup tsunami," *Proc., Coastal Structures 2007*, ASCE, Venice, Italy, in press.

Noguchi, K., Sato, S. and Tanaka, S. (1997). "Large-scale experiments on tsunami overtopping and bed scour around coastal revetment," *Proc., Coastal Eng.*, JSCE, Vol. 44, pp. 296-300 (in Japanese).

Salvetti, M. V. and Banerjee, S. (1995). "A priori tests of a new dynamic subgrid-scale model for finite difference large-eddy simulations", *Phys. Fluids*, Vol. 7, No. 11, pp. 2831-2847.

Tonkin, S., Yeh, H., Kato, F. and Sato, S. (2003). "Tsunami scour around a cylinder," *J. Fluid Mech.*, Vol. 496, pp. 165-192.

Uda, T., Omata, A. and Yokoyama, Y. (1987). "Experimental study on tsunami run-up – the effects of coastal topography and structures against tsunami run-up," *Technical Note of Public Works Research Institute*, No. 2486 (in Japanese).

Zang, Y., Street, R. L. and Koseff, J. R. (1993). "A dynamic mixed subgrid-scale model and its application to turbulent recirculating flows," *Phys. Fluids A*, Vol. 5, No. 12, pp. 3186-3196.

Study on Beach Profile Change of Ida Beach of Shichiri-Mihama Coast

Norimi Mizutani[1], Hyun-Ho Ma[2], Shu Eguchi[3]

[1] *Dept. of Civil Engineering, Nagoya University, Furo-cho, Chikusa-ku, Nagoya 464-8603 Japan*
[2] *Marine Research Institute, Samsung Heavy Industries Co.,Ltd, 530, Jangpyeong-ri, Sinhyeon-up, Geoje, Kyeongsangnam-do, 656-717, Korea*
[3] *Nagoya City Government, 3-1-1 Sannomaru, Naka-ku, Nagoya 460-8508 Japan*

Abstract

In this study, the velocity inside the breaking zone over permeable beach has been measured in laboratory experiments. Beach profile changes are also measured for different types of bed materials. Considering the balance of wave force acting on a bed material and restoring force, the mechanism of the sediment movement and resultant beach profile are investigated. It is revealed that the mechanism of beach profile change and types of sediment transport can be well explained by considering wave forces on bed materials.

1. INTRODUCTION

Ida beach of Schiri-mihama coast, which locates the southern part of Mie Prefecture, Japan suffers from severe beach erosion. There may be several reasons causing the beach erosion, however, quantitative estimation of each cause is difficult. It is very important to protect the beach from the erosion and some countermeasures, like installation of artificial reefs and beach nourishment, have been conducted. However, situation is not improved and beach erosion is still remained as severe problem. To establish an effective countermeasure, it is important to investigate the mechanism of sediment movement in relation with the flow field. It is known that the complicated flow field is formed in onshore side of breaking zone and wash zone.

Ida beach (Fig.1) is a gravel beach consisting of sand and gravel mixture. It is also well known that the grading occurs in the beach consisting of sand and gravel (e.g., Yoshida et al, 2002; Mizutani et al, 2003). Main cause of the grading can be attributed to the coexistence of different types of sediment movement according to the grain size of bed materials. Underwater weight is one of the important factors because it governs the mode of sediment movement. However, how the underwater weight affects the sediment movement seems not to be discussed quantitatively.

In this study, the cantilever-type velocimeter which has been developed to measure the velocity inside the breaking zone (Iwata et al, 1983) is manufactured, and then it is used to measure the velocity in the breaking and swash zones. Beach profile changes are also measured for different types of bed materials. Considering the balance of wave force acting on a bed material and restoring force, the mechanism of the sediment movement and resultant beach profile are investigated.

2. LABORATORY EXPERIMENTS

2.1 Experimental equipments and procedure

The experiments are conducted using a two-dimensional wave tank (30-m length, 0.7-m width, 0.9-m depth) at Nagoya University. As shown in Fig.2, an impermeable beach with a slope of 1:7 has been constructed in the flume, which starts 18.6m from the wave generator. On this slope, different types of permeable beach have been made with different materials such as sand, gravel and mixture of both. Water depth on the horizontal bottom is 0.4m for all experimental runs. Regular waves (H_i=6cm, T=1.7s)

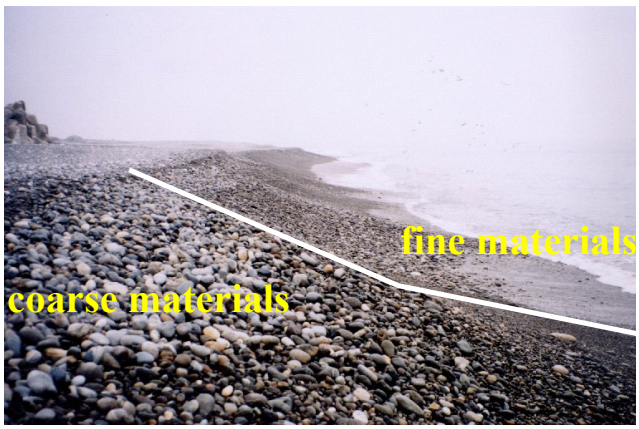

Fig.1 Photo of Ida beach

is generated and the hydrodynamics and movement of bed material in surf zone are investigated.

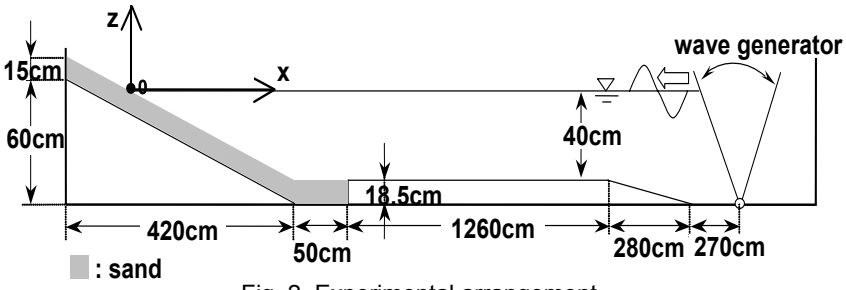

Fig. 2 Experimental arrangement

To measure the velocity distribution in breaking and swash zones, the permeable beach has been made using a gravel of d_{50}=5mm. The thickness of permeable beach has been changed in two ways (d=8cm and 15cm). To keep the initial beach profile during the velocity measurements, the metal mesh has been installed on the permeable bed during the measurements. In the measurements, the cantilever-type velocimeter (Iwata et al, 1983) has been used. Measurements have been done at 3cm interval from run-up point to x=120cm and 6cm interval from x= 120cm to x=150cm in horizontal direction and 3cm intervals from bottom to z=6cm and 6cm intervals from z=6cm to surface in vertical diection. A schematic diagram of the velocity measuring points is shown in Fig. 3.

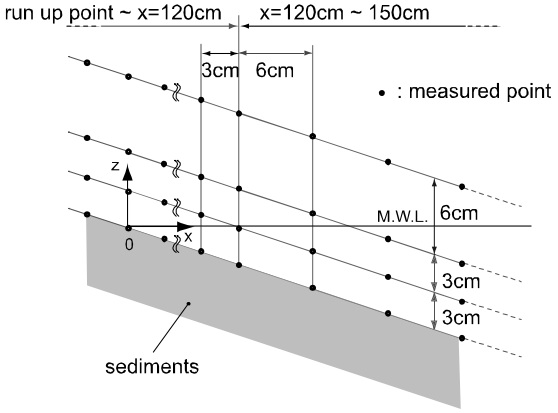

Fig. 3 Measuring point of velocity

In the experiments of the beach profile change, time variation of the beach profile and sediment transports have been investigated. In these experiments, waves have been generated for 6 hours. In this series of experiments, to discuss the effects of size and density of bed materials on the beach profile change and sediment transport, four kinds of beach of different bed conditions have been tested, that is, two kinds of single-layered beach made of fine and coarse materials respectively, and two kinds of mixed materials, that is mixture of fine material and coarse material with same density and mixture of materials with different density but same diameter. Bed materials used in these cases are follows; sand (d_{50}=0.1mm, ρ=2.65g/cm^3), gravel (d_{50}=5mm, ρ =2.65g/cm^3) and plastic ball (d_{50}=5mm, ρ =1.81g/cm^3). In Table 1, the bed conditions are summarized, where the initial bed profiles in all cases are uniform slope of 1/7.

Table 1. Bed conditions in experiments

Bed condition	material size (mm)	density (g/cm^3)	layer thickness(cm)
Single-layered	0.1	2.65	15
Single-layered	5	2.65	8, 15
Mixed	0.1 and 5	2.65	15
Mixed	5	2.65 and 1.81	15

In each experimental run, water surface elevations at two different points were measured by the capacitance-type wave gages to check the incident wave parameter. And beach profile changes at 0.5, 1, 3, 6 hrs after wave generation have been measured with sand profile meter. Also the movement of bed materials has been recorded by video to analyze the sediment transport.

3. EXPERIMENTAL RESULTS AND ANALYSIS

3.1 The variation of beach profile

Processes of beach profile change are shown in Fig.4 (beach of fine material) and Fig.5 (beach of coarse material). The beach of fine material is subjected to erosion type deformation caused by the offshoreward sediment movement in the swash zone and breaking zone. On the other hand, the beach of

coarse material presents an accretion type deformation caused by the onshoreward sediment movement in the surf zone. It takes about 30minutes for the beach deformation of coarse material to reach an equilibrium profile. On the other hand, beach profile of the fine material doesn't reach its equilibrium state even after 3hours and more.

The equilibrium beach profiles of gravel beaches with two different thickness and beach of mixture of gravel and plastic ball are shown in Fig.6. In the all of the equilibrium beach profiles, it is seen that the erosion occurs in surf zone and accumulation occurs in the swash zone. The beach profile observed in the swash zone is quite similar to that observed in real gravel beach as shown in Fig.1. It is interesting that erosion and accumulation are more in thicker beach than thinner one.

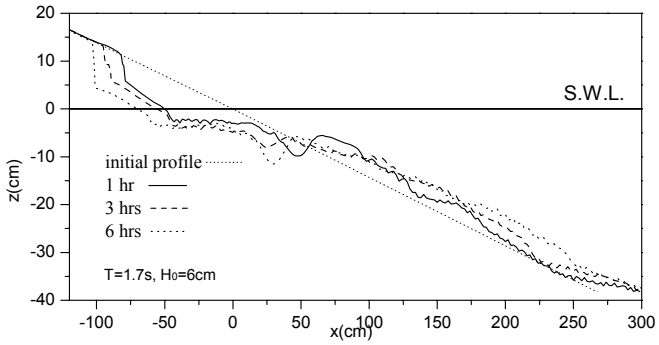

Fig. 4. Deformation process with time (single-layered sand beach)

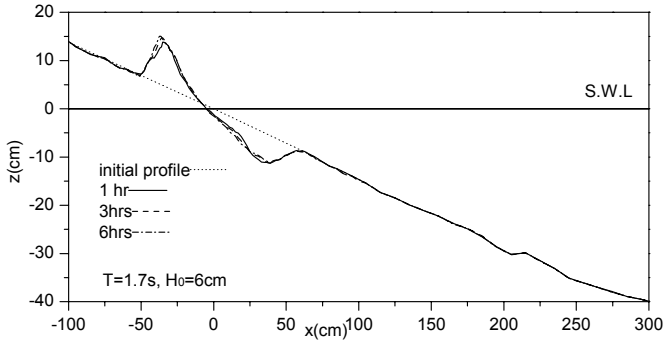

Fig. 5. Deformation process with time (single-layered gravel beach)

3.2 Hydrodynamics of surf and swash zone

The distributions of the measured maximum onshore and offshore velocities along the beach surface are shown in Fig.7. In the figure, it is obvious that the magnitude of the onshoreward velocity is larger than that of the offshoreward velocity. This indicates that the larger wave force in the direction of onshoreward than that in the direction of offshoreward acts on the bed materials. The values of the maximum onshoreward velocities are little larger than those of the offshoreward in the surf zone, while the difference between onshoreward and offshoreward velocities are much larger in the swash zone. This tendency is prominent in case of thick layer beach (d=15cm) than that of thin layer beach (d=8cm) as shown in Fig.7.

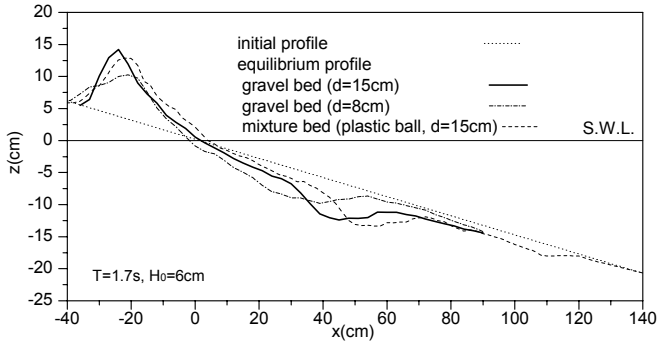

Fig. 6. Equilibrium profile of gravel beach

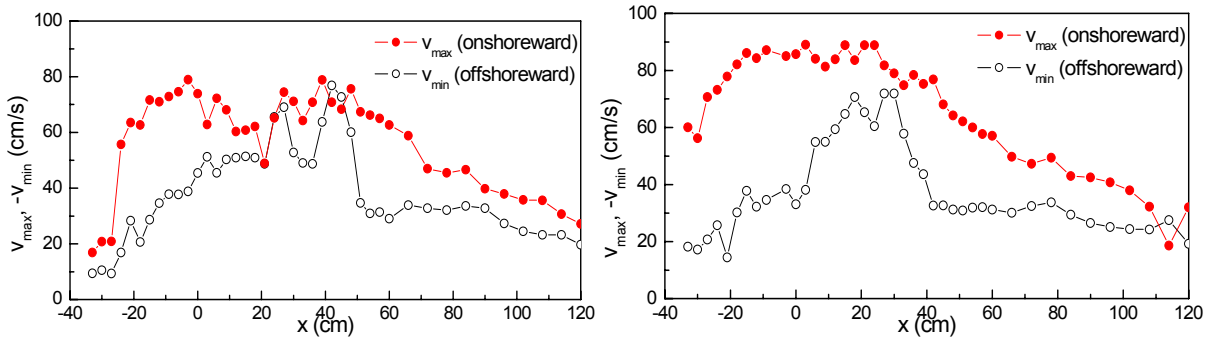

(a) d=8cm (b) d=15cm

Fig. 7. Maximum velocity distribution along the bed

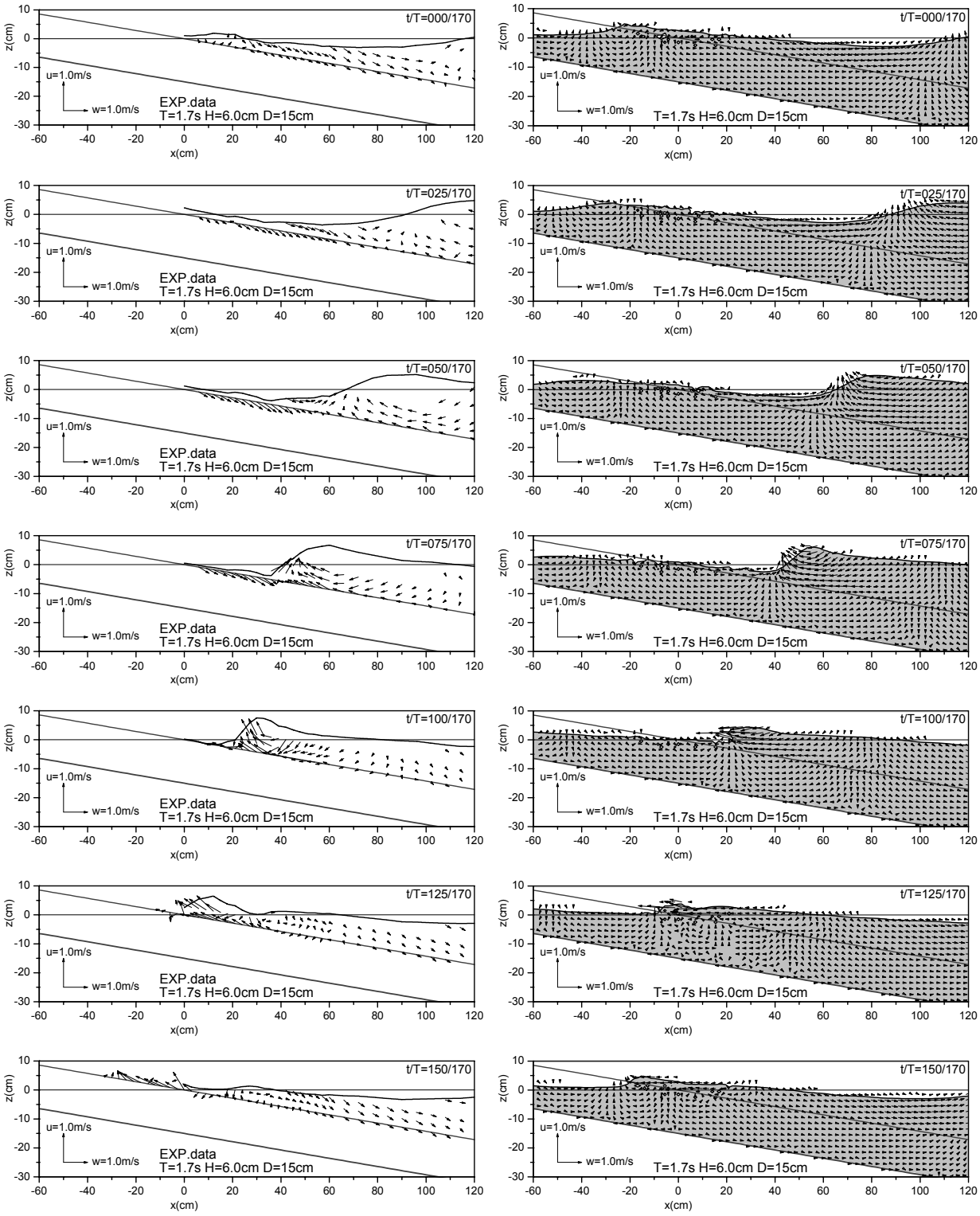

Fig. 8. Distributions of instantaneous measured velocity (Left:measured, Right:simulated)

The distributions of instantaneous velocity vectors above the beach of layer thickness of 15cm are shown in Fig. 8. The velocity vectors are obtained by taking phase average over five wave periods. Based on the video images and observation in the experiments, the run-rush meets wave run-up around x=45cm , then they generate the vortex and wave breaking occurs when wave crest is passing there. Velocity vectors at t/T=050/170~t/T=100/170 shows formation of vortex when the wave crest is passing x=45cm. Then, the maximum onshoreward velocity appears just after the wave breaking (t/T=125/170). It is noted that the infiltration flow (velocity toward inside permeable layer) exists during wave run-down. This may reduce

the amount of the run-down flow on the beach surface, which results in the difference of onshoreward and offshoreward velocity magnitude shown in Fig.7.

4 STABILITY OF SEDIMENT AND WAVE FORCES

Mizutani et al. (1994) discussed the stability of spherical armor units of the submerged breakwater by considering the acting wave force and resistance force due to its own weight. Stability of bed material is also treated in the same manner by assuming a spherical shape. Two idealized spherical sediment motions are considered here, that is rotating and suspension movements. The rotating movement takes place when overturning moment acting on the sediment overcomes the restoring moment. On the other hand, the suspension movement occurs when the uplifting force is larger than the normal resisting force.

Two typical placement referred as Case-1 and Case-2 are considered. These arrangements are based on the analysis of movement on a given geometry of four spherical materials of the most densely packed arrangement as shown in Fig.9. For rotating movements, the spherical material resting on the top of the pyramid formed by the assemblage of these four spherical materials requires a much greater external force to move the sphere along the median line connecting the vertex of the triangle (Case-2) than to move the spherical material along the median line connecting the base of the triangle (Case-1). Stability conditions are summarized as follows (Mizutani et al, 1994);

a) Case-1

$$W_b \cos\alpha \geq Fz \quad \text{(for suspension)} \tag{1}$$

$$(W_b \cos\alpha - Fz)\sin\beta \geq (W_b \sin\alpha - Fx)\cos\beta - (2\varepsilon/D)Fx \quad \text{(for rolling down)} \tag{2}$$

$$(W_b \cos\alpha - Fz)\sin\beta \geq 2[(Fx - W_b \sin\alpha)\cos\beta + (2\varepsilon/D)Fx] \quad \text{(for rolling up)} \tag{3}$$

b) Case-2

$$W_b \cos\alpha \geq Fz \quad \text{(for suspension)} \tag{4}$$

$$(W_b \cos\alpha - Fz)\sin\beta \geq 2[(W_b \sin\alpha - Fx)\cos\beta - (2\varepsilon/D)Fx] \quad \text{(for rolling down)} \tag{5}$$

$$(W_b \cos\alpha - Fz)\sin\beta \geq (Fx - W_b \sin\alpha)\cos\beta + (2\varepsilon/D)Fx \quad \text{(for rolling up)} \tag{6}$$

Assuming that the transverse force acting on sediments can be negligibly small compared with inline forces (drag and inertia forces), Morison equation can be applicable to estimate the forces acting on a bed material as follows;

$$F_x = \frac{1}{8}C_{Dx}\rho\pi D^2 u\sqrt{u^2+w^2} + \frac{1}{6}C_{Mx}\rho\pi D^3\dot{u} \tag{7}$$

$$F_z = \frac{1}{8}C_{Dz}\rho\pi D^2 w\sqrt{u^2+w^2} + \frac{1}{6}C_{Mz}\rho\pi D^3\dot{w} \tag{8}$$

where F_x and F_z are the wave force in x(tangential)-direction and z(normal)-direction, respectively. C_{Dx} and C_{Dz} are the drag coefficients for x and z components, C_{Mx} and C_{Mz} are the inertia coefficients for x and z components, u and w are respectively the horizontal and vertical velocities, and $\dot{u}$ and $\dot{w}$ are the accelerations in corresponding directions. ρ is the density of fluid and D is the diameter of bed material.

The time variation of the wave force has been calculated by substituting the measured velocity and acceleration evaluated from measured velocity. The drag and inertia coefficient estimated by Iwata and Mizutani (1989) are adopted.

Fig.10~13 give comparisons between time variations of the force acting on a bed material and stability limits for three modes of movements, in which both typical two arrangements, Case-1 and Case-2, are con-

sidered. The stability limits were computed based on the assumption that the wave force is acting all over the exposed spherical materials (ε=0) and the friction force is considered to be negligibly small as compared to the other forces (μ=0). Also, in the figures, normal and tangential wave forces are normalized by underwater weight of bed material.

As shown in Fig.10, in the surf zone like x=36cm, difference in the magnitudes of onshoreward and offshoreward forces are not so large and wave forces exceed the limitations for both onshoreward and offshoreward rotations, without exceeding the limitation of suspension. This indicates that the bed material motion is bed load and it oscillates onshore and offshore directions. In the swash zone like x=-24cm shown in Fig.11, the onshoreward wave force exceeds the onshoreward rotation limit, whereas the offshoreward wave force does not exceed any limit because of weakened velocity due to the infiltration occurred in the swash zone.

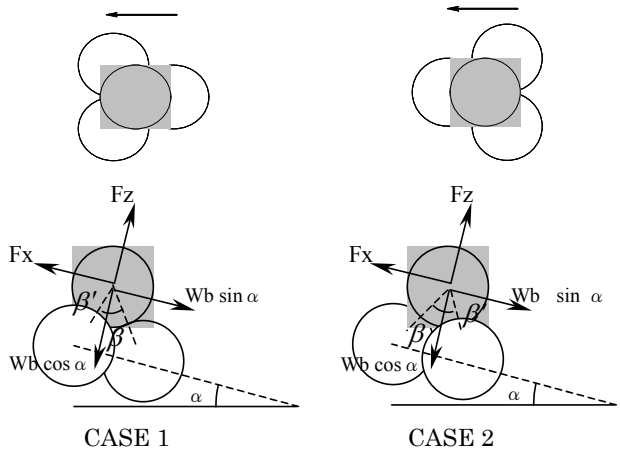

Fig. 9. Assumed arrangement of ideal bed material

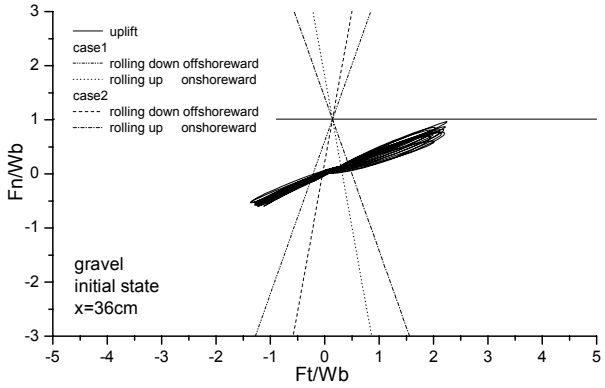

Fig.10 Comparison between stability limit and wave force (gravel , x= 36cm)

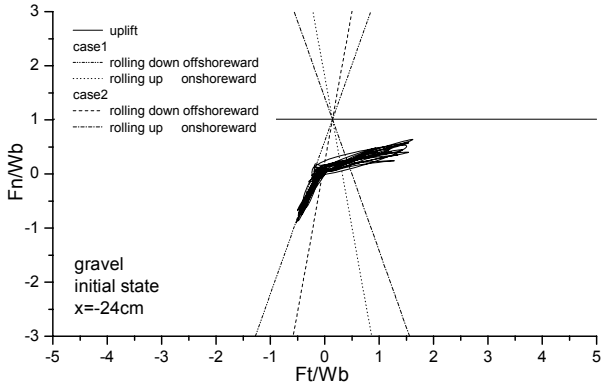

Fig.11 Comparison between stability limit and wave force (gravel , x= -24cm)

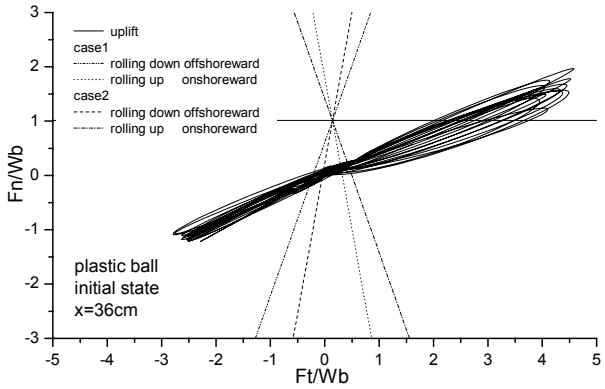

Fig.12 Comparison between stability limit and wave force (plastic ball , x= -24cm)

This implies that the onshoreward sediment transport is dominating in the swash zone, and therefore the precipitous beach profile shown in Fig.5 is formed. The effect of the infiltration is more significant when the thickness of beach is large. Thus, the slope of the beach with 15cm thickness is more precipitous as seen in Fig. 6.

Fig.12 shows comparison of the stability limits for sediment movements and wave forces acting on a plastic ball. As shown in Fig.12, in the surf zone like x=36cm, the the magnitude of dimensionless onshoreward and offshoreward wave forces are larger than those of gravel as shown in Fig.11, and wave force exceeds the limitation of suspension. Thus, this material is easily suspended and moved offshoreward by return flow. Moreover, in the swash zone like x=-24cm, the wave force acting on a plastinc ball in offshoreward as well as onshoreward exceeds the rotating limit and it moves both onshoreward and offshoreward, although the corresponding figure is not shown here. Because of these properties, the plastic ball is spread over the gravel by wave excitation as shown in Photo 1.

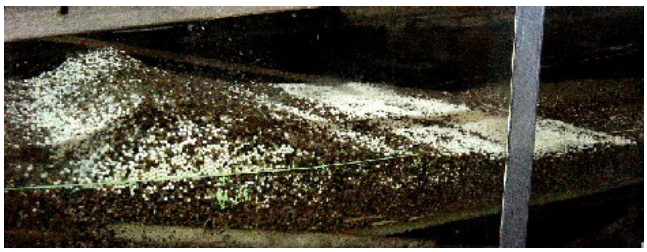

Photo 1 Graded process of mixture bed (gravel and plastic material)

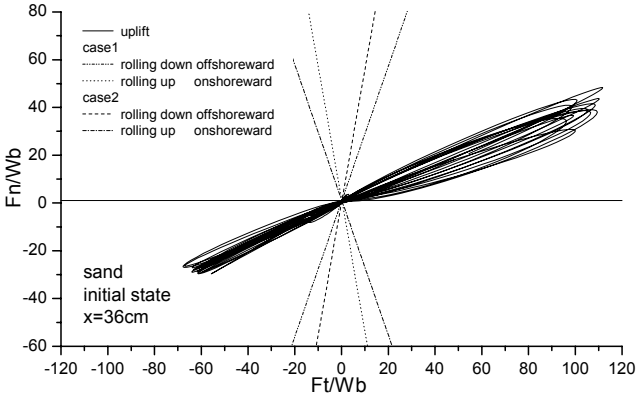

Fig.13 Comparison between stability limit and wave force (sand, x= -24cm)

Such a comparison for gravel on the equilibrium beach is shown in Fig. 14. Above the still water level, beach slope becomes steep and limitation of rolling motions shift to right. Under this condition, wave force easily exceeds the limitation for rolling down, which forms equilibrium beach profile.

Fig.15 shows measured cross-shore profile of Ida beach above the water level. The profiles observed at Ida beach are very similar to those obtained in the experiments (Fig.5 and Fig.6). Thus, the mechanism explained by Fig.9 through Fig.13 can be applicable to Ida beach. Fig.16 shows the simulated mean flows in gravel beach. It is noted that the circulation flow in the counterclockwise direction is formed. This circu-

lation flow plays an important roe in forming the beach profile shown in Fig.5 and Fig.6. In other words, infiltration flow above the still water level and exfiltraion flow around a breaking point encourage the accretion.

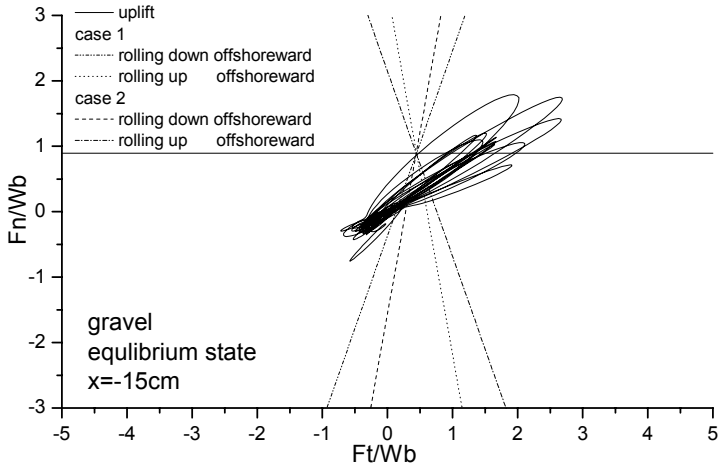

Fig.14 Comparison between stability limit and wave force (gravel, x= -15cm, equilibrium state)

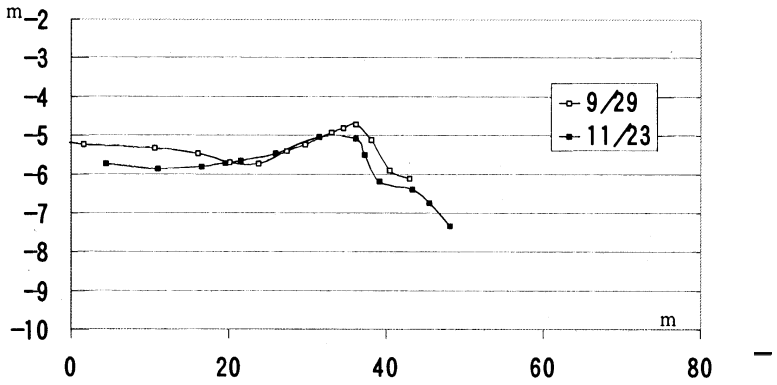

Fig.15 Measured beach profile at Ida beach

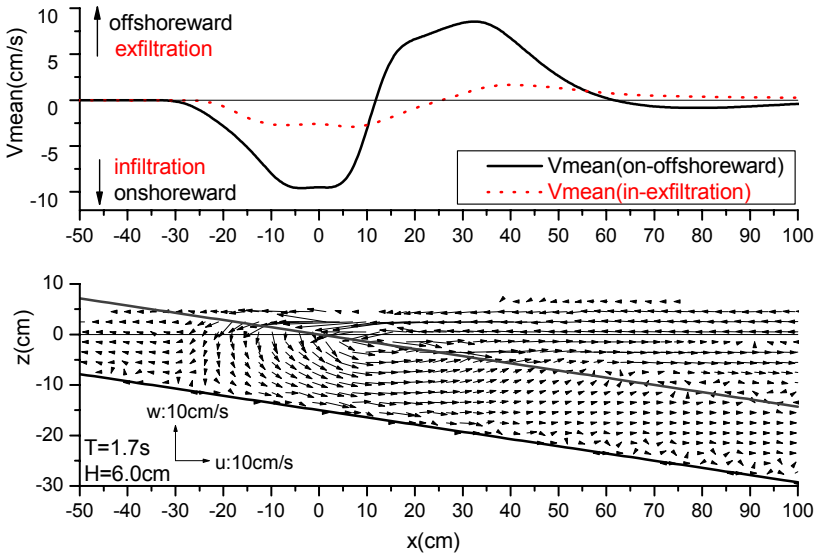

Fig.16 Simulated mean flow

5 CONCLUDING REMARKS

Hydrodynamics in the surf and swash zone is investigated based on the measured and simulated velocity by cantilever-type velocimeter. To analyze the sediment movement, the wave forces acting on bed materials are estimated with measured velocity, and then they are compared with theoretically derived stability limits for idealized spherical sediment. Analysis gives good explanation of sediment movement and resultant beach profile. Investigation in this study suggests that the wave force on bed material is important to consider the beach profile change. Moreover, it is found that the infiltration flow plays an important role on sediment movement of the beach.

References

Iwata, K. and N. Mizutani, N. 1989. Experimental Study on Wave Force Acting on a Submerged Sphere, Proc. of 8th International Conference on Offshore Mechanics and arctic Engineering, ASME, Vol.3, pp.145-152.

Iwata, K., H. Koyama and S. Futoh: Experimental Study on Variation of Wave Energy after Breaking, Proceedings of 30th Japanese Conference on Coastal Engineering, JSCE, pp.10-14 (in Japanese).

Mizutani, N., T.M. Rufin, Jr. and K. Iwata. 1994. : Stability of Armor Stones of a Submerged Wide-crown Breakwater, Proc. of 24th International Conference on Coastal Engineering, ASCE, 1439-1453.

Yoshida, E., S. Araki, I. Deguchi and T. Ikeda. 2002. : Sorting of Bed Material on Mixed Grain Size Beach and Topography Change, Proceedings of Coastal Engineering, JSCE, Vol.49, pp.461-465 (in Japanese).

Mizutani N., Ma H. H., Eguchi S. (2003): An experimental Study on the Beach Profile Change and Grading Process of Beach Material, Proc. 13th ISOPE, Vol.III, pp.862-867.

A Numerical Model for Gravel Beach Deformation Based on Two-way Method

Kwang-Ho Lee[1], Norimi Mizutani[2], Toshikai Fujii[3]

[1] *Department of Civil Engineering, Nagoya University, Nagoya, Japan.*
leekh@civi.nagoya-u.ac.jp
[2] *Department of Civil Engineering, Nagoya University, Nagoya, Japan.*
mizutani@civi.nagoya-u.ac.jp
[3] *Department of Civil Engineering, Nagoya University, Nagoya, Japan.*

Abstract

Fluid motions of waves interact with bed materials mainly through the bottom shear stress caused by water particle velocity near the bottom, which leads to topographical changes. The altered bottom profile, in turn, affects the wave fields, and changes in these fields can lead sequential bottom profile change. Most of the studies on the sediment problems, however, have not considered the effects of the altered bottom profile on wave fields. To predict topographical changes more accurately, the changed bottom profile should be reflected in calculation of wave fields over time, i.e., the two-way method is required. In this study, a numerical model considering dynamic interactions between wave fields and topography change caused by on-offshore sediment transports is proposed to estimate the topographic change of gravel beaches. The model is composed of a wave model and a sediment model. Comparison between numerical and existing experimental results showed that the present model is useful to simulate wave fields and beach topographical change of gravel beaches.

KEY WORDS: Topographic change, sediment, two-way method, gravel beach, wave field

INTRODUCTION

Beach erosion caused by broken coastal balance is one of the serious important problems and of large interest in coastal engineering. So far, various attempts have been made to assess beach deformations. However, it is not simple to simulate beach morphodynamics directly because of the complexity of the underlying mechanisms involved in sediment transport. Therefore, most numerical models for predicting beach evolutions are based on the quantitative relationships for the sediment transport and fluid motion, mainly established by laboratory experiments. As a consequence, various empirical and semi-empirical formulations have been proposed, and used to achieve topographic changes in most numerical investigation. For example, Madsen and Grant (1976) found a relationship between an averaged sediment transport rate and the Shields parameter under unidirectional flow. Watanabe(1981) and Watanabe et al. (1984) proposed the semi-empirical sediment transport equation considering the effect of return flow, and developed the three-dimensional beach deformation model under wave-current coexistence fields. Shibayama and Horikawa (1982) performed laboratory and field investigations to formulate a predictive model of two-dimensional beach profile change, and proposed sediment formula based on the observed transport patterns. Sato and Kabilling (1994) found the sediment transport equation capable of calculating the instantaneous local sediment transport rate with time development according to the bed load and suspended load of sediment transport, and succeeded in predicting sediment transport in the swash zone. Pedrozo-Acuña et al. (2006) applied the sediment transport equation considering the effect of slope corrections and friction angle by revising the formula for sediment transport rate proposed by Meyer-Peter and Muller (1948) to gravel beaches. Also, from a sensitivity analysis, they showed that the topographic changes could be reproduced to some degree although it couldn't get enough quantitative agreement between experimental and calculation profile. However, most numerical process-based models currently used for predicting beach profile are based on a one-way method in which topographical change is updated based on the information of already computed fluid motions, i.e., in these approach, the effects of the altered bottom profile on fluid fields or vice versa are perfectly neglected. The alternative to the one-way method is the two-way method in which the dynamic interaction between fluid motion and sediments can be considered through feedback process between two phenomena. Generally, fluid motions of waves interact with sediments mainly by the means of the bottom shear stress caused by water particle velocity near the bottom, which leads to topographical changes. The altered bottom profile, in turn, affects the flow fields, and changes in these fields can lead to further alterations of the bottom profile. Therefore, to predict gravel

beach deformation more exactly, the changed bottom profile should be reflected when calculating fluid fields over time.

Only very recently a limited number of numerical investigations have considered the fluid-sediment interactions in morphodynamic model to predict the evolution of the bed. Liang et al. (2005) proposed the two-way-based numerical model for assessing local scour below offshore pipelines under the unidirectional steady flow. Kuroiwa et al. (2007) developed a coastal area model, based on the depth-averaged nearshore current model, to predict shoreline changes and formation of sand bar, sand spits around river-mouth under various wave and river flow conditions. In these models, however, movable seabed was considered impermeable because of the relatively low permeability of sand beach; the effects of in- or ex-filtration on beach face were neglected. In particular, these flows on beach face with high permeability may influence sediment motion (Conley and Inman, 1994; Nielsen, 2001, Lee et al, 2007). Therefore, these models are unsuitable for predicting gravel beach deformation. Most previous studies mainly confine their objects for discussion to sandy beach, and gravel beach models are fewer in number. Within the limits of authors' knowledge, the modeling for gravel beach deformations based on two-way method has not been performed. In this paper, a new numerical model is presented based on the two-way method to predict cross-shore deformation of gravel beach. In this proposed model, the changed bottom profile can be reflected when calculating flow fields over time, and thus accurate assessment of sediment transport can be achieved. The newly developed beach deformation model is validated through the comparisons with existing experimental results (Lee et al., 2007).

HYDRODYNAMIC MODEL

The numerical model developed in this study is comprised of a hydrodynamic model to analyze the fluid fields and a sediment model to predict the bottom topography. The basic approach for the hydrodynamic model is similar to that of Hur and Mizutani. (2003) except the computational scheme for the pressure. This section introduces the description for modeling methodology for fluid fields.

Governing Equation

In hydraulic model, the governing equations express the continuity equation (1) and the unsteady incompressible Navier-Stokes equation (2). The free surface is traced by Eq. (3) in terms of the volume of fluid (VOF) function, F, which represents the rate of volume in a cell occupied by the fluid to the whole volume of the cell.

$$\frac{\partial m u_i}{\partial x_i} - \widetilde{q} = 0 \tag{1}$$

$$\hat{m}\frac{Du_i}{Dt} = -\frac{1}{\rho}\frac{\partial p}{\partial x_i} + \nu\frac{\partial^2 u_i}{\partial x_j \partial x_j} - R_i - g_i - \beta u_j \delta_{j3} + \frac{\nu}{3m}\frac{\partial \widetilde{q}}{\partial x_i} \tag{2}$$

$$\frac{\partial mF}{\partial t} + \frac{\partial (Fmu_i)}{\partial x_i} = F\widetilde{q} \tag{3}$$

where u_i is the velocity vector, t is time, p is the pressure, ρ is the fluid density, g_i is the acceleration due to gravity, m is the porosity in porous medium, β is a wave dissipation factor that equals zero except the wave dissipation zone, ν is the dynamic viscosity, R_i is the resistance force, F is the VOF function varying at the range of $0 \le F \le 1$, and $\widetilde{q}$ is the source term for generating waves with flux density q at the source position ($x = x_s$) and defined as

$$\widetilde{q}(y,z,t) = \begin{cases} q(y,z,t)/\Delta x_s & \text{at } x = x_s \\ 0 & \text{at } x \neq x_s \end{cases} \tag{4}$$

where Δx_s is the width in x-direction of the mesh including $x = x_s$. The resistance force, considering the size effect of porous media, is expressed as follows:

$$R_i = \frac{6C_{D2}\nu(1-m)}{m{d_{50}}^2}u_i + \frac{C_{D1}(1-m)}{2m^2 d_{50}}u_i\sqrt{u_j^2} \tag{5}$$

where C_{D1} and C_{D2} are non-linear and linear drag coefficient, respectively. Also, $\hat{m}$ is defined as

$$\hat{m} = 1 + C_M \frac{1-m}{m} \tag{6}$$

Numerical Implementation

The governing equations are discretized using the first-order forward time difference for the time derivative, the central difference for the pressure and stress terms, and the third-order Kawamura-Kuwahara scheme for the convection term. A two-step projection method, predictor-corrector procedure, is then used to solve the discretized governing equations. The temporary velocities $\tilde{u}_i^{n+1}$ at the next time step as follows:

$$\frac{\tilde{u}_i^{n+1} - u_i^n}{\Delta t} = \begin{bmatrix} -u_j \dfrac{\partial u_i}{\partial x_j} + \hat{m}^{-1}\nu \dfrac{\partial^2 u_i}{\partial x_j \partial x_j} - R_i - g_i \\ -\beta u_j \delta_{j3} + \dfrac{\nu}{3m}\dfrac{\partial \tilde{q}}{\partial x_i} \end{bmatrix}^n \tag{7}$$

where Δt is the time step size, and the superscript represents the time-level. The intermediate velocities, $\tilde{u}_i^{n+1}$, is the only unknown in above equation, and can therefore be computed explicitly. The correct velocity and pressure are then calculated with the following correction step.

$$\frac{u_i^{n+1} - \tilde{u}_i^{n+1}}{\Delta t} = -\hat{m}^{-1}\frac{1}{\rho^n}\frac{\partial p^{n+1}}{\partial x_i} \tag{8}$$

In above equation, the correct pressure, p^{n+1}, is the solution of the Poisson pressure equation (PPE) derived by substituting Eq. (7) for the continuity equation

$$\frac{\partial}{\partial x_i}\left(\frac{m}{\hat{m}\rho^n}\frac{\partial p^{n+1}}{\partial x_i}\right) = \frac{1}{\Delta t}\left(\frac{m\tilde{u}_i^{n+1}}{\partial x_i} - \tilde{q}\right) \tag{9}$$

In solving the PPE, however, the interpolation or extrapolation procedure is required because the actual free surface position is not always coincided with the definition position of the pressure in a cell. Natural coordinates (ξ, ζ) are used to obtain the correct pressures without complicate inter- or extrapolation near the free surface. The computational mesh is a uniform with spacing $\Delta\xi = \Delta\zeta = 1$. The use of natural coordinates permits finite difference methods to be effective in computational domains with complicated boundary shapes, primarily by making the boundaries coincide with particular generalized coordinate lines and thereby avoiding a local interpolation to implement the boundary conditions (Fletcher, 1991). Using the chain rule of partial derivatives and applying the relation between the computational cell and the Jacobian of the transportation, $J = (\partial x/\partial\xi)(\partial z/\partial\zeta)$, PPE can be expressed as:

$$\begin{aligned} &\frac{\partial}{\partial\xi}\left(\frac{m}{\hat{m}\rho^n}\dot{\alpha}\frac{\partial p^{n+1}}{\partial\xi} - \frac{m}{\hat{m}\rho^n}\dot{\beta}\frac{\partial p^{n+1}}{\partial\zeta}\right) \\ &+\frac{\partial}{\partial\zeta}\left(\frac{m}{\hat{m}\rho^n}\dot{\gamma}\frac{\partial p^{n+1}}{\partial\zeta} - \frac{m}{\hat{m}\rho^n}\dot{\beta}\frac{\partial p^{n+1}}{\partial\xi}\right) = \frac{1}{\Delta t}\left\{\frac{\partial}{\partial x_i}\left(\tilde{u}_i^{n+1}\right) - \tilde{q}\right\} \end{aligned} \tag{10}$$

where $\dot{\alpha}, \dot{\beta}$, and $\dot{\gamma}$ are the geometric coefficients defined as follows:

$$\dot{\alpha} = \left(\frac{\partial^2 z}{\partial\zeta^2} + \frac{\partial^2 x}{\partial\zeta^2}\right) \tag{11}$$

$$\dot{\beta} = \left(\frac{\partial z}{\partial\zeta}\frac{\partial z}{\partial\xi} + \frac{\partial x}{\partial\zeta}\frac{\partial x}{\partial\xi}\right) \tag{12}$$

$$\dot{\gamma} = \left(\frac{\partial^2 z}{\partial\xi^2} + \frac{\partial^2 x}{\partial\xi^2}\right) \tag{13}$$

Then, the advection of VOF function (3) is computed to reconstruct the free surface at a new time, based on the computed velocity. The above procedures are repeated in each time step, and wave fields are calculated with the time development. In addition, appropriate boundary conditions must be specified to numerically

SEDIMENT MODEL

As described earlier, the numerical description for the sediment movement is very difficult because of its complex mechanism. In this paper, to estimate sediment transport quantitatively, the sediment formula proposed by Pedrozo-Acuña et al. (2006) was adopted. This formula is able to assess the instantaneous sediment transport rate with considering slope corrections and friction angle for a moving grain, and thus it is suitable to estimate the cross-shore movement by feedback algorithm. Furthermore, only bed load transport, moving immediately above the bed, was considered in assessing the sediment transport rate due to the relatively large grain sizes on gravel beach, and given by

$$q_b(t) = \frac{C\sqrt{(s-1)gd_{50}^3}}{1+\dfrac{\tan\beta}{\tan\phi}} \max\left[\theta(t)-\theta_{\beta cr},0\right]^{3/2} \frac{u_b(t)}{|u_b(t)|} \tag{14}$$

where q_b is the bed load transport rate, C is the empirical sediment transport coefficient, s is the specific gravity, β is slope correction, ϕ is friction angle for a moving grain, d_{50} is the sediment median diameter, u_b is the bed velocity, and $\theta(t)$ and $\theta_{\beta cr}$ are the instantaneous and critical shields parameters, respectively, given by

$$\theta(t) = \frac{0.5\rho f (u_b)^2}{\rho g d_{50}(s-1)} \tag{15}$$

$$\theta_{\beta cr} = \frac{\tau_{\beta cr}}{\rho g d_{50}(s-1)} \tag{16}$$

where f is the bed friction factor caused by wave motion, $\tau_{\beta cr}$ is a threshold bed shear stress. The bed friction factor was calculated with Nielsen's formula (1992).

$$f = \exp\left\{-6.3+5.5\left(\frac{2.5d_{50}}{A_{ms}}\right)^{0.2}\right\} \tag{17}$$

where A_{ms} is the amplitude of orbital motion. Also, the critical $\theta_{\beta cr}$ is adjusted to consider the influence of the slope, using equations (17) and (18). These equations cope with the flow up and down the slope, respectively.

$$\frac{\theta_{\beta cr}}{\theta_{cr}} = \cos\beta + \frac{\sin\beta}{\tan\phi} \tag{18}$$

$$\frac{\theta_{\beta cr}}{\theta_{cr}} = \cos\beta - \frac{\sin\beta}{\tan\phi} \tag{19}$$

In these equations, it is clear that the critical shields parameter becomes large with flow up the slope and small with flow down. Form these approach, the amount of local sediment transport is calculated with time development. Bottom profile changes are then computed from the mass balance of the bed materials, given by

$$\frac{\partial z_b}{\partial t} = \frac{\partial q_b}{\partial x} \tag{20}$$

where z_b is the bed level including the bed porosity.

COUPLED MODEL

The hydrodynamic model and the sediment model are linked by feedback way, i.e., the computed results of each model are used to update the computational conditions mutually in each model. Since the flow motion and sediment interact at the same time, these two models have to be solved simultaneously. To do so, however, enormous calculation time is necessary, and this is impractical from an engineering perspective. To alleviate this burden, a time-marching scheme was used for linking the hydrodynamic model and the sediment mode. The concept of this scheme is basically the same as that in Liang and Cheng (2005). In the time-marching scheme, the time increment of the sediment model is far greater than that for fluid fields because the time scale of topographical changes is greater than that of fluid field changes.

In this approach, the fluid field is first simulated, and its limited information (i.e., from a limited number of wave cycles) is used in calculating the topographical changes as input data. In calculating the sediment model, the fluid fields are assumed to be steady state, i.e., some fluid field calculations are skipped. Using this time-marching scheme, it is possible to speed up the numerical calculation. In the present study, fluid fields for grave beach under wave attack are first computed for 10 periods to incident wave period, at which time the incident wave generated by the wave source had fully spread in the defined calculation area. After calculation for fluid fields, the topographic changes are updated with the sediment model for three minutes under the assumption fluid fields by wave are not extremely deformed for this time. Fig. 1 shows the comparison of the calculation procedure between the two-way method used in the current study and a one-way method.

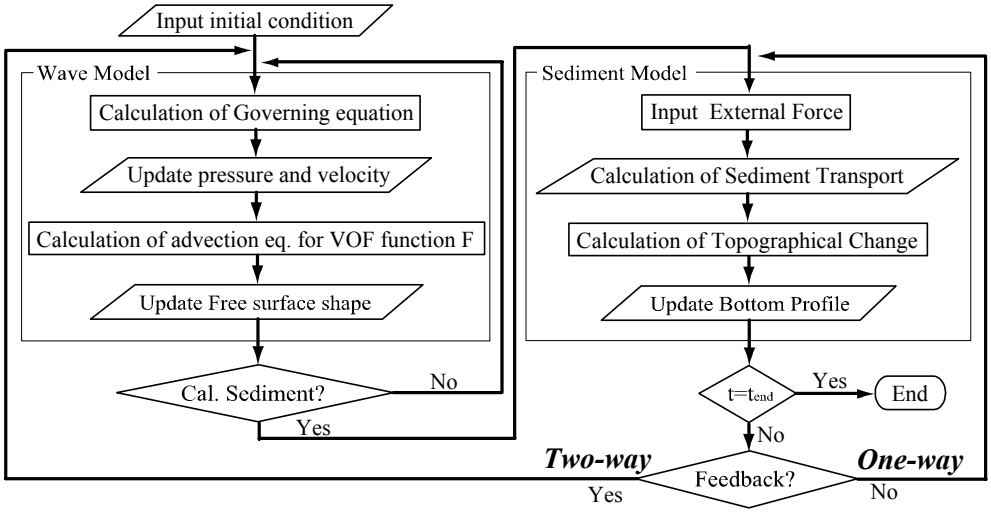

Fig. 1 Flow chart of computational procedure

RESULTS AND DISCUSS

Topographic Change

In order to survey the accuracy of the newly proposed numerical model for gravel beach deformations, the very much simplified representation of Ida beach, Shichiri-Mihama coast, Japan is applied as a test case.

The numerical simulation was performed within the numerical wave tank (NWT). The NWT is a powerful tool that can directly simulate the flow fields under conditions almost the same as in experimental tests without excessive effort required for laboratory experiments. In the NWT adopted in this study, several functional systems are equipped similar to those in a laboratory wave flume; i.e. a source to generate waves instead of a wave paddle in a real wave tank, an added fictitious dissipation zone as a wave absorber to prevent wave reflection at both the lateral open boundaries, and a VOF method for tracking the free surface of the water. Fig. 2 presents a schematic sketch of the NWT model used in this study. As shown in Fig. 2, the grid size in the added fictitious dissipation zone increased linearly to the lateral boundary of the NWT, whereas the uniform grids of $\Delta x = 2.0$ and $\Delta y = 1.0$ cm are used in the calculation region. Also, a gravel beach with initially uniform slope of 1:7 was considered as the initial movable bed condition. The averaged wave condition at Ida beach is adopted as the incident wave condition, the incident wave height

of $H_i = 6.0$ cm and a wave period of $T = 1.7$ s at a water depth of $h = 40.0$ cm. The still water depth was kept constant at 40 cm during the calculation.

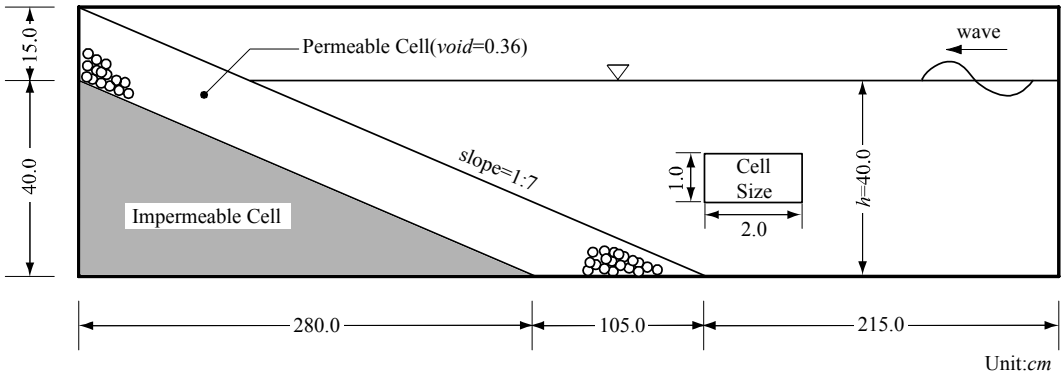

Fig. 2 Schematic illustration of the numerical wave tank

Fig. 3 gives a comparison for the topographical changes of gravel beach computed respectively by the one-way method and by the two-way method newly proposed in this study, after 1 hour of run time. The distance from the shoreline is normalized by the wavelength of the incident wave, L. For the comparisons with the laboratory experiment, the experimental result by Lee et al. (2007) is also presented simultaneously in figure. The consideration for the gravel beach deformation obtained by the laboratory experiments is useful to investigate the applicability of the newly developed numerical model because it allows the qualitative analysis. Mizutani et al. (2003) and Lee et al. (2007) found that gravel beach has the characteristics of the accretion type deformation by laboratory experiments, which is mainly caused by onshore sediment movement through surf zone, and there is little difference of the shore line between the initial condition and the end result. These deformation patterns on gravel beach are somewhat different to the erosive beach found previously for fine sandy beach. Also, the berm is formed in the upper portion of the shoreline ($-0.1 < x/L < 0.0$) and the slope toward offshore side is steeper than that of the other side. On the other hand, the beach surface below the still water depth ($0.0 < x/L < 0.2$) has a gentle slope compared to that of berm. As shown in Fig. 3, it is clear that both computed results reproduce these overall characteristics of gravel beach deformations well although the some quantitative differences in bed level are observed in both models. In particular, the predicted beach deformation and its range by the one-way method are far larger than the laboratory experimental result, whereas the predicted beach profile by the two-way method is closer to the laboratory experimental result. Moreover, the computed result by the two-way method and the experimental measurement agree well for the berm occurring position. These discrepancies between the two methods may result form the assessment of the instantaneous shields parameter used as the criterion of the incipient motion for the sediment particles; the one-way method overestimate the sediment transport rate because the predicted bed velocities under the initial beach slope are only used to assess the external force on the sediment particles, not considering the change of the fluid fields by the altered bottom profile. From the comparisons for the predicted beach profiles by two different models, it can be concluded that the two-way method gives more precise results for the beach deformation, i.e., consideration of the interaction between seabed and fluid fields through feedback may lead to more accurate prediction of the beach deformation.

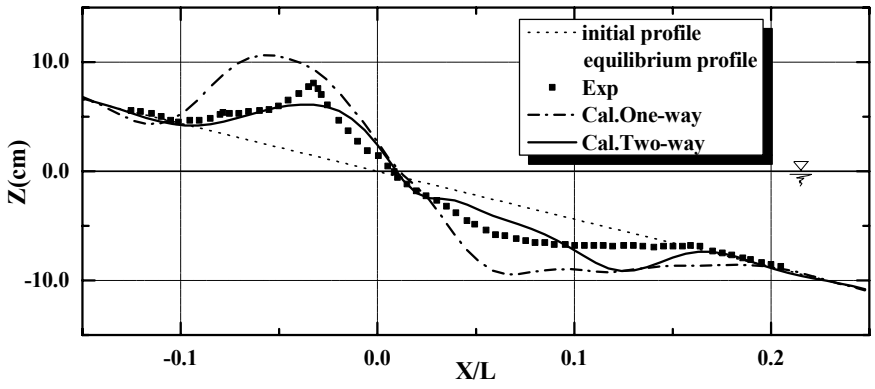

Fig. 3 Comparison of the topographical changes of gravel beach

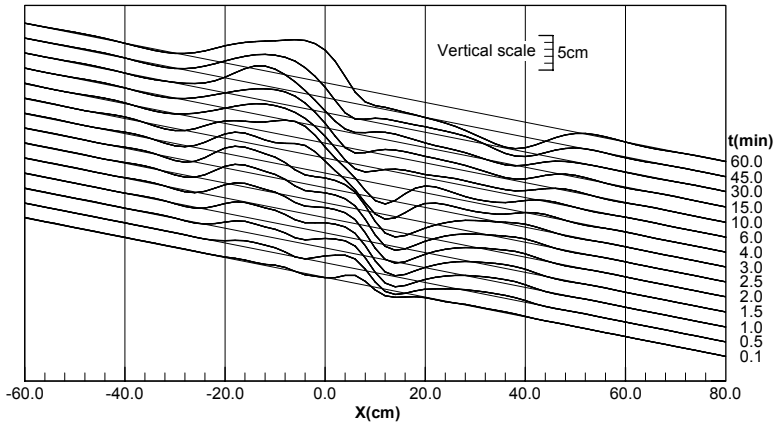

Fig. 4 Computed cross-shore profile as time develop

For more understanding for the progress of the gravel beach deformation with time development, the cross-shore profile was computed as time develop, based on the two-way method. Fig. 4 shows the time development of the computed cross-shore profile. The right axis shows the capture time of the beach profiles. This figure indicates that the first topographic change occurs by the strong velocities within the small range of the surf zone, where wave is breaking and wave-induced currents is generate, and deformational regime spreads gradually in the cross-shore direction with time development.

Time Development of Amount of Erosion

Fig. 5 presents the amount of erosion computed by two different models, the one-way method and the two-way method, with respect to time. The amount of erosion is computed by integrating the eroded part from the initial cross-shore shape in each time step. As seen, in the case of the one-way method, beach erosions are exponentially increased as time progress. Meanwhile, in the case of the two-way method, the beach erosion is rapidly increased with the calculation start, similar to that in the one-way method, but its increasing rate becomes gentle gradually as time progress. For this, a possible explanation is that in the two-way method the beach slope ranging from the top of the berm to the extremely erosive point approaches gradually a stable state caused by the movement of gravel, which lead to the decrease of the sediment rate. As already pointed out in the preceding section, however, in the one-way method because the predicted bed velocities under the initial beach slope are only used for predicting the sediment transport rate, the amount of the erosion continues to increase although the effect of the local slope is implemented in the sediment model.

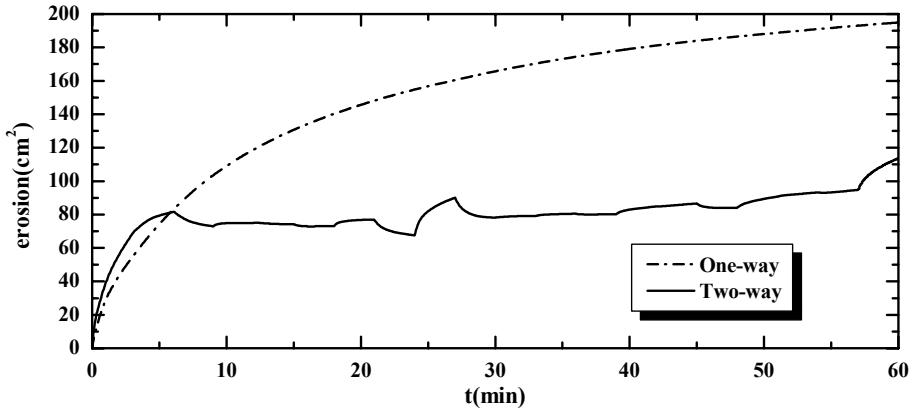

Fig. 5 Amount of erosion by the one-way and two-way method

The difference observed in the predicted results suggest that the approach based on the two-way method with feedback way presents the prospect for the prediction of an equilibrium beach profile, as shown in Figs. 4 and 5. But, local changes by an influence to feedback bottom profile around 45, 60 minutes occurs and discontinuous is recognized. More investigation is necessary for this point.

Time Development of Velocity Vector

The investigation of fluid fields under the different bed conditions may be helpful to understand beach deformations. In this section, to investigate the effect of beach profiles on fluid fields and vice versa, the flow motions by waves for the two different beach profiles, the initially uniform slope beach and the presumptive beach deformed by wave attacks, were simulated, using the proposed hydrodynamic model. In these calculations, the fixed-bed condition was used and the other calculation conditions including incident wave condition are the same to that in the previous section. Figs. 6(a) and (b) show the calculated velocity vector plots for each case over a wave cycle, respectively. Water surface configurations were plotted as the VOF function, $F = 0.5$, indicating the interface between water and gas (air) in the each computational cell. Also, the 15th wave cycle after generating wave the velocity fields was selected to capture fully developed velocity fields. As seen in Figs. 6(a) and (b), it is clear that the proposed numerical model reproduces the typical process of the wave deformations including wave breaking on the beach well in each model run. In both cases, the seaward flow due to backwash after wave breaking occurs at $t/T = 000/170 \sim 025/170$, leading to seaward sediment movements, and this flow collides with the seaward flow at $t/T = 025/170 \sim 050/170$. Subsequently, strong velocity components occur near the bottom at $t/T = 100/170$, which are concerned with the offshore sediment transport. As expected, however, some discrepancies in the flow motions are observed between two cases. Considering the velocity components in the breaker zone, the relatively stronger bottom velocity vectors are observed as compared to those in the case of the deformed beach. This implies that in the case of the uniform beach the exerting force acting on the sediment particles becomes larger, i.e., the morphologic evolution can be more active, and these sediment movements become difficult as topographic change proceeds. As a result, the morphologic evolution predicted by the two-way method with feedback way is smaller than that by the one-way method, as shown in Fig. 4. Also, these mechanisms can explain the difference in the amount of erosion in Fig. 5 discussed in the previous section. Significantly, in the case of the deformed beach, the strong up-rush and return flows parallel to the deformed beach surface occurs around $x =$ -20~20 cm at $t/T = 125/170$ and 150/170. These flows explain the berm formation and gentle beach slope beneath the still water depth in Fig 4. Furthermore, it is expected that as the beach slope steepens from the initial beach profile, the seaward sediment mobility is increased due to the decrease of the stabilizing force, which compensates the eroded beach profiles by the wave breaking and consequential up-rush.

CONCLUSIONS

In this paper, the coupled numerical model linking a hydrodynamic model and a sediment model has been proposed to simulate cross-shore deformations on a gravel beach. The difference from existing beach deformation models is in the consideration of the interaction between fluid fields and sediments based on the two-way method. In the hydrodynamic model, the modified governing equations based on a porous model have been used to describe the flow motions within the porous media of a gravel beach. The quantitative relationships for the sediment particles and the external force by flow motions have been utilized in the sediment model. These two models are successfully linked by the time-marching scheme. The analysis capability of the proposed two-way method on the prediction of gravel beach profiles has been compared to available experiment results. Although quantitative agreement between the computed profiles and the measurements by the laboratory test is not fully satisfactory, it has been concluded that the newly developed model based on the two-way method greatly improves prediction of the gravel beach profiles. Furthermore, the bed profile during the computation converged on an equilibrium profile for the two-way method.

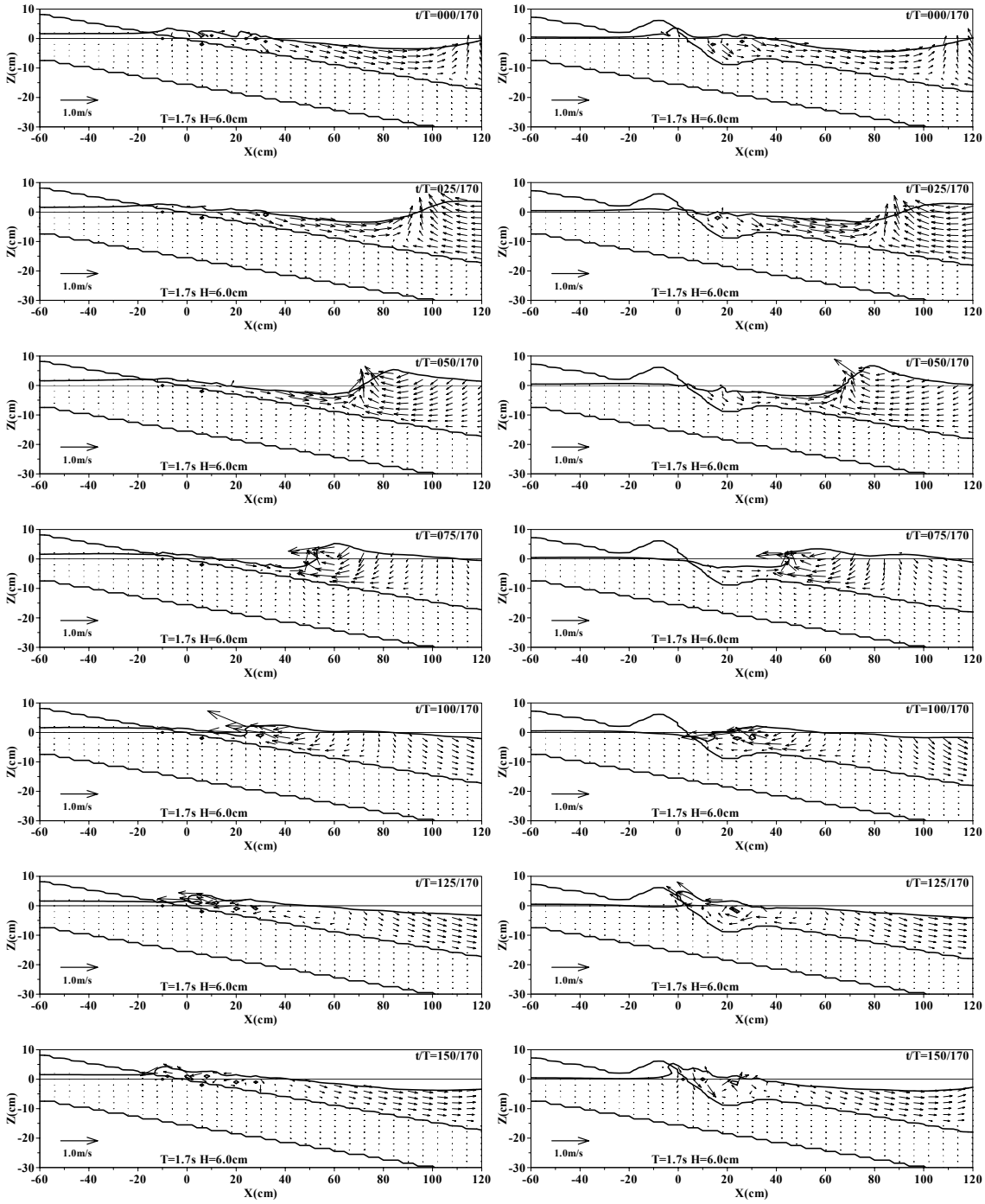

(a) initial bed profile (b) deformed bed profile

Fig. 6 Velocity vector fields under the different bed profile

References

Conely, D.C., Street, R.L. (1994) "Ventilated oscillatory boundary layers" *Journal of Fluid Mechanics*, Vol. 273, pp.261-284.

Fletcher, C.A.J. (1991) "Computational Technique for fluid dynamics: Volume 2" *Springer-Verlag*, 494p.

Hur, D.S. and Mizutani, N. (2003) "Numerical estimation of the wave forces acting on a three-dimensional body on submerged breakwater", *Coastal Engineering*, Vol. 47, pp. 329-345.

Lee, K.H., Mizutani N., Hur, D.S. and Kamiya, A. (2007). "The effect of groundwater on topographic

changes in a gravel beach", *Ocean Engineering*, Vol. 34, pp. 605-615.
Madsen, O.S. and Grant, W.D. (1976). "Quantitative description of sediment transport by waves", *Proc. 15th Coastal Eng. Conf.*, pp. 1093-1112.
Meyer-Peter, E. and Müller, R. (1948) "Formulas for bed load transport", *2nd Congress of the Int. Association of Hydraulics Structures Res., Stockholm, Sweden*.
Mizutani, N., Ma, H.H, Eguchi, S. (2003) "An experimental study on the beach profile change and grading process of beach material", *Proceedings of the 13th International offshore and Polar Engineering Conference, ISOPE*, pp.864-869.
Nielsen, P., Robert, S., Moller-Christiansen, B., Oliva, P. (2001) "Infiltration effects on sediment mobility under waves" *Coastal Engineering*, Vol. 42, pp.105-114.
Nielsen, P. (1992) "Coastal bottom boundary layers and sediment transport" *Advanced series on Ocean Engineering Volume 4*, World Scientific, 324p.
Kuroiwa, M., Kuchiishi, T. and Matsubara Y. (2007) "Numerical simulation on 3d morphodynamic around river-mouth" *Annual Journal of Civil Engneering in the Ocean, JSCE*, Vol. 23, pp.1177-1181.
Liang, D. and Cheng, L. (2005) "Numerical modeling of flow and scour below a pipeline in currents: Part 2. Scour simulation", *Coastal Eng.*, Vol. 52, pp.43-62.
Sato, S. and Kabiling, M. (1992) " Numerical simulation of nonlinear wave interacting with permeable breakwaters", *Proc.39th Conf. on Coastal Eng., JSCE*, Vol. 41, pp. 401-405.
Shibayama, T. and Horikawa, K. (1982) "Sediment transport and beach transformation", *Proc. 18th Coastal Eng. Conf.*, pp. 1440-1458.
Pedrozo-Acuña, A., Simmonds, D.J., Otta, A.K. and Chadwick, A.J. (2006) "On the cross-shore profile change of gravel beaches", *Coastal Eng.*, Vol. 53, pp. 335-347.
Watanabe et al. (1981) "Numerical simulation of nearshore current and beach transformation", *Proc. 28th Conf. on Coastal Eng.*, *JSCE* Vol. 28, pp. 285-289.
Watanabe et al. (1984) "Numerical prediction model of three-dimensional beach deformation around coastal structures", *Proc. 31th Conf. on Coastal Eng.*, *JSCE* Vol. 31, pp. 406-410.

APPENDIX

APPENDIX 1

International Conference on the Mitigation of Natural Disasters in the Tsunami Affected Coastal Regions of Tropical Asia

Workshop: Pearl Hotel (Phuket City, Thailand), 31st August 2006
Field excursion: Phuket, Khao Lak, Nam Khem and Ranong, Southwest Thailand, 1st September 2006

Support from: Japan Society for the Promotion of Science
Nagoya University, Japan
Prince of Songhla University, Thailand
Kasetsart University, Thailand
Coastal Research Committee, Japan Quaternary Science Association
Chief Organizer: Professor Masatomo Umitsu (Nagoya University, Japan)
Local Organizer: Dr Charlchai Tanavud (Prince of Songkhla University, Thailand)
Secretariat: Dr Taro Sasaki (Forest Economic Research Institute, Japan)
Dr Makoto Takahashi (Nagoya University, Japan)

Program of Workshop

Opening speech (Masatomo Umitsu)
Keynote speech: Masataka Ando (Nagoya University, Japan): How do Earthquakes Generate Tsunamis?
Paper presentation I (Chair: Norimi Mizutani)
Md. Shahidul Islam and Nayon Kumar Barua (University of Chittagong, Bangladesh): Impact of the Giant Sumatra Tsunami of 26 December, 2005 on the Northeastern Part of the Bay of Bengal, Bangladesh: a Preliminary Study
Ryota Nagasawa (Tottori University, Japan) and Boonrak Patanakanog: Topographic Assessment on the TSUNAMI Attacked Areas Using Digital Photogrametry
Satoshi Ishiguro (Nagoya University, Japan), Toshiro Sugimura, Shigeki Sano and Yasuhiro Suzuki: DSM Accuracy Generated by Combining Single-images from IKONOS and QuickBird: a Case Study of Nam Khem Plain, Thailand
Suharyadi, Taufik Heri and Barandi Sapta (Gadjah Mada University, Indonesia): Quick Assessment & Mapping of Earthquake Damage Using Remote Sensing Imagery: Case Yogyakarta, Indonesia
Paper presentation II (Chair: Sumiko Kubo)
Sitthisak Moukomla and Thudchai Sansena (Geo-Informatics and Space Technology Development Agency, Thailand): GISTDA Rapid Responded to Tsunami
Kaori Hayashi and Shigeko Haruyama (University of Tokyo, Japan): Coastal Vulnerability Assessment of Phuket Island to Mitigation of Tsunami Hazards
Masatomo Umitsu (Nagoya University, Japan), Charlchai Tanavud and Boonrak Patanakanog: Effects of Landforms on Tsunami Flow Caused by the Giant Earthquake off Smatra in the Plains of Nam Khem, Thailand and Banda Aceh, Indonesia
Abdul Hoque and Md. Shahidul Islam (University of Chittagong, Bangladesh): Vulnerability of the Coastal Belt of Bangladesh to Tsunami and Storm-Surges: New Challenge in Coastal Disaster Management
Paper presentation III (Chair: Ryota Nagasawa)
Djati Mardiatno (Gadjah Mada University, Indonesia), Johann Stoetter, Adi Widagdo, Ananta Purwoarminta, Mujiono, Juniawan Priyono, Sutikno, Sunarto, and Franck Lavigne: The Impact of Java Tsunami 17th July 2006 to the South Coast of Java Island: A Preliminary Result from the Field Survey
Agussalim (Syiah Kuala University, Indonesia): Characteristic of Damaged Buildings Caused by December 2004 Tsunami in Great Aceh District
Norimi Mizutani and Tomoaki Nakamura (Nagoya University, Japan): Three-Dimensional Numerical Analysis on Impact Loads Due to Run-up Tsunami
Sabaruddin Zakaria and Helmi (Syiah Kuala University, Indonesia): Improving Farmers Awareness on Onion Cultivation Sytem in Tsunami: Destructed Land by Participatory Student Research
Culminating discussion (Taro Sasaki and Makoto Takahashi)
Closing speech (Charlchai Tanavud)

List of Poster Presentations

Sumiko Kubo: Geomorphological Mapping of the Lower Mekong Plain (Cambodia)
Idawati Arsyad, Ulrich Polom, and Didik Sugiyanto: Shallow Shear-wave Reflection Seismic Applications in The Krueng Aceh River Delta

Didik Sugiyanto, Irwan Meilano, Yusaku Oota, Takeo Ito and Fumiaki Kimata, and Takao Tabei: GPS Observations of Fault Afterslip Follow ing the 2004 Aceh-Andaman Earthquake

Hiromi Kataoka: Supply of Disaster Information to
Foreigners in Hamamatsu-city, Shizuoka Pref. (JAPAN)

Naruekamon Janjirawuttikul, Kannisa Saridsiri, Salila Iamittipon, and Aumpaiwan Sunawan: Land Use Planning in Tambon Bang Muang and Khuk Khak, Amphoe Takuapa, Phan-Nga Province, Thailand

Helmi: Community Mobilization in Land Rehabilitation and Reclamation of Tsunami Affected Area: A Case Action in Aceh Besar, Indonesia

Sciences Research Team of Nagoya University + Suhirman: People, Community and Government in the Post-tsunami Rehabilitation/Reconstruction Processes in Banda Aceh

Masatomo Umitsu, Charlchai Tanavud, and Boonrak Patanakanog: Spatial Distribution of the Tsunami Deposits in the Nam Khem, Thailand

Remote Sensing Department – Geography, Gadjah Mada University: Quick Damage Assessment and Mapping; GIS – RS For Damage Assessment & Mapping

Photo of the Phuket Conference

Group photo of the Phuket Conference Excursion at Coastal Research Center, Kaset Sart University

APPENDIX 2

International Conference on Mangroves: Important Issue for the Coastal Environment

Workshop:	Tan Son Nhat Hotel (Ho Chi Minh City, Vietnam), 25th August 2007
Field excursion:	Can Gio Mangrove Biosphere Reserve, 26th August 2007
Host:	Japan Society for the Promotion of Science Nagoya University, Japan Nanzan University, Japan Vietnamese Academy of Science and Technology (VAST) Nong Lam University, Vietnam
Support:	Coastal Research Committee, Japan Quaternary Science Association International Society for Mangrove Ecosystems (ISME)
Chief Organizer:	Professor Masatomo Umitsu (Nagoya University, Japan)
Co-organizer:	Professor Kiyoshi Fujimoto (Nanzan University, Japan)
Local Organizer:	Dr. Nguyen van Lap (Vietnamese Academy of Science and Technology) Dr. Vien Ngoc Nam (Nong Lam University, Vietnam)

Program of Workshop

Opening Address: Masatomo Umitsu
Keynote Speech: Shigeyuki Baba: What we can learn from mangroves
Invited Lecture: Vien Ngoc Nam: Status and problems of mangrove ecosystems in Southern Vietnam
Invited Lecture: Mai Sy Tuan: Present status and problems of mangrove ecosystems in Northern Vietnam
SESSION 1: ENVIRONMENT
- Nguyen Tien Cong, and Nguyen Thanh Phuong: An assessment of the changes of the ecological significance of wetlands and mangroves in the Red River coastal zone, Vietnam
- Ta Thi Kim Oanh, Nguyen Van Lap, Bui Thi Luan, and Masatomo Umitsu: Diatom and foraminifera as indicators of environmental change in mangrove swamps of Ca Mau Peninsula, Vietnam

SESSION 2: DISASTER
- Sakhan Teejuntuk, Decha Duangnamon, Preedamon Kamwachirapitak, and Jon-grak Wacharinrat: Impact of tsunami disaster to forests in Ranong Coastal Resources Research Station
- Gay D. Defiesta: Valuation of selected ecosystem functions of oil spill-affected mangrove areas in the Visayas, Philippines: a benefit transfer approach

SESSION 3: REMOTE SENSING
- Nguyen Thi Thuy Hang: Remote sensing for monitoring vegetation structure in coastal wetlands
- Sanjeevi Shanmugam, and Aparna Bhaskar: A sub-pixel approach for accurate change detection in Pichavaram mangroves, southern India, using satellite images

SESSION 4-5: MANAGEMENT
- Rene N. Rollon and Maricar S. Samson: Growth performance of planted mangroves in the Philippines: revisiting forest management strategies
- Jon P. Altamirano and Hisashi Kurokura: Effective ground-based mapping of manageable mangrove forests
- Bui Thi Nga and Huynh Quoc Tinh: The mangrove-shrimp system in the Mekong Delta, Vietnam: present status, researches, and conservation
- Somying Soontornwong and Tanongsak Janthong: Mangrove community institutional development: experience of Pred Nai, Trat, Thailand

SESSION 6: EMPOWERMENT
- Taro Sasaki and Makoto Takahashi: Community forestry and land ownership in the coast
- Dao Huy Giap and David Brown: Lessons from the EcoBoat project: teaching teenagers the value of mangrove forests

Closing Address: Kiyoshi Fujimoto

List of Poster Presentations

Chanchai Thanawood: Natural barrier to tsunami disasters
Fujimoto Kiyoshi1, Umitsu Masatomo, Kawase Kumiko, Nguyen Van Lap, Ta Thi Kim Oanh, Huynh Duc Hoan: Geomorphological evolution and mangrove habitat dynamics of the Northern Mekong River Delta and Dong Nai River Delta
Helmi: Management of mangrove ecosystem for coastal rehabilitation in Aceh Province, Indonesia
Ishihara Shuichi, Fujimoto Kiyoshi, Vien Ngoc Nam and Huynh Duc Hoan: Growth and mortality of mangroves for four years in a reforested area, Cán Gio, Vietnam

Janjirawuttikul Naruekamon and Umitsu Masatomo: Geo-environment and acid sulfate soil in the Lower Central Plain, Thailand

Junun Sartohadi, Langgeng Wahyu Santosa, and Wirastuti Widyatmanti: The conservation problems of mangrove forest in Segara Anakan – Central Java – Indonesia

Maricar S. Samson, and Rene N. Rollon: A decade of mangrove forest management in Tayabas and Calauag Bays, Philippines: our focus onwards?

Mkrtchyan Ferdenant A., Krapivin V. F., and Golovachev S. P.: An adaptive microwave radiometry technology for the monitoring for-est ecosystems and coastal zones

Ngo Thi Phuong Uyen, Nguyen Van Lap, and Ta Thi Kim Oanh: Coastline change in Ben Tre Pprovince, Mekong River Delta

Nguyen Van Lap, Ta Thi Kim Oanh, Masaaki Tateishi, and Yoshiki Ssaito: Geomorpho- sedimentary and coastal changes at the Mekong River Delta, Vietnam

Muslim Abdul Djalil: Community based economic activities in the tsunami affected areas in the Province of Aceh, Indonesia (key success and challenges)

Pham Minh Hai: Change detection of the mangrove forest in Balat estuary by remote sensing

Pham Thi Lan: Multidate image analysis applied to change detection of mangrove cover in coastal communes of Thai Binh Province, Red River Delta, Vietnam

Pham Van Manh: Application of remote sensing and GIS for assessing mangrove forest for aquaculture in Hai Phong coastal zone

Resurreccion B. Sadaba: Oil spill in mangroves: the case of Solar 1 Oil Spill in Southern Gui-maras, Philippines

Huynh Duc Hoan, Pham Van Quy, and Vien Ngoc Nam: Initial nursing of *Lumnitzera littorea* fruit

Wijarn Meephol and Wijit Ongsomwang: Current status and rehabilitation of mangroves in Thailand

Photo of the Ho Chi Minh Conference

Group photo of the Ho Chi Minh Conference Excursion

APPENDIX 3

International Conference on Mangroves: Coastal Erosion: Its Dynamics and Impact to Human Life

Workshop: The Cozy Beach Hotel (Pattaya City, Chonburi, Thailand), 3rd November 2007
Field excursion: Coastal Area of the East Coast and the Upper Gulf of Thailand, 4th November 2007

Support: Japan Society for the Promotion of Science
Nagoya University, Japan
Chulalongkorn University, Thailand
Chief Organizer: Professor Masatomo Umitsu (Nagoya University, Japan)
Local Organizer: Dr. Thanawat Jarpongsakul (Chulalongkorn University, Thailand)

Program of Workshop

Opening Address: Masatomo Umitsu (Nagoya University, Japan)
Address of Local Organizer: Thanawat Jarupongsakul (Chulalongkorn University, Thailand)
Session 1: Coastal Erosion and Environment (Chaired by Masatomo Umitsu)
- Yoshiki Saito (Geological Survey of Japan, National Institute of Advanced Industrial Science and Technology, Japan): Coastal erosion of mega-deltas in Asia: deltas at risk
- Thanawat Jarupongsakul (Department of Geology, Faculty of Science, Chulalongkorn University,Thailand): Effectiveness of the disintegrated wave-power barrier in protecting coastal erosion of muddy shore at Ban Khun Samut Chin, Upper Gulf of Thailand
- Nguyen Van Lap (Sub-Institute of Geography, Vietnamese Academy of Science and Technology, Vietnam), Ta Thi Kim Oanh, Masaaki Tateishi, and Yoshiki Saito: Sedimentary environments and coastal erosion of the active delta plain, Mekong River Delta, Vietnam
- Ta Thi Kim Oanh (Sub-Institute of Geography, Vietnamese Academy of Science and Technology, Vietnam), and Nguyen Van Lap: Erosion process of Ca Mau coastline since the last 100 years in Mekong River Delta, Vietnam

Session 2: Coastal Erosion and Ecosystem (Chaired by Yoshiki Saito)
- Masatomo Umitsu (Department of Geography, Nagoya University, Japan), Naruekamon Janjrawuttikul, Charlchai Tanavud, and Kumiko Kawase: Late Holocene evolution of the Songkhla Coastal Plain in Southern Thailand
- Pramote Sojisuporn (Department of Marine, Faculty of Science, Chulalongkorn University, Thailand), and Supichai Tangjaitrong: Effectiveness of bamboo rows in protecting coastal shoreline erosion
- Vu Van Phai (Hanoi University of Science, Vietnam National University, Vietnam): Coastal erosion of Vietnam: actual state and reasons

Session 3: Coastal Change and Impact (Chaired by Tanawat Jarupongsakul)
- Nguyen Ngoc Thach (Hanoi University of Science, Vietnam National University, Vietnam), and Pham Ngoc Hai: Assess effects of sea-level rising and river activity to changing in the coastal zone of the Red River Delta by using remote sensing and GIS
- Junun Sartohadi (Faculty of Geography, Gadjah Mada University, Indonesia), Rino Cahyadi Giyanto, Wirastuti Widyadmanti, and Suratman Worosuprojo: The coast line changes from 1934 to 2006 in the Kulonprogo District Yogyakarta – Indonesia
- Abdul Hoque (Department of Geography and Environmental Studies, University of Chittagong, Bangladesh), and Mahbub Murshed: Impact of flash floods and water logging to the human life in Matamuhuri Delta of Cox'sbazar due to the river bank erosion and other associated factors
- Suratman Worosuprojo (Faculty of Geography, Gadjah Mada University, Indonesia), Rino Cahyadi Srijaya Giyanto, Junun Sartohadi, and Langgeng Wahyu Santosa: Identification of coastal area damage using remote sensing and geographic information system: the impact of July 17th, 2006 Tsunami in Parangtritis, Yogyakarta Special Province – Indonesia
- Futoshi Nanayama (Geological Survey of Japan, National Institute of Advanced Industrial Science and Technology, Japan): Coastal erosion and sand transportation associated with past huge tsunamis at Kiritappu marsh, eastern Hokkaido

Session 4: Coastal Change and Engineering (Chaired by Charlchai Tanavud)
- Tomoaki Nakamura (Department of Civil Engineering, Nagoya University, Japan), Norimi Mizutani, and Yasuki Kuramitsu: Effects of pore water pressure on scour – in case of local scour due to runup tsunami –

Norimi Mizutani (Department of Civil Engineering, Nagoya University, Japan), Hyunho Ma, and Shu Eguchi: Study on beach profile change of Ida Beach of Shichiri-Mihama Coast

Kwang-Ho Lee (Department of Civil Engineering, Nagoya University, Japan), Norimi Mizutani, and Toshiaki Fujii: A numerical model for gravel beach deformation based on 2-way method

Winai Ouypornprasert, Somchai Ouypornprasert and Natamon Kampananon (Faculty of Engeneering, Rangsit University,Thailand): Protection of coastal erosion at Ban Khunsamut Chin, appear Gulf of Thailand: Coastal engineering aspects

Culminating Discussion: Moderated by Taro Sasaki (International Cooperation Center for Agricultural Education, Nagoya University, Japan)

Closing Address: Norimi Mizutani (Department of Civil Engineering, Nagoya University, Japan)

Photo of the Pattaya Conference

Group photo of the Pattaya Conference

Condolence

At the time of Pattaya Conference Field Excursion on November 4, 2007, we took a boat for the access to the observation site. On the way back from the site, our boat with 36 participants hit a pole in a canal and sank very quickly. Among the participants, three young brilliant scientists passed away due to the accident.

They are Mr. Wiman Wedchakul, an assistant of the Dr. Thanawat Jarpongsakul's laboratory at Churalongkorn University, Ms. Nongnuch Paiboon, an Officer at Department of Marine and Coastal Resources, Thailand, and Mr. Rino Cahyadi Giyanto, a master course student at the University of Gadjah Mada in Indonesia.

We are extremely sad and very sorry that the bright three young scientists passed away by the unexpected accident. We would like to offer our deepest condolences to those to the deceased persons and their families.